

THE CARDIOPROTECTIVE MECHANISMS OF DIETARY FLAVONOIDS

JAMES DAUBNEY

A thesis submitted in partial fulfilment of the
requirements of Nottingham Trent University for the
degree of Doctor of Philosophy

July 2015

This work is the intellectual property of the author. You may copy up to 5% of this work for private study, or personal, non-commercial research. Any re-use of the information contained within this document should be fully referenced, quoting the author, title, university, degree level and pagination. Queries or requests for any other use, or if a more substantial copy is required, should be directed in author.

Proceedings and Publications

Data from this thesis has been published in *Basic & Clinical Pharmacology & Toxicology*, and has been presented at the 6th Annual School of Science and Technology Research Conference held by Nottingham Trent University (2012).

- Daubney J, Bonner PL, Hargreaves AJ and Dickenson, JM (2015) Cardioprotective and Cardiotoxic Effects of Quercetin and Two of Its In Vivo Metabolites on Differentiated H9c2 Cardiomyocytes, *Basic & Clinical Pharmacology & Toxicology*, **116**, 96–109

Abstract

Mitotic rat embryonic cardiomyoblast-derived H9c2 cells are widely used as a model cardiomyocyte to study the protective mechanisms of dietary flavonoids, but they lack features of fully differentiated cardiomyocytes. Therefore, this present study aimed to investigate the cytoprotective and cytotoxic effects of the dietary flavonoids quercetin, kaempferol, myricetin and two major quercetin metabolites, quercetin-3-glucuronide and 3'-O-methylquercetin, on fully differentiated H9c2 cells for the first time. The cardiomyocyte-like phenotype of the differentiated H9c2 cells was confirmed by monitoring the expression of cardiac specific troponin T, as well as through the identification of other cardiac specific cytoskeletal markers using MALDI-TOF MS/MS. The cytoprotective effect of quercetin, kaempferol, myricetin, quercetin-3-glucuronide and 3'-O-methylquercetin against hypoxia and H₂O₂-induced cell death was assessed by monitoring MTT reduction and LDH release. Furthermore the effect of quercetin pre-treatment on ERK1/2, PKB, JNK and p38 MAPK phosphorylation was monitored using western blotting. It was shown that quercetin was the most potent flavonoid at inducing a protective effect, and 3'-O-methylquercetin the most potent metabolite. Using western blotting it was shown that this protective effect is most likely due to quercetin-mediated inhibition of ERK1/2, PKB, JNK and p38 MAPK. Specific inhibitors of these protein kinases did not modulate the observed cytoprotective effect, or cause significant protection alone. The cytotoxic effects of dietary flavonoids, particularly quercetin, was monitored with MTT reduction, LDH release, western blotting to monitor phosphorylation of ERK1/2, PKB, JNK and p38 MAPK and activation of caspase-3, and monitoring intracellular ROS generation with DCFDA assay. The cytotoxic effect of quercetin was shown to be linked to intracellular ROS generation, caspase-3 activation and phosphorylation of ERK1/2, PKB, JNK and p38 MAPK. MALDI-TOF MS for the first time identified several proteins associated with the flavonoid-mediated cytoprotective effect and flavonoid pre-treatment in differentiated H9c2 cells. Most were shown to be linked to the regulation of MAPK and PI3K cell signalling pathways. This present study for the first time demonstrates the cytoprotective and cytotoxic effects of flavonoids on differentiated H9c2 cells, and has identified novel proteins associated with the cytoprotective effect.

Acknowledgements

I'd like to extend a huge thank you to my supervisory team, John, Phil and Alan. In particular John, your constant reminders that "It's your PhD" kept me motivated and your help, support and understanding have been an invaluable asset to me, a better director of studies I could not have asked for.

For his help in mass spectrometry I thanks David in JvG, for their help in flow cytometry Stephanie and Steve, and for his help in microscopy a special thanks to Gordon.

My thanks also go to my stalwart lab mates in Lab 107 and everyone else in the IBRC top floor, without whom my time in the lab would have been boring and uneventful. A special thanks to Shatha, you spent the most time with me in the lab and still haven't left, this takes a very special type of scientist.

For all my other friends at NTU and elsewhere, you have my sincere thanks for putting up with me and keeping me 'sane' during my PhD studies, you have a friend for life in me.

Finally, my thanks go to my beloved family, you have made me what I am today, without you I couldn't have achieved what I have so far, and I hope to achieve much more to make you even more proud.

Contents

1.0 Introduction.....	11
1.1 Cardiovascular disease.....	12
1.2 Ischaemia induced cell death.....	12
1.3 Reactive oxygen species and cell signalling.....	16
1.4 Pharmacological preconditioning.....	16
1.5 Cardioprotective properties of flavonoids.....	17
1.6 Flavonoids.....	20
1.7 Flavonoid structure.....	21
1.8 Quercetin.....	23
1.9 Kaempferol.....	24
1.10 Myricetin.....	24
1.11 Bioavailability of flavonoids.....	25
1.12 Pro-oxidant intracellular metabolism of quercetin.....	30
1.13 MAPK proteins.....	31
1.14 PI3K/Akt pathway.....	34
1.15 H9c2 cells.....	36
1.16 H9c2 cell differentiation.....	37
1.17 Aims of this project.....	39
2.0 Methods.....	41
2.1 Cell Culture.....	41
i) H9c2 cell differentiation.....	41
2.2 Immunocytochemistry.....	41
2.3 Oxidative stress and Hypoxia-induced cell death.....	42

2.4 Cell viability assays.....	43
i) MTT assay.....	43
ii) Lactate dehydrogenase assay.....	43
iii) Coomassie blue staining.....	44
2.5 DCFDA assay for intracellular ROS.....	44
2.6 Western Blot.....	45
i) Cell lysis.....	45
ii) Protein estimation.....	45
iii) SDS-PAGE.....	46
iv) Western blot.....	47
2.7 Proteomic analysis.....	48
i) 2D gel electrophoresis.....	48
ii) SameSpot Analysis.....	50
iii) De-staining.....	50
iv) ZipTip reverse phase chromatography.....	51
v) MALDI-TOF MS/MS.....	51
2.8 Statistical analysis.....	52
2.9 Materials	52
3.0 Differentiation of H9c2 cells.....	55
3.1 Morphological change during differentiation	57
3.2 Expression of cardiac specific troponin.....	57
3.3 Proteomic analysis.....	61
3.4 Summary of findings.....	67
3.5 Discussion of Differentiation.....	67

i) Characterisation of differentiated H9c2 cells.....	67
ii) Proteomic investigation into the differentiated H9c2 cell phenotype.....	68
iii) Confirmation of tropomyosin expression.....	70
iv) Conclusion.....	70
4.0 Cytoprotective potential of flavonoids.....	73
4.1 Determining optimal H ₂ O ₂ treatment conditions.....	76
4.2 Hypoxia model design.....	81
4.3 Cytoprotective effects of flavonoid pre-treatment against Hydrogen peroxide induced cell death.....	81
4.4 Cytoprotective effects of flavonoid pre-treatment hypoxia induced cell death.....	89
4.5 Protective effects of quercetin metabolites.....	94
4.6 Protein kinase phosphorylation during flavonoid mediated cardioprotection against hydrogen peroxide.....	96
4.7 Protein kinase phosphorylation during flavonoid mediated cardioprotection against hypoxia.....	99
4.8 protein kinase inhibitors and flavonoids mediated cardioprotection.....	102
4.9 Results summary.....	106
4.10 Discussion of flavonoid mediated cytoprotective effect.....	107
i) Mitotic and differentiated cell comparison.....	107
ii) Flavonoid-mediated cytoprotection from H ₂ O ₂ exposure.....	107
iii) Flavonoid-mediated cytoprotection from hypoxia.....	109
iv) Cytoprotective effect of quercetin metabolites.....	109
v) Involvement of protein kinases in flavonoid-mediated cytoprotection.....	110
vi) Implications of flavonoid induced cytoprotection.....	113
5.0 Cytotoxicity of flavonoids.....	115

5.1 Cytotoxicity of flavonoids on proliferating cardiomyoblasts.....	117
5.2 Cytotoxicity of flavonoids on differentiating cardiomyoblasts.....	121
5.3 Cytotoxicity of flavonoids on differentiated cardiomyocytes.....	125
5.4 Cytotoxicity of quercetin metabolites on differentiated cardiomyocytes.....	130
5.5 Protein kinase expression associated with flavonoid induced cytotoxicity.....	133
5.6 Intracellular ROS associated with prolonged flavonoid exposure.....	136
5.7 Summary of findings.....	137
5.8 Discussion of flavonoid-mediated cytotoxicity.....	137
i) Cytotoxicity of Flavonoids.....	137
ii) Cytotoxicity of quercetin metabolites.....	138
iii) Role of cell signalling in flavonoid-mediated cytotoxicity.....	139
iv) Implications of flavonoid induced cytotoxicity.....	140
6.0 Proteomic identification of flavonoid mediated cardioprotection associated proteins.....	143
6.1 Two-dimensional gel electrophoresis.....	144
6.2 Progenesis SameSpot analysis.....	148
6.3 MALDI-TOF MS identification of proteins.....	155
6.4 Western blot confirmation of CBR-1 expression.....	157
6.5 Proteomics Discussion.....	158
i) CBR1.....	159
ii) Gelectin-1.....	160
iii) PEBP-1.....	160
iv) PRKC apoptosis WT1 regulator protein (PAWR).....	161
v) Annexin-III.....	161

vi) Calumenin.....	162
vii) Glutamate receptor (ionotropic kainate 4).....	163
viii) Summary.....	163
7.0 Conclusions and further work.....	164
7.1 Results summary and further work.....	165
7.2 Conclusions.....	168
7.3 Concluding remarks.....	168
8.0 References.....	170
Appendix 1.....	183
Appendix 2.....	184

Chapter 1:

Introduction

1.0 Introduction

1.1 Cardiovascular disease

In the developed world cardiovascular disease is the leading cause of death. In 2011 alone cardiovascular disease was responsible for approximately 160,000 deaths in the United Kingdom (British heart foundation). Factors such as diet, alcoholism, lack of exercise, smoking and longer life expectancy have led to an increased risk of cardiovascular disease in developed nations. Cardiovascular disease is also the leading cause of premature death of adults in the United Kingdom. Atherosclerotic plaques or thrombi causing a blockage of the coronary arteries is the major cause of ischaemic heart disease (coronary heart disease). This blockage causes a decrease in blood flow to the myocardium resulting in the myocardial tissue experiencing ischaemia. This ischaemia can lead to angina pectoris and myocardial infarction. Cardiovascular disease represents a significant burden to health authorities worldwide as risk factors and the overall age of the population increases, thus plentiful research on protection from ischaemia has been conducted. The potential protective effect of flavonoids against ischaemia in general and ischaemic heart disease in particular is still being studied. Flavonoids represent an interesting avenue in combating ischaemic heart disease, since they are already a ubiquitous component in the human diet, and some varieties are already available as dietary supplements. The interactions of flavonoids with the complex cellular mechanisms involved in ischaemia and cardioprotection could identify potential targets for prophylactic therapy against cardiovascular disease, and therefore reduce the overall burden of cardiovascular disease on the human population.

1.2 Ischaemia induced cell death

Adequate oxygen supply is vital for normal functioning of cardiac tissue. During an ischaemic attack the reduced availability of oxygen can lead to impaired contractile ability and cell death (de Moissac *et al*, 2000). This cell death can be divided into two classes, namely apoptosis and necrosis. Apoptosis is a “programmed cell death” where the cell destroys itself to minimise the leakage of cellular content into the extracellular microenvironment. Apoptosis is identified by nuclear condensation, fragmentation of chromosomal DNA and packaging the cellular content into apoptotic bodies, as well as

zeiosis of the plasma membrane. *In vivo* these apoptotic bodies are then recognised and phagocytosed, thus minimising the inflammatory response of the surrounding tissue. Apoptosis can be characterised by the activation of caspases (cysteine-dependent aspartate-directed proteases), cell death by apoptosis also requires ATP (Edinger and Thompson, 2004).

A number of studies have shown that hypoxia is able to induce apoptosis in a number of cell lines. Hypoxia has been shown to induce apoptosis via the activation of cytochrome c, which goes on to activate caspases, in Jurkat cells (Malhotra *et al*, 2001). The study by Malhotra, *et al* (2001) specified the involvement of caspase-3 in hypoxia mediated apoptosis in Jurkat cells. In adult rat cardiomyocytes caspase-3 was shown to be activated by mitochondrial cytochrome c and specifically target the DNA repair enzyme PARP (poly ADP ribose polymerase), which when cleaved results in the fragmentation of DNA and apoptosis (de Moissac *et al*, 2000). It has also been suggested that a caspase-independent pathway for apoptosis exists in certain cell lines (Malhotra *et al*, 2001). Overall there is strong evidence that ischaemia induces apoptosis in cardiomyocytes.

In opposition to the programmed cell death of apoptosis, necrosis has been described as a passive form of cell death, as well as it being much less concerned with contamination of the extracellular microenvironment with cellular debris. Necrosis results from a “bioenergetics catastrophe” where ATP levels are depleted to such a level to become incompatible with cellular life (Edinger and Thompson, 2004). Specifically during ischaemia the reduced availability of oxygen, other metabolites, and important sources of energy such as glucose, that would normally arrive via the blood stream become so depleted as to be insufficient for normal oxidative phosphorylation. This triggers anaerobic respiration, which reduces the intracellular production of ATP and increases the intracellular accumulation of hydrogen ions (H^+). This further leads to the intracellular accumulation of Sodium ion (Na^+) via the inhibition of ATP-dependant sodium/potassium pumps (Na^+/K^+ -ATPase) and activation of sodium/hydrogen exchangers (NHE). Intracellular Calcium ions (Ca^{2+}) are also accumulated by various mechanisms, including activation of Na^+/Ca^{2+} exchangers and reduced uptake of Ca^{2+} by sarcoplasmic reticulum due to decreased ATP in myocytes. Intracellular levels of Ca^{2+} go on to activate Ca^{2+} -dependant proteases which damage cytoskeletal and membrane bound proteins. Cellular osmotic swelling also occurs

due to the influx of water and Cl^- ions. The weakening of the cytoskeleton and cell membrane by the Ca^{2+} -dependant proteases and influx of osmotic swelling leads to membrane rupture and necrosis. This particular ischaemic cell death mechanism is mostly referred to as necrosis, but has been more specifically named oncotic necrosis (Schaper and Kostin, 2005). Rather than being separated it is now believed that apoptosis and necrosis represent different outcomes of the same pathway. Initially apoptosis is favoured by cardiomyocytes in hypoxia, but when ATP levels are depleted to a low enough level necrosis takes over as the dominant form of cell death, since it is not dependent on energy derived from ATP (Tatsumi *et al*, 2003). The proposed pathway of ischaemic attack leading to cell death is outlined in Fig 1.1.

In addition to apoptosis and necrosis a third cell death mechanism has been variously described, the theory of non-apoptotic programmed autophagy, or 'Programmed Necrosis' is gaining scientific momentum. A cell undergoing autophagy (self-digestion) forms a double membrane around organelles and cytoplasmic components, which then fuses with the lysosome. This fusion leads to the digestion of the content of the vesicle, which are then recycled. It has been suggested that this mechanism can be used by the cell as a method of suicide, leading to the complete digestion of itself (Edinger and Thompson, 2004). Autophagy is generally thought to be a method of self-preservation, where the cell content is recycled during times of famine in certain mammalian cells, as well as in plants species, yeasts and nematodes. The debate as to if autophagy represents a viable form of programmed cell death is ongoing, but it goes to prove that the apoptosis-independent mechanisms of cell death do occur, and therefore provide a potential for therapeutic targets (Edinger and Thompson, 2004).

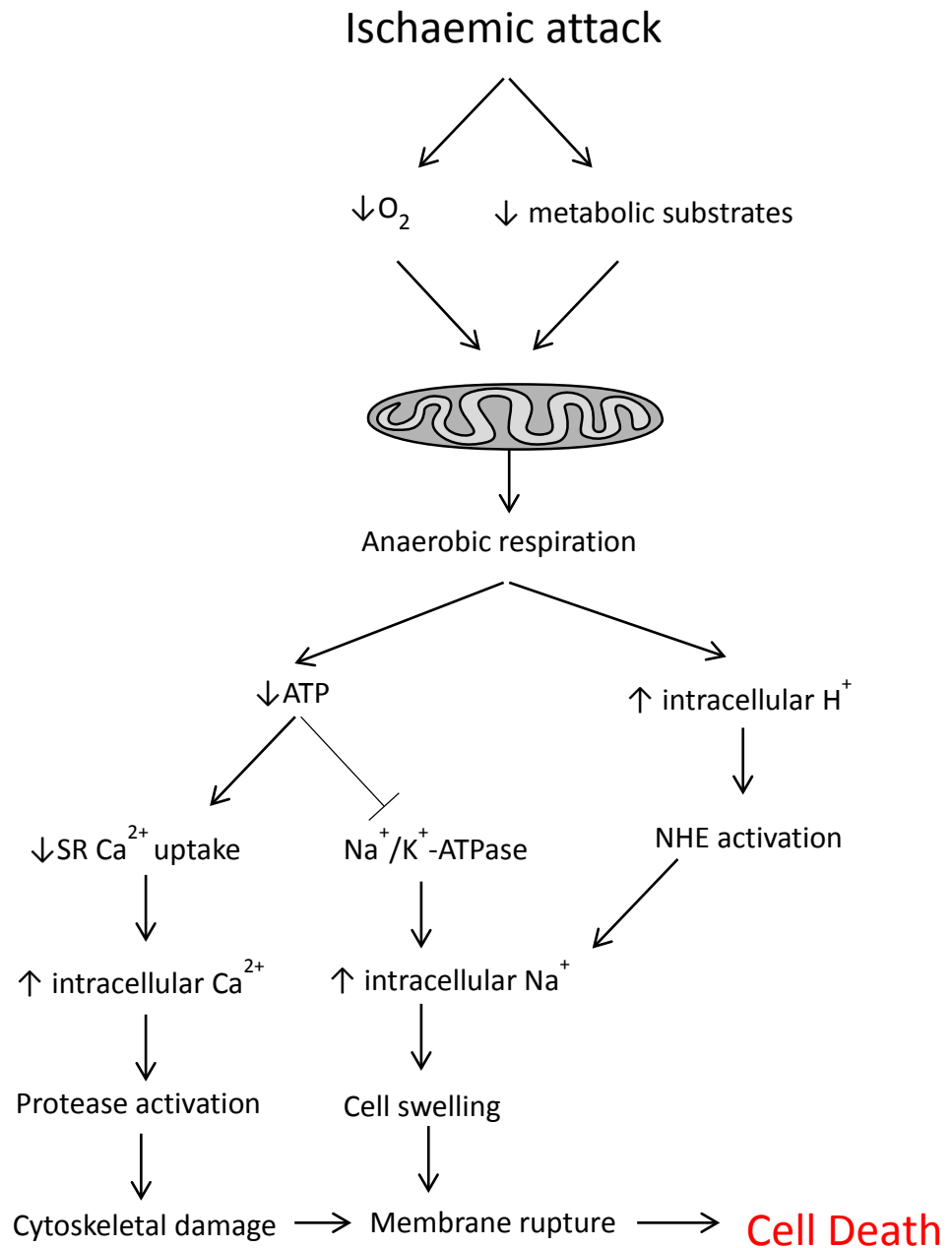


Fig. 1.1 Proposed scheme of events from ischaemia to cell death. Reduced oxygen and metabolic substrates leads to lack of ATP and intracellular acidosis. Cell swelling and damage leads to necrosis. (NHE: sodium/hydrogen exchangers).

1.3 Reactive oxygen species and cell signalling

The intracellular environment in cells under normal conditions is highly reducing. Reactive oxygen species (ROS) such as superoxides and peroxides are generated as a by-product of mitochondrial metabolism, and are eliminated from the cell via internal cellular antioxidants, reductants and other scavengers (Kamata and Hirata, 1999). Despite this mechanism some production of the highly reactive $\text{OH}\cdot$ occurs, which can lead to damage to the cell via the Haber-Weiss and Fenton reactions (Kamata and Hirata, 1999). These reactions can be artificially stimulated by adding H_2O_2 to the cellular environment. Oxidative stress caused by ROS has been shown to activate several cell signalling pathways, including Ras, the upstream activator of MEKs and the PI3K/Akt pathway. Furthermore oxidative stress can cause the activation of the caspases including caspase-3. Oxidative stress has a drastic effect on the intracellular regulation of Ca^{2+} , causing an intracellular increase through the modulation of the activity of $\text{Ca}^{+2}\text{-Na}^+$ exchangers and $\text{Ca}^{+2}\text{-ATPase}$ (Kamata and Hirata, 1999).

1.4 Pharmacological preconditioning

The effect known as ischaemic preconditioning (IPC) was first described by Murry *et al* (1986). The group was able to successfully precondition *in vivo* canine hearts to long periods of ischaemia by briefly and repeatedly occluding the coronary artery. This study showed that intermittent episodes of ischaemia resulted in a protective effect on the myocardium, visible upon histological inspection (Murry *et al*, 1986). It has since been the goal of many studies to recreate this effect pharmacologically. Studies have shown that a number of cell signalling pathways are associated with IPC, including MEK1/2, ERK1/2, RAS, PI3K and AKT (Hausenloy and Yellon, 2007). It is known now that flavonoids are able to act upon these cell signalling molecules in a number of ways, this opens the possibility of using flavonoids as a cardioprotective agent. Given the ubiquitous nature of flavonoids in the human diet, they present a good prospect for pharmacological preconditioning of the heart in humans.

1.5 Cardioprotective properties of flavonoids

Flavonoids, in particular quercetin, have been extensively reported to possess many pharmacological properties, including anti-proliferation effects on cancer cell lines, as well as a strong antioxidant effect. Quercetin also possesses a broad range of effects that promote its reported cardioprotective action, including anti-inflammatory, anti-platelet aggregation and anti-hypercholesterolemia effects. In the past it was thought the majority of quercetin's cardioprotective effect was due to its potent antioxidant activity, but it is now also becoming evident that quercetin is able to modulate certain cell signalling pathways which may have an effect on the post-ischaemic survival of heart cells (Choi *et al*, 2005).

It has been shown that quercetin is able to bind to the ATP-binding sites of a large number of proteins which can cause competitive inhibition of these proteins (Williams *et al*, 2004). Proteins that have been shown to be inhibited by quercetin include proteins important to cell signalling pathways, such as protein kinase C (PKC), mitogen-activated protein kinase (MAPK) family proteins, Phosphoinositide 3-kinase (PI3K) and myosin-light chain kinases (MLCK) (Russo *et al*, 2012). These cell signalling pathways are associated with cell survival, growth arrest and apoptosis.

Supplementation with quercetin (730 mg/day) for 28 days has been demonstrated to cause a reduction in mean systolic, diastolic and arterial pressure in a cohort of patients suffering hypertension (Edwards *et al*, 2007). Similarly, a study on a cohort of overweight patients with high risk of cardiovascular disease showed that supplementation with 150 mg/day quercetin for 42 days caused a reduction in systolic blood pressure, and reduced atherogenic-oxidised low density lipoproteins (LDL) (Egert *et al*, 2009). These studies show the diverse range of effects quercetin possesses which lead to cardioprotection.

This body of work will focus on the effect flavonoids have on heart cells during ischaemic attack as a way to investigate the potential benefits of flavonoids on CVD development. Generally *in vivo* a number of other physiological events occur before damage to the heart cells develops due to ischaemia. These events, namely the development and progression of atherosclerosis, also have the potential to be effected by flavonoids.

Atherosclerosis is typified by the development of lesions, called atheromas or atherosclerotic plaques, located in the intimal layer of cells in the blood vessels. These lesions consist of a fatty core of lipids, mostly cholesterol, capped with a fibrous layer consisting of smooth muscle, macrophages, foam cells, collagen and elastins. These lesions lead to the mechanical obstruction of blood vessels which can lead to ischaemic attack, furthermore the lesion can rupture causing vessel thrombosis and aneurysm formation.

There have been a number of risk factors identified with regard to developing atherosclerosis, these include hyperlipidaemia (*hypercholesterolaemia*), hypertension, tobacco smoking and diabetes (Chambless *et al*, 2002).

Atherosclerosis has been characterised as a chronic inflammatory condition where healing responses in the endothelium of the artery lead to injury. The development of an atherosclerotic lesion follows a series of pathological events, starting with endothelial injury which leads to increased endothelial permeability and leukocyte adhesion. Lipoproteins, mostly in the form of LDL (low density lipoproteins) then accumulate in the vessel wall. Monocytes then migrate into the area and transform into macrophages and foam cells. Platelet adhesion, along with the presence of macrophages, then leads to factor release which induces smooth muscle cell recruitment. The smooth muscle in response proliferates and the ECM (extracellular matrix) production is increased. Finally lipids further accumulate leading to the formation of the lesion (Ross, 1999).

The initial injury to the endothelium of the blood vessel is the keystone in the sequence of events that lead to the formation of the atherosclerotic plaque. The thickening of the intima can be a result of a range of different injurious stimuli, such as immune complex desposition, irradiation, chemical injury or haemodynamic forces. Coupled with high-lipid diets, this leads to the formation of the plaque. Furthermore, endothelial dysfunction is a key factor in the development of an atherosclerotic plaque, specifically regarding increased endothelial permeability and increased leukocyte adhesion. Currently the specific pathways and factors leading to this dysfunction are not fully understood, etiologic studies suggest hypertension, hyperlipidaemia, toxins from tobacco smoking and infectious agents are key factors. However, haemodynamic disturbance and hypercholesterolaemia are considered the main contributing factors.

The prominence of haemodynamic disturbance in the formation of atherosclerotic plaques is demonstrated principally by the observation that lesions tend to form at the branch points and the dorsal wall of the abdominal aorta where disturbed flow patterns of blood are common (Chatzizisis et al, 2007).

The evidence implicating hypercholesterolaemia as a dominant factor in atherogenesis includes the observation that cholesterol and cholesterol esters form the dominant lipids in atherosclerotic plaques. Furthermore, disorders that cause hypercholesterolaemia, such as diabetes and hypothyroidism, lead to premature atherosclerosis. The mechanism by which hypercholesterolaemia is thought to contribute to atherogenesis is mainly due to increasing oxygen free radical production, which leads to tissue injury and decreased vasodilatory action due to accelerated nitric oxide decay. Furthermore, lipids that are accumulated in the intima are oxidised in the presence of the oxygen free radicals generated by macrophages and the endothelium. The oxidised LDLs are then phagocytised by macrophages, accumulate and form foam cells. Oxidised LDL also stimulates the release of cytokines, chemokines and growth factors that lead to increased amassing of monocytes. Endothelial cell dysfunction is further stimulated by oxidised LDL as it has a cytotoxic effect on smooth muscle and endothelial cells (Gau *et al*, 2006).

Progression of atherosclerotic lesions is also heavily influenced by inflammatory cells and pathways. dysfunctional endothelial cells express adhesion molecules that encourage immune cells adhere. Once adhered to the endothelium these immune cells are able to migrate into the intima, attracted by locally produced chemokines. The differentiation of monocytes into macrophages and foam cells is considered protective as this removes harmful lipid particles. However oxidised LDL augments the macrophages leading to more leukocyte adhesion and chemokine production, leading to mononuclear cell infiltration. Activated macrophages also produce ROS that increase LDL oxidation. The recruitment of T-lymphocytes to the intima can generate a chronic inflammatory state by producing pro-inflammatory cytokines when they interact with the macrophages, the exact reason for this remains unknown. Furthermore activated leukocytes and the cells of the vascular wall release growth factors that lead to smooth muscle proliferation and ECM synthesis (Hansson, 2005).

Flavonoids, in particular quercetin and its metabolites, have been demonstrated to have anti-atherogenic properties in a number of studies. Flavonoids are known to inhibit LDL oxidation, inhibit platelet aggregation and adhesion, have a detrimental effect on the uptake of lipids into macrophages, induce vasodilation and lower LDL cholesterol (Reed, 2002). Specifically, quercetin and quercetin-3-glucuronide have been demonstrated to prevent endothelial dysfunction *in vitro* at 1 $\mu\text{mol/L}$ (Lodi *et al*, 2009). Similarly, quercetin and the glucuronidated metabolite was able to prevent ROS release at concentrations less than 10 $\mu\text{mol/L}$ in aortic smooth muscle cells in culture (Lodi *et al*, 2009). Quercetin was found to modulate the effect of inflammatory enzymes such as cyclooxygenase, lipoxygenases, myeloperoxidase and nitric oxide synthase in rabbits with a hypercholesterolemic diets when administered at 25mg/kg body weight (Bhaskar *et al*, 2013). Quercetin was also demonstrated to modulate PKC activity induced by superoxide production and endothelial dysfunction in rat aortas (Romero *et al*, 2009).

Various studies have demonstrated how quercetin and its metabolites effect atherogenesis. In the diet, these flavonoids will lead to a decreased risk of atherosclerosis and therefore a decreased risk in overall CVD, representing a significant mechanism of cardioprotection. In this present study the protective effects of flavonoids were investigated with regard to heart cells, to further elaborate on the effects of flavonoids on the progression of CVD in general.

1.6 Flavonoids

Flavonoids are a diverse family of plant metabolites, which form a ubiquitous part of the human diet. Over 4000 types of flavonoids have been identified, and can be found in the leaves, bark, fruits, seeds and flowers of many plants (Hiem, *et al*, 2002). The intake of flavonoid in the human diet varies by region, and with cultural practices such as drinking tea or wine also having an influence. The average daily flavonoid intake in a western developed nation has been reported to be approximately 23 mg (Hiem, *et al*, 2002). Many years of research has been dedicated to the investigation of the antioxidant capacity of flavonoids, and their ability to protect cells from damage from oxidative stress. Recent studies have also been concerned with the potential ability of flavonoids to interact directly with cell signalling molecules that also play a role in the survival of cells after oxidative stress.

1.7 Flavonoid structure

Flavonoids are all based on a standard central structure called the flavan nucleus (Fig 1.2). Subtypes of flavonoid are classified by the substitutions on this standard structure. Dietary flavonoids differ by the number and arrangement of hydroxyl, methyl and glycosidic groups on the central flavan nucleus. Tannins, a related chemical to flavonoids, are formed by the polymerisation of the underlying flavan nucleus.

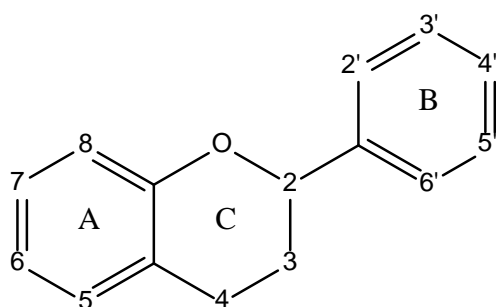


Fig. 1.2 The flavan nucleus.

The structure of flavonoids, being polyphenolic, gives the molecule great antioxidant capacity, as well as the potential to influence cell signalling. Research suggests that the number and arrangement of hydroxyl group substitutions effects the antioxidant capacity of flavonoids in a positive way. Particular substitutions such as hydroxyl groups on position 3 and 5 of the A ring and C2-C3 double bonding result in higher antioxidant activity (Chang *et al*, 2007). There are a number of subtypes of flavonoid, all based on the underlying flavan nucleus structure.

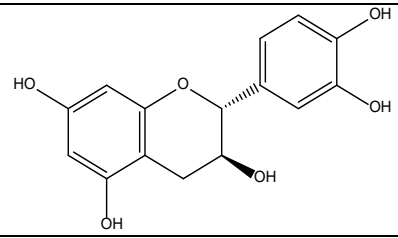
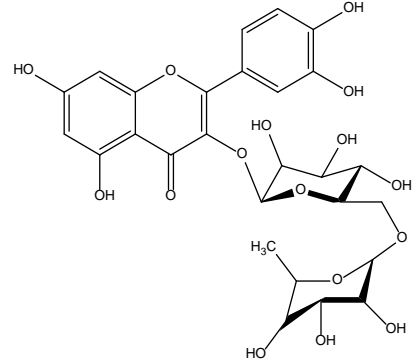
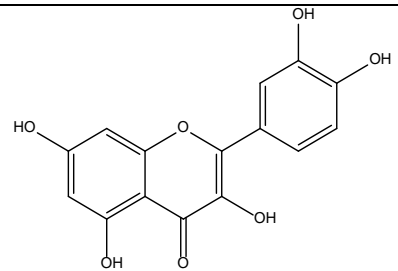
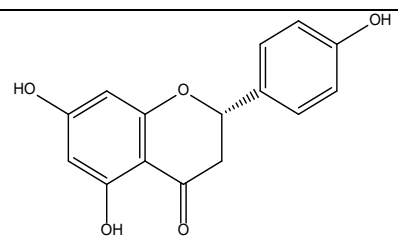
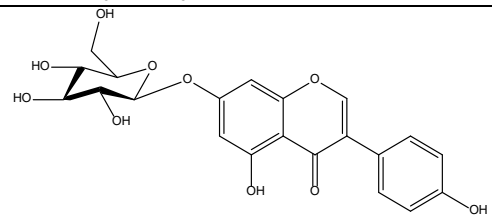
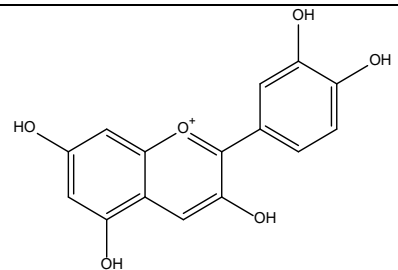
Class	Example flavonoid	Structure	Dietary source
Flavanol	(+)-catechin		Tea
Flavone	Rutin		Red wine, Buckwheat, tomato skin, Citrus
Flavonol	Quercetin		Onion, lettuce, broccoli, Tomato, tea red wine, berries, olive oil, apple skin
Flavanone	Naringenin		Citrus (Grapefruit)
Isoflavone	Genistin		Soybean
Anthocyanidin	Cyanidin		Cherry, Raspberry, strawberry

Table 1.3 Classes of flavonoid and their associated structure (Hiem, *et al*, 2002).

Certain subtypes of flavonoid generally possess specific structural traits, for example flavanols all exhibit hydroxyl groups on the 3,5,7,3' and 4' locations on the flavan nucleus.

This particular subtype contains molecules such as (-)-epicatechin which is found in high quantities in tea (Heim, 2002).

1.8 Quercetin

Quercetin, a member of the flavonol subfamily, is one of the most frequently researched members of the flavonoid family. It has been shown to exhibit a structure that is both an effective antioxidant and a potent effector of cell signalling molecules. The structure of quercetin is based on the flavan nucleus, with hydroxyl groups on the 3,5,7,3' and 4' carbons and a ketone group located on the at position 4 of the C ring of the flavan nucleus, as shown in Fig. 1.4.

Quercetin has been demonstrated to be able to bind directly to the ATP binding pocket of some enzymes, this ability is directly linked to the hydroxyl group substitutions on the B ring of the flavonoid, as well as an unsaturated C2-C3 bond (Williams *et al*, 2004). Quercetin has been found to be one of the most abundant flavonoids in the human diet and is found in high levels in red wines, tomatoes, red berries, certain teas and onions. Naturally, it is responsible for the red pigmentation in a wide variety of plants, in its pure form it has a yellow coloration due to the ketone group on position 4 of the C ring of the flavan nucleus.

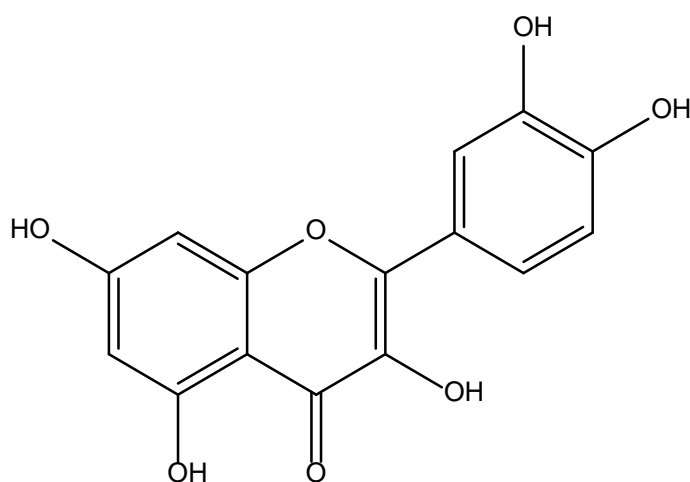


Fig. 1.4 Structure of quercetin. Based on the flavan nucleus with hydroxyl groups on the 3,5,7,3' and 4' carbons, a ketone group located on the at position 4 of the C ring of the flavan nucleus.

1.9 Kaempferol

Kaempferol is a flavonol, and is found in high levels in kale, broccoli, chives and other green plants (Choi, 2011). Studies have demonstrated that kaempferol can inhibit the phosphorylation of JNK and p38 MAPK in several cell lines, resulting in prevention of oxidative stress and apoptosis (Mansuri *et al*, 2014). Like quercetin, kaempferol has been shown to have antioxidant and cell signal modulating activities. Structurally, kaempferol has hydroxyl groups on the 4', 3, 5 and 7 positions of the flavan nucleus with an unsaturated C2-C3 bond, and a ketone group located at position 4 of the C ring of the flavan nucleus, as shown in Fig. 1.5. This unsaturated bond, similar to quercetin, may allow kaempferol to bind directly to ATP binding pockets of some enzymes (Williams *et al*, 2004).

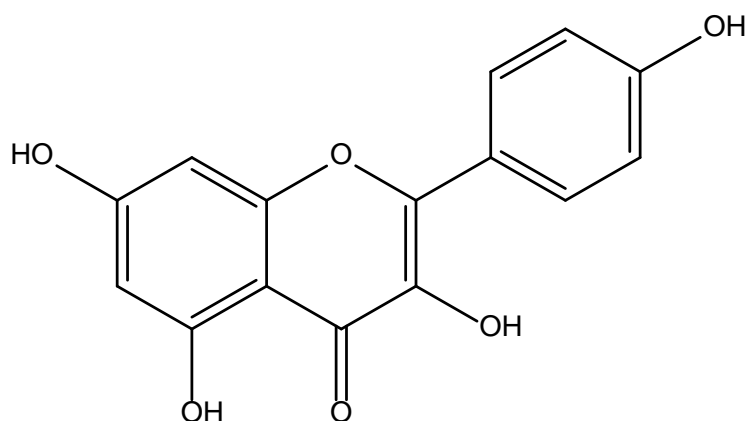


Fig 1.5 Structure of kaempferol.

1.10 Myricetin

Myricetin has been found to act as a direct antioxidant and also acts to induce antioxidant enzyme expression, specifically catalase (Wang *et al*, 2010). Myricetin has also been shown to directly interact with the PI3K/Akt and MAPK pathways (Kyoung *et al*, 2010). Myricetin can down-regulate the phosphorylation of p38 MAPK and JNK, suggesting anti-apoptotic effects (Mansuri *et al*, 2014). Structurally similar to quercetin and kaempferol, myricetin has hydroxyl groups on the 3', 4', 5', 3, 5 and 7 positions of the flavan nucleus with an unsaturated C2-C3 bond, and a ketone group located at position 4 of the C ring of the flavan nucleus, as shown in Fig. 1.6.

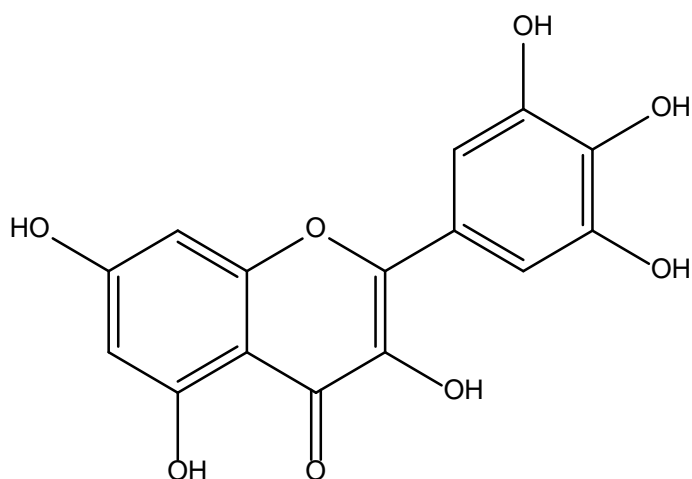


Fig. 1.6 Structure of myricetin.

1.11 Bioavailability of flavonoids

Given the ubiquity of flavonoids in plants, flavonoids form a universal non-nutritious element of the human diet. They are particularly concentrated in luxury products such as red wine, chocolate and tea. The flavonoid content can be as high as 21.6 μM in chocolate and 14.3 μM in certain varieties of red wine (Pimentel *et al*, 2008). Consumption of flavonoids by humans varies for a number of geographical, cultural and economic reasons. The consumption of a wide variety of fruits and vegetables will be the leading contributor to dietary flavonoid intake. Using Japan as an example, daily consumption of quercetin specifically was estimated to be 16.2 mg/day based the consumption of common foods in the Japanese diet containing quercetin, such as onions, asparagus and lettuces (Nishimuro *et al*, 2015). Although based in Japan, these estimates could be applied to a balanced western diet, given that the majority of foods used to create the estimate are widely available. Furthermore, the estimate produced by Nishimuro *et al* (2015) does not take into account the consumption of wine. In the west the consumption of onions is the biggest contributor to flavonol (quercetin and kaempferol) intake, containing approximately 120-160 mg/100 g (Peluso and Palmery, 2015). Average dietary consumption of kaempferol is slightly lower, and ranges from 2 – 11 mg/day (Calderón-Montaña *et al*, 2011). Dietary

intake of myricetin, principally from tea consumption, has been found to be 1.4 mg/day (Geybels *et al*, 2012).

Despite the ubiquitous nature of flavonoid in the human diet, the bioavailability is further dependent on the absorption and metabolism of the flavonoids. Firstly the flavonoid is absorbed through the small intestine. Flavonoids from the diet usually possess a saccharide group, making them a glycoside. These must be first deglycosylated prior to absorption into the blood. This reaction is catalysed intracellularly by the enzyme β -glucosidase. The loss of the sugar moiety increases the hydrophobicity of the flavonoid, allowing them to pass through the epithelial cells. However, in some cases, glycosylated flavonoids are actively transported through the cell by glucose transporter proteins (Viskupičová *et al*, 2008). Flavonoids, specifically quercetin and its metabolites, are known to enter cells by both passive diffusion and active transport via organic anion transporters (Glaeser *et al*, 2014). Although because of the lack of specific transporters the majority of flavonoid enters cells passively, with hydrophobic flavonoids more able to cross cellular membranes (Barnes *et al*, 2011). A further regulator of flavonoid absorption is intestinal efflux, where various membrane transport proteins transport flavonoid back into the intestinal lumen. Quercetin specifically is thought to be transported out of the intestinal epithelium by multidrug-resistance protein 2 (MRP 2), the mechanism of intestinal absorption and metabolism is shown in Fig. 1.7. Quercetin is transported very efficiently back into the intestinal lumen, and therefore intestinal efflux is a major factor in the bioavailability of quercetin for the rest of the organs in the body (Viskupičová *et al*, 2008).

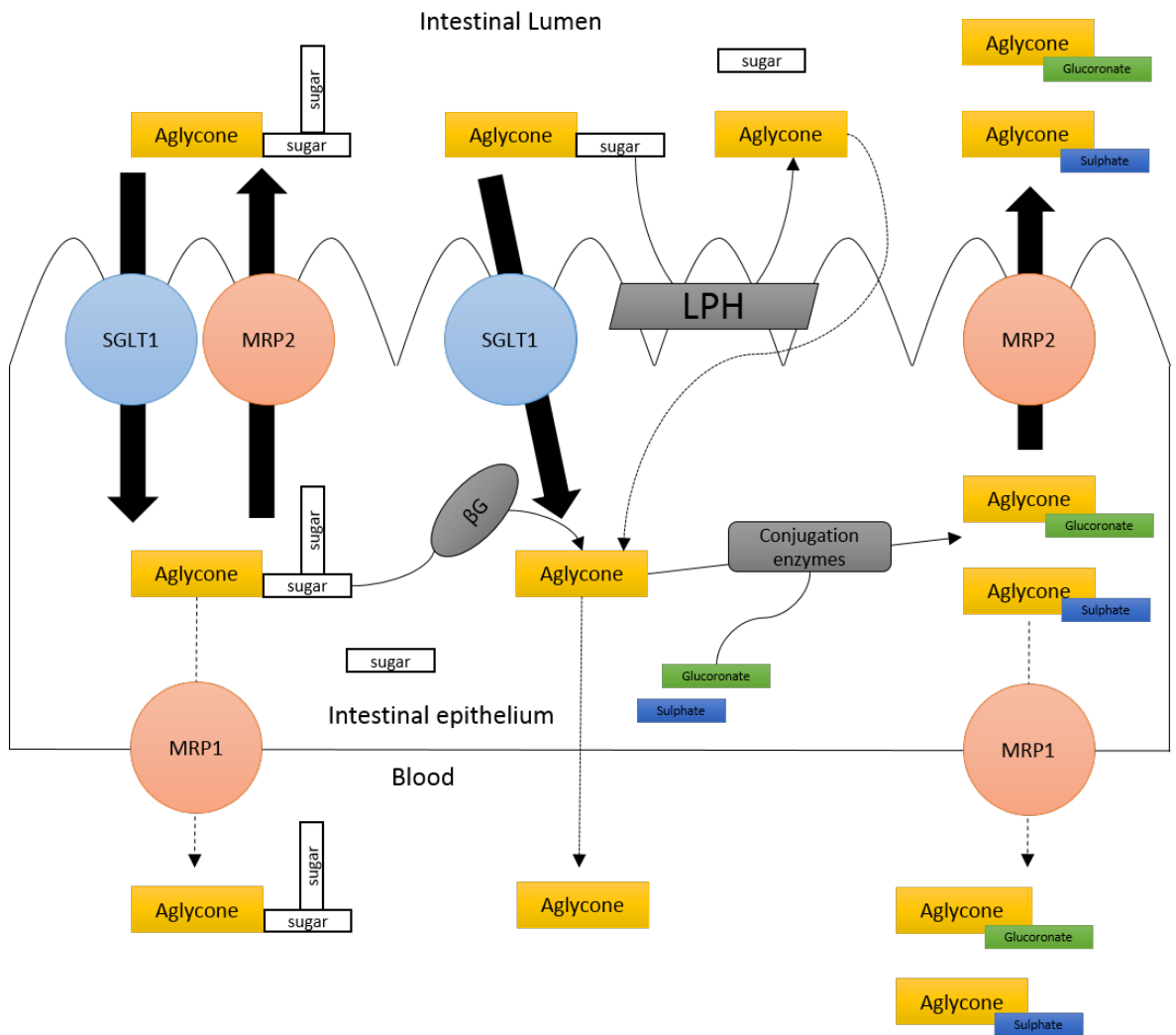


Fig 1.7 Mechanism of Intestinal flavonoid absorption and metabolism. The transport of the flavonoid is facilitated by MRP1 & 2 (Multidrug resistance protein) and SGLT (Sodium-dependent glucose transporter). βG; β-Glucosidase, LPH; lactase phloridzin hydrolase (Adapted from Kanazawa, 2011).

In a study using radiolabelled quercetin, after ingestion the absolute availability of quercetin in humans was estimated at 44.8 %, although this was likely enhanced by the experimental presence of ethanol (Guo and Bruno, 2015). In a separate study participants ingested 10 mg quercetin aglycone in a grape drink, and the average maximum plasma concentration was shown to be 0.16 μM , approximately 1.4 % of the ingested flavonoid. When sourced from onions (containing approximately 100 mg quercetin) the maximum plasma concentration of quercetin was approximately 6.4 % of the dose (Guo and Bruno, 2015). In a similar study using onions as a dietary source, a peak concentration of quercetin and its metabolites was observed to be 7.6 μM after a meal of onions containing the equivalent of 100 mg quercetin (Labbé *et al*, 2009). After administration in a liquid medium a maximum plasma concentration of 2.01 μM quercetin aglycone was achieved. Similarly,

when in an alcoholic medium a maximum plasma concentration of 3.44 μM quercetin aglycone was achieved (Guo and Bruno, 2015). These observations demonstrate that the form in which the quercetin is injected has a dramatic effect on the maximal plasma concentrations observed, and with the observation that ethanol increases the maximal plasma concentration, wine consumption could contribute to a higher flavonoid plasma concentration achieved (Guo and Bruno, 2015). Furthermore, the half-lives of quercetin metabolites, which range from 11 – 28 h, favours the theory that plasma concentrations of flavonoids could increase due to accumulation with repeated intakes, as would be the case with dietary intake (Labbé *et al*, 2009).

Once absorbed into the blood the flavonoids are transported to the liver via the portal vein to undergo extensive metabolism before they enter the systemic blood stream. In the liver the flavonoid can undergo a number of different metabolic changes, the most common of which are hydrolysis, oxidation, reduction or conjugation with one of several possible moieties; either sulphate, glucuronate or *O*-methyl groups. Of these possibilities conjugation with glucuronic acid or sulphate groups are reported to be the most common. As well as taking place in the liver, glucuronidation of the flavonoids can also occur in the small intestine. This reaction is catalysed uridine-5'-diphosphate glucuronosyltransferases (UGTs) and is very efficient.

A small proportion of the dietary flavonoids are not absorbed in the small intestine, and instead move on to the colon. In the colon flavonoids can be extensively metabolised by the native microflora (Serra *et al*, 2012).

Once arrived at the target cells via the blood and diffused into the target cells flavonoids can then be subjected to further intracellular metabolism that converts the metabolite forms of the flavonoid back to the native aglycone. The enzyme β -Glucuronidase, located in the endoplasmic reticulum and lysosomes of cells, has been demonstrated to have a key role in the metabolism of flavonoids. Specifically it has been demonstrated to free the aglycone form of luteolin from its glucuronidated metabolite (Shimoi *et al*, 2001).

Intracellular accumulation of quercetin and 3'-*O*-methylquercetin has been demonstrated previously in mitotic H9c2 cells. Peak intracellular quercetin levels were measured at ≈ 2 nmol/mg protein, which was achieved in mitotic H9c2 cells after 1 h of exposure to 30 μM

quercetin (Angeloni *et al*, 2007). Interestingly, ≈ 1 nmol/mg protein of 3'-O-methylquercetin was observed after 24 h exposure to 30 μ M 3'-O-methylquercetin (Angeloni *et al*, 2007). These findings highlight the potential for cell in general, and H9c2 cells in particular, to accumulate flavonoids and their metabolites during constant exposure. This accumulation may play an important role in the protective effect of flavonoids *in vivo*, as relatively high concentrations of flavonoid may be present intracellularly due to the constant exposure of cells to flavonoids from the diet.

Once absorbed the flavonoids will eventually undergo excretion. Quercetin is mainly eliminated from the body via the bile in the form of its two major metabolites, 3'-O-methylquercetin (3',4',5,7-tetrahydroxy-3-methoxyflavone) and quercetin-3-glucuronide, the structures of which are shown below in Fig. 1.8 (Viskupičová *et al*, 2008).

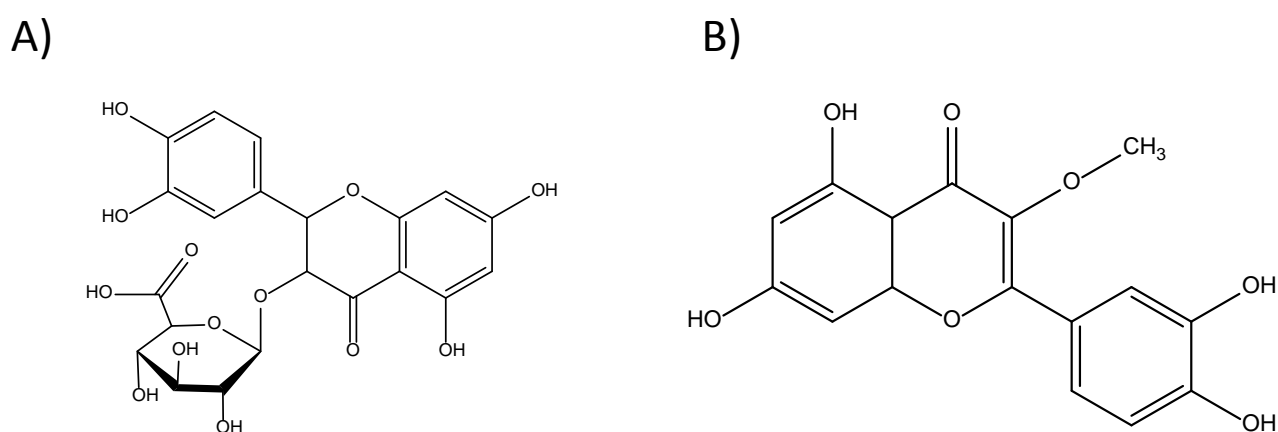


Fig 1.8 Major quercetin metabolite structures. A) quercetin-3-glucuronide B) 3'-O-methylquercetin.

1.12 Pro-oxidant intracellular metabolism of quercetin

The structure of quercetin is an indicator of its antioxidant ability, which is believed to contribute to its cardioprotective effect in addition to modulation of cell signalling cascades. Conversely the intracellular metabolism of quercetin into the prooxidants quinone and semiquinone could potentially increase intracellular ROS and lead to adverse effects (Metodiewa *et al*, 1999). The generation of intracellular ROS by oxidative degradation of quercetin and quinone reduction has been previously identified as concentration dependent.

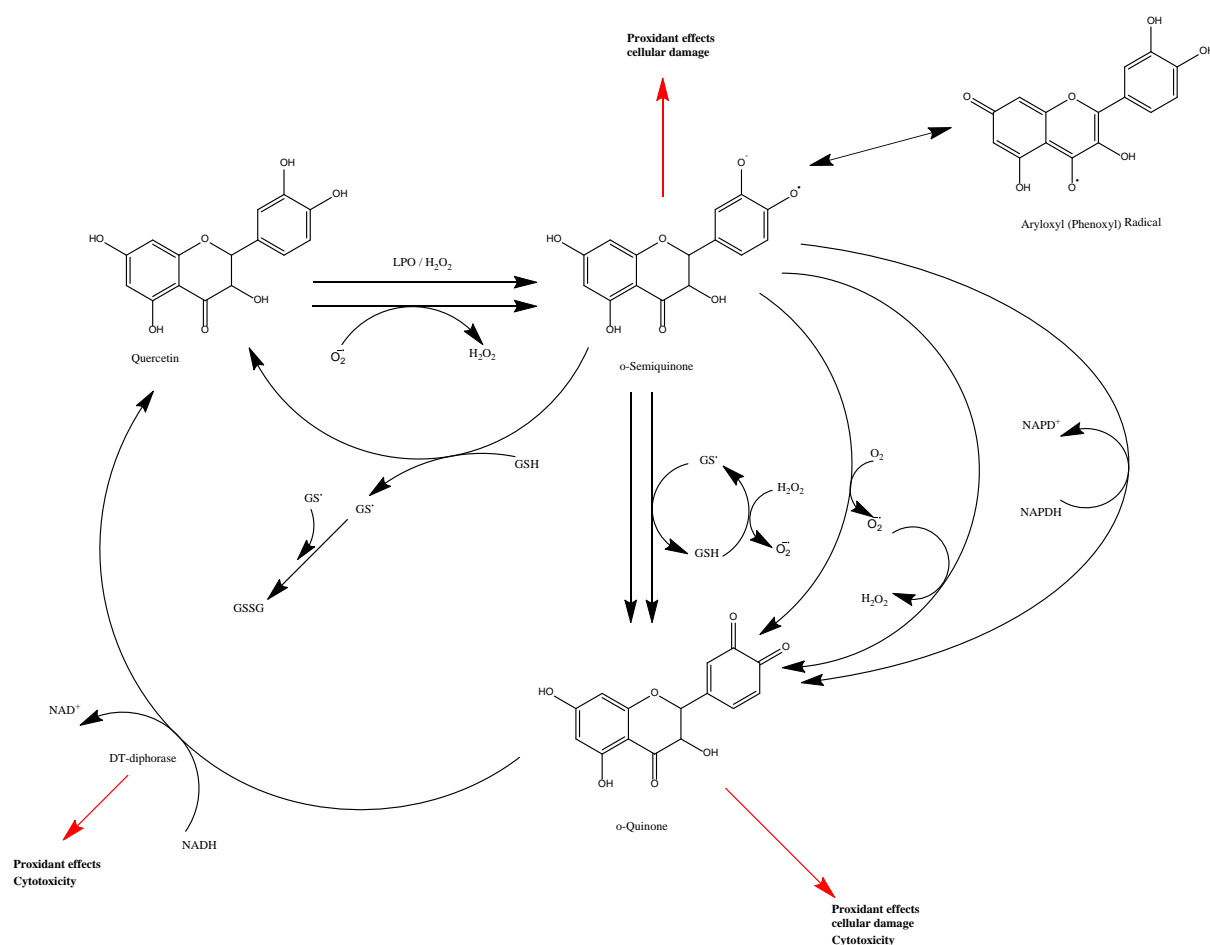


Fig. 1.9 Intracellular metabolism of quercetin leading to prooxidant products. A summary of the intracellular ROS scavenging activity resulting in the formation of semiquinone and quinone from quercetin, stoichiometry not shown. (abbreviations: GSH; reduced Glutathione. LPO; Lactic peroxidase. DT-diphorase; NAD(P)H quinone oxidoreductase.) (Metodiewa *et al*, 1999).

As shown in Fig. 1.9, quercetin is converted to *o*-semiquinone in the presence of H₂O₂ and catalysed by LPO. *o*-semiquinone, containing oxygen radicals can then go on to cause potentially cytotoxic activities. Some *o*-semiquinone is converted back into the parent molecule quercetin, the remainder going on to be converted into *o*-quinone. In the presence of oxygen, *o*-semiquinone can also produce O₂^{•-} superoxide and *o*-quinone. The O₂^{•-} superoxide can then go on to produce more *o*-semiquinone from quercetin with an additional H₂O₂ production. Furthermore the O₂^{•-} superoxide can react with *o*-semiquinone to form *o*-quinone and H₂O₂. *o*-semiquinone can also form *o*-quinone with the biological reducing agent GSH, form during the reduction reaction from GS[•]. This GSH can go on to form quercetin from *o*-semiquinone resulting in GS[•] in a reversible reaction. In addition, GSH can go on to form GS[•] and H₂O₂ in the presence of H⁺ ions (Metodiewa *et al*, 1999). These intracellular reactions illustrate that in the presence of oxygen, quercetin can give rise to the prooxidant products *o*-semiquinone and *o*-quinone. The major quercetin metabolite 3'-*O*-methyl quercetin can also undergo intracellular demethylation to form quercetin, which then goes on to participate in the scavenging of ROS. Eventually, GSH conjugates with *o*-quinone to form 2'-glutathionyl quercetin which, along with other unknown potentially prooxidant intermediates, is exported from the cell and excreted (Spencer *et al*, 2003).

1.13 MAPK proteins

The MAPK cell signalling pathway is involved in most aspects of cell biology, and is essential for proper cell function. It is a family that encompasses important proteins such as extracellular signal-regulated protein kinase 1 & 2 (ERK1/2), p38 MAPK and c-Jun N-terminal kinase (JNK). It is well associated with essential cell functions such as adhesion, differentiation, proliferation and cell survival.

ERK1 and ERK2 are a pair of proteins that share 84 % protein sequence as well as most, if not all functions, thus it is common that they are referred to as ERK1/2. They are a ubiquitously expressed non-receptor protein, integral to the MAPK signalling cascade. ERK1/2 is activated by a signalling cascade that starts with H-Ras, K-Ras and N-Ras, which are produced in response to mitogenic stimuli. H-Ras, K-Ras and N-Ras then convert Ras-

GDP to Ras-GTP. Ras-GTP then goes on to activate the Raf kinase family of proteins (A-, B- and C-Raf), which specifically catalyse the phosphorylation of MEK1 and MEK2. MEK1 and MEK2 phosphorylate the tyrosine and threonine in ERK1/2, which activates ERK1/2. The phosphorylated ERK1/2 can then act upon a number of its 175 cytoplasmic and nuclear substrates (Roskoski, 2012). Quercetin has been shown to be able to bind to the activation loop of MEK1 at pharmacologically relevant concentrations (1-2 μ M).

Studies on the cardioprotective mechanisms of flavonoids often monitor the phosphorylation of ERK1/2 as it is known to be a pro-survival cell signalling molecule. Previous studies using mitotic H9c2 cardiomyoblast cells have shown that the modulation of MAPK pathways and PI3K/Akt pathways by quercetin has a cardioprotective effect against oxidative stress (Angeloni *et al*, 2007).

The MAPK, specifically the Raf-1/MEK/ERK1/2, pathway has been shown to be associated with proliferation of cardiac smooth muscle cells through mitogens such as 5-HT and platelet derived growth factor, and is also involved in cardiac injury. Hypoxia is known to cause phosphorylation of ERK1/2 in both rat and human cell lines (Morecroft *et al*, 2011). Furthermore, unopposed activation of ERK1/2 is a major contributing factor to hereditary pulmonary arterial hypertension. The activation of the Raf-1/MEK/ERK1/2 pathway is proposed to be linked with the activation of the PKC ζ , particularly during hypoxia.

The Raf-1/MEK/ERK1/2 pathway is highly regulated, particularly during hypoxia. The enzyme PEBP-1 (Phosphatidylethanolamine-binding protein 1) also known as RKIP (Raf kinase inhibitor protein) has been identified as one of the regulatory mechanisms of the Raf-1/MEK/ERK1/2 pathway during hypoxia (Morecroft *et al*, 2011). The unregulated phosphorylation of ERK1/2 during hypoxia, in PEBP-1 knockout mice, was shown to cause more drastic symptoms of pulmonary arterial hypertension, suggesting that inhibition of ERK1/2 is cardioprotective (Morecroft *et al*, 2011). Both Raf and MEK protein kinases are specific inhibition targets of quercetin, and has been shown to be a more efficient inhibitor of MEK than the specific inhibitor PD098059 (Russo *et al*, 2012). It is proposed that quercetin forms a hydrogen bond with ser²¹² in the MEK backbone, which causes an inactive form of the protein to stabilise. The inhibition of MEK would consequently lead to

decreased phosphorylation of ERK1/2, p38 MAPK and JNK, causing a cardioprotective effect (Russo *et al*, 2012). Pharmacologically relevant (2 μ M) concentrations of quercetin are also known to be a potent inhibitor of 16 other kinase family enzymes involved in the cell cycle, and is able to cause arrest in the G2/M or G1 phase of the cell cycle (Russo *et al*, 2012).

JNK, also known as stress-activated protein kinase (SAPK), is a regulator of several cellular processes including apoptosis. Its pro-apoptotic action is thought to be mediated through the regulation of c-Jun and activated protein 1 (AP1). Similarly p38 MAPK is known to be involved in apoptosis. Activation of p38 MAPK occurs in response to a number of cellular stresses (Mansuri *et al*, 2014). A summary of the MAPK pathway, with particular regard to ERK1/2, JNK and p38 MAPK is shown below in Fig. 1.10.

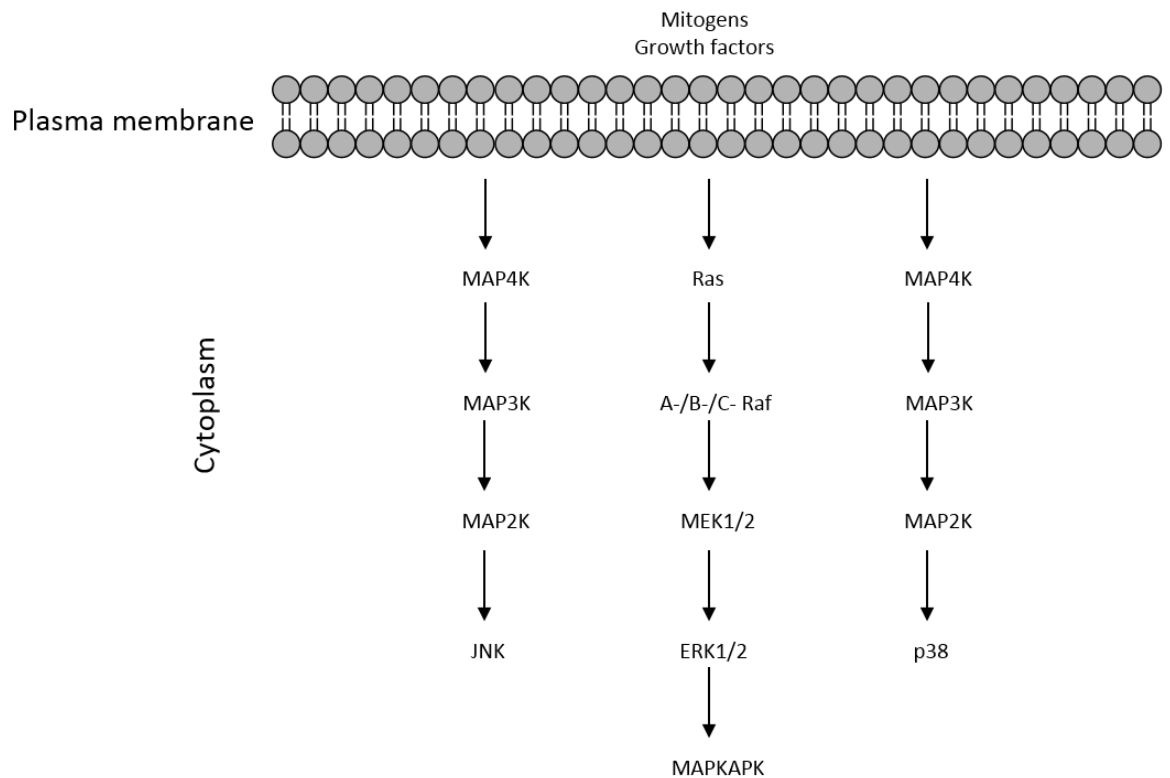


Fig. 1.10 ERK1/2, JNK and p38 MAPK cascades. MEK1/2 leads to the activation of JNK, ERK1/2 and p38 MAPK, which catalyses the phosphorylation of proteins in the cytoplasm and nuclear transcription factors (adapted from Roskoski, 2012).

1.14 PI3K/Akt pathway

The PI3K/Akt pathway is a strong intracellular pro-survival system, that is known to be modulated by flavonoids and their metabolites (Mansuri *et al*, 2014). The pathway regulates a variety of cell functions including survival, division, differentiation and transformation. Phosphoinositol 3-kinases (PI3Ks) catalyse the reaction that transfers the γ -phosphate group from ATP to the hydroxyl group at the 3' position of three substrates; phosphatidylinositol (PI), phosphatidylinositol-4-phosphate (PI4P) and phosphatidylinositol-4,5-bisphosphate (PIP₂). PI3K signalling modulates many cellular processes, such as cell growth, differentiation, motility, gluconeogenesis and glycolysis.

PI3Ks can be grouped into 3 classes. Class I PI3Ks catalyse PIP₂ to PIP₃ (Phosphatidylinositol (3,4,5)-trisphosphate), and can be further divided based on their activation pathway. The conversion of PIP₂ to PIP₃ is regulated by the lipid phosphatase PTEN (Phosphatase and tensin homolog) (Mendoza *et al*, 2011). Class 1A are activated through tyrosine kinases (RTKs) and class 1B through G protein-coupled receptors (GPCRs) Class II PI3ks regulate membrane trafficking through clathrin-coated vesicles, and Class III PI3Ks produce PI(3)P and have a role in autophagy.

Structurally, class I PI3Ks consist of two subunits, regulatory and catalytic. The regulatory subunit binds to intracellular RTK phosphotyrosine residues or adaptor proteins, which leads to the relieving of intramolecular inhibition of the catalytic subunit and localises the catalytic subunit near the plasma membrane and its PIP₂ substrate. PI3K can also be stimulated by Ras which binds directly to the catalytic subunit (Mendoza *et al*, 2011). The RTK signal is propagated by PI3K products binding to specific regions of downstream target proteins such as FYVE zinc-finger, pleckstrin homology and phox-homology domains (Courtney *et al*, 2010). A major target of PI3K is AKT, also known as PKB, the complete activation of which requires dual phosphorylation by PDK1 (3-phosphoinositide dependent protein kinase-1) and mTORC2 (mechanistic target of rapamycin complex 2) (Mendoza *et al*, 2011).

It is a false to assume that cell signalling pathways work in isolation, and there is significant cross-talk between pathways and many share common core signalling molecules, which can lead to inhibition of multiple pathways by one target (Rozenfurt *et al*, 2010).

Cross-talk between cell signalling pathways can be summarised by four types of interactions: 1) negative feedback loop, where a downstream molecule of a pathway inhibits the activation of an upstream molecule from the same signalling pathway; 2) cross-inhibition, where a core molecule of a pathway inhibits a core member of a different pathway; 3) cross-activation, where a core member of a pathway upregulates an upstream molecule of another pathway; 4) pathway convergence, two or more signalling pathways directly act on the same protein (Mendoza *et al*, 2011). Furthermore, pathways can exhibit all four or any combination of these interactions.

There is a great deal of cross-talk between the MAPK/ERK and PI3K/AKT pathways. Firstly, both pathways can be activated through RTK or GPCRs, therefore cross-talk begins at the receptor level. Cross-inhibition between the MAPK/ERK and PI3K/AKT pathways has been observed when MAPK/ERK is inhibited, furthermore AKT and Ras can cross-inhibit when AKT is stimulated by IGF-1 (Insulin-like growth factor 1) (Mendoza *et al*, 2011). MAPK/ERK can activate the PI3K pathway through several means. Ras-GTP can directly bind and activate PI3K, and active ERK can phosphorylate TSC2 (Tuberous Sclerosis Complex 2) and promote the activity of mTORC1 (Mendoza *et al*, 2011). Several core kinase components of the MAPK/ERK and PI3K/AKT pathway affect the same downstream targets, including FOXO3A (Forkhead box O3), BAD (Bcl-2-associated death promoter), c-Myc and GSK3 (Glycogen synthase kinase 3) (Mendoza *et al*, 2011).

Interestingly several pro-apoptotic and anti-apoptotic transcription factors can be activated by Akt/PKB. Flavonoids are known modulators of the PI3K/Akt pathway. Kaempferol has been demonstrated to protect MC3T3-E1 cells from toxicity by modulation of the PI3K/Akt pathway (Choi, 2011). Similarly myricetin induces cell survival via the PI3K/Akt pathway, after H₂O₂ induced cell death with 30 µM myricetin treatment (Kyoung *et al*, 2010).

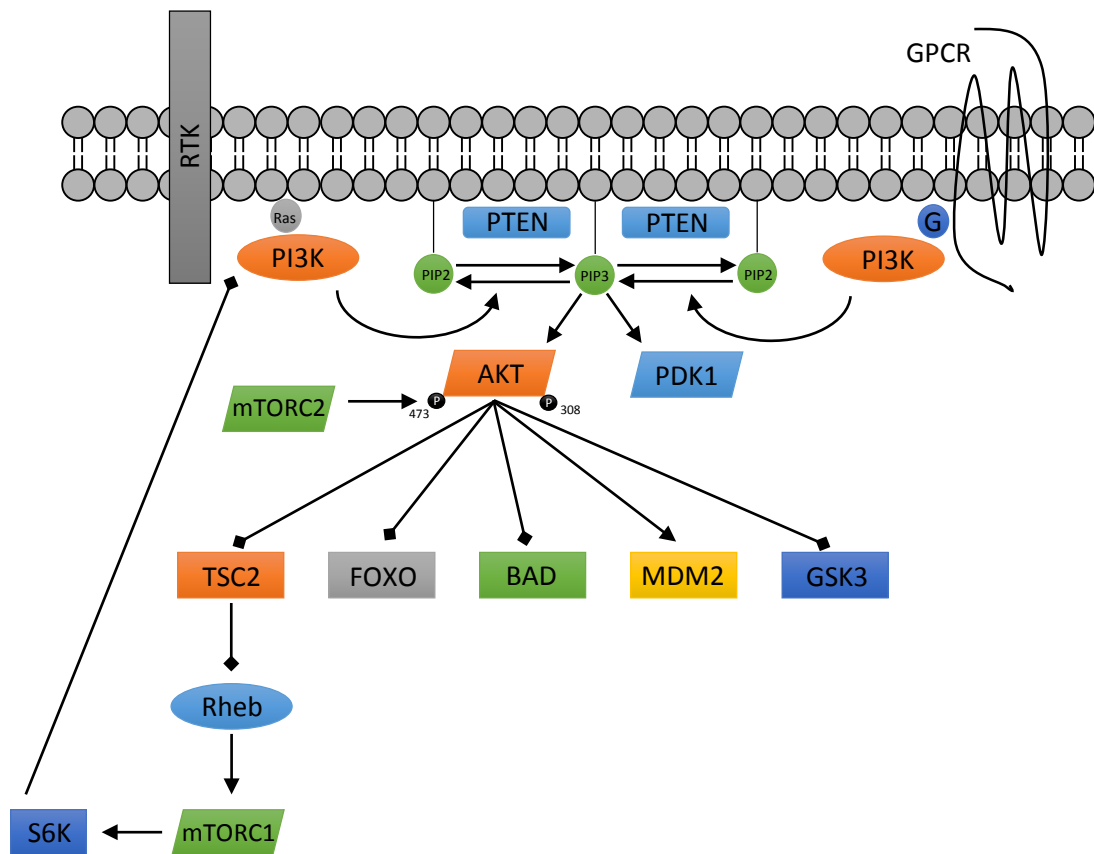


Fig. 1.11 The PI3K signalling cascade. The cascade has many effects on cell growth, differentiation, survival and metabolic activity, and can be activated by both RTKs and GPCRs. Arrows indicate activation, squared arrow heads represent inhibition. Abbreviations: RTK, receptor tyrosine kinase; GPCR, G-protein coupled receptor; P, phosphate; G, G-protein; PTEN, phosphatase and tensin homolog; PDK1, Pyruvate dehydrogenase lipoamide kinase isozyme 1. (Adapated from Courtney *et al*, 2010).

1.15 H9c2 cells

H9c2 is a rat embryonic cardiomyoblast-derived cell line (Kimes and Brandt, 1976). H9c2 cells have been used in a large number of studies as a model system for the characterisation of cardioprotective mechanisms of flavonoids (Gutiérrez-Venegas *et al*, 2010; Angeloni *et al*, 2012; Angeloni *et al*, 2007; Sun *et al*, 2012; Kim *et al*, 2010; Mojzisoová *et al*, 2009). These studies have all used the H9c2 cell line in its mitotic form which, although electrophysiologically and biochemically similar to cardiomyocytes, are not fully differentiated (Hescheler *et al*, 1991). In their mitotic form H9c2 cells lack some properties of cardiomyocytes, they do not fuse to form multinucleated myotubes nor do they express gap junctions (Hescheler *et al*, 1991). The loss of myotube formation is attributed to dedifferentiation due to increased passage number and time spent in cell culture. It is

notable therefore that this present study is currently unique in the use of differentiated H9c2 cells to investigate the cardioprotective effects of flavonoids.

1.16 H9c2 cell differentiation

H9c2 cells can be made to differentiate into a more cardiomyocyte-like phenotype in culture, by supplementation with *all-trans* retinoic acid (RA) in a medium with decreased (1 %) serum content (Ménard *et al*, 1999). The final differentiated form of H9c2 consists of fusing and forming thin, elongated, multinucleated myotubes. The differentiated cells also form a more organised linear structure, with well organised actin filaments. This final differentiated form of H9c2 cells is obtained by chronic treatment of the cells with RA, meaning the cells are exposed to fresh RA every 48 hours (Ménard *et al*, 1999). The differentiation of H9c2 cardiomyoblasts into the more cardiomyocyte-like phenotype is regulated heavily by PI3K (Kim *et al*, 1999). It has been demonstrated that external signals such as insulin, insulin growth factor 1 (IGF-1), epidermal growth factor *etc.* activate PI3K signalling cascades via p85. This activation of PI3K leads to the downstream activation of PKB/Akt, which is activated by binding with the PI3K products phosphatidylinositol-3,4-bisphosphate (PtdIns(3,4)P₂), or phosphatidylinositol-3,4,5-trisphosphate (PtdIns(3,4,5)P₃). This signal is then further propagated by phosphorylation of serine/ threonine residues of other proteins (Kim *et al*, 1999). pPKC δ has also been shown to be involved in the differentiation of H9c2 cells, mostly by its interaction with SC35 (Zara *et al*, 2010). Interestingly it has also been reported that ERK1/2 is not involved in the differentiation of H9c2 cells, despite it being a downstream signal of PI3K (Kim *et al*, 1999). It is a combination of these crucial events that result in the downstream transcription of genetic components that lead to the changes in morphology relating to the differentiation into the cardiomyocyte-like phenotype. The similitude of the cardiomyocyte-like differentiated H9c2 cell to *in vivo* cardiomyocytes will provide for a better model for the study of flavonoid dependent cardioprotection compared to previous studies using the mitotic form of the cell.

Some of the characteristics of differentiated H9c2 cells compared to the mitotic form have been described in various studies, mostly focussing on differences in cytoskeletal contractile proteins and morphological changes, other studies have described the

metabolic differences between differentiated and mitotic H9c2 cells (Pereira *et al*, 2011; Dangel *et al*, 1996; Branco *et al*, 2013). Table 1.12 provides a summary of the main differences observed between a number of studies.

Mitotic H9c2 cells	Differentiated H9c2 cells
Polygonal/fibroblast morphology Mono-nucleated Multiple nucleoli Dense cytoskeletal network Non-expression of gap junctions Prominent rough endoplasmic reticulum Surface microvilli Striated muscle-like G protein expression Favour "Warburg effect" like glycolysis	Multiple nuclei Myotube formation Cardiac troponin expression Parallel cellular arrangement Cardiac L-type voltage-dependent calcium channel upregulation Troponin-T expression Myosin expression T-tubule expression Z-disc development Increased mitochondrial mass Increased ATP synthesis Increased cytosolic calcium Decreased β 1-AR expression Increased oxygen consumption

Table 1.12 Summary of the observed differences between differentiated and mitotic H9c2 cells. Differentiated H9c2 cells express cardiac muscle-specific cytoskeletal features, as well as having different metabolic activity and differing expression of certain receptors (Pereira *et al*, 2011; Dangel *et al*, 1996; Branco *et al*, 2013).

1.17 Aims of this project

The aims of the present study can be surmised as four main aims:

- To differentiate H9c2 cardiomyoblasts into a more cardiomyocyte-like phenotype, and characterise this phenotype using immunocytochemistry, western blotting and MALDI-TOF MS/MS.
- To investigate the cytoprotective mechanisms of quercetin, myricetin, kaempferol, quercetin-3-glucuronide and 3'-O-methylquercetin against oxidative stress caused by H₂O₂ exposure or hypoxic incubation.
- To investigate the cytotoxic activity of quercetin, myricetin, kaempferol, quercetin-3-glucuronide and 3'-O-methylquercetin on mitotic, differentiated and differentiating H9c2 cells.
- Use MALDI-TOF MS/MS to investigate proteomically the mechanism of flavonoid-mediated cytoprotection and flavonoid exposure to differentiated H9c2 cardiomyocytes.

Chapter 2:

Materials and

Methods

2.0 Methods

2.1 Cell Culture

Rat embryonic cardiomyoblast-derived H9c2 cells were obtained from the European Collection of Animal Cell Cultures (Porton Down, Salisbury, UK). Mitotic cells were cultured in 25 cm² cell culture flasks in Dulbecco's modified Eagle's Medium (DMEM) supplemented with 10 % (v/v) Foetal Bovine Serum (FBS), 2 mM L-glutamine, penicillin (100 U/ml) and Streptomycin (100 µg/ml). Cell cultures were maintained in a humidified incubator at 37°C with a controlled atmosphere of 95 % air/5 % CO₂ until 70-80 % confluence was observed under light microscopy. Cells were sub-cultured first by detaching using trypsin (0.05 % w/v)/EDTA (0.02 % w/v) in sterile phosphate buffered saline (PBS). Once detached cells were sub-cultured using a 1:5 split ratio.

i) H9c2 cell differentiation

Differentiation of H9c2 cells was induced by culturing the cells for 7 days in the continued presence of 10 nM *all-trans* retinoic acid in DMEM growth medium supplemented with 1 % (v/v) FBS. The differentiation medium was replaced every 48 h. The cells were observed to confirm differentiation to a cardiomyocyte-like phenotype by the formation of multinucleated elongated myotubes. The differentiation was further confirmed with western blotting and immunocytochemistry monitoring the expression of cardiac specific troponin T.

2.2 Immunocytochemistry

The expression of cardiac specific troponin T was monitored using immunocytochemistry. H9c2 cells were seeded into an 8 well chamber slide (BD Falcon™ CultureSlide) at a density of 15,000 cells/well and cultured in fully supplemented DMEM growth medium for 24 h. The growth medium was aspirated and replaced with differentiation medium and cultured for 7 days as described above. The differentiation medium was then aspirated and adherent differentiated H9c2 cells were washed three times with 37°C PBS for 5 min each wash. Cells were then fixed using 3.7 % (v/v) paraformaldehyde (Sigma-Aldrich, UK) in PBS for 15 min at room temperature without agitation, then washed in PBS three times for 5 min each time. The cellular location of the troponin T being inside the cell, it is then necessary to

permeabilise the fixed cells. Permeabilisation of the cells was performed by incubation with 0.1% (v/v) Triton X-100 in PBS for 15 min at room temperature without agitation, followed by three washes with PBS for 5 min each wash. Fixed cells were then incubated in 3% (w/v) bovine serum albumin (BSA) in PBS for 2 h at room temperature to prevent non-specific binding of antibodies. After blocking, cells were then incubated overnight at 4°C in a humidified chamber with anti-cardiac specific troponin T primary antibody (1:1000) in 3% (w/v) BSA in PBS. The primary antibody was then removed and the cells washed in three times in PBS for 5 min each wash. Cells were then incubated for 2 h at 37°C in a humidified chamber with the secondary anti-mouse antibody (1:1000; Abcam, UK) which possesses a FITC (Fluorescein isothiocyanate) fluorescent dye conjugate in 3% (w/v) BSA in PBS. The culture slides were then washed three times in PBS for 5 min and air dried. Cell culture slides were then mounted using Vectashield® mounting medium (Vector laboratories Ltd, Peterborough, UK) containing DAPI (4',6-diamidino-2-phenylindole) nuclear counterstain to allow for nuclear visualisation. The slides were cover-slipped and sealed using clear, colourless nail varnish and visualised (FITC: EX₄₉₃/EM₅₂₈; DAPI: EX₃₆₀/EM₄₆₀) using an Olympus DP71 fluorescent microscope system, equipped with an argon/krypton laser.

2.3 Oxidative stress and Hypoxia-induced cell death

To induce oxidative stress, fully differentiated or mitotic H9c2 cells were incubated in fully supplemented DMEM growth medium containing 600 µM hydrogen peroxide (H₂O₂) for 2 h at 37°C. Alternatively, hypoxic cell death was induced by incubating fully differentiated H9c2 cells in un-supplemented DMEM growth medium (containing no FBS or L-Glutamine) in a hypoxic incubator set at the following conditions; O₂ 0.5 %, CO₂ 5.0 %, 37 °C, for 24 h. To assess the cytoprotective effects of the flavonoids or flavonoid metabolite, H9c2 cells were pre-treated with quercetin (100 µM, 30 µM, 10 µM, 3 µM or 1 µM) for 24 h prior to hypoxia or H₂O₂ treatment in fully supplemented DMEM growth medium, which was removed and replaced with the appropriate assay medium after pre-treatment.

Where appropriate cell were also pre-treated for 30 min with one of the following protein kinase inhibitors; LY 294002 (30 µM; PI3K inhibitor), Wortmannin (100 nM; PI3K inhibitor), PD 98059 (50 µM; MEK1/2 inhibitor), SB 203580 (30 µM; p38 MAPK inhibitor) or SP 600125 (10 µM; JNK1/2 inhibitor) prior to the quercetin pre-treatments, with the continued

presence of the inhibitors during the quercetin pre-treatment. Cells were also treated with the inhibitors for 24 h followed by H₂O₂ treatment and viability assessment.

2.4 Cell viability assays

i) MTT assay

The viability of the H9c2 cells in culture was assessed using the MTT (thiazolyl blue tetrazolium bromide, Sigma-Aldrich) assay. Undifferentiated H9c2 cells were seeded at a density of 15,000 cells per well in 24-well cell culture plates (Sarstedt, Leicester, UK) and incubated overnight at 37°C in fully supplemented DMEM growth medium. Cells were then induced to differentiate for 7 days using the H9c2 cell differentiation method described above. The cells were then treated according to the protocol of the particular experiment being undertaken. Cells were incubated for 1 h in 0.5 µg/ml MTT solution in DMEM (fully supplemented) at 37°C. The medium in each well was aspirated, taking care to leave the blue, insoluble formazan crystals at the bottom of the well intact. The formazan crystals were dissolved in 500 µl of DMSO (dimethyl sulphoxide) and the plate was agitated to ensure sufficient dissolution of the crystals. After which, 200 µl of the resulting solution was transferred into a 96-well plate (Sarstedt, Leicester, UK) and the absorbance of the solutions was read at 570 nm using a standard 96-well plate reader. The absorbance of the blank was subtracted from each assay absorbance reading, the viability of the cells is then directly proportional to the magnitude of the MTT reduction determined by the absorbance at 570 nm.

ii) Lactate dehydrogenase assay

Lactate dehydrogenase (LDH) leakage was assessed using the CytoTox 96[®] non-radioactive cytotoxic assay kit (Promega, Southampton, UK). This kit allowed LDH release to be measured via a coupled chemical reaction that leads to the production of a coloured formazan product. Firstly, LDH released from the cells catalyses the formation of pyruvate and NADH from lactate and NAD⁺. The secondary reaction is catalysed by the dehydrogenase enzyme diaphorase (present in the substrate mix in the kit), and involves the formation of NAD⁺ and a red formazan product from NADH and a tetrazolium salt. LDH release is proportional to the red formazan product. H9c2 cells were seeded into 96-well

plates at a density of 5000 cells/well, and cultured for 24 h in fully supplemented DMEM growth medium. Cells were then differentiated for 7 days in differentiation medium as described above. Incubations were performed in 200 μ l of the appropriate medium. Cellular debris was compacted to the bottom of wells by centrifugation (5 min, 300g) and fifty μ l of supernatant was transferred to a non-sterile 96-well plate. 50 μ l reconstituted assay buffer (10 ml assay buffer added to one bottle of substrate mix, in kit) was added to each well, the plates were then incubated in the dark for 30 min at room temperature with gentle agitation. The reaction was then terminated using 50 μ l of assay stop solution (1 M acetic acid, in the kit). Change in absorbance was measured at 490 nm using a standard plate reader. LDH release was calculated as a percentage of basal LDH release acquired from an untreated control.

iii) Coomassie blue staining

Cells were stained for visualisation with light microscopy with Coomassie blue. To stain, growth medium was aspirated and the cells were washed with PBS three times. The cells were then fixed with -20 °C 90 % (v/v) methanol solution for 15 min. The fixing solution was aspirated and replaced with Coomassie blue staining solution (0.1% (w/v) Coomassie brilliant blue G, 50 % (v/v) methanol, 10 % acetic acid) and stained for 10 min. Staining solution was aspirated and stained cells were washed three times with deionised water and left to air dry.

2.5 DCFDA assay for intracellular ROS

To analyse intracellular ROS levels in differentiated H9c2 cells exposed to quercetin, the DCFDA (2',7'-dichlorofluorescein diacetate) ROS assay (Abcam, Cambridge, UK) was performed. H9c2 cells were cultured in 25 cm² cell culture flasks and differentiated for 7 days as per the H9c2 cell differentiation method. Differentiated cells were exposed to 100 μ M quercetin for 24, 48 or 72 h and detached from the growth surface using trypsin (0.05 % w/v)/EDTA (0.02 % w/v) and centrifuged for 5 min at 1000 RPM. The resulting pellet was re-suspended in 500 μ l PBS containing 5 μ M DCFDA dye and incubated for 30 min at 37°C in the dark. In the presence of ROS, DCFDA is oxidised to form the highly fluorescent 2', 7'-

dichlorodihydrofluorescein, with the amount of fluorescence being directly proportional to the levels of intracellular ROS. After incubation, the cell suspension was transferred to FACS tubes (Fisher scientific, Loughborough, UK) and the DCFDA fluorescence was measured using a Gallios™ flow cytometer (Beckman Coulter), reading at a maximum excitation and emission spectra of 495 nm and 529 nm respectively. The flow cytometer was set to count 10,000 cells in each treatment, and positive fluorescence was gated in relation to the untreated control. Results were reported as the percentage of cells showing positive fluorescence. Fluorescence data was further analysed using Kaluza Flow Cytometry Analysis (v1.2) software.

2.6 Western Blot

i) Cell lysis

Western blotting was used to monitor the expression and/or activation of cell signalling molecules. Cells were cultured in 25 cm² cell culture flasks, differentiated for 7 days as described above. Following experimentation cells were lysed using boiling 300 µl 0.5 % (w/v) sodium dodecyl sulphate (SDS) solution in Tris buffered saline (TBS; 20 mM Tris base, 150 mM NaCl). Cells were removed from the growth surface of the flasks using a scraper to ensure complete lysis. The resulting lysates were transferred to 1.5 ml Eppendorf™ tubes and boiled for 10 min. Samples could then be stored at -20 °C if required.

ii) Protein estimation

The protein content of the lysates was calculated using the Bio-Rad *DC* Protein assay (Bio-Rad laboratories, Hertfordshire, UK) method. Briefly, in a 96 well plate 5 µl samples of cell lysates were added to 25 µl of assay reagent A' (prepared as per manufacturer's instructions; 20 µl of reagent S and 1 ml of reagent A) and 200 µl assay reagent B. Samples were then incubated at room temperature in the dark under gentle agitation of 30 min. Absorbance was read at 620 nm using a standard 96 well plate reader. These absorbance readings were compared to a standard curve produced using BSA standards (Fig 2.1) to calculate the protein content of the samples.

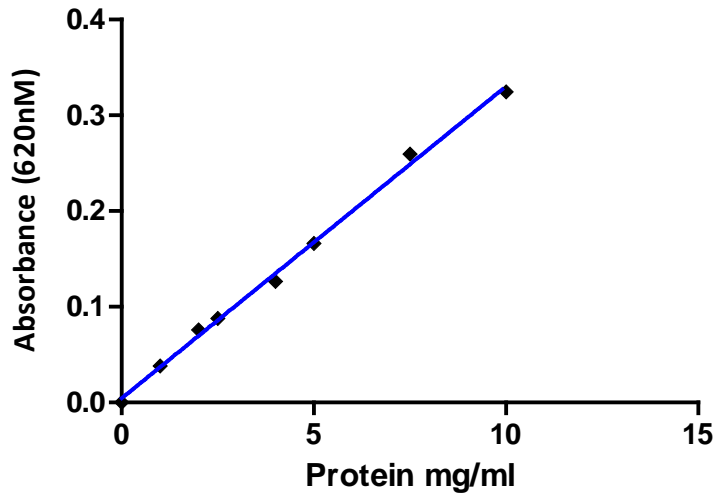


Fig 2.1 protein standard curve produced with DC Lowry method and known BSA concentrations.

iii) SDS-PAGE

75 µl of each lysate sample was suspended in 25 µl of 4x Laemmli buffer (8 % w/v SDS, 40 % (v/v) glycerol, 10 % (v/v) β-mercaptoethanol, 0.01 % (w/v) bromophenol blue, 250 mM Tris-HCl pH 6.8, in deionised water) and boiled for 10 min. 0.75 mm thickness 15 % acrylamide gels (Resolving gel; 23 % (v/v) deionised water, 50 % (v/v) ProtoGel® acrylamide mix (30 % acrylamide solution 37.5:1 ratio, Geneflow Ltd, Staffordshire, UK), 25 % (v/v) 1.5 M Tris-HCl pH 8.8, 1 % (v/v) SDS solution (10 % (w/v) Sodium dodecyl sulphate in deionised water) 1 % (v/v) APS solution (10 % (w/v) Ammonium persulfate in deionised water), 0.04 % (v/v) TEMED) were cast using a Bio-Rad Mini-Protean III system with a layer of stacking gel (Stacking gel; 68 % (v/v) deionised water, 17 % (v/v) ProtoGel® acrylamide mix, 12.5 % (v/v) 1.0 M Tris-HCl pH 6.8, 1 % (v/v) SDS solution (10 % (w/v) Sodium dodecyl sulphate in deionised water) 1 % (v/v) APS solution (10 % (w/v) Ammonium persulfate in deionised water), 0.1 % (v/v) TEMED). The buffered lysate samples containing 30 µg of protein and 5 µl of protein ladder (Precision Plus Protein™ dual standards, Bio-Rad laboratories, Hertfordshire, UK) were then loaded into the gel. Electrophoresis was then performed at 200 V for 45 min, with the gels submerged in 1x electrophoresis buffer (2.5 mM Tris, 19.2 mM glycine, 0.01 % (w/v) SDS, pH 8.3). The migration of the proteins was monitored visually by observation of the dye front movement, with additional running time added where appropriate to facilitate optimal separation. Once protein separation was achieved the gels were removed from the electrophoresis tank and from the glass casting frames. Gels were

then placed in 4 °C western blot transfer buffer (25 mM Tris, 192 mM glycine and 20% (v/v) MeOH) for 5 min.

iv) Western blot

Proteins were transferred to a nitrocellulose membranes of appropriate size using Bio-Rad Trans-Blot system. Briefly, gels were layered in the system in the following order; Sponge, filter paper, gel, nitrocellulose membrane, filter paper, sponge. Layers were clamped into western blotting cassettes and placed into a tank containing transfer buffer and a cooling block. The western blot transfer was performed at 100 V for 1 h, or alternatively at 20 V for 16 h at 4 °C. Nitrocellulose membranes were placed in Ponceau red stain (Sigma-Aldrich, UK) to visualise the protein bands and cut at the required molecular weight. Membranes were de-stained by washing in PBS for 5 min with agitation. Nitrocellulose membranes were blocked using blocking buffer (5 % (w/v) skimmed milk powder and 0.1% v/v Tween-20 in TBS) for 1 h at room temperature with gentle agitation. Blocking solution was replaced with fresh blocking buffer and one of the following primary antibody was added (1:1000 unless stated otherwise); phospho-specific ERK1/2, phospho-specific PKB (1:500), phospho-specific p38 MAPK, phospho-specific JNK or cleaved active caspase-3 (1: 500), and incubated overnight at 4°C under gentle agitation. The primary antibody was removed and the membranes washed vigorously for 5 min with TBS/tween 20 three times. Blocking solution and the appropriate secondary antibody coupled with horseradish peroxidase (HPR) was added (1:1000) and membranes incubated at room temperature for 2 h with gentle agitation. Following removal of secondary antibody, membranes were washed vigorously in TBS/Tween-20 three times for 5 min at room temperature. Blots were developed using the Ultra Chemiluminescence Detection System (Cheshire Sciences Ltd, Chester, UK) and quantified by densitometry using Advanced Image Data Analysis (AIDA) Software (Fuji; version 3.52). Replicates of each experiment were analysed on separate blots using primary antibodies specific to total unphosphorylated ERK1/2, PKB, JNK, p38 MAPK or GAPDH (1:1000) to confirm uniform protein loading in the gels.

2.7 Proteomic analysis

i) 2D gel electrophoresis

2D gel electrophoresis was used to separate cellular proteins by two parameters, molecular weight and isoelectric point (pH), to allow the protein samples to be identified using MALDI-TOF MS/MS. Cell cultures were grown in T75 cell culture flasks and treated according to the experimental protocol. The cell culture was then lysed totally using 300 µl urea lysis buffer (8 M urea, 50 mM DTT, 4 % (w/v) CHAPS, 0.2 % (v/v) Biolite® ampholytes (pH 3-10) (Bio-Rad laboratories, Hertfordshire, UK), in deionised water). The protein content of the cell lysate was then isolated using acetone precipitation, the cell lysate was added to -20 °C acetone in a proportion of 10 % (v/v) lysate to 90 % (v/v) acetone for 15 h and incubated at -20 °C. After the incubation the proteins form a visible precipitate, the lysate-acetone mixture was then centrifuged at 10,000 RCF for 10 minutes at 4 °C to pellet the proteins. The supernatant was decanted and the pellet left to dry out for 1 h in a fume cupboard, covered to prevent contamination. The dried protein was then suspended in 1X TBS buffer and further purified using a commercially available 2D clean-up kit from GE healthcare, following the manufacturer's protocol. A 5 µl aliquot of the protein sample was used to perform a DC Lowry protein assay, to determine the protein content of the sample. With the protein concentration determined, 300 µg of protein was suspended in 120 µL rehydration buffer (8 M urea, 50 mM DTT, 4% (w/v) CHAPS, 0.2% (v/v) Biolite® ampholytes (pH 3-10), 0.0002% (w/v) bromophenol blue, made in deionised water). The 120 µl sample was transferred into an IEF focusing tray, ensuring an even spread on the bottom of the tray with the liquid making contact with both anode and cathode wires. A 7 cm 3-10 pH IGP ReadyStrip™ (Bio-Rad laboratories, Hertfordshire, UK) was positioned on top of the protein sample, ensuring correct orientation and full contact with the protein sample without bubbles. The samples were allowed to undergo passive rehydration, where the sample is absorbed into the IPG gel, for 1 h at room temperature. The samples underwent active rehydration at 50 V for 16 h, with a layer of mineral oil (Bio-Rad laboratories, Hertfordshire, UK) placed on top of the IPG strip to prevent buffer evaporation. After rehydration IEF system electrode wicks (Bio-Rad laboratories, Hertfordshire, UK) were inserted in-between the IPG strip and the top of the electrodes in the focusing tray, these function to remove excess salts and ensure an effective focusing. The IPG strips were

focused with the following protocol, which separates the proteins in the first dimension; linear voltage slope up to 250 V was applied for 20 min. A second linear voltage slope increasing to 4000 V was applied for 2 h. A rapid voltage slope to 4000 V for 10,000 Volt-hours was then applied. Finally a rapid voltage slope down to 500V was applied to the gel for 25 h. After focusing the IPG strips were equilibrated in preparation for the second dimension SDS gel electrophoresis. IPG strips were placed in an equilibration tray and 2500 μ l of equilibration buffer 1 (6 M urea, 2 % (w/v) SDS, 1.5 M Tris/HCl pH 8.8, 50 % (v/v) glycerol, 2 % (w/v) DTT, in deionised water) was added for 10 min at room temperature with gentle agitation. Buffer 1 was removed and replaced with 2.5 ml equilibration buffer 2 (6 M urea, 2 % (w/v) SDS, 1.5 M Tris/HCl pH 8.8, 50 % (v/v) glycerol, 2.5 % (w/v) iodoacetamide, in deionised water) and incubated at room temperature for 10 min with gentle agitation.

Once equilibrated the IPG strip were positioned on top of a 15 % (w/v) SDS acrylamide gel (incorporating a stacking gel). A 0.5 cm strip of filter paper was soaked in a mixture of 10 % (v/v) protein ladder (Precision Plus Protein™ dual standards, Bio-Rad laboratories, Hertfordshire, UK) and 90 % (v/v) 4x laemmli buffer (8 % w/v SDS, 40 % (v/v) glycerol, 10 % (v/v) β -mercaptoethanol, 0.01 % (w/v) bromophenol blue, 250 mM TRIS-HCL pH 6.8, in deionised water) and placed at the side of the IPG strip to allow for molecular weight comparison. The IPG strip and ladder were then sealed to the gel with molten ReadyPrep™ overlay agarose (Bio-Rad laboratories, Hertfordshire, UK), which was allowed to solidify. The second dimension separation was then carried out by electrophoresing the gel at 200 V for 45 min, in a electrophoresis tank (Bio-Rad laboratories, Hertfordshire, UK) containing 1 x electrophoresis buffer. The bromophenol blue present in the IPG strips allowed for visible tracking of the dye front to ensure optimal separation of protein. After electrophoresis the gels were removed from the glass backing plates and washed for 5 min three times in deionised water. The gels were stained for 16 h using ProtoBlue™ safe colloidal coomassie G-250 stain (Bio-Rad laboratories, Hertfordshire, UK). After staining the gels were washed for 1 h in deionised water to remove any background staining. The stained gels were then photographed using a Syngene G-box with Genesnap software. The gels were then stored in a 0.001 % w/v sodium azide solution in deionised water at 4 °C. The gels were kept flat by placing them in-between two layers of acetate plastic.

ii) SameSpot Analysis

Photographed gels were analysed using Progenesis SameSpot (V 3.1.3030.23662, Non-linear Dynamics, UK) software. Gel images were aligned to a gel selected to be a control, either untreated differentiated or untreated mitotic H9c2 cells. Densitometric analysis of the gel spots was then performed by the software, which identifies gel spots that are more densely stained in the gels. This allows the software to locate proteins that have increased or decreased in expression. The significance of the change in density of the gel spots is then reported with $p < 0.05$ being reported as a significant change. The significantly changed spots were assigned a number, and spot picking map of the gel were produced, highlighting the significantly changed protein spots and labelling them with their respective number.

iii) De-staining

Proteins identified as being significantly changed were picked out of the gels using a pipette tip cut to an appropriate size and the gel spot was placed in a 1 ml Eppendorf™ tube containing a mixture of equal volumes 50 mM ammonium bicarbonate, deionised water and acetonitrile. The spots were incubated in this mixture for 5 min at 37 °C under gentle agitation. The supernatant was carefully removed and replaced with a mixture containing equal volumes of 50 mM ammonium bicarbonate, deionised water and acetonitrile and incubated at room temperature for 15 min with gentle agitation. The gel spots were then dehydrated by adding an equal volume of 100 % acetonitrile to the mixture and incubated for 5 min at room temperature with gentle agitation. The supernatant was then removed and replaced with 50 mM ammonium bicarbonate solution and incubated for 5 min at room temperature with gentle agitation. An equal volume of 100 % acetonitrile was added to the 50 mM ammonium bicarbonate solution and incubated for 15 min at room temperature under gentle agitation. This supernatant was then removed and replaced with 100 % acetonitrile for 1 min at room temperature, which was then removed and replaced with deionised water for 5 min to ensure the gel spots were fully rehydrated. The supernatant was then removed and replaced with the trypsin digestion mixture (1 µl Mass spectrometry grade Promega gold trypsin, 7.6 µl deionised water and 16.6 µl 100 mM ammonium bicarbonate) and incubated for 16 h at 37 °C. The digestion reaction was then terminated by adding 1 µl 1 % (v/v) Trifluoroacetic acid (TFA).

iv) ZipTip reverse phase chromatography

After tryptic digestion the protein digests were prepared for MALDI-TOF MS by using C₁₈ ZipTips (200 Å pore size) (Millipore, Hertfordshire, UK) to purify and concentrate the peptide sample. A Millipore C₁₈ ZipTip was prepared first by cleaning in 80 % v/v acetonitrile by cycling 10 µl through the pipette tip three times, followed by cycling 10 µl 0.1 % v/v TFA three times. The peptide digest was then bound to the C₁₈ ZipTip chromatography medium by cycling 10 µl of the peptide digest sample 25 times. The C₁₈ ZipTip was then washed by cycling 10 µl 0.1 % TFA three times. The bound peptides were then eluted from the chromatography medium by the uptake of 5 µl of 80 % acetonitrile and cycling through the C₁₈ ZipTip 25 times into a sterile 0.5 ml Eppendorf™ tube. 1.5 µl of the peptide digest was then spotted onto a MTP 384 ground steel Mass Spectrometry target plate (Bruker, UK) and 1.5 µl of CHCA matrix mixture (5.0 mg/ml α-Cyano-4-hydroxycinnamic acid (Bruker, UK), 50 % v/v acetonitrile, 0.1 % v/v TFA) was added to the peptide digest spot and allowed to air dry for 15 min, covered to prevent contamination. 1 µl peptide calibrant mixture (Bruker peptide calibration standard II; see appendix I) along with 1 µl CHCA matrix mixture was spotted onto the target plate adjacent to the protein samples.

v) MALDI-TOF MS/MS

The target plate was inserted into a Bruker Ultraflex extreme MALDI-TOF TOF Mass Spectrometer, which was operated by Bruker-Daltonics FlexControl (v 3.3, build 108) software. Peptides were analysed in reflectron positive ion mode, with the mass range of 800-3500 Da. The mass spectrometer was calibrated using the calibrant mixture. Once calibrated samples were analysed with laser power and shots (≈ 1000-3000 shots) optimised for each individual sample to give the best signal-to-noise ratio (SNR). The peptide mix mass spectrum was then exported to Bruker-Daltonics FlexAnalysis (v3.3, build 80) software to produce a peak list of *m/z* and intensity, using the SNAP algorithm. Known trypsin self-digestion product *m/z* peaks were removed from the spectrum. Protein identification was determined using Bruker-Daltonics Biotools (v 3.2, build 2.3) software linked to mascot (v 2.1) server. Database search parameters were set to the following: Search: peptide mass fingerprint (PMF); Database: SwissProt (May 2012a); Variable modifications: Carbamidomethylation (C), Methone oxidation (M); Mass Tolerance: 150

ppm; Mass values: Monoisotopic; Max missed cleavages: 2; Charge state: 1+; Enzyme: Trypsin; Taxonomy: Rattus. Protein identity was reported as significant ($p < 0.05$) according to protein score.

Protein identification was further investigated using MALDI-TOF MS/MS. m/z peaks of identified sample protein peptide fragments were selected for further investigation according to intensity and SNR. Selected peptide fragments were fragmented using LIFT (MS/MS) mode and the resulting fragment spectra were analysed using Bruker-Daltonics Biotoools (v 3.2, build 2.3) software linked to mascot (v 2.1) server, using the same parameters as the previous PMF database searches except the type of search was changed to MS/MS ion search and Fragment Mass Tolerance was set to ± 0.8 Da.

2.8 Statistical analysis

Statistical analysis was performed using GraphPad Prism 6. One-way ANOVA (analysis of variance of means) was used to compare three or more sets of data, with T-test being used to compare two sets of data. Tukey's multiple comparison *post hoc* analysis was used to further demonstrate significant differences between multiple data sets. Significance was deemed to be represented as $p < 0.05$ and highlighted with an asterix (*), all data is presented as the mean \pm S.E.M.

2.9 Materials

Quercetin, quercetin 3-glucuronide, and *all-trans* retinoic acid were purchased from Sigma-Aldrich I Co. Ltd. (Poole, Dorset, UK). 3'-O-methyl quercetin was purchased from Extrasynthese (France). LY 294002, PD 98059, SB 203580, SP 600 125 and wortmannin were inhibitors were obtained from Tocris Bioscience (Bristol, UK). Dulbecco's modified Eagle's Medium (DMEM), foetal bovine serum (FBS), trypsin (10 \times), L-glutamine (200 mM), penicillin (10,000 U/ml)/streptomycin (10,000 μ g/ml) were purchased from Lonza Group Ltd. Antibodies were obtained from the following suppliers: monoclonal anti-phospho-specific ERK1/2 (Thr²⁰²/Tyr²⁰⁴) from Sigma-Aldrich; polyclonal anti-phospho-specific PKB (Ser⁴⁷³), polyclonal anti-total unphosphorylated PKB, monoclonal anti-total unphosphorylated ERK1/2, polyclonal anti-total unphosphorylated JNK, polyclonal anti-

total unphosphorylated p38 MAPK, monoclonal anti-phospho-specific p38 MAPK, monoclonal anti-total tropomyosin-1, monoclonal anti- α -tubulin and polyclonal anti-cleaved active caspase 3 were from New England Biolabs (UK) Ltd; monoclonal anti-phospho-specific JNK was from Santa Cruz Biotechnology Inc; monoclonal anti-cardiac specific troponin T, monoclonal anti-CBR1 and monoclonal anti-GAPDH from Abcam (Cambridge, UK). All other chemicals were of analytical grade. Stock concentrations of quercetin (100 mM) were dissolved in DMSO, which was present in all treatments including the control at a final concentration of 0.1 % (v/v).

Chapter 3:

Differentiation of

H9c2 cells

3.0 Differentiation of H9c2 cells

The use of differentiated H9c2 cells in the context of this present study is essential, given the numerous differences between mitotic and differentiated H9c2 and what they represent when oxidative stress is considered. Mitotic H9c2 cells have been observed to exhibit metabolism similar to the “Warburg effect” (Pereira *et al*, 2011). This effect is primarily observed in cancer cells and describes the propensity for cells to produce energy at a higher rate due to accelerated glycolysis and lactic acid fermentation, as opposed to the more usual oxidation of pyruvate. This effect in mitotic H9c2 cells would allow them to continue production of high amounts of energy even during ischaemic attack, decreasing their sensitivity to oxidative stress, indeed the “Warburg effect” is thought to be an adaptation to low-oxygen environments (Pereira *et al*, 2011). This is further supported by observations that differentiated H9c2 cells have a reduced oxidative capacity when compared to mitotic H9c2 cells (Comelli *et al*, 2011). Although several studies into the cytoprotective effects of flavonoids have used mitotic H9c2 cells (Gutiérrez-Venegas *et al*, 2010; Angeloni *et al*, 2012; Angeloni *et al*, 2007; Sun *et al*, 2012; Kim *et al*, 2010; Mojzisoová *et al*, 2009), given the innate resistance and tolerance to oxidative stress of mitotic H9c2 cells, differentiated H9c2 represent a better model for the study of those effects. Therefore, this current chapter will establish a repeatable model for H9c2 cell differentiation, confirm this differentiation and investigate proteins expressed in H9c2 cells after differentiation.

H9c2 cells can be made to differentiate into a more cardiomyocyte-like phenotype in culture by supplementation with *all-trans* retinoic acid (RA) in a medium with decreased (1%) serum content (Ménard *et al*, 1999). Phenotypically differentiated H9c2 cells form thin, elongated, multinucleated myotubes, and are expected to express cardiac specific markers.

To develop a better model for *in vivo* cardiomyocytes, the differentiation of H9c2 cells will be assessed using several criteria. As shown in Table 1.12 it is known that differentiated H9c2 cells express cardiac specific markers, therefore to assess the differentiation of H9c2 cells the expression of cardiac specific troponin T Will be determined (Pereira *et al*, 2011). This will be coupled with the observation of morphological features including myotubule development and multiple nuclei, as these are also known markers of H9c2 differentiation (Branco *et al*, 2013).

There are currently no studies that have used proteomics to investigate the difference in proteins expressed between mitotic and differentiated H9c2 cells. Therefore, this present study will use two-dimensional electrophoresis and MALDI-TOF MS/MS to elucidate the proteomic differences between mitotic and differentiated H9c2 cells.

This chapter aims to monitor the differentiation of H9c2 cells in the following ways:

- Using Coomassie staining and light microscopy to characterise the phenotypical change in differentiated H9c2 cells.
- Using fluorescent immunocytochemistry to monitor the expression of the cardiac specific marker troponin T and phenotypical change in differentiating H9c2 cells.
- Using western blotting to quantify the expression on troponin-T in differentiating H9c2 cells.
- Using proteomic methods to identify novel protein(s) that significantly change in expression after differentiation.
- Using western blotting to confirm the findings of proteomic analysis.

3.1 Morphological change during differentiation

Mitotic H9c2 cardiomyoblasts have been used extensively in the study of the cardioprotective effects of flavonoids. H9c2 cells were differentiated for 7 days and then fixed and stained using Coomassie blue to assess visually the morphological changes. After 7 days the cells change markedly in appearance, becoming more cardiomyocyte-like. The morphological changes after differentiation can be observed in Fig. 3.1.

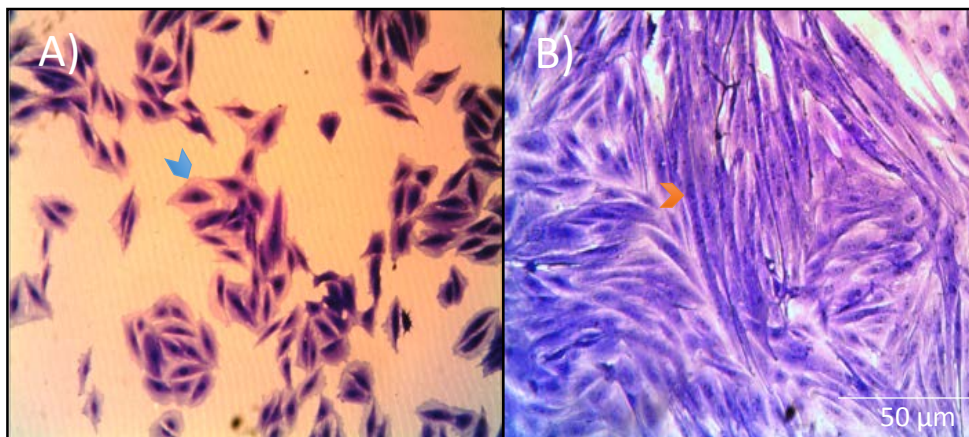


Fig. 3.1 Light micrograph of H9c2 cells. Mitotic H9c2 cells in fully supplemented DMEM medium (A) have a fibroblast like structure, with densely staining nuclei and cytoskeleton (blue arrowhead). After 7 days differentiation in differentiation medium (B) the cells phenotype has changed to thin, elongated, multinucleated myotubes (red arrowhead).

3.2 Expression of cardiac specific troponin

To create a model more similar to *in vivo* cardiomyocyte-like phenotype, in terms of morphology, electrophysiology and biochemistry, H9c2 cells were differentiated by culturing in differentiation medium for 1, 3, 7 and 9 days. Differentiated H9c2 cells were expected to express the cardiac specific marker cardiac troponin T, along with other cytoskeletal markers (Ménard *et al*, 1999). *In vivo*, troponin proteins are an essential part of the contractions mechanism of muscles, through their interaction with tropomyosin, actin and myosin (Zara *et al*, 2010). Immunocytochemical staining of cardiac troponin T was performed on H9c2 cells at different stages of differentiation, namely 1, 7 and 9 days, along with an undifferentiated control, shown in Fig. 3.2.

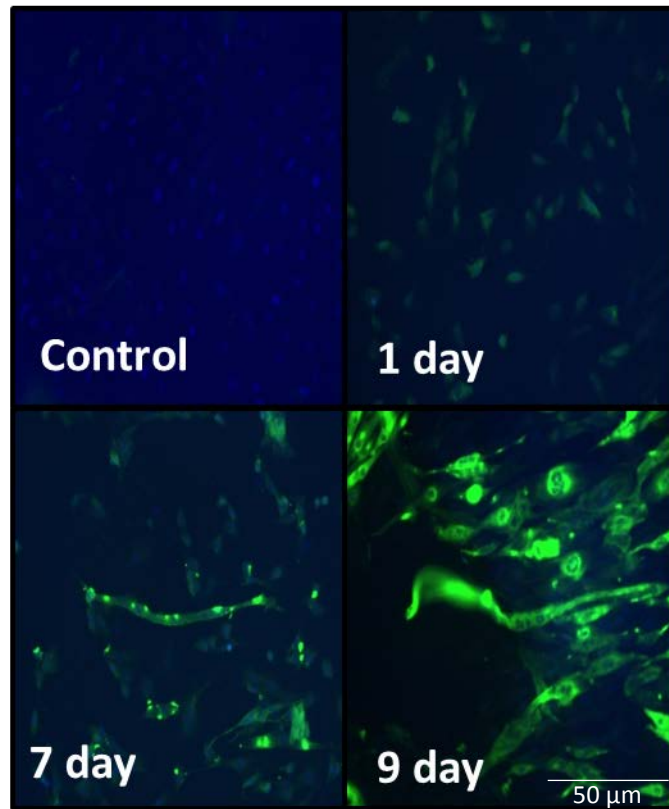


Fig. 3.2 Cardiac specific troponin expression during the differentiation of H9c2 cells. Immunocytochemistry using florescent microscopy was used to visualise the expression of cardiac troponin T, using anti-cardiac specific antibody and a FITC tagged secondary antibody (green) and DAPI nuclear counterstain (blue). Images are representative of 3 separate experiments.

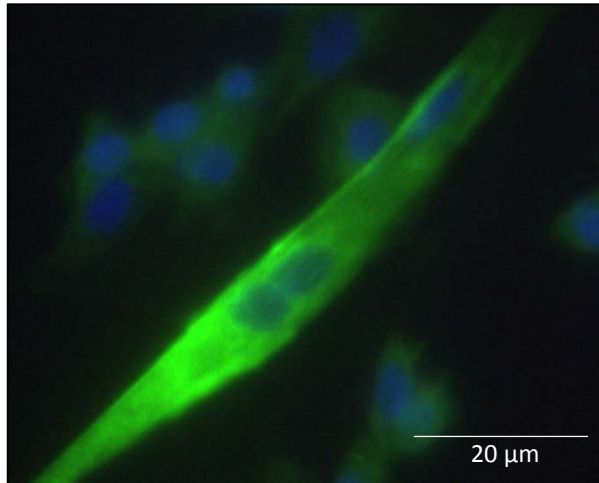


Fig. 3.3 Cardiac specific troponin expression after 7 days differentiation of H9c2 cells. The multinucleated, spindle phenotype of differentiated H9c2 cells is further demonstrated through the use of immunocytochemistry to stain cardiac troponin T, using anti-cardiac specific antibody and a FITC tagged secondary antibody (green) and DAPI nuclear counterstain (blue). Images are representative of 3 separate experiments.

The immunocytochemistry demonstrates the development of the multinucleated spindle-like myotubule morphology typical of cardiomyocytes after 7 days differentiation. Furthermore the expression of cardiac specific troponin T is visible with the increase in green fluorescence (Fig 3.1). To further demonstrate the increase in expression of cardiac specific troponin, western blotting was performed on cells at various stages of differentiation.

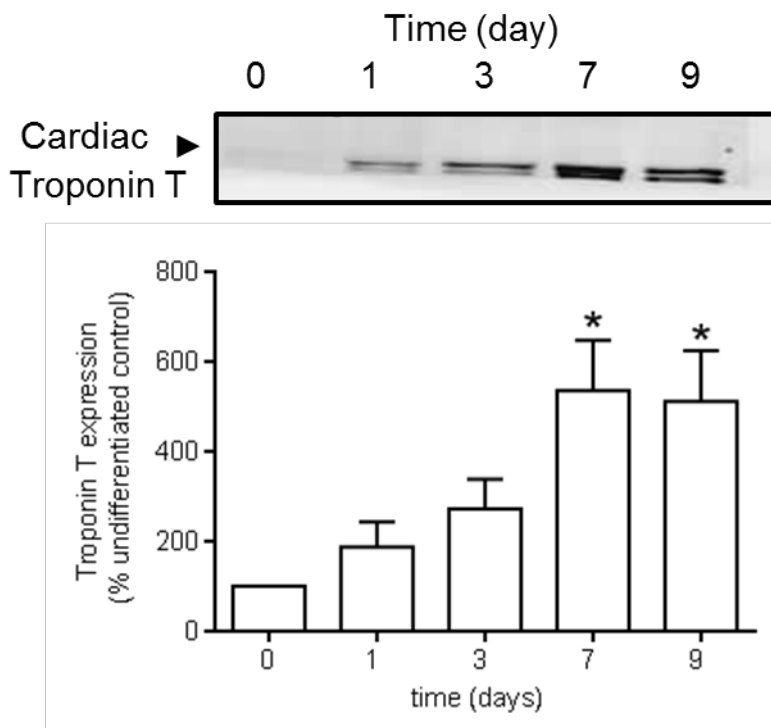


Fig. 3.4 Cardiac troponin 1 expression was assayed for after 1, 3, 7 and 9 days of exposure to differentiation medium. Cardiac specific troponin expression assayed by western blot, data expressed as percentage of undifferentiated control cells, after 7 and 9 days cardiac troponin is expressed at a significantly increased level (* $p < 0.05$ vs. control). Data are expressed as a percentage of control cells (0 days = 100%) and represent the mean \pm S.E.M of three independent experiments.

As shown in Figure 3.4 the expression of cardiac specific troponin was significantly ($p < 0.05$) increased after 7 days exposure to differentiation medium, confirming the differentiation of the H9c2 cells into a more cardiomyocyte-like phenotype.

3.3 Proteomic analysis

To identify novel proteins associated H9c2 cell differentiation, cell lysates were prepared from differentiated H9c2 cells and mitotic H9c2 cells. The lysates were prepared using specific 2D gel electrophoresis lysis buffer, two-dimensional gel electrophoresis was then performed, the gels stained and imaged according to the section 2.7 Proteomic analysis. A representative gel from undifferentiated cell lysate is shown in Fig 3.5 and differentiated cell lysate is shown in Fig. 3.6, all proteomic gels can be seen in Appendix 2.

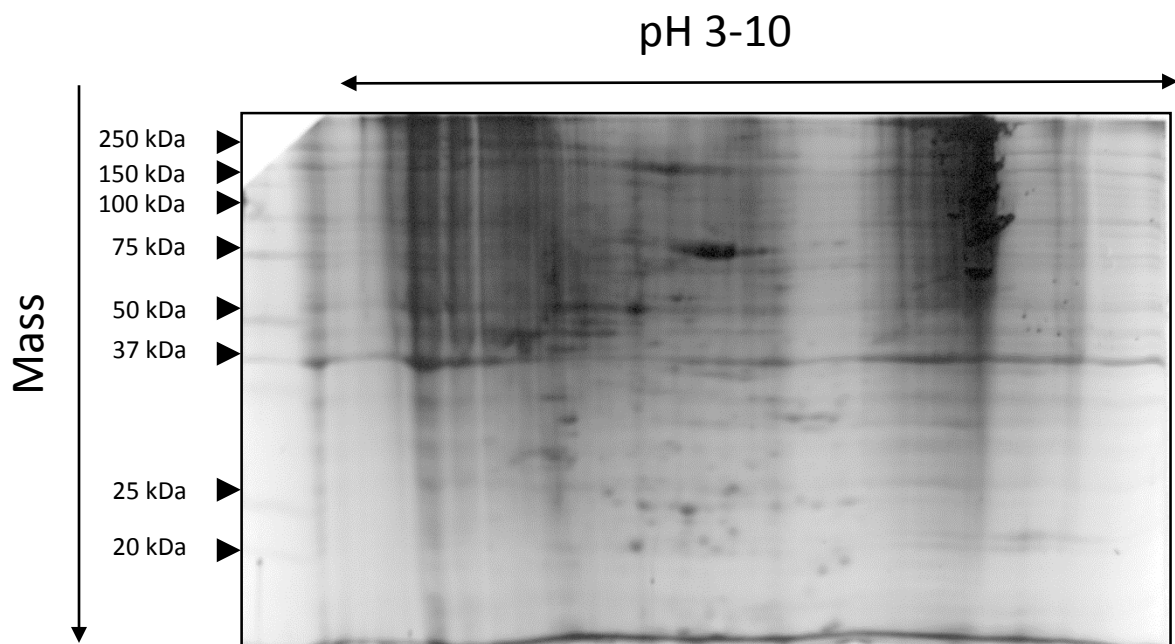


Fig 3.5 Expression pattern of proteins undifferentiated H9c2 cells. Proteins are separated first according to isoelectric point along a pH gradient, and then according to mass with polyacrylamide gel. Mass (kDa) has been highlighted using protein standards. Image is a representative gel of three separate experiments performed separately.

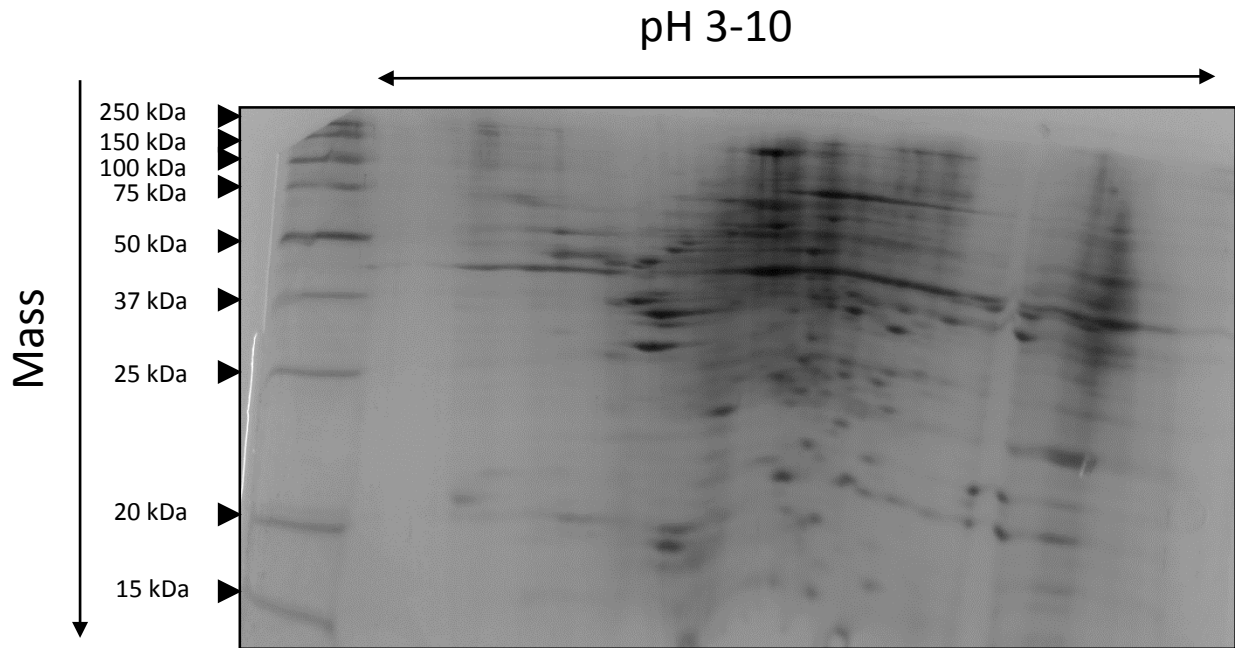


Fig 3.6 Expression pattern of proteins from differentiated H9c2 cells. Visual analysis shows potential density differences in some of the protein spots when compared to the undifferentiated cell gel image in fig 3.4. The image shown is a representative gel of three separate experiments performed separately.

Images of three separate 2D gels of differentiated H9c2 cells and mitotic H9c2 cells were analysed using Progenesis SameSpot software as described in section 2.7 part ii. Images were aligned to a selected control image, in this case a representative 2D gel of mitotic H9c2 cells. Protein spots were identified by the software and assigned an identity number. The relative density of the protein spots was then calculated and the change in density of the protein spots between the two sets of gels was analysed using the software. The significance of the difference in density was calculated using ANOVA and the protein spots ranked according to their significance, shown in Fig. 3.7, and highlighted on a spot picking map of a reference gel image, Fig. 3.8. Spot ID numbers 1, 20, 57 and 36 were found to be significantly changed in density in differentiated H9c2 cells when compared to mitotic H9c2 cells.

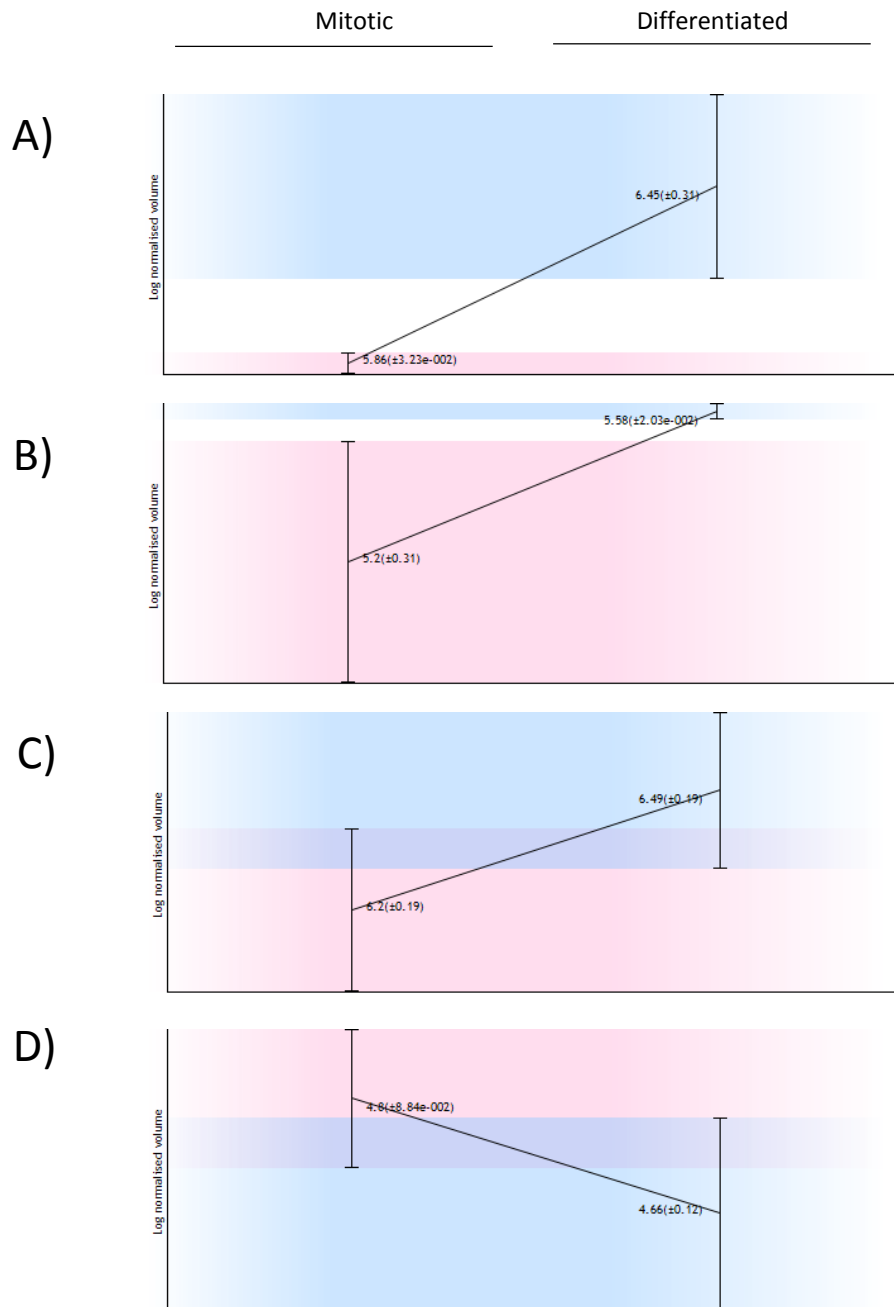


Fig. 3.7 Progenesis SameSpot analysis of protein spot densities. The difference in density between the two sets of gels, differentiated H9c2 cells and mitotic H9c2. Protein spots A) spot ID 1, B) spot ID 20, C) spot ID 36 and D) spot ID 57. A, B and C was shown to be of a higher density consistently in the gels of differentiated H9c2. The difference in density of protein spot was found to be significant for each spot using ANOVA analysis. A) *: $p < 0.005$ B) **: $p < 0.02$ C) *: $p < 0.032$ D) *: $p < 0.043$. Data are expressed as the mean log normalised volume of protein spot \pm S.E.M of three independent experiments in each group.**

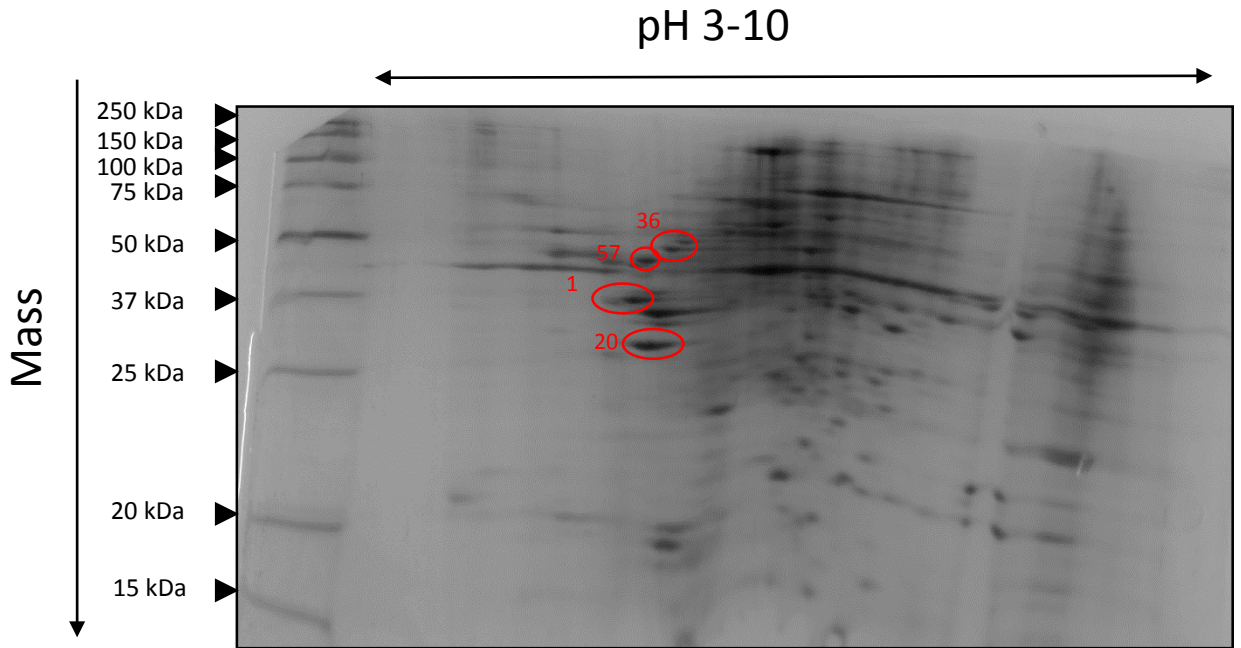


Fig. 3.8 Spot picking map of significantly changed protein spots in differentiated H9c2 cells. Spot ID 36 and Spot ID 57 are shown to be approximately 50 kDa, spot ID 1 is shown to be approximately 37 kDa and spot ID 20 between 37 and 25 kDa.

These significantly changed protein spots were then picked from the three gels of the lysates from the differentiated H9c2, according to the spot picking map (Fig 3.8). The spots were tryptically digested, and purified in preparation for MALDI-TOF MS/MS according to section 2.7 part iii and iv. The identity of the proteins within the spot was determined using MALDI-TOF MS/MS according to section 2.7 part V. Mass spectra of the protein fragments from MS/MS analysis are shown in Appendix 2.

The analysis of spot ID 20 identified it as possibly being tropomyosin α 4-chain or tropomyosin α 1-chain, as both tropomyosin α 1-chain and tropomyosin α 4-chain are the same weight it is likely that they are both present within the same protein spot when resolved with 2D gel electrophoresis. The findings of the MALDI-TOF MS/MS are summarised below in table 3.9.

Progenesis spot number	mass	RMS error (ppm)	Identification	PMF Score*	PMF Sequence Coverage (%)	Progenesis score	MS/MS Score#	MS/MS Peptides
1	32817	106	Tropomyosin beta chain	77.6	9	p < 0.005	73	K.LVILEGELER.S R.KLVILEGELER.S
20	28492	118	Tropomyosin alpha-1 chain	88	39	p < 0.02	76.2	R.KLVIIESDLER.A R.IQLVEEELDR.A R.RIQLVEEELDR.A
20	28492	26	Tropomyosin alpha-4 chain	63.6	45	p < 0.02	92.5	R.KIQALQQADDAE
57	41710	97	Actin (Cytoplasmic)	67.3	53	p < 0.043	79.5	K.IWHHTFYNELR.V
36	53700	55	Vimentin	103.8	56	p < 0.032	79.7	R.ISLPLPNFSSLNLR.E R.SLYSSSPGGAYVTR.S

Table 3.9 Proteins significantly up-regulated in differentiated H9c2 cells identified using MALDI-TOF MS/MS. The identity of the four spots tested were found to be tropomyosin β -chain , tropomyosin α -1 chain, tropomyosin α -4 chain, cytoplasmic actin and vimentin. *PMF score > 51 considered significant ($p > 0.05$). #MS/MS score > 21 considered significant ($p > 0.05$). PMF sequence coverage, PMF score, RMS error and MS/MS score are expressed as the mean of scores from 3 separate protein spots from different gels.

MALDI-TOF MS/MS identified five proteins that are expressed in a significantly different concentration in differentiated H9c2 cells. All five are cytoskeletal proteins, three of which were identified to be part of the tropomyosin family. The up-regulation of various tropomyosin subtypes further demonstrates the differentiation of the H9c2 cells into a more cardiomyocyte-like phenotype.

To further demonstrate the up-regulation of tropomyosin in differentiated H9c2 cells western blot for tropomyosin-1 was performed. As shown in Fig. 3.10 tropomyosin was significantly up-regulated in the differentiated cells when compared to the undifferentiated control. This finding confirms those of the MALDI-TOF MS/MS.

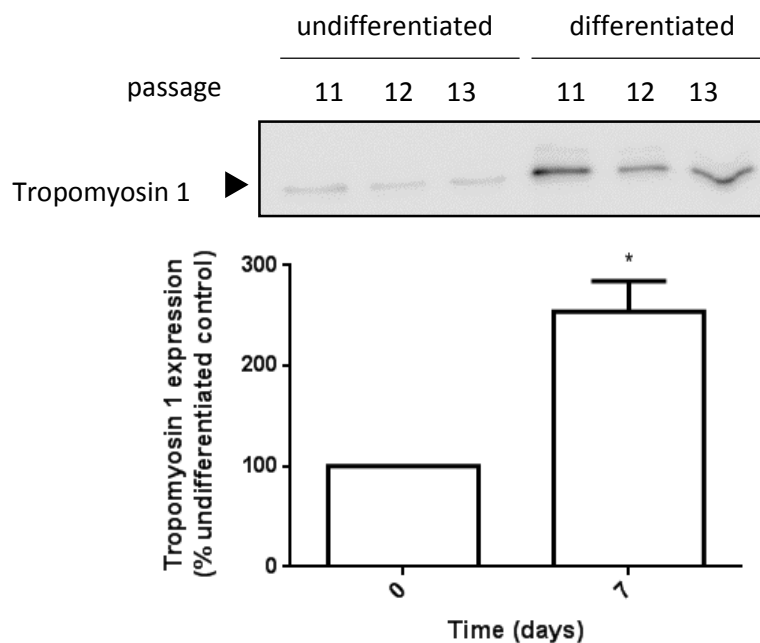


Fig. 3.10 Cardiac specific Tropomyosin-1 expression in 7 day differentiated of H9c2 cells. Expression of Tropomyosin-1 is significantly (*: $p < 0.05$) increase after 7 days of differentiation. Data are expressed as a percentage of control cells (0 days = 100%) and represent the mean \pm S.E.M of three independent experiments.

From these observations it can be said that the H9c2 cells become differentiated after 7 days exposure to differentiation medium. This is demonstrated by the expression of cardiac specific troponin T and tropomyosin, as well as the development of a more cardiomyocyte-like phenotype, with multinucleated, spindle shaped myotubules. Therefore, for the rest of the present study, cells differentiated for 7 days in differentiation medium were used as a standard model for differentiated H9c2 cardiomyocytes.

3.4 Summary of findings

It was demonstrated that the method for differentiating H9c2 cells in culture described in 2.1 cell culture was effective in causing differentiation. This was assessed by quantitative measurement of cardiac specific troponin-1 over the differentiation period, and visually confirmed using immunocytochemical staining of troponin-1 in differentiated H9c2 cells. Proteomic analysis using two-dimensional gel electrophoresis and MALDI-TOF MS/MS identified several more cytoskeletal proteins associated with H9c2 cell differentiation, namely tropomyosin β -chain, tropomyosin α -1 chain, tropomyosin α -4 chain, cytoplasmic actin and vimentin. The increased expression of tropomyosin was further demonstrated using western blotting.

3.5 Discussion of Differentiation.

Previous studies into the protective mechanisms of flavonoids have used mitotic H9c2 cells as a model system (Gutiérrez-Venegas *et al*, 2010; Angeloni *et al*, 2012; Angeloni *et al*, 2007; Sun *et al*, 2012; Kim *et al*, 2010; Mojzisoová *et al*, 2009). Mitotic H9c2 cells are generally accepted as a reliable model for cardiomyocytes, since they are electrophysiologically and biochemically similar to cardiomyocytes, but mitotic H9c2 cells lack certain features that would make them ideal of modelling *in vivo* cardiomyocytes (Hescheler *et al*, 1991). In mitotic form H9c2 cells do not form the classic myotubule structures associated with cardiomyocytes, and features such as gap junctions are not present. A novel element of this present study is the use of the differentiated H9c2 cells as a more cardiomyocyte-like model for the investigation of the effects of dietary flavonoids.

i) Characterisation of differentiated H9c2 cells

H9c2 cells have the potential to differentiate into either cardiac or skeletal myocytes, this differentiation is dependent on the conditions of the differentiation medium (Comelli *et al*, 2011). The differentiation method used in the present study, namely the incubation of the mitotic cells for 7 days with 1 % FBS supplemented DMEM and 10 nM *all-trans* retinoic acid, is in line with several previous studies using differentiated H9c2 cells (Ménard *et al*, 1999, Kageyama *et al*, 2002 and Comelli *et al*, 2011). To confirm the differentiation of the H9c2

cells in the present study into the cardiac myocyte phenotype it was necessary to measure the expression of cardiac markers in the cells during the differentiation and after the differentiation period. The cardiac specific marker troponin-1 has been used in previous studies to monitor the differentiation of H9c2 cells (Comelli *et al*, 2011). Using immunocytochemistry cardiac specific troponin-T was shown to be expressed after 7 days exposure to the differentiation conditions (Fig. 3.2 & Fig. 3.3). Western blotting was used to further demonstrate the increased expression of troponin-T during differentiation. As shown in Fig. 3.4 troponin-T expression increased to significantly high levels after 7 days incubation with differentiation media. After 9 days differentiation the expression of troponin-T appears to decrease, this may be due to death of the differentiated cells, as the differentiated H9c2 cells no longer mitotically divide (Comelli *et al*, 2011). Based on cardiac troponin-T expression and observable phenotypical change, the method of differentiation used in this present study was effective in differentiation of H9c2 cardiomyoblast in a more cardiomyocyte-like phenotype.

ii) Proteomic investigation into the differentiated H9c2 cell phenotype

The expression of novel proteins after H9c2 cardiomyocyte differentiation was analysed proteomically with a MALDI-TOF MS/MS approach. To the author's knowledge, no studies have used a proteomic approach to investigate the difference of expression of proteins between H9c2 cells in cardiomyoblast phenotype and the differentiated cardiomyocyte-like phenotype. Protein spots from two-dimensional gel electrophoresis gels of both cardiomyoblast and cardiomyocyte-like phenotypes were selected for MALDI-TOF MS/MS from their significance score after progenesis SameSpot analysis and their visual distinctiveness. The proteins highlighted in section 3.3 proteomic analysis represent those that were observed and significantly identified on three separate occasions from three independent experiments. Proteins that were not identified in three independent experiments were omitted. Furthermore, difficult to distinguish protein spots were not selected for MALDI-TOF MS/MS. These omissions explain the relatively small number of verifiable protein identities despite the apparent abundance of proteins spots identified by progenesis SameSpot analysis. This also explains why troponin-T was not identified by MALDI-TOF MS/MS despite being a well-known marker of the cardiomyocyte-like

phenotype of H9c2 cells (Comelli *et al*, 2011). All the proteins identified and highlighted in section 3.3 proteomic analysis (Table 3.9) were consistently identified with a combination of MALDI-TOF MS and MALDI-TOF MS/MS and had distinctive protein spots on the two-dimensional gel electrophoresis gels. MS/MS MALDI-TOF was performed on the proteins identified using MALDI-TOF to provide further evidence of their identity, and all proteins detailed on Table 3.9 were shown to have a very strong MS/MS score, representing a confident identification. All the proteins that were reliably identified were cytoskeletal in nature. It is known that the differentiation of H9c2 cells into the cardiomyocyte-like phenotype confers cytoskeletal changes to the cell, principally in the formation of cardiomyocyte-like ultrastructural features such as myofilament bundles (Comelli *et al*, 2011). Myofilament formation is a precursor to the development of sarcomere like structural development in the differentiated H9c2 cell. Several sub-types of tropomyosin and actin were identified as being significantly increased in expression in differentiated H9c2 cells when compared to the cells in their mitotic form. It is likely that the cardiac cytoskeletal elements such as tropomyosin and actin identified from the MALDI-TOF MS/MS are directly associated with the formation of the myofilaments known to occur in differentiated H9c2 cells (Comelli *et al*, 2011). The filamentary structure of the cytoskeleton, the more organised, linear arrangement can also be visualised using immunocytochemistry (Fig. 3.2 & 3.3) and chemical staining techniques (Fig. 3.1). From the MALDI-TOF MS/MS analysis vimentin was also identified as being increased in expression in differentiated H9c2 cells. Vimentin has been previously identified as a marker for H9c2 cardiomyocyte differentiation, therefore the finding that vimentin was increased in expression in the present study further demonstrates the efficacy of the differentiation method and supports the conclusion that the cells have differentiated into a more cardiomyocyte-like phenotype (Selmin *et al*, 2005). Vimentin has also been investigated for potential links with flavonoid mediated cytoprotection, using the flavonoid epigallocatechin-3-gallate (Hsieh *et al*, 2013). Epigallocatechin-3-gallate was shown to form complexes with vimentin that could lead to cytoprotective effects due to the potent anti-oxidant activity of epigallocatechin-3-gallate (Hsieh *et al*, 2013). Given the structural similarity between epigallocatechin-3-gallate and other flavonoids such as quercetin, the potential for other flavonoids to form conjugations with vimentin and other cytoskeletal proteins such as β -actin and myosin may augment the protective effect of the flavonoids and increase the

protective effect observed in differentiated H9c2 cells when compared to their mitotic form, since the expression of these cytoskeletal structures is comparatively lower in the H9c2 cells cardiomyoblast form (Hsieh *et al*, 2013).

iii) Confirmation of tropomyosin expression

The increased expression of tropomyosin-1 after differentiation was further demonstrated using western blotting (Fig 3.10). Studies have identified that differentiation of H9c2 cells causes mitochondrial developments specifically demonstrating that the mitochondria increase in size and undergo ultrastructural changes (Comelli *et al*, 2011). Differentiated H9c2 cells are also shown to have reduced oxidative capacity when compared to the undifferentiated cardiomyoblast form. This reduced oxidative capacity will allow for a more effective characterisation of the protective effects of dietary flavonoids, as any observed protective effect will be most likely due to the inducement of the effect from the flavonoid rather than the innate oxidative capacity of the H9c2 cells themselves. The identification of vimentin up regulation in the present study further suggests mitochondrial development in differentiated H9c2 cells, since vimentin is known to be associated with the development of organelles, such as mitochondria and the sarcoplasmic reticulum, in muscle cells (Comelli *et al*, 2011).

iv) Conclusion

In conclusion, from the results shown in chapter 3, the method of differentiation used in this present study was shown to be effective in the differentiation of H9c2 cells. This differentiation was demonstrated through the expression of cardiac specific troponin, and the subsequent novel identification of the increased expression of vimentin, tropomyosin and actin, known cardiac muscle and general muscle markers in the differentiated H9c2 cells, through the use of MALDI-TOF MS/MS (Selmin *et al*, 2005). The myofilament development, as evidenced by the presence of tropomyosin, vimentin and actin, shows that the differentiated H9c2 cell is similar to primary cardiomyocyte cell cultures, further demonstrating that the differentiated H9c2 cells is of a cardiomyocyte-like phenotype. The differentiated H9c2 cells will provide a novel model, which are phenotypically and

electrophysiologically similar to *in vivo* cardiac cells, for the purpose of investigating the cytoprotective and cytotoxic effects of dietary flavonoids (Hescheler *et al*, 1991). The proteins identified by MALDI-TOF MS/MS provide new information about the cardiomyocyte-like phenotype of H9c2 cells acquired after differentiation through the use of *all-trans* retinoic acid and serum depleted DMEM growth medium.

Chapter 4:
Cytoprotective
potential of
flavonoids

4.0 Cytoprotective potential of flavonoids

This chapter aims to demonstrate the cytoprotective effect of flavonoids and their metabolites on differentiated H9c2 cells against oxidative stress induced by hypoxia and H₂O₂ exposure. Although the protective effect of flavonoids is known to occur in mitotic H9c2 cells, differentiated H9c2 cells provide a more cardiomyocyte-like phenotype model to study the cytoprotective effects of flavonoids. As demonstrated in Chapter 3, the differentiation of H9c2 cells leads to the expression of cardiac specific markers and a change in morphology. As described previously mitotic H9c2 cells exhibit certain metabolic characteristics that increase its survivability in conditions of oxidative stress (Pereira *et al*, 2011). Firstly the difference in survivability of mitotic and differentiated H9c2 cells will be investigated by assaying the viability of both mitotic and differentiated H9c2 cells after exposure to hypoxia and H₂O₂.

Once differentiated cells are shown to be more susceptible to oxidative stress-induced cell death the cytoprotective effects of flavonoids and their metabolites will be investigated. This will be achieved by assaying the viability of differentiated H9c2 cells after pre-treatment with three flavonoids (kaempferol, myricetin and quercetin) and exposure to hypoxia and H₂O₂. There is considerable variation in the exposure time and concentration of flavonoids used previously to investigate the cytoprotective effect of flavonoids in mitotic H9c2 cells (Gutiérrez-Venegas *et al*, 2010; Angeloni *et al*, 2012; Angeloni *et al*, 2007; Sun *et al*, 2012; Kim *et al*, 2010; Mojzisová *et al*, 2009). When obtained via diet the peak plasma concentration of quercetin and its metabolites was shown to be 7.6 μM (Labbé *et al*, 2009). Plasma half-lives of quercetin metabolites have been shown to be between 11-28 h, therefore after repeated intake of flavonoid rich food such as onions, these metabolites may accumulate in the plasma (Labbé *et al*, 2009). Furthermore, flavonoids and their metabolites have also been observed to accumulate intracellularly and undergo metabolism, with aglycone forms of the flavonoid being formed from their metabolites by β-Glucosidase enzymes (Kanazawa, 2011). Reportedly peak intracellular concentrations of quercetin were 2 nmol/mg protein after 1 h exposure to 30 μM quercetin (Angeloni *et al*, 2007). Considering the bioavailability of the flavonoids, previous investigations, and the possibility of intracellular flavonoid accumulation, a range of 1-100 μM concentrations of flavonoid will be used when exposing the differentiated H9c2 cells. Although the dietary

intake of kaempferol and myricetin is considerably lower than quercetin, the same exposure concentrations will be used, as to reflect the intracellular and plasma accumulation. Previous studies investigating flavonoid induced cytoprotection have used a range of exposure times, most commonly 1-24 h (Gutiérrez-Venegas *et al*, 2010; Angeloni *et al*, 2012; Angeloni *et al*, 2007; Sun *et al*, 2012; Kim *et al*, 2010; Mojzisoová *et al*, 2009). The use of a 1 h exposure time reflects the *in vivo* exposure of the cells shortly after a meal, and has been shown to be adequate time to allow for intracellular flavonoid accumulation (Angeloni *et al*, 2007). As the half-life of quercetin metabolites surpass 24 h, an exposure time of 24 h reflects the exposure of *in vivo* cells after one or several meals (Labbé *et al*, 2009). A 24 h exposure time may also lead to greater intracellular flavonoid accumulation and a greater cytoprotective effect. Considering this, 1 h and 24 h exposure times to the flavonoid will be used to investigate the cytoprotective effect.

The effect of flavonoid pre-treatment on protein kinases associated with cytoprotection, namely PKB, ERK1/2, JNK and p38 MAPK will be investigated using western blotting. Both these signalling cascades (PI3K and MAPK) are associated with cell survival and have been investigated previously in mitotic H9c2 cells with respect to flavonoid induced cytoprotection (Angeloni *et al*, 2007). There is considerable cross-talk between these two cascades, therefore if flavonoids are able to modulate the phosphorylation of one or several key molecules in one cascade it is likely to have an effect on the other (Mendoza *et al*, 2011). Quercetin has been shown to form a hydrogen bond with ser²¹² in the MEK backbone, inactivating the protein. Inhibition of MEK would consequently lead to decreased phosphorylation of ERK1/2, p38 MAPK and JNK (Russo *et al*, 2012). PI3K inhibition has also been observed when ERK1/2 is inhibited (Mendoza *et al*, 2011). Quercetin was also predicted to be able to form 14 hydrogen bonds inside a computer modelled ATP binding motif at the Tyr¹⁰⁴⁴, Thr¹⁰⁴⁶, Arg¹⁰⁴⁷, Gly¹⁰⁷³, Gly¹⁰⁷⁵, Lys¹⁰⁷⁶, Ser¹⁰⁷⁷, Tyr¹⁰⁸⁷, and Glu¹²⁰¹ amino acids (Qian *et al*, 2004). This predicted binding may be a major contributing factor to the observed inhibition of MEK.

As the inhibitory effect of flavonoids on cell signalling cascades is a suspected mechanism of flavonoid-induced cytoprotection the effects of specific inhibitors of PKB, ERK1/2, JNK and p38 MAPK will be investigated using western blot, specifically PD98059 (50 µM, MEK1/2 inhibitor) and LY294002 (30 µM, PI3K inhibitor), Wortmannin (100 nM, PI3K

inhibitor), SB203580 (30 μ M, p38 MAPK inhibitor) and SP600125 (10 μ M, JNK inhibitor). The exposure time and concentrations of inhibitors used followed the manufacturer's recommendations. Firstly the specific inhibitors will be used to compare to the effects of flavonoids. The effect of the specific inhibitors on cell viability using the same exposure times to those used to investigate the effect of flavonoids will be investigated. Furthermore, the cytoprotective effect of the inhibitors will be investigated, to determine if the inhibition of a specific signal is responsible for the cytoprotective effect of flavonoids.

4.1 Determining optimal H₂O₂ treatment conditions

Treatment with H₂O₂ was used in the present study as a chemical inducer of oxidative stress, to simulate ischaemic attack *in vitro*. To ascertain the appropriate time and concentration of hydrogen peroxide exposure MTT reduction and LDH release cell viability assays were used. Firstly to determine optimal concentration differentiated H9c2 cells were treated with a range of concentrations of H₂O₂ (200-100 µM) for 2 h. The results of the cell viability assays are shown in Fig. 4.1. Differentiated H9c2 cells were also exposed to 600 µM H₂O₂ for various time points to determine the optimal time for H₂O₂ treatment with regard to cell death. This was assayed using MTT reduction and LDH release cell viability assays. Results of these cell viability assays is shown in Fig. 4.2.

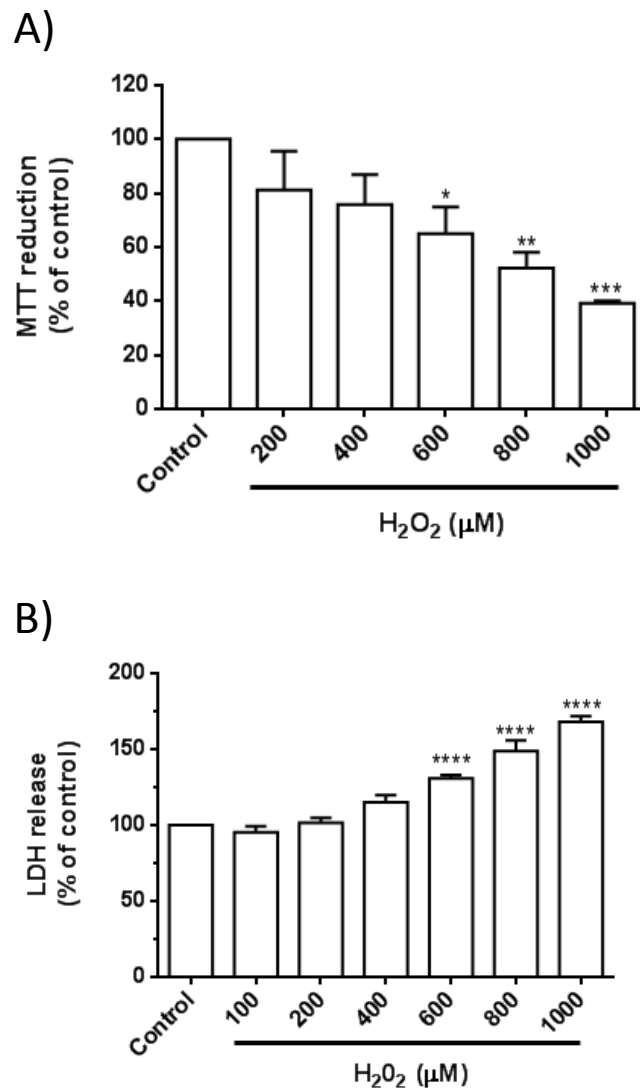


Fig. 4.1 The effects of concentration of H₂O₂ on differentiated H9c2 cell viably after 2 h exposure as measured by A) MTT reduction and B) LDH release assays. Both assays show that a minimum of 600 μM H₂O₂ is required to illicit significant (*: p < 0.05; **: p < 0.01; ***: p < 0.005; ****: p < 0.001) cell death. Data are expressed as the percentage of control cells (C =100%) and represent the mean ± SEM of three independent experiments.

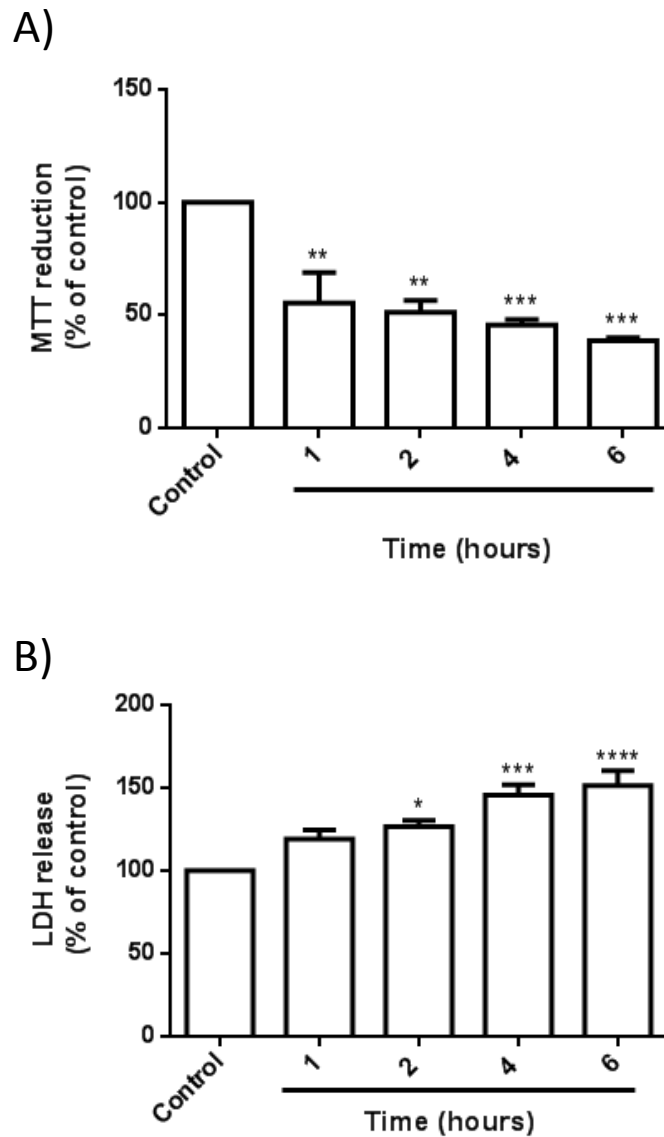


Fig 4.2 The effects of exposure time of 600 μM H_2O_2 on differentiated H9c2 cell viability. Measured by A) MTT reduction and B) LDH release assays. Both assays show that time points 6, 4 and 2 h 600 μM H_2O_2 exposure caused significant (*: $p < 0.05$; **: $p < 0.01$; ***: $p < 0.005$; ****: $p < 0.001$) cell death. Data are expressed as the percentage of control cells (C =100%) and represent the mean \pm SEM of five independent experiments.

From the data shown in figs. 4.1 and 4.2 it is clear that a minimum of 2 h exposure to 600 μM H_2O_2 on differentiated H9c2 cells causes significant decrease in viability as measured by MTT reduction and LDH release assays. Undifferentiated H9c2 cardiomyoblast cells showed less sensitivity to H_2O_2 induced cell death as measured by MTT reduction and LDH release, as shown in Fig. 4.3 and Fig. 4.4. This may be a reflection of the more immature phenotype of the undifferentiated H9c2 cardiomyoblast cells.

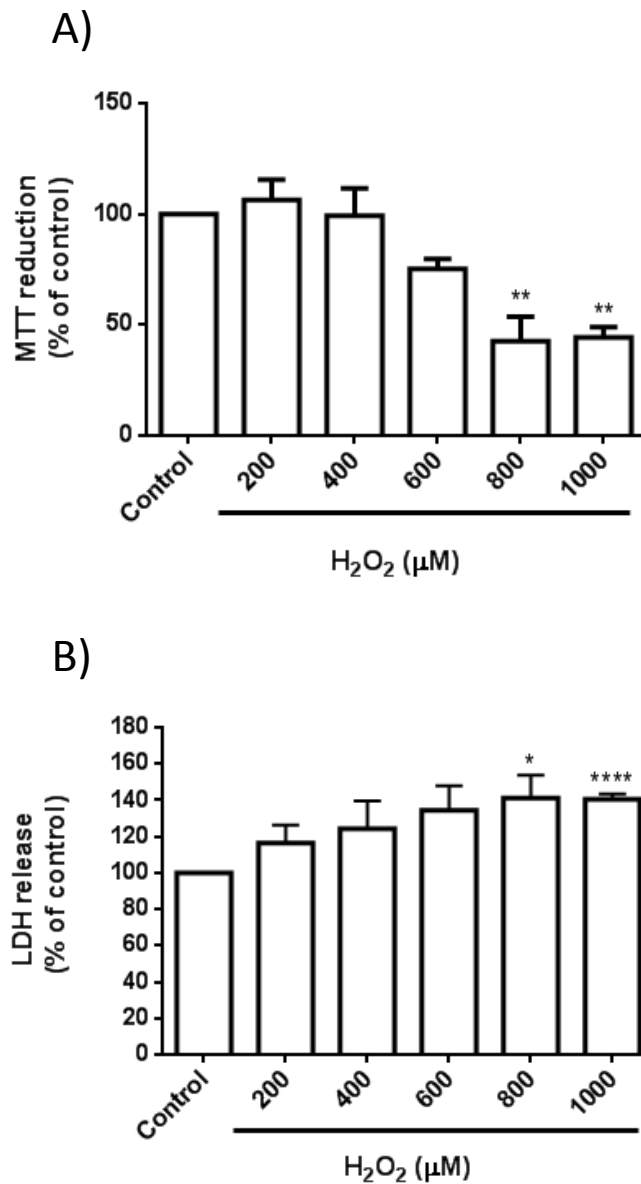


Fig. 4.3 The effects of concentration of H₂O₂ on undifferentiated H9c2 cell viably after 2 h exposure. Measured by A) MTT reduction and B) LDH release assays. Both assays show that a minimum of 800 μM H₂O₂ is required to illicit significant (*: p < 0.05; **: p < 0.01; ****: p < 0.001) cell death. Data are expressed as the percentage of control cells (C =100%) and represent the mean ± SEM of three independent experiments.

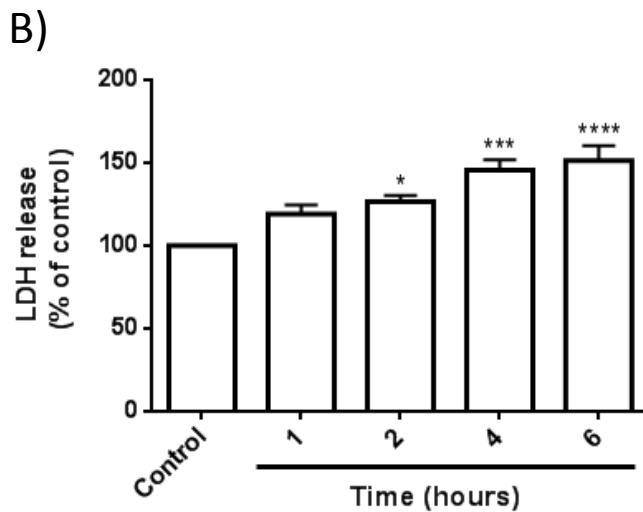
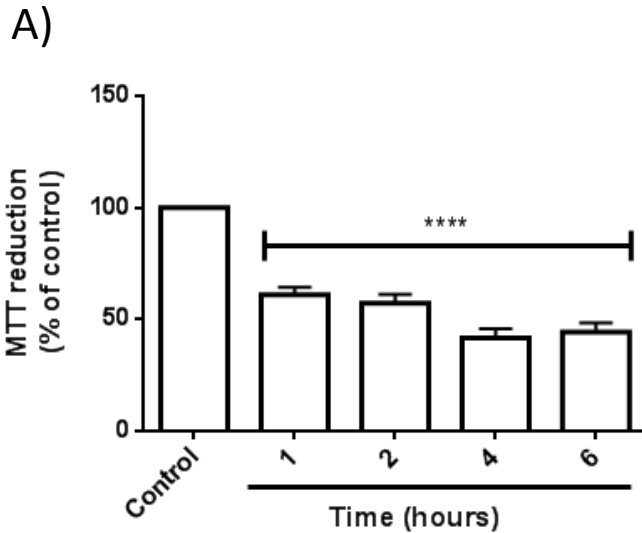


Fig 4.4. The effects of exposure time of 800 μM H_2O_2 on undifferentiated H9c2 cell viability. Measured by A) MTT reduction and B) LDH release assays. Both assays show that a minimum of 2 h treatment with 800 μM H_2O_2 causes significant (*: $p < 0.05$; ***: $p < 0.005$; ****: $p < 0.001$) cell death. Data are expressed as the percentage of control cells (C=100 %) and represent the mean \pm SEM of four independent experiments.

Fig 4.3 and 4.4 demonstrate that undifferentiated H9c2 cells are less sensitive to H_2O_2 induced cell death, as shown by the necessity of a minimum 800 μM treatment to elicit a significant loss in viability as measured by LDH release and MTT reduction, as compared to the minimum 600 μM required for differentiated cells. This is also reflected in the increased exposure time required to induce a loss in viability in undifferentiated H9c2 cardiomyoblasts, as shown in Figs 4.2 and 4.4.

4.2 Hypoxia model design

To determine the optimal duration of hypoxia differentiated H9c2 cells were exposed to 6 or 24 h of hypoxia (0.5 % O₂) and viability was assayed using MTT reduction. The viability of the cells was then compared to a normoxia control. From this assay (Fig. 4.5) it was demonstrated that 24 h hypoxia causes a significant loss in cell viability as measured by MTT reduction. Therefore for the duration of the present study, 24 h was used as the standard incubation time to induced significant cell death from hypoxia.

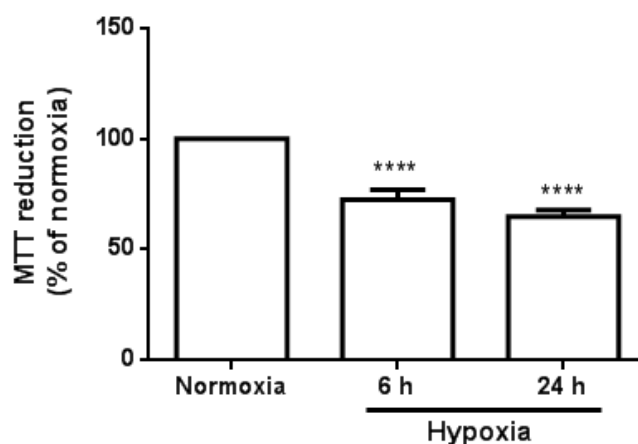


Fig. 4.5 The effects of duration of Hypoxia on differentiated H9c2 cell viably as measured by MTT reduction. Significant (****: $p < 0.001$) cell death occurred during both treatment times when compared to normoxic control, although 24 hours in hypoxia caused a more significant ($p < 0.0001$) cytotoxic effect than 6 hours ($p = 0.0003$). Data are expressed as the percentage of control normoxia cells (Normoxia = 100 %) and represent the mean \pm SEM of nine independent experiments.

4.3 Cytoprotective effects of flavonoid pre-treatment against Hydrogen peroxide induced cell death

With the optimal conditions for simulating oxidative stress with H₂O₂ determined, as described in section 4.1, differentiated H9c2 cardiomyocytes were pre-treated with various concentrations of three different flavonoids; myricetin, kaempferol and quercetin. Initially, the experimental design also included the flavonoid naringenin, but due to time constraints investigations were not continued. The preliminary investigations into the protective effects of naringenin showed no significant effects (data not presented). Firstly, differentiated H9c2 cells were pre-treated with 30 μ M or 100 μ M of flavonoid for 1 h and

the exposed to 600 μM H_2O_2 for 2 hours, viability was then measured using LDH release and MTT reduction.

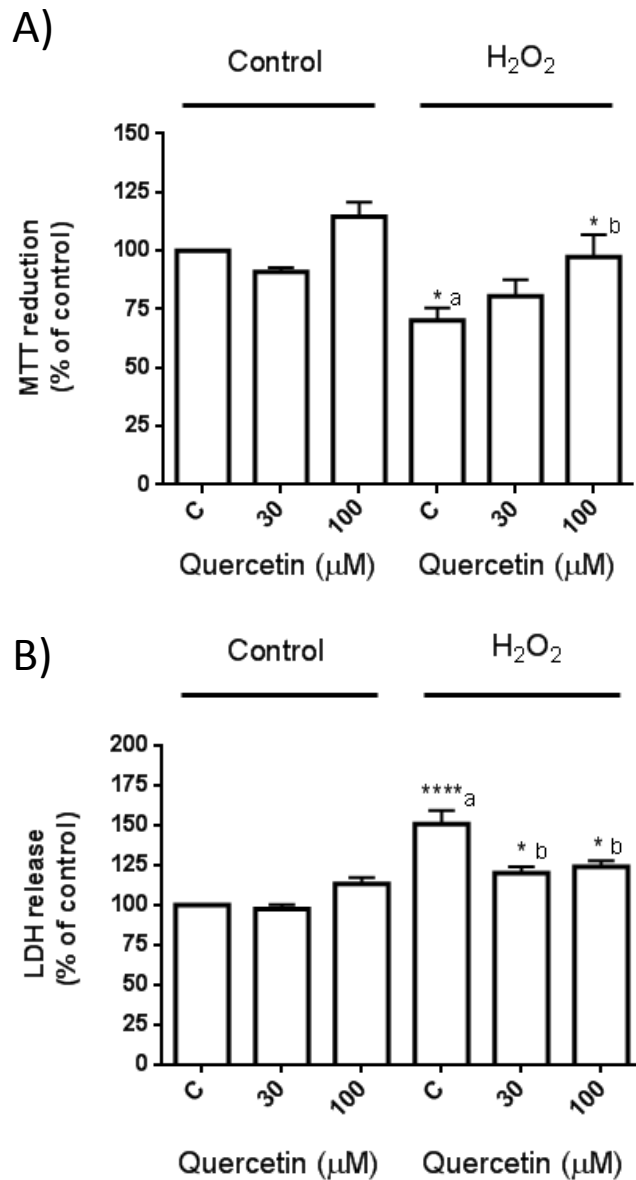


Fig 4.6 Effect of 1 h quercetin pre-treatment on cell viability during 600 μM H_2O_2 induced oxidative stress. Measured by A) MTT reduction assay and B) LDH release assay. Hydrogen peroxide caused significant cell death compared to control cells (a denotes significance vs untreated control cells). The MTT reduction assay showed that 100 μM concentration of quercetin, induced significant protection from cell death compared to hydrogen peroxide treatment. The LDH release assays showed that 100 μM and 30 μM pretreatment caused significant protection compared to hydrogen peroxide treatment. (*: $p < 0.05$; **: $p < 0.01$; ***: $p < 0.005$; ****: $p < 0.001$; b denotes significance vs H_2O_2 treatment). Data are expressed as the percentage of control cells (C = 100 %) and represent the mean \pm SEM of seven independent experiments

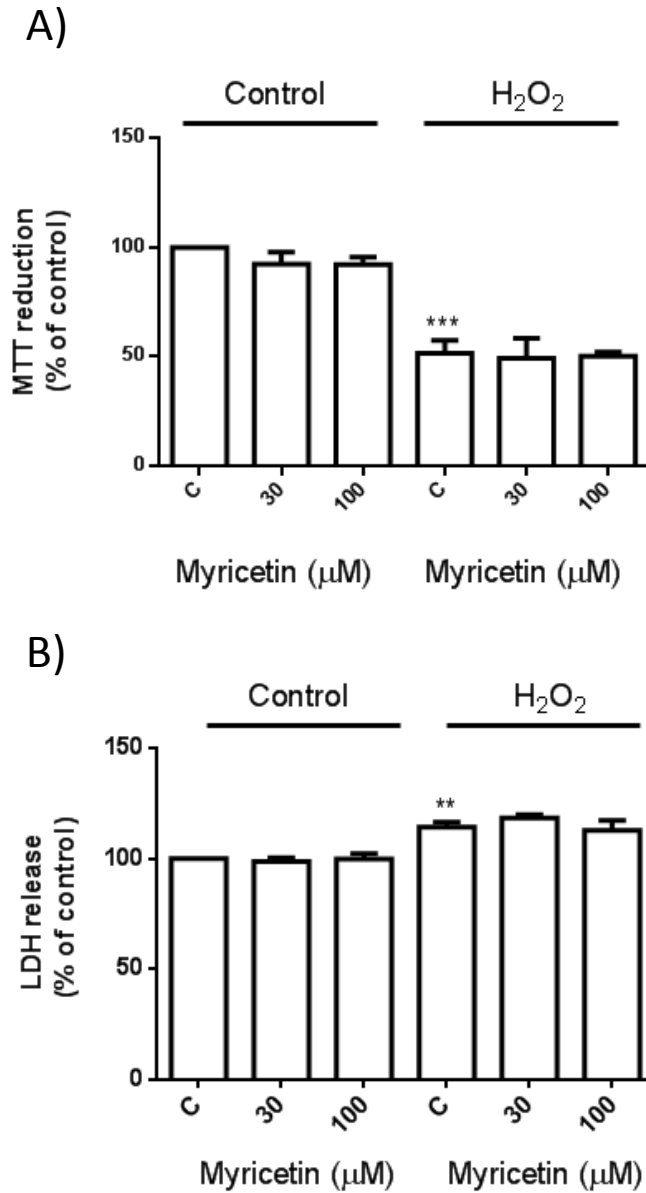


Fig 4.7 Effect of 1 h myricetin pre-treatment on cell viability during 600 μM H₂O₂ induced oxidative stress. Measured by A) MTT reduction assay and B) LDH release assay. Hydrogen peroxide caused significant cell death compared to control cells. The MTT reduction assay and LDH release assays showed no concentrations of myricetin were able to illicit a significant protective effect after 1 h pretreatment (**: $p < 0.01$; ***: $p < 0.005$). Data are expressed as the percentage of control cells (C = 100 %) and represent the mean \pm SEM of three independent experiments.

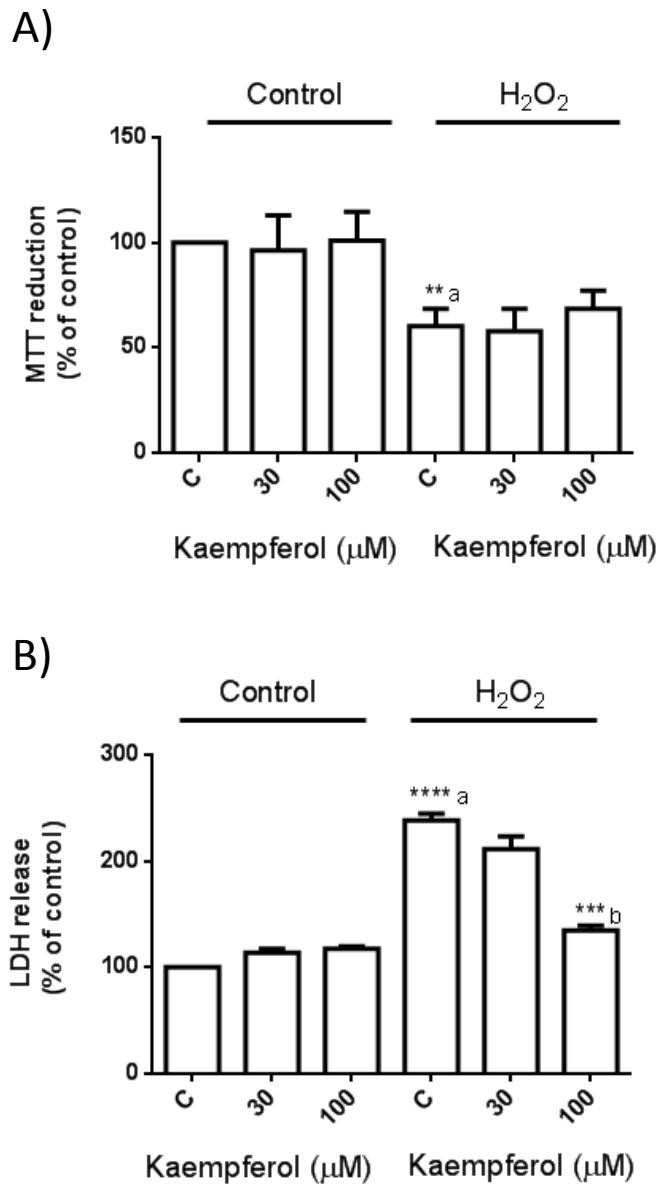


Fig 4.8. Effect of 1 h kaempferol pre-treatment on cell viability during 600 μM H₂O₂ induced oxidative stress. Measured by A) MTT reduction assay and B) LDH release assay. Hydrogen peroxide caused significant (a denotes significance vs untreated control cells) cell death compared to control cells. The MTT reduction assay and LDH release assays show 1 h pretreatment with 100 μM kaempferol was able to illicit a significant protective effect. (: p < 0.01; ***: p < 0.005; ****: p < 0.001; b denotes significance vs H₂O₂ treatment). Data are expressed as the percentage of control cells (C = 100 %) and represent the mean ± SEM of three independent experiments.**

As demonstrated by Figs. 4.6, 4.7 and 4.8, quercetin was shown to be the most potent flavonoid in terms of inducing a protective effect against H₂O₂ induced cell death after 1 h pre-treatment. Therefore, flavonoid pre-treatment time was increased to 24 h to further investigate the protective effect of the three flavonoids. Differentiated cells were pre-treated with a range of concentrations of one flavonoid for 24 h and then exposed to 600 µM H₂O₂ for 2 h. Firstly, a range of concentrations of quercetin were used to pre-treat differentiated cells for 24 h, the cells were exposed to 600 µM H₂O₂ for 2 h and the viability was assayed using MTT reduction and LDH release assays. The protective effect of 24 h pretreatment with the other two flavonoids, kaempferol and myricetin, against 2 h exposure to 600 µM H₂O₂ was assayed using MTT reduction.

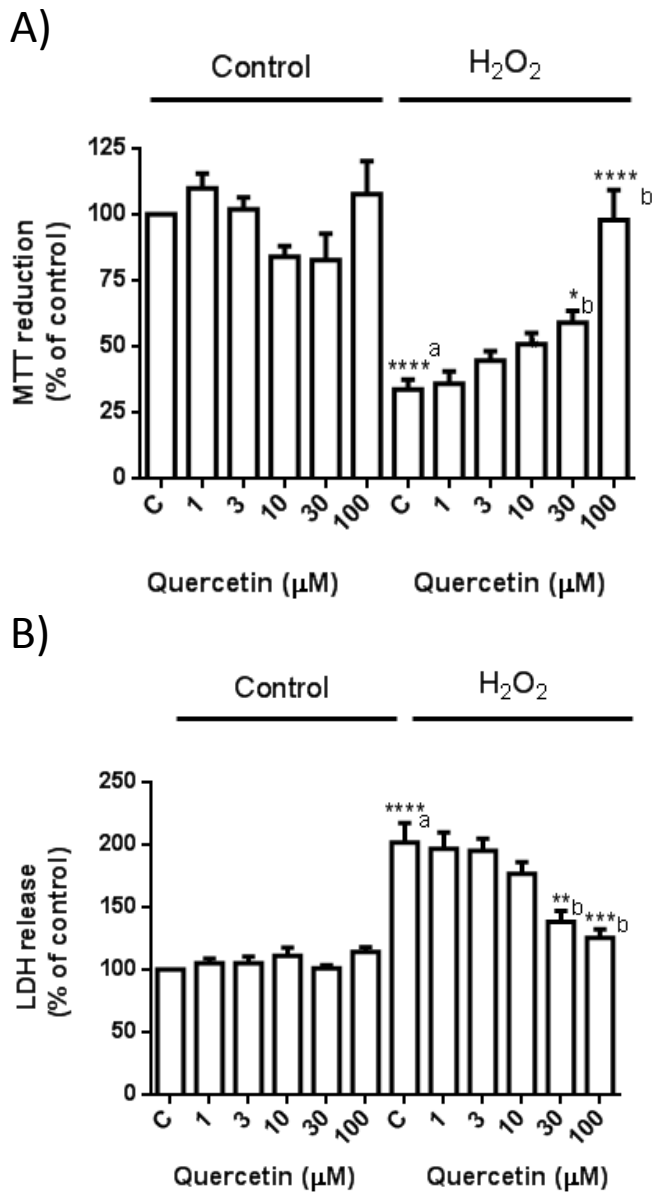


Fig. 4.9 Effect of 24 h quercetin pre-treatment on cell viability during H₂O₂ induced oxidative stress. Measured by A) MTT reduction assay and B) LDH release assay. Hydrogen peroxide caused significant (****: $p < 0.001$; a denotes significance vs untreated control cells) cell death compared to control cells. The MTT reduction assay showed that several concentrations of quercetin induced significant protection; 100 μM (****: $p < 0.001$) and 30 μM (*: $p < 0.05$) from cell death compared to hydrogen peroxide alone (b denotes significance vs H₂O₂ treatment). LDH assays showed that 100 μM (****: $p > 0.005$) and 30 μM (**: $p > 0.01$) caused significant protection compared to hydrogen peroxide treatment. Data are expressed as the percentage of control cells (C = 100 %) and represent the mean \pm SEM of six independent experiments.

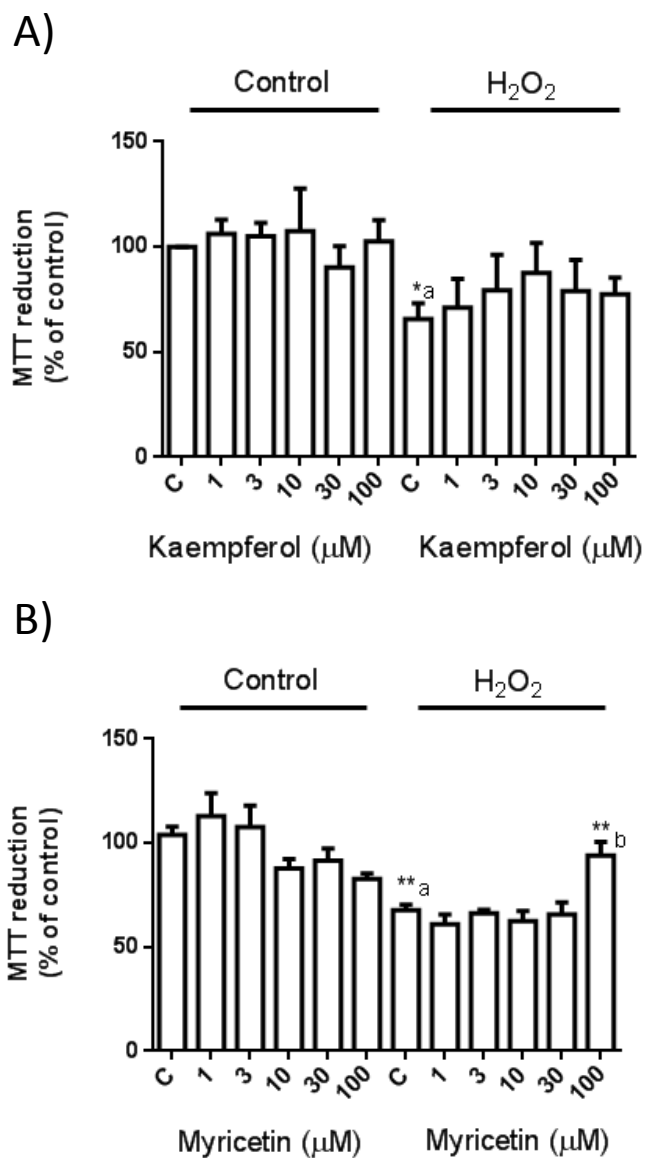


Fig. 4.10 Protective effect of 24 h flavonoid pretreatment on differentiated H9c2 cell viability after H₂O₂ treatment. H₂O₂ treatment caused a significant decrease in MTT reduction in both experiments (A, *: $p > 0.05$; B, **: $p > 0.05$; a denotes significance vs untreated control cells). 24 h kaempferol pretreatment caused no significant protective effect with any concentration tested, whereas 100 μM myricetin caused a significant (**: $p > 0.01$; b denotes significance vs H₂O₂ treatment) protective effect as measured by MTT reduction. Data are expressed as the percentage of control cells (C = 100 %) and represent the mean \pm SEM of three independent experiments.

As demonstrated by Figs. 4.9 and 4.10, quercetin was again shown to be the most potent flavonoid in terms of inducing a protective effect against H₂O₂ induced cell death after 24 h pre-treatment. The protective effect of 24 h pretreatment with myricetin was only induced with 100 μM concentration, and Kaempferol showed no significant protective effect. This protective effect can be further demonstrated by observing the cellular morphology, as shown in Fig. 4.11. The cellular damage induced by H₂O₂ treatment is visible in the form of damaged cells in cells treated with H₂O₂ and those pre-treated with 100 μM kaempferol, whereas cells pre-treated with 100 μM quercetin and myricetin show little damage, further illustrating the cytoprotective effect.

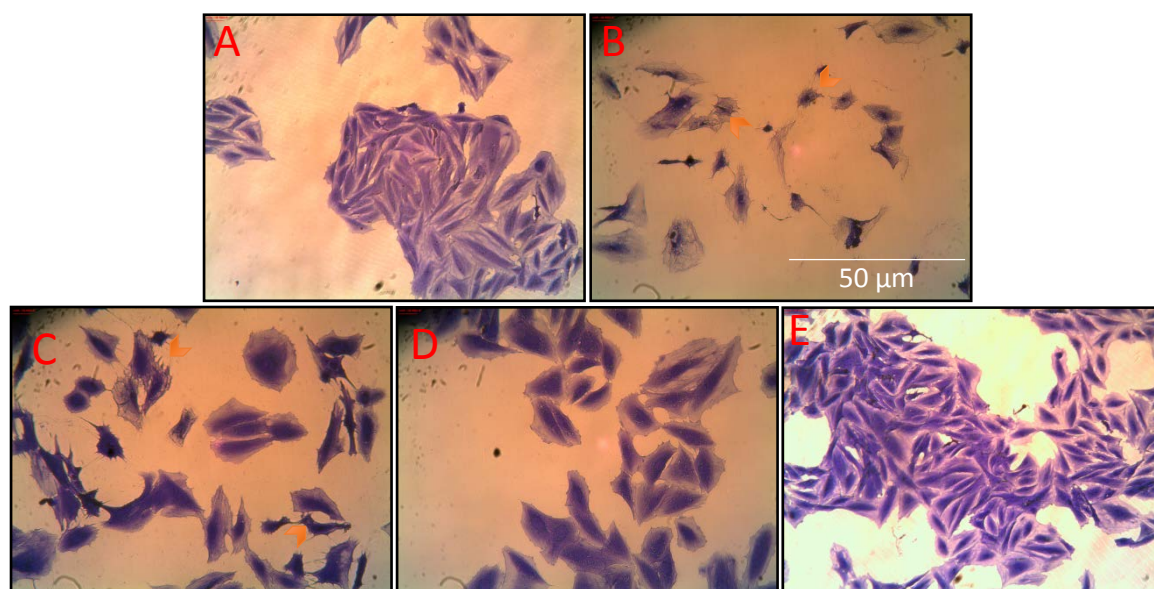


Fig. 4.11 The effect of flavonoid pre-treatment on visible cellular damage from H₂O₂ exposure. A) Untreated differentiated H9c2 cells. B) differentiated H9c2 cells exposed to 600 μM H₂O₂ for 2 h. C) Differentiated H9c2 cells pretreated for 24 h with 100 μM kaempferol and exposed to 600 μM H₂O₂ for 2 h. D) Differentiated H9c2 cells pretreated for 24 h with 100 μM myricetin and exposed to 600 μM H₂O₂ for 2 h. E) Differentiated H9c2 cells pretreated for 24 h with 100 μM quercetin and exposed to 600 μM H₂O₂ for 2 h. Visible cellular damage (red arrowheads) is present in images B and C. Stained with Coomassie blue.

4.4 Cytoprotective effects of flavonoid pre-treatment hypoxia induced cell death

Differentiated H9c2 cardiomyocytes were pre-treated with various concentrations of three different flavonoids; myricetin, kaempferol and quercetin. Firstly, differentiated H9c2 cells were pre-treated with 30 μM or 100 μM of flavonoid for 1 h and then exposed to 24 h hypoxia (0.5 % O_2), viability was then measured using MTT reduction

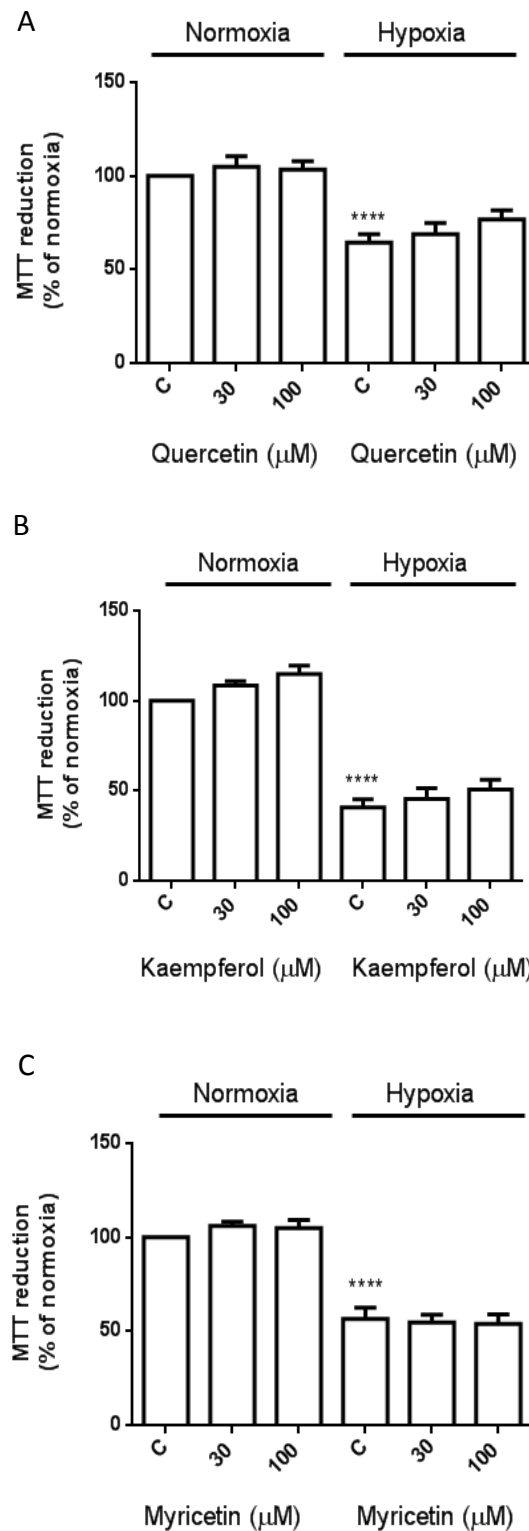


Fig 4.12 Effect of 1 h flavonoid pretreatment on differentiated H9c2 cell viability after 24 h hypoxia. In each experiment 24 h hypoxia caused a significant (****: $p < 0.001$) loss in cell viability as measured by MTT reduction assay. With all flavonoids tested (A: Quercetin, B: Kaempferol, C: Myricetin) 1 h pretreatment with 100 μM or 30 μM was not sufficient to cause any significant protective effect. Data are expressed as the percentage of control normoxia cells (normoxia C = 100 %) and represent the mean \pm SEM of three independent experiments.

As evidenced by Fig. 4.12, 1 h pretreatment with flavonoids proved to be insufficient to stimulate a protective effect with the concentrations tested. Therefore the effect of 24 h pretreatment with flavonoids was assayed with regard to the ability to induce a protective effect against 24 h hypoxia exposure using MTT reduction assay.

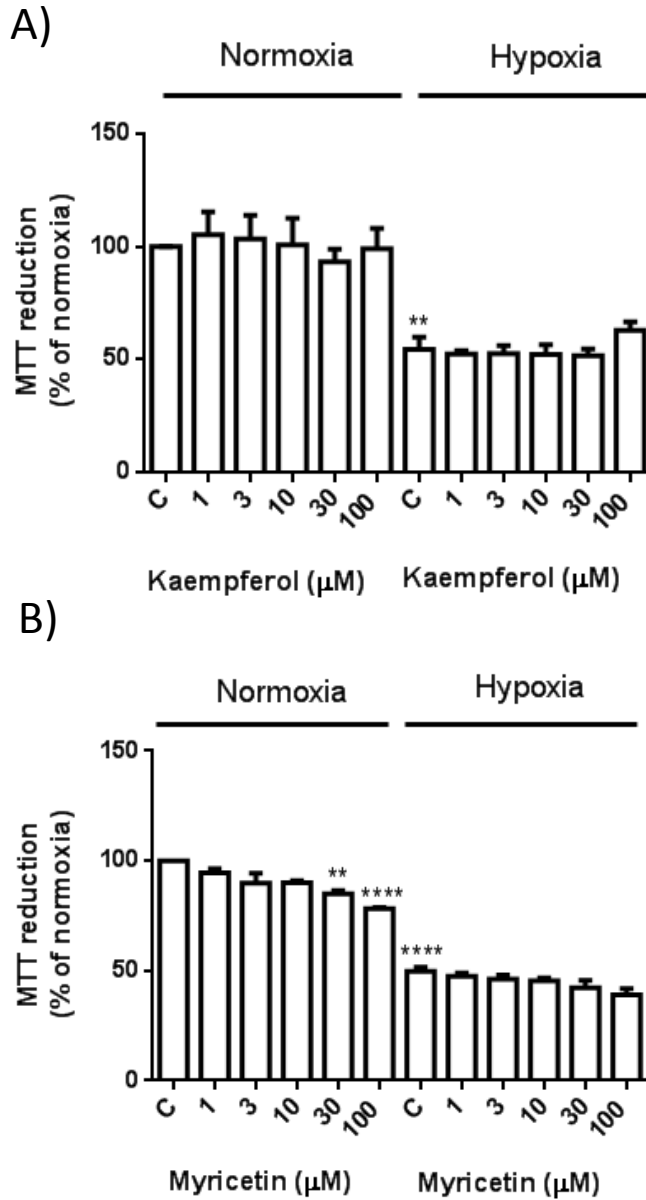


Fig. 4.13 Effect of 24 h flavonoid pretreatment on H9c2 cell viability after 24 h hypoxia. In both incidences 24 h hypoxia caused a significant decrease in MTT reduction compared to normoxia controls. Kaempferol (A) and myricetin (B) at all concentrations tested failed to induce a significant protective effect in differentiated H9c2 cells after 24 h pretreatment. 24 h pretreatment with 30 μM and 100 μM myricetin caused a significant decrease in MTT reduction after 24 h pretreatment in normoxic conditions (**: $p < 0.01$; ****: $p < 0.001$). Data are expressed as the percentage of control normoxia cells (normoxia C = 100 %) and represent the mean \pm SEM of three independent experiments.

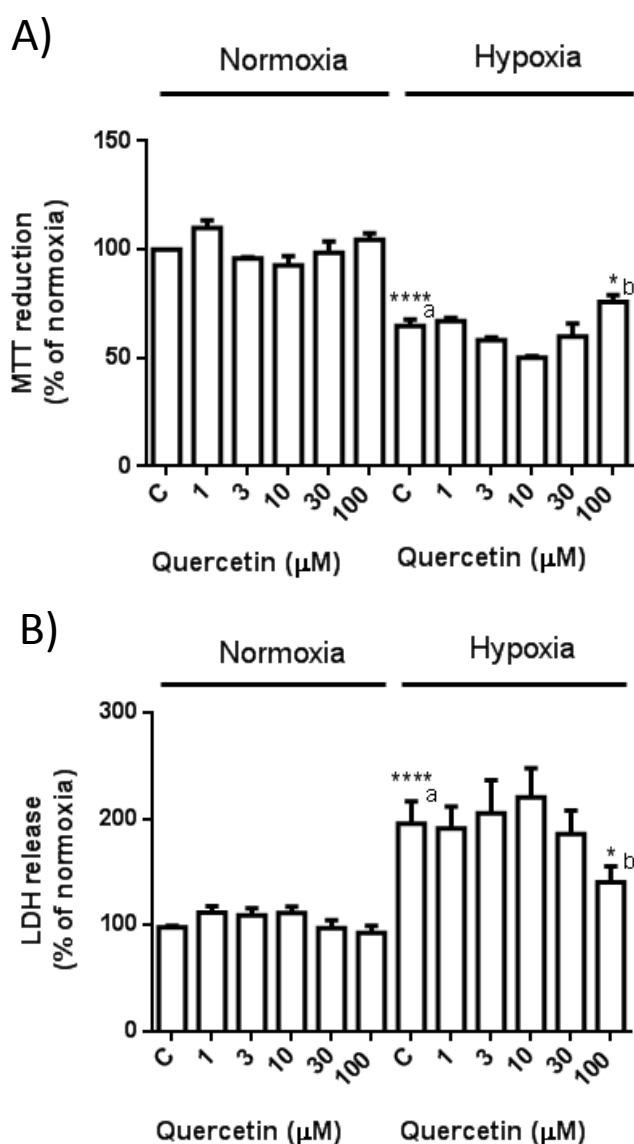


Fig. 4.14 Effect of 24 h quercetin pre-treatment on cell viability during 24 h hypoxia induced oxidative stress. Measured by A) MTT reduction assay and B) LDH release assay. 24 h hypoxia caused significant (****: $p < 0.001$; a denotes significance vs untreated control cells) cell death. Both MTT reduction and LDH release assays showed 24 h pre-treatment with 100 μM quercetin induced significant (*: $p < 0.05$; b denotes significance vs H_2O_2 treatment) protection from cell death compared to hypoxia cells alone. Data are expressed as the percentage of control normoxia cells (normoxia C = 100 %) and represent the mean \pm SEM of nine independent experiments.

As demonstrated in figures 4.13 and 4.14 24 h pre-treatment with 100 μM quercetin was able to significantly protect differentiated H9c2 cells from oxidative stress caused by both hypoxia and H_2O_2 treatment. Furthermore, 30 μM quercetin pretreatment was shown to be protective against H_2O_2 treatment with both assay methods. Therefore, 100 and 30 μM quercetin pretreatment was selected to be used for investigations into the cell signaling pathways involved in quercetin mediated cytoprotection.

4.5 Protective effects of quercetin metabolites

The protective effect of the two major metabolites of quercetin, 3'-*O*-methyl quercetin (Q3M) and quercetin-3-glucuronide (Q3G), against 2 h 600 μ M H₂O₂ exposure was tested using MTT reduction and LDH release assays. Fig. 4.15 shows that 100 μ M Q3M pre-treatment for 24 h was sufficient to illicit a significant protective, whereas Q3G showed no such effect, this may be a consequence of the less lipophilic nature of Q3G.

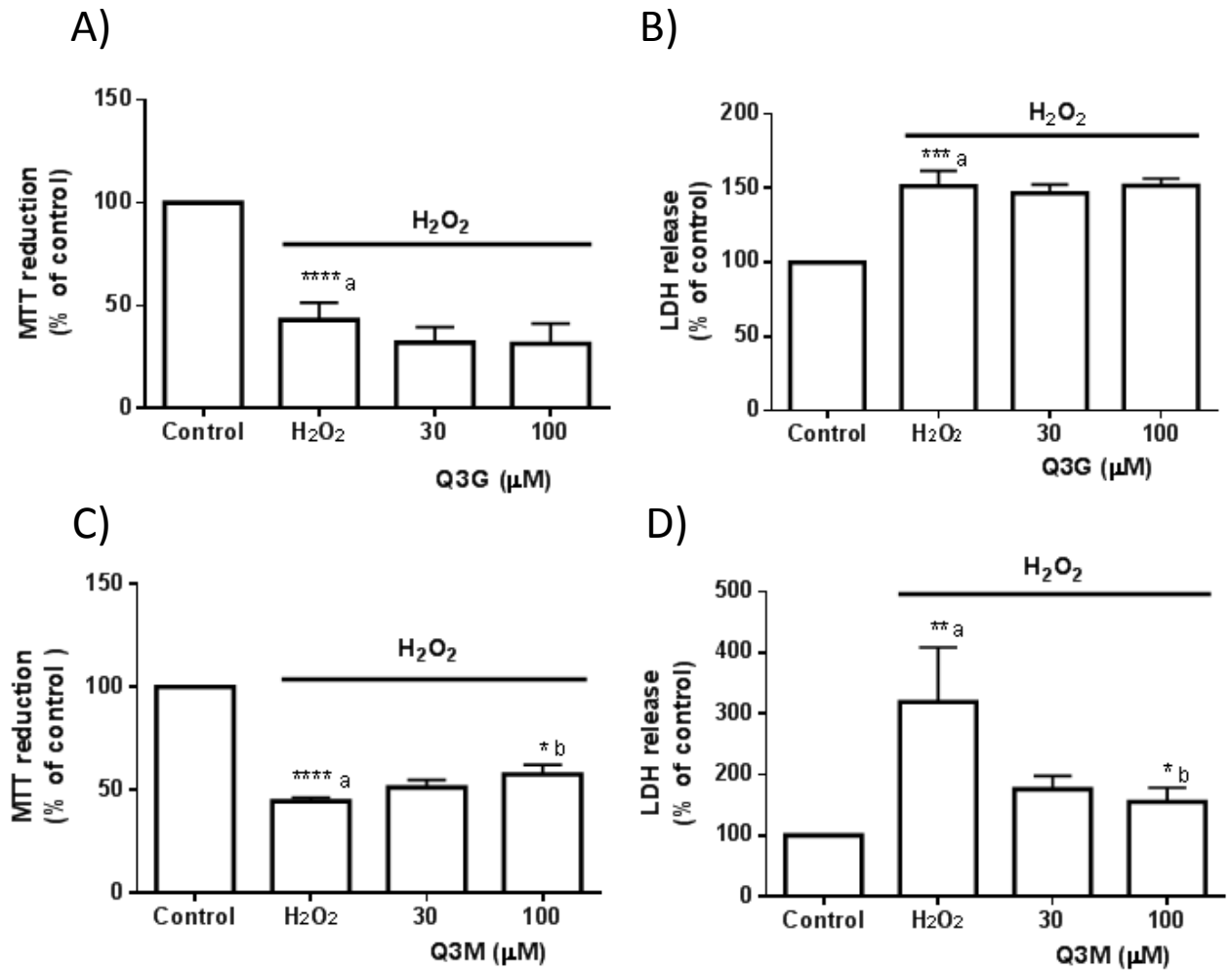


Fig. 4.15 Protective effect of 24 h quercetin metabolite pretreatment on differentiated H9c2 cell viability after H₂O₂ treatment. H₂O₂ treatment caused a significant decrease in MTT reduction and increase LDH release in all experiments (A and C, ****: $p > 0.001$; B, ***: $p > 0.005$; D, **: $p < 0.01$; a denotes significance vs untreated control cells). 24 h Q3G pre-treatment caused no significant protective effect with any concentration tested (A and B), whereas 100 μM Q3M caused a significant (*: $p > 0.05$; b denotes significance vs H₂O₂ treatment) protective effect as measured by MTT reduction and LDH release. Data are expressed as the percentage of control cells (C = 100 %) and represent the mean ± SEM of five independent experiments.

4.6 Protein kinase phosphorylation during flavonoid mediated cardioprotection against hydrogen peroxide

As previously observed 30 μM and 100 μM concentrations of quercetin was able to induce a significant cardioprotective effect after 24 h pre-treatment in differentiated H9c2 cardiomyocytes against oxidative stress caused by exposure to 600 μM H_2O_2 . To investigate the mechanism of this cardioprotective effect western blotting was used to monitor the phosphorylation of four protein kinases involved in cell survival and cell death; ERK1/2, PKB, p38 MAPK and JNK. Differentiated H9c2 cells were pre-treated for 24 h with 30 μM or 100 μM quercetin, the flavonoid was removed and the cells then exposed to 600 μM H_2O_2 for 2 h, after which the cells were lysed and western blotting performed.

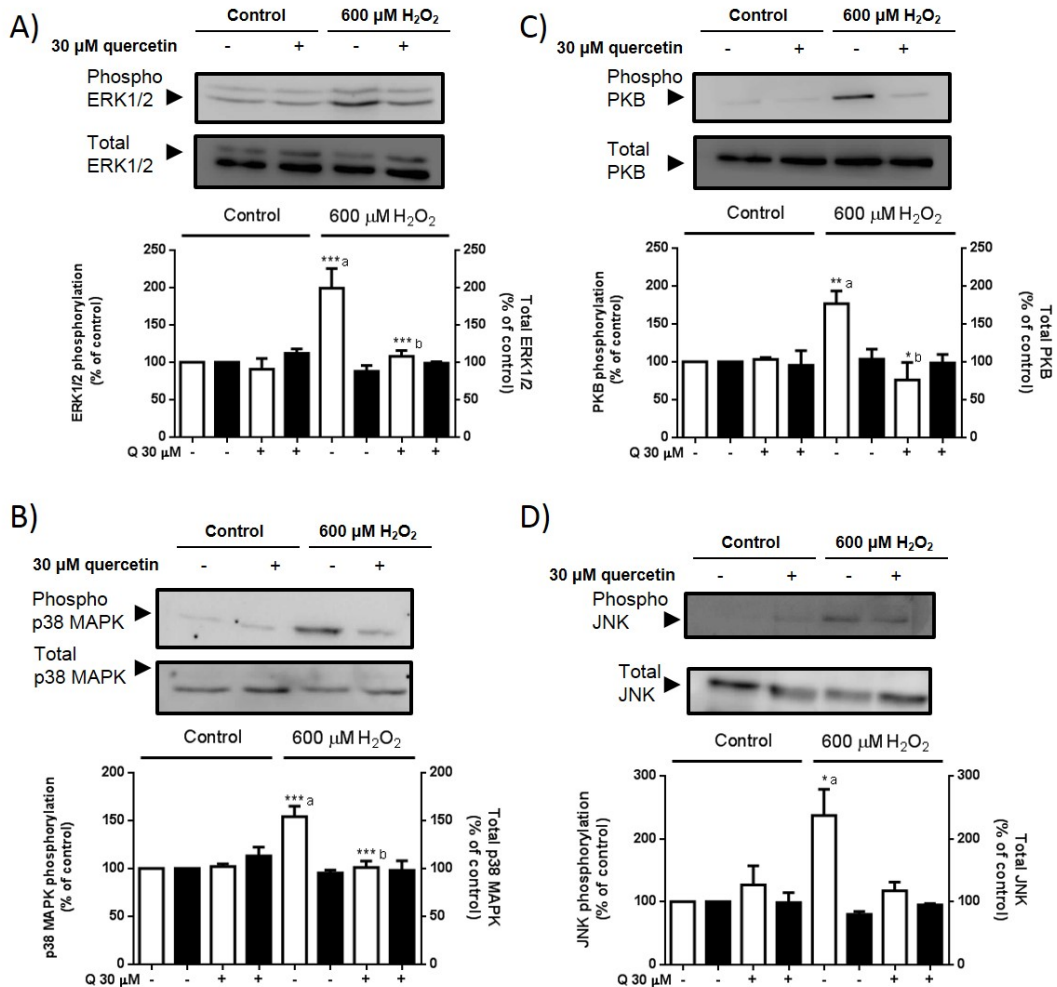


Fig. 4.16 Effect of 30 μM quercetin on H₂O₂-induced protein kinase activation. Differentiated H9c2 cells (7 days) were treated with 30 μM quercetin 24 h prior to 2 h insult with 600 μM H₂O₂, cells were then lysed and western blotting performed using specific antibodies for phosphorylated and total A) ERK1/2, B) p38 MAPK, C) PKB and D) JNK. In all incidences exposure with 600 μM H₂O₂ caused a significant increase in phosphorylation of the protein kinases (A & B, ***: p < 0.005; C, **: p < 0.01; D, *: p < 0.05; a denotes significant vs control cells). A significant reduction in phosphorylation of ERK1/2, PKB and p38 MAPK was observed in cells pre-treated for 24 h with 30 μM quercetin and then exposed to 600 μM H₂O₂ (A & B, ***: p < 0.005; C, *: p < 0.05; b denotes significance vs H₂O₂ treated cells). No significant variation was observed in total specific blots of each protein kinase. Data are expressed as a percentage of control cells (control = 100%) and represent the mean ±S.E.M of three independent experiments.

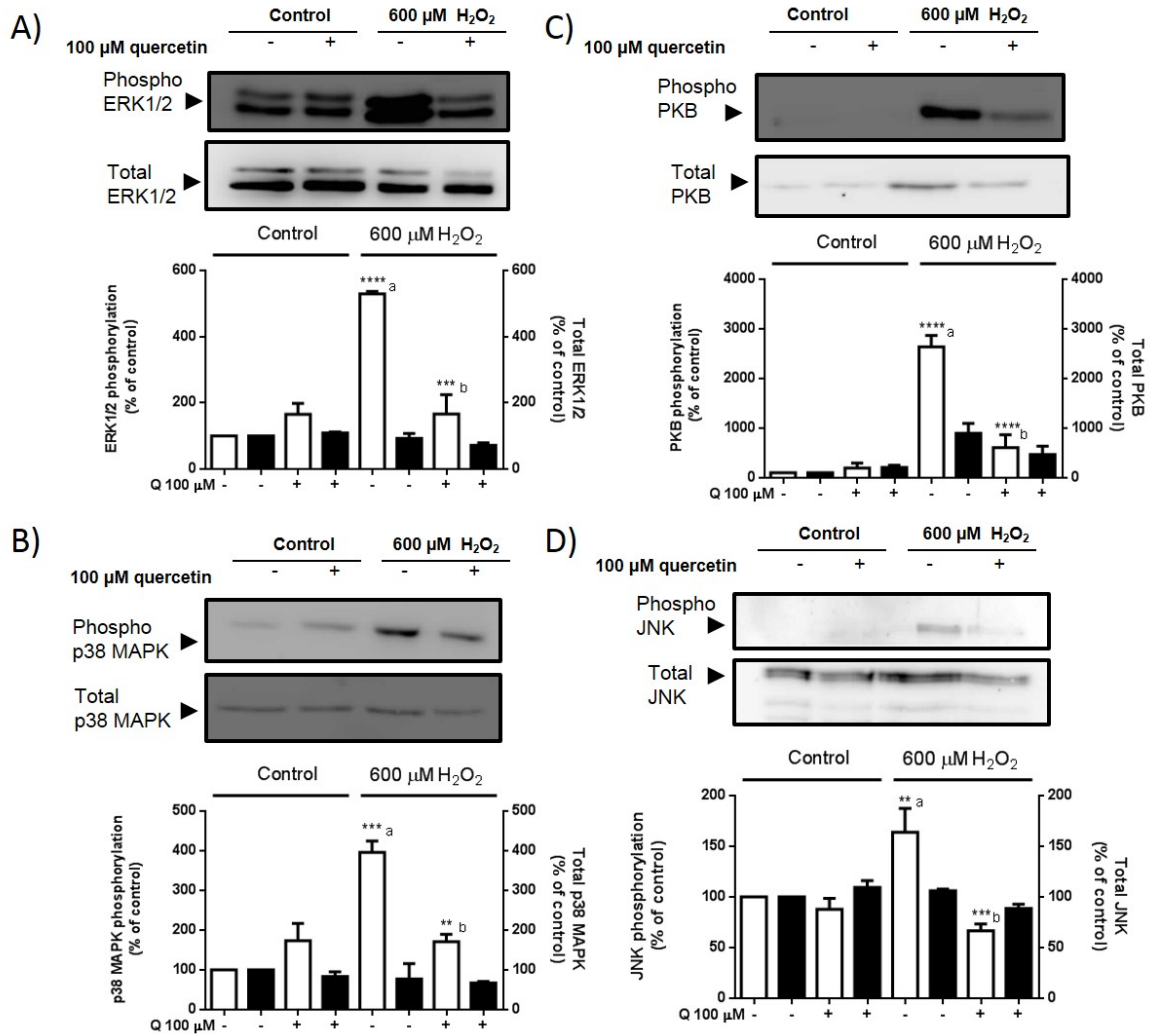


Fig. 4.17 Effect of 100 μM quercetin on H_2O_2 -induced protein kinase activation. Differentiated H9c2 cells (7 days) were treated with 100 μM quercetin 24 h prior to 2 h insult with 600 μM H_2O_2 , cells were then lysed and western blotting performed using specific antibodies for phosphorylated and total A) ERK1/2, B) p38 MAPK, C) PKB and D) JNK. In all incidences exposure to 600 μM H_2O_2 caused a significant increase in phosphorylation of the protein kinases (A & C, ****: $p < 0.001$; B, ***: $p < 0.005$; D, **: $p < 0.01$; a denotes significant vs control cells). A significant reduction in phosphorylation of ERK1/2, PKB, p38 MAPK and JNK was observed in cells pre-treated for 24 h with 100 μM quercetin and then exposed to 600 μM H_2O_2 (C, ****: $p < 0.001$; A & D, ***: $p < 0.005$; B, **: $p < 0.01$; b denotes significance vs H_2O_2 treated cells). No significant variation was observed in total specific blots of each protein kinase. Data are expressed as a percentage of control cells (control = 100 %) and represent the mean \pm S.E.M of three independent experiments.

As can be observed in Figs. 4.16 and 4.16, exposure to 600 μM H_2O_2 for 2 h consistently induces a significant increase in phosphorylation of ERK1/2, PKB, p38 MAPK and JNK in differentiated H9c2 cardiomyocytes. Generally it can be seen that in after pre-treatment with quercetin the protein kinases expression is inhibited when compared to the activation that occurs during the treatment with H_2O_2 .

4.7 Protein kinase phosphorylation during flavonoid mediated cardioprotection against hypoxia

As previously observed 100 μM concentration of quercetin was able to induce a significant cardioprotective effect after 24 h pre-treatment in differentiated H9c2 cardiomyocytes against ischaemic damage caused incubation in hypoxic conditions for 24 h. Four cell signalling molecules; ERK1/2, PKB, p38 MAPK and JNK were once again used to investigate the mechanism of the flavonoid mediated cardioprotective effect. Differentiated H9c2 cells were pre-treated for 24 h with 30 μM or 100 μM quercetin, the flavonoid was removed and the cells then incubated in hypoxic condition (0.5 % O_2) for 24 h, after which the cells were lysed and western blotting performed.

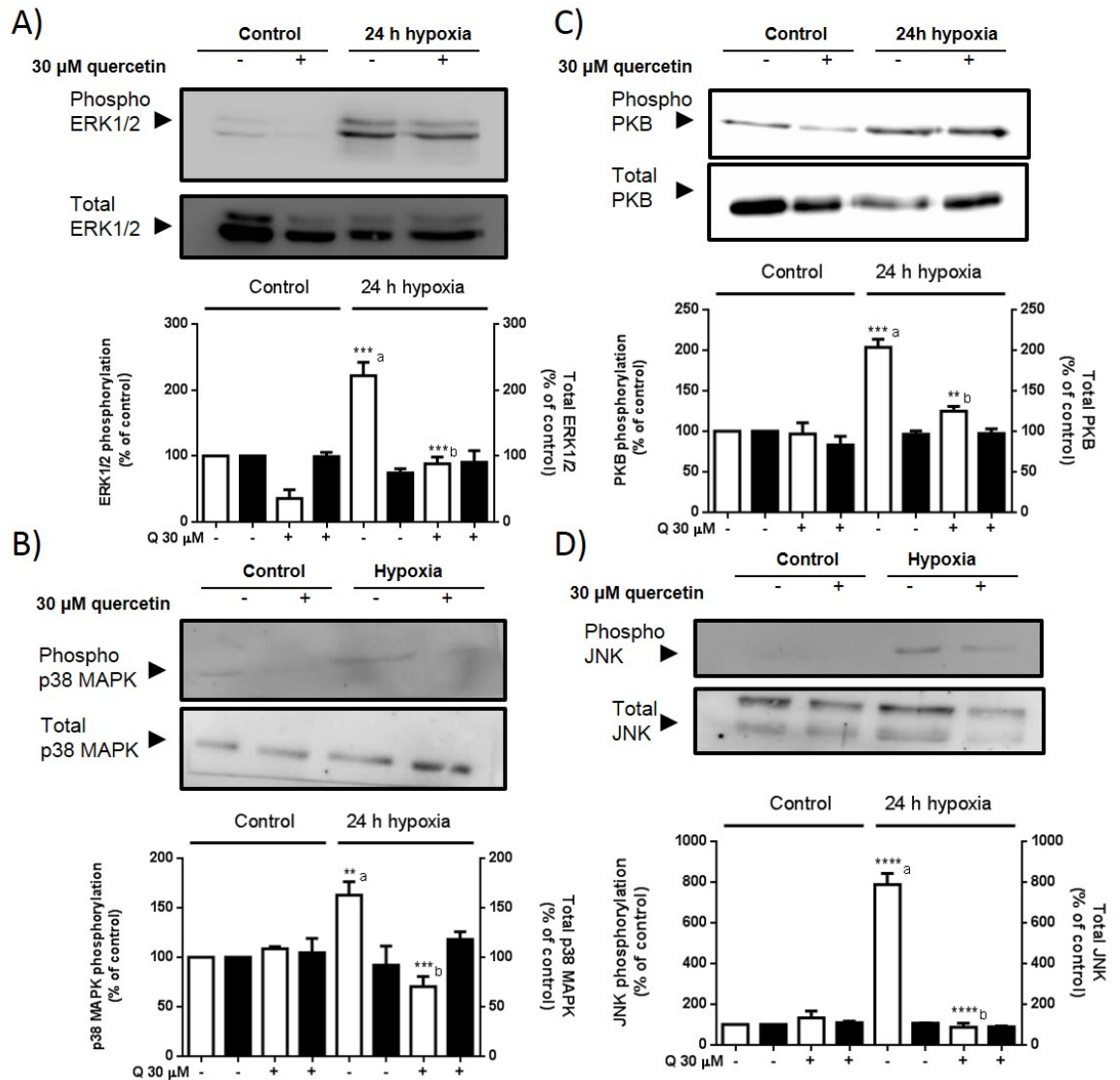


Fig. 4.18 Effect of 30 μM quercetin on hypoxia-induced protein kinase activation. Differentiated H9c2 cells (7 days) were treated with 30 μM quercetin 24 h prior to 24 h incubation in hypoxic conditions, cells were then lysed and western blotting performed using specific antibodies for phosphorylated and total A) ERK1/2, B) p38 MAPK, C) PKB and D) JNK. In all incidences hypoxic incubation caused a significant increase in phosphorylation of the protein kinases (D, ****: $p < 0.001$; A & C, ***: $p < 0.005$; B, **: $p < 0.01$; a denotes significant vs control normoxia cells). A significant reduction in phosphorylation of ERK1/2, PKB, p38 MAPK and JNK was observed in cells pre-treated for 24 h with 30 μM quercetin prior to hypoxic incubation for 24 h (D, ****: $p < 0.001$; A & B, ***: $p < 0.005$; C, **: $p < 0.01$; b denotes significance vs hypoxia incubated cells). Data are expressed as a percentage of control cells in normoxic conditions (control = 100%) and represent the mean \pm S.E.M of three independent experiments.

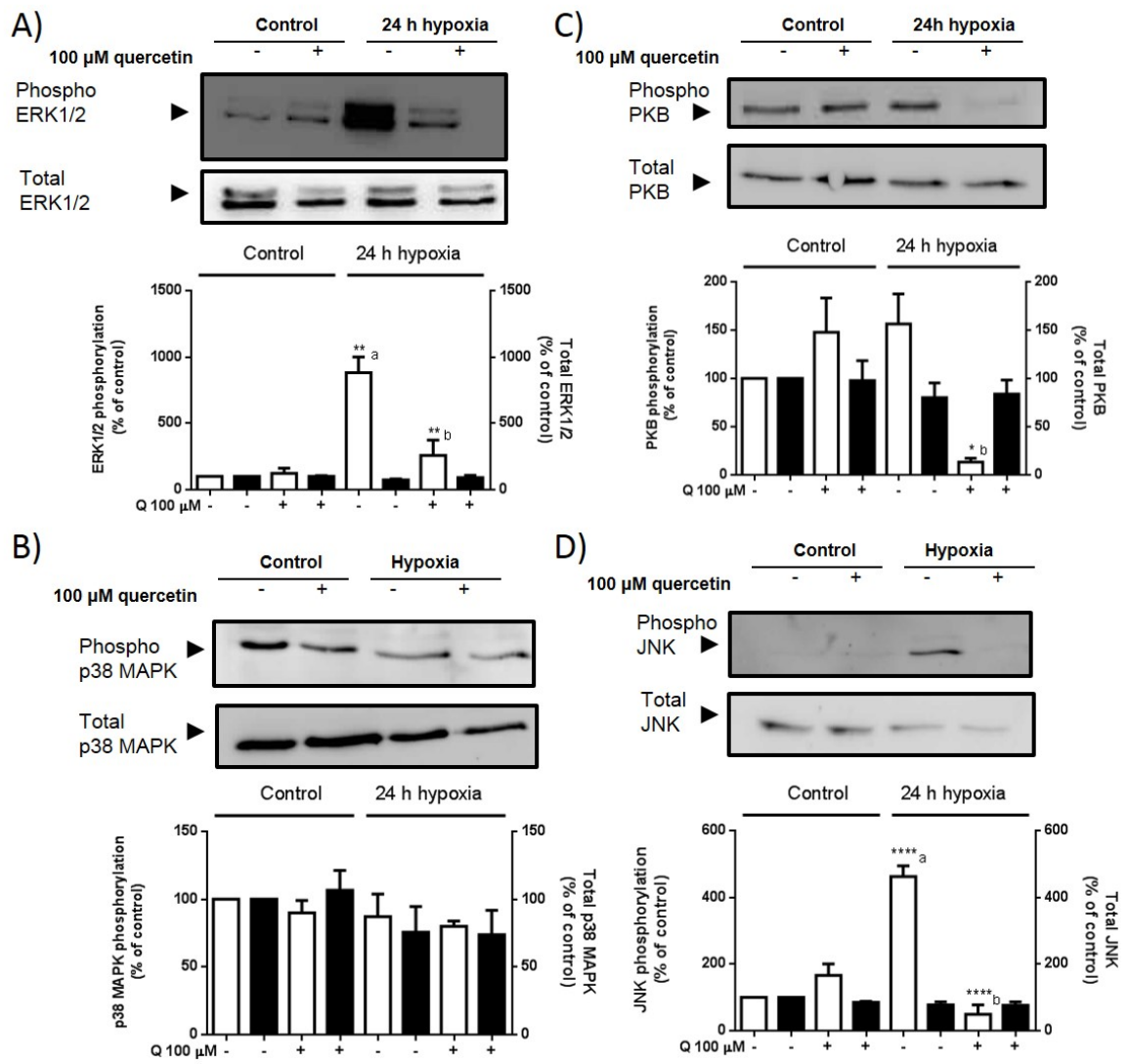


Fig. 4.19 Effect of 100 μM quercetin on hypoxia-induced protein kinase activation. Differentiated H9c2 cells (7 days) were treated with 100 μM quercetin 24 h prior to 24 h incubation in hypoxic conditions, cells were then lysed and western blotting performed using specific antibodies for phosphorylated and total A) ERK1/2, B) p38 MAPK, C) PKB and D) JNK. Only ERK1/2 and JNK saw a significant increase in phosphorylation after hypoxic incubation (A, **: $p < 0.01$; D, ****: $p < 0.001$; a denotes significant vs control normoxia cells). A significant reduction in phosphorylation of ERK1/2, PKB and JNK was observed in cells pre-treated for 24 h with 100 μM quercetin prior to hypoxic incubation for 24 h (D, ****: $p < 0.001$; A, **: $p < 0.01$; B, *: $p < 0.05$; b denotes significance vs hypoxia incubated cells. Data are expressed as a percentage of control cells in normoxic conditions (control = 100%) and represent the mean \pm S.E.M of three independent experiments.

As shown in figs. 4.18 and 4.19 24 h pre-treatment with 30 μ M and 100 μ M quercetin has a significant effect on the phosphorylation of protein kinases during hypoxic incubation. Mainly the protein kinases are present in their phosphorylated form at higher levels during hypoxia, and 24 h pre- treatment with quercetin causes this to decrease. This reduction in phosphorylation of protein kinases may be involved in the cardioprotective mechanism of flavonoids.

4.8 protein kinase inhibitors and flavonoids mediated cardioprotection

Inhibition of protein kinases by quercetin may be part of the mechanism of flavonoid mediated cardioprotection. Specific protein kinase inhibitors were used to investigate the effect of inhibition of these protein kinases, and to potentially mimic the inhibitory characteristics and cardioprotective effect of quercetin in particular and flavonoids in general.

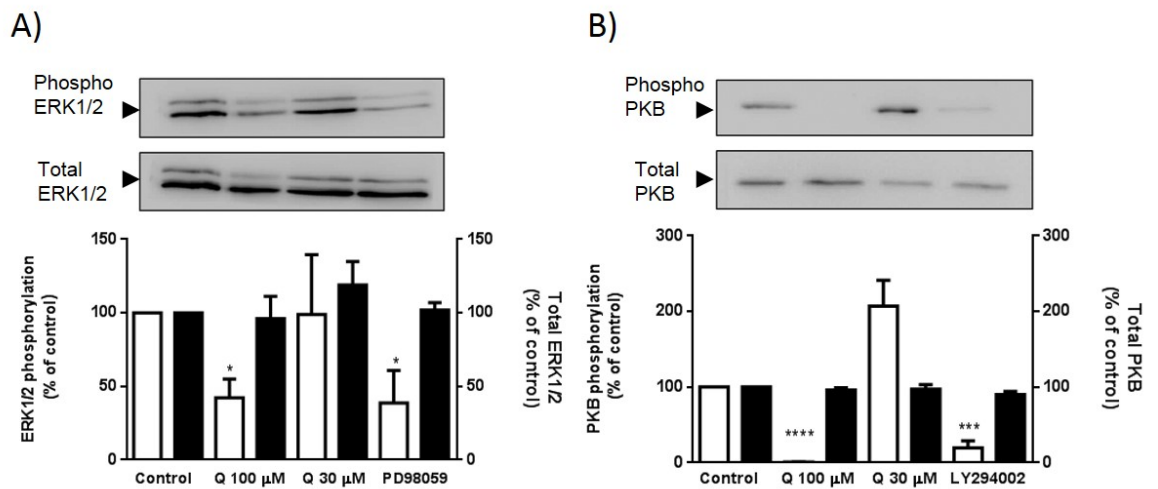


Fig. 4.20 Effect of quercetin on ERK1/2 and PKB phosphorylation. Differentiated H9c2 cells (7 days) were treated with 100 μM, 30 μM quercetin for 24 h or PD98059 (50 μM, MEK1/2 inhibitor) and LY294002 (30 μM, PI3K inhibitor) for 30 min. Cells were then lysed and analysed using western blotting for A) Phospho-ERK1/2 or B) Phospho-PKB using phosphor-specific antibodies. Separate samples were analysed using antibodies that recognise total ERK1/2 and PKB. Treatment with 100 μM quercetin (Q 100 μM) was shown to cause a significant inhibitory effect (A, *: $p < 0.05$; B, ****: $p > 0.001$) on both ERK1/2 and PKB that is comparable with the effect of the specific inhibitors PD98059 and LY294002 (A, *: $p < 0.05$; B, ***: $p > 0.005$). Data are expressed as a percentage of control cells in conditions (control = 100%) and represent the mean \pm S.E.M of three independent experiments.

The effects of the specific inhibitors PD98059 and LY294002 were shown to be comparable to 100 μM quercetin after 24 h exposure. The protective effect of protein kinase inhibition against 600 μM H_2O_2 exposure and the potential ameliorative effect of these specific inhibitors on quercetin mediated cardioprotection was then investigated by MTT reduction assay. In addition to PD98059 (50 μM , MEK1/2 inhibitor) and LY294002 (30 μM , PI3K inhibitor), Wortmannin (100 nM, PI3K inhibitor), SB203580 (30 μM , p38 MAPK inhibitor) and SP600125 (10 μM , JNK inhibitor) were used to investigate the effect of protein kinase inhibition of cardioprotection.

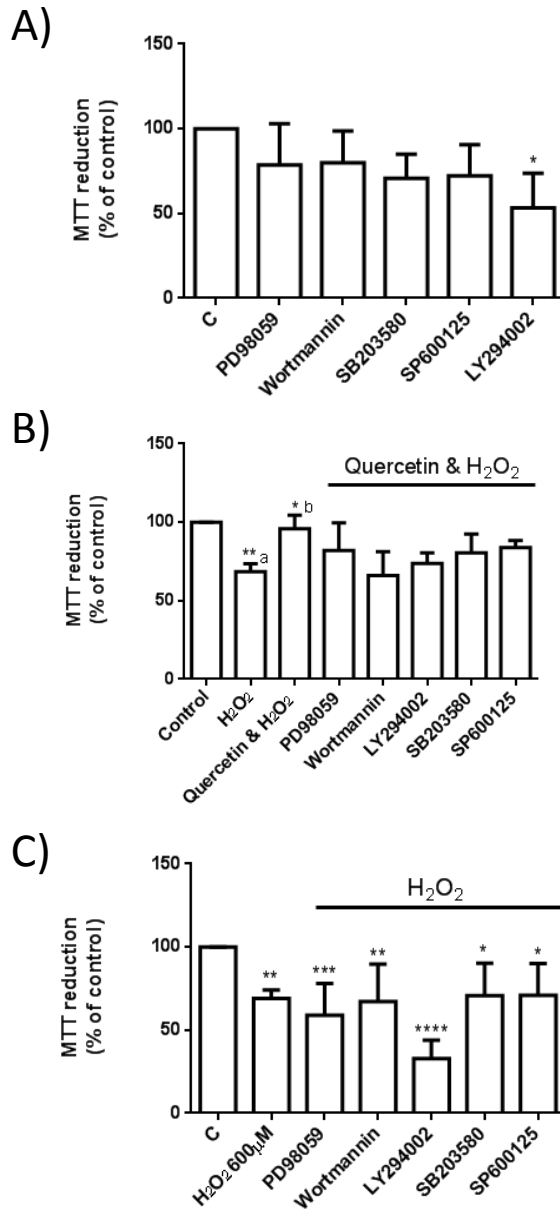


Fig. 4.21 Effect of protein kinase inhibitors on quercetin-induced cardioprotection. **A)** differentiated H9c2 cells were exposed to protein kinase inhibitor for 24 h. 24 h exposure to LY294002 caused a significant (*: $p < 0.05$) decrease in MTT reduction. **B)** Differentiated H9c2 cells were treated with kinase inhibitor for 30 min prior to 24 h exposure to 30 μM quercetin, after which the cells were exposed to 600 μM H_2O_2 for 2 h. Exposure to 600 μM H_2O_2 for 2 h caused a significant (**: $p < 0.01$; a denotes significance vs untreated control) decrease in MTT reduction. Without inhibitor pre-treatment, 30 μM quercetin pre-treatment for 24 h induced a significant (*: $p < 0.05$; b denotes significance vs H_2O_2 treated control) protective effect. No significant difference was observed vs the untreated control or and H_2O_2 treated control in those cells pre-treated with inhibitor prior to 24 h exposure to 30 μM quercetin. **C)** Differentiated H9c2 cells were exposed to protein kinase inhibitor for 24 h and then exposed to 600 μM H_2O_2 for 2 h. Exposure to 600 μM H_2O_2 for 2 h caused a significant (**: $p < 0.01$) decrease in MTT reduction vs untreated control. 24 h exposure to inhibitors induced no significant protective effect as each was shown to have a significant decrease in MTT reduction compared to the untreated control (PD98059, **: $p < 0.01$; Wortmannin, ***: $p < 0.005$; LY294002, ****: $p < 0.001$; SB203580 & SP600125, *: $p < 0.05$). Data are expressed as a percentage of control cells in conditions (control = 100%) and represent the mean \pm S.E.M of six independent experiments.

From Fig. 4.21 it can be seen that acting singularly protein kinase inhibitors do not confer a protective effect that is comparable to that of quercetin, nor was the protective effect of quercetin perturbed by the presence of inhibitors.

4.9 Results summary

Quercetin was shown to have a cytoprotective effect on differentiated H9c2 cells, as it was able to protect differentiated H9c2 cells from damage from H₂O₂ treatment with a pre-treatment time of 1 h as well as 24 h. The results further demonstrated that this protective effect can be elicited by a concentration of 30 µM quercetin, which may be achievable pharmacologically *in vivo*, considering intracellular and plasma accumulation after repeated doses. Quercetin was able to protect differentiated H9c2 cells from death caused by hypoxia at 100 µM with a pre-treatment time of 24 h. Of the two quercetin metabolites tested 3'-O-methyl quercetin was found to exhibit a similar protective effect to quercetin against cell death caused by H₂O₂ exposure, whereas quercetin-3-glucorinde showed no protective effect. The protective effect of quercetin pre-treatment is likely associated with the inhibitory effect on protein kinases demonstrated in 4.6. The inhibitory effect of 30 µM and 100 µM quercetin pre-treatment on the phosphorylation of ERK1/2, PKB, JNK and p38 MAPK during H₂O₂ treatment and hypoxia further suggests that this is a potential mechanism of the protective effect of quercetin.

4.10 Discussion of flavonoid mediated cytoprotective effect

This chapter investigated the potential cytoprotective effects of quercetin, kaempferol, myricetin and two of the major quercetin metabolites, 3'-O-methyl quercetin and quercetin-3-glucuronide. Specifically with regard to their ability to protect differentiated H9c2 cells from oxidative induction of cell death from H₂O₂ exposure or incubation in hypoxic conditions.

i) Mitotic and differentiated cell comparison

Firstly the optimal concentration and exposure time for H₂O₂ treatment on differentiated and mitotic H9c2 cells was determined in order to compare the susceptibility to oxidative cell death. As illustrated in Figs. 4.3 and 4.4 mitotic H9c2 cells require exposure to a higher concentration of H₂O₂ compared to differentiated H9c2 cells (Figs 4.1 and 4.2). The observed increased susceptibility of the differentiated H9c2 cells to cell death from H₂O₂ exposure is in agreement with the observation made in previous studies, which have shown that differentiated H9c2 cells have a reduced oxidative capacity (Comelli *et al*, 2011). This finding further demonstrates the value of using differentiated H9c2 cells as a model cell line for the present study. The reduced oxidative capacity of the cardiomyocyte-like phenotype of the differentiated H9c2 cell is more similar to *in vivo* cardiomyocytes than that of the embryonic cardiomyoblast undifferentiated H9c2 cell. The cytoprotective effect of the studied flavonoids will thus be better reflective of the actions of flavonoids on cardiomyocytes *in vivo*. The susceptibility of the differentiated H9c2 cells to cell death from incubation in hypoxic conditions for various times was investigated. Incubation for 24 h was shown to have the most significant effect on cell viability, measured by MTT reduction (Fig 4.5).

ii) Flavonoid-mediated cytoprotection from H₂O₂ exposure

With the establishment of the optimal conditions of inducing cell death through H₂O₂ exposure and incubation in hypoxic conditions the cytoprotective effect of the flavonoids and the major quercetin metabolites could then be assayed. Firstly, 1 h pre-treatment with myricetin was shown to be ineffective in inducing cytoprotection against H₂O₂ exposure. Quercetin was able to induce a consistent protective effect after 1 h pre-treatment, observed with both LDH release and MTT reduction assays. The protective effect of

kaempferol was observed only with the LDH release assay. The observation that kaempferol did not show a protective effect after 1 h pre-treatment measured by the MTT reduction assay makes it difficult to confirm if a protective effect was induced, as the LDH release assay has been previously shown to be less reliable in terms of detecting cytotoxic insults compared to MTT reduction (Fotakis *et al*, 2006). It is preferable therefore to observe a protective effect with both MTT reduction and LDH release. After 24 h pre-treatment quercetin was able to induce a significant cytoprotective effect with 30 μ M and 100 μ M concentrations. This finding is in agreement with other studies using mitotic H9c2 cells as a model system, it is of note that this present study is the first to identify this cytoprotective effect of quercetin in differentiated H9c2 cells (Angeloni *et al*, 2007). No observable cytoprotective effect was induced by 24 h pre-treatment with myricetin at the concentrations tested. This contrasts with studies that have previously shown myricetin to be able to protect cells from oxidative stress induced apoptosis, although these studies were not using cardiomyocyte cells as a model system (Kyoung *et al*, 2010). Cardiac effects induced by myricetin have been observed using a Langendorff perfused heart, where myricetin induced an increased concentration of intracellular cAMP, which may be related to cytoprotective effects (Angelone *et al*, 2011). Kaempferol was observed to have a potential cytoprotective effect against H₂O₂ exposure with 24 h pre-treatment with 100 μ M concentrations. This finding is the first concerning kaempferols cytoprotective effect on differentiated H9c2 cells against H₂O₂ exposure. Kaempferol has been previously shown to have a protective effect on mitotic H9c2 cells against simulated ischaemia/reperfusion injury, which may be partly mimicked by H₂O₂ exposure (Kim *et al*. 2008). The protective effect observed by Kim *et al*. (2008) was elicited from 10 μ M kaempferol, although this was using mitotic H9c2 cells as a model which have an inherently greater oxidative capacity (Comelli *et al*, 2011). The protective effect induced by the flavonoids myricetin and quercetin can be observed with morphological analysis (Fig. 4.11).

iii) Flavonoid-mediated cytoprotection from hypoxia

Pre-treatment (1 h) with myricetin, kaempferol and quercetin was not able to induce a significant cytoprotective effect from cell death caused by 24 h incubation in hypoxic conditions. The non-induction of a cytoprotective effect was also observed with myricetin and kaempferol when differentiated H9c2 cells were pre-treated for 24 h with the flavonoid. This contrasts with the protective observation of a cytoprotective effect being observed with 24 h pre-treatment with myricetin against H₂O₂ exposure. As stated previously, kaempferol has been shown to have a protective effect against ischaemia/reperfusion injury. Several differences in methodology between the present study and that of Kim *et al.* (2008) may explain why no protective effect was observed in the present study with kaempferol pre-treatment. A protective effect using kaempferol was observed, ischaemia was induced for 12 h without the use of a hypoxic incubator and mitotic H9c2 cells were used as a model system. Furthermore cells were in the constant presence of kaempferol, in comparison to the present study where flavonoid was removed from the cell growth medium after pre-treatment and prior to hypoxic incubation (Kim *et al.* 2008). The present study is the first to use myricetin with differentiated H9c2 cells and a hypoxic model of oxidative stress induced cell death. Pre-treatment for 24 h with 100 µM quercetin was shown to have a cytoprotective effect against hypoxia induced cell death. This observation shows that when compared to the other two flavonoids tested, quercetin was the most effective in inducing a cytoprotective effect, as it was observed to protect cells from both hypoxic and H₂O₂ exposure induced oxidative stress cell death, generally at 100 µM concentrations.

iv) Cytoprotective effect of quercetin metabolites

The protective effects of 24 h pre-treatment with the two major quercetin metabolites, 3'-*O*-methylquercetin and quercetin-3-glucuronide, against H₂O₂ exposure was investigated (Fig. 4.15). It was demonstrated that 24 h pre-treatment with 100 µM 3'-*O*-methyl quercetin was able to induce a significant protective effect on the differentiated H9c2 cells. In contrast, quercetin-3-glucuronide was not able to produce any significant protective effect. The partition coefficient (LogP) of both metabolites and quercetin was calculated as follows; quercetin 3-glucuronide (-0.49), quercetin (1.68) and 3'-*O*-methyl quercetin (1.96). These LogP values show that quercetin and 3'-*O*-methylquercetin are similarly lipophilic, whereas

the negative LogP of quercetin 3-glucuronide suggests a greater lipophobicity. The lipophobic nature of quercetin-3-glucuronide may partially explain why no protective effect was elicited from 24 h pre-treatment. Migration through the cellular membrane and binding of quercetin-3-glucuronide to membrane bound proteins would be ameliorated by its lipophobic structure, which would prevent intracellular ROS scavenging (Chang *et al*, 2007). The hydroxyl group substitutions on the B ring of quercetin, as well as an unsaturated C2-C3 bond, allow it to bind with ATP binding sites in some enzymes (Williams *et al*, 2004). The hydroxyl group substitutions on the B ring of quercetin-3-glucuronide are changed from those of quercetin (Figs 1.4 & 1.7) (Williams *et al*, 2004). The structural differences between quercetin, kaempferol and myricetin may also partially explain why myricetin is able to induce a protective effect in differentiated H9c2 cells when insulted with H₂O₂ exposure. The partition coefficient of myricetin, 1.392, is quite similar to that of quercetin, were the partition coefficient of kaempferol was calculated as 2.172. These calculations suggest that all three flavonoids are lipophilic, and thus able to migrate through the cell membrane and potentially associate with membrane bound proteins. Structurally, both myricetin and kaempferol have the unsaturated C2-C3 present in quercetin, and myricetin has similar hydroxyl group substitutions on the B ring of the flavan nucleus structure. The structural similarity and LogP of myricetin to quercetin may explain partly why myricetin is able to induce a protective effect in differentiated H9c2 cells, as it would allow myricetin to potentially bind to similar or the same proteins as quercetin.

v) Involvement of protein kinases in flavonoid-mediated cytoprotection

To understand the mechanism of flavonoid mediated cardioprotection, the effects of quercetin on H₂O₂- and hypoxia induced protein kinase (ERK1/2, PKB, JNK and p38 MAPK) activation in differentiated H9c2 cells was investigated using western blotting. Quercetin was selected as a model flavonoid for this investigation as previous findings in the present study identify quercetin as the most potent flavonoid in inducing a cytoprotective effect in differentiated H9c2 cells. Previous studies have shown that several protein kinases, including the ones investigated in the present study, are activated in response to reactive oxygen species (Kamata and Hirata, 1999). This increased activation of protein kinase activity by ROS has been demonstrated in cardiomyocytes (Clerk *et al*, 1998; Pham *et al*, 2000; Takeishi *et al*, 1999). As demonstrated in section 4.6 Figs 4.16 and 4.17, 2 h exposure

to 600 μM H_2O_2 caused a significant increase in phosphorylation of ERK1/2, PKB, JNK and p38 MAPK in differentiated H9c2 cells, in agreement with previous reports. Pre-treatment for 24 h with both 30 μM and 100 μM quercetin significantly reduced the phosphorylation of ERK1/2, PKB, JNK and p38 MAPK when compared to H_2O_2 treated cells. Quercetin pre-treatment (30 μM) failed to significantly reduce the phosphorylation of JNK (Fig. 4.16), although not significant the phosphorylation is noticeably reduced, and lack of significance is most likely due to the large variance observed in H_2O_2 induced phosphorylation of JNK. Similarly, 24 h incubation in hypoxic conditions lead to an increased activation of protein kinases (Fig. 4.18). Unusually this was not observed clearly in Fig. 4.19 with PKB and p38 MAPK. Pre-treatment for 24 h with 100 μM and 30 μM quercetin was shown to significantly reduce the phosphorylation induced by hypoxia incubation, except for p38 MAPK with 100 μM . Basal expression of ERK1/2 and PKB was shown to be unaffected by quercetin after 24 h pre-treatment in terms of significant inhibition (Figs. 4.16 - 4.19), despite the fact that quercetin is known to be a competitive inhibitor of MEK1 and PI3K γ , upstream regulators of ERK1/2 and PKB respectively. Significant inhibition of basal ERK and PKB expression by 24 h pre-treatment with 100 μM quercetin was observed in Fig. 4.20, though not by 24 h pre-treatment with 30 μM quercetin. This basal level inhibition was compared to the inhibition induced from PD98059 (50 μM) and LY 294002 (30 μM), specific inhibitors for MEK1 and PI3K respectively. The observed inhibition of ERK1/2 and PKB during oxidative stress is likely therefore to be induced through a pathway independent of MEK1 and PI3K inhibition. As shown in Fig. 4.21 24 h incubation with specific inhibitors for protein kinases caused no significant loss in cell viability, save for LY294002. Furthermore, the specific inhibitors had no effect on quercetin induced cardioprotection, and the inhibitors alone caused no significant protective effect. Inhibition of a single kinase by a selective inhibitor caused no protective effect, whereas the protective effect of quercetin was associated with the inhibition of several kinases. As quercetin is a non-selective inhibitor, the inhibition of multiple kinases at the same time may be conducive to a cytoprotective effect. Therefore, using several specific inhibitors in conjunction to induce a cytoprotective effect should be considered in future investigations. Contrary to the observations made in the present study, it has been suggested that the principal mechanism of quercetin induced cytoprotection in mitotic H9c2 cells is the activation of ERK1/2 and PI3K (Angeloni *et al*, 2007). This discrepancy may be a result of using differentiated H9c2 cells as a model system, which have been shown

to be more physiologically similar to *in vivo* cardiomyocytes, rather than mitotic H9c2 cells. The mechanism of quercetin induced cytoprotection from hypoxia and H₂O₂ exposure most likely involves the modulation of oxidative stress induced protein kinase activation that are involved in apoptosis and cell survival. Cell death from oxidative stress has been linked with the mitochondria-dependent or intrinsic apoptotic pathways, which have been shown to be inhibited by the flavonoid isorhamnetin in mitotic H9c2 cells through the inactivation of ERK1/2 (Sun *et al*, 2012). Isorhamnetin is almost structurally identical to quercetin, and therefore it is plausible that quercetin acts in a similar manner. A major mechanism of quercetin induced cytoprotection is therefore inactivation of ERK1/2, inhibiting downstream pro-apoptotic signalling. Quercetin has been shown to also inhibit ERK1/2, PKB, JNK and p38 MAPK activation in mitotic H9c2 cells in response to other stimuli (Gutiérrez-Venegas *et al*, 2010). Furthermore, myricetin and kaempferol have also been shown to inhibit the activation of JNK and p38 MAPK in a number of different cell lines, resulting in prevention of oxidative stress induced apoptosis (Mansuri *et al*, 2014). The observations made in the present study agree that quercetin is a potent inhibitor of several protein kinases, which will contribute majorly to the observed cytoprotective effect. It is notable that specific inhibitors alone did not induce a significant protective effect against oxidative stress induced cell death, despite the inhibition of these protein kinases being a major mechanism of quercetin mediated cytoprotection. Previous studies on quercetin mediated cardioprotection in H9c2 cells have also identified several other mechanisms that contribute to the cytoprotective effect (Dong *et al*, 2014). Quercetin was shown to induce upregulation of the mitochondrial regulatory protein Bmi-1, decrease ROS production by inhibiting Nox1 and inhibiting Ca²⁺- dependant ATP hydrolysis, ATP-dependant Ca²⁺ uptake and Ca²⁺ release (Dong *et al*, 2014). This suggests that quercetin specifically, and flavonoids in general, induce a protective effect as a result of synergistic inhibition of multiple protein kinases, rather than inhibition of single protein kinases, combined with decreasing ROS generation and ROS scavenging activity (Dong *et al*, 2014).

After ingestion quercetin is glycosylated, therefore native quercetin levels in the plasma are often undetectable (Russo *et al*, 2012). After metabolism in the liver to the glucuronidated, sulphated or methylated metabolites, the quercetin metabolites can be absorbed by cells and de-conjugated to form native quercetin, which has been shown to

be more potent in terms of cytoprotectivity (Kawai *et al*, 2008). Metabolites of quercetin have been shown to be less potent in inducing a cytoprotective effect when compare to quercetin, the present study agrees with this observation, as 3'-O-methyl quercetin was only effective at 100 μ M concentrations (Williamson *et al*, 2005). The findings of this present study also suggest the inability of differentiated H9c2 cells to de-conjugate quercetin 3-glucuronide as no significant cytoprotective effect was observed using this metabolite.

vi) Implications of flavonoid induced cytoprotection

Quercetin was shown to induce a cytoprotective effect with concentrations ≥ 30 μ M after 24 h exposure and subsequent exposure to H₂O₂. Similarly, 3'-O-methyl quercetin induced a protective effect at 100 μ M concentration after exposure to H₂O₂. To protect against hypoxia induced cell death a concentration of 100 μ M quercetin was required. The bioavailability of flavonoids and the maximum achievable plasma concentrations (7.6 μ M quercetin and quercetin metabolites) without supplementation are a great deal lower than these concentrations (Labbé *et al*, 2009). Therefore, based on these observations, the cytoprotective effects observed in this chapter are unlikely to be achievable *in vivo* from dietary flavonoids. Further investigations into the intracellular accumulation of quercetin and other flavonoids, resulting from exposure to the aglycone or metabolites followed by their intracellular deconjugation, are required to determine more accurately the concentrations required to induce a cytoprotective effect *in vivo*. In addition, the results of this chapter highlight that quercetin has a potent and significant effect on cell signalling molecules under laboratory conditions, which may form the basis of a cytoprotective effect.

Chapter 5:

Cytotoxicity of

flavonoids

5.0 Cytotoxicity of flavonoids

In the presence of oxygen the intracellular metabolism of quercetin, its metabolites, and other flavonoids has been shown to lead to the creation of reactive oxygen species (ROS) and other pro-oxidant effects (Metodiewa *et al*, 1999). Although short term exposure to quercetin was shown to reduce intracellular ROS (Dong *et al*, 2014). Extended periods of exposure to ROS leads to apoptosis, although the mechanism by which ROS induce apoptosis is still unclear. It is proposed that ROS leads to the oxidation of mitochondrial pores, leading to the release of cytochrome-c and the activation of pro-apoptotic cell signals and enzymes such as Caspase-3 (Simon *et al*, 2000). Therefore, prolonged exposure to flavonoids may induce apoptosis due to their intracellular accumulation and metabolism. Therefore, this chapter aims to investigate the cytotoxic effects of prolonged exposure to dietary flavonoids and major quercetin metabolites on H9c2 cells for the first time.

The effect of prolonged (≥ 24 h) exposure to concentrations of quercetin, kaempferol, myricetin and the quercetin metabolites quercetin-3-glucuronide and 3'-O-methylquercetin on cell viability will be investigated using MTT reduction and LDH release assays. As with the investigation into the cytoprotective effects of flavonoids (Chapter 4) the range of concentrations (1-100 μM) used reflect the bioavailability of flavonoids *in vivo*, as well as the potential for intracellular and plasma accumulation of flavonoid following repeated dietary intake (Labbé *et al*, 2009).

The differences in the metabolic activity of mitotic (proliferating) and differentiating H9c2 may impact on the potential cytotoxic effect of prolonged flavonoid exposure, as mitotic H9c2 cells are known to be less sensitive to oxidative stress, which in this case would be caused by intracellular ROS generation (Pereira *et al*, 2011). Furthermore, as differentiated H9c2 cells are known to have an increased mitochondrial mass, this may contribute to an increased sensitivity to cytotoxicity induced by flavonoid dependant ROS generation (Branco *et al*, 2013). Considering this, the effect of prolonged (≥ 24 h) exposure to flavonoids and flavonoid metabolites will be investigated in mitotic (proliferating), differentiating and fully differentiated H9c2 cells using cell viability assays.

The direct modulation of cell signalling molecules represents another mechanism by which flavonoids may induce cytotoxicity. Quercetin is known to inhibit MEK, and consequently the PI3K pathway; furthermore Apoptosis is also heavily regulated by the MAPK and PI3K cell signalling pathways (Russo *et al*, 2012; Mendoza *et al*, 2011; Simon *et al*, 2000). To investigate how prolonged flavonoid exposure affects these cell signals will be determined using western blotting to monitor the phosphorylation of ERK1/2, PKB, p38 MAPK and JNK. Caspase-3 activation will also be monitored using western blotting, as the activation of Caspase-3 is a significant marker of apoptosis and may be induced by the mitochondrial damage caused by intracellular ROS generation as well as the cell signalling activity modulated by flavonoids (Simon *et al*, 2000).

It is proposed that flavonoids will undergo pro-oxidant intracellular metabolism to produce ROS in H9c2 cells after prolonged exposure (Metodiewa *et al*, 1999). To quantify intracellular ROS generation arising from flavonoid exposure the DCFDA ROS assay will be used in conjunction with flow cytometry, where intracellular ROS levels will be measured after 24, 48 and 72 h exposure to flavonoid. Combined with cell viability observations and the monitoring of cell signal phosphorylation and Caspase-3 activation, a clearer picture of flavonoid induced cytotoxicity can be produced.

5.1 Cytotoxicity of flavonoids on proliferating cardiomyoblasts

To measure the effects of exposure to flavonoids on proliferating cardiomyoblasts, undifferentiated H9c2 cells were exposed to a range of concentrations (100, 30, 10, 3 and 1 μM) of a particular flavonoid, either quercetin, myricetin or kaempferol. Cells were exposed for 24, 48 or 72 h, after which the viability of the cells was assayed using LDH release and MTT reduction assays.

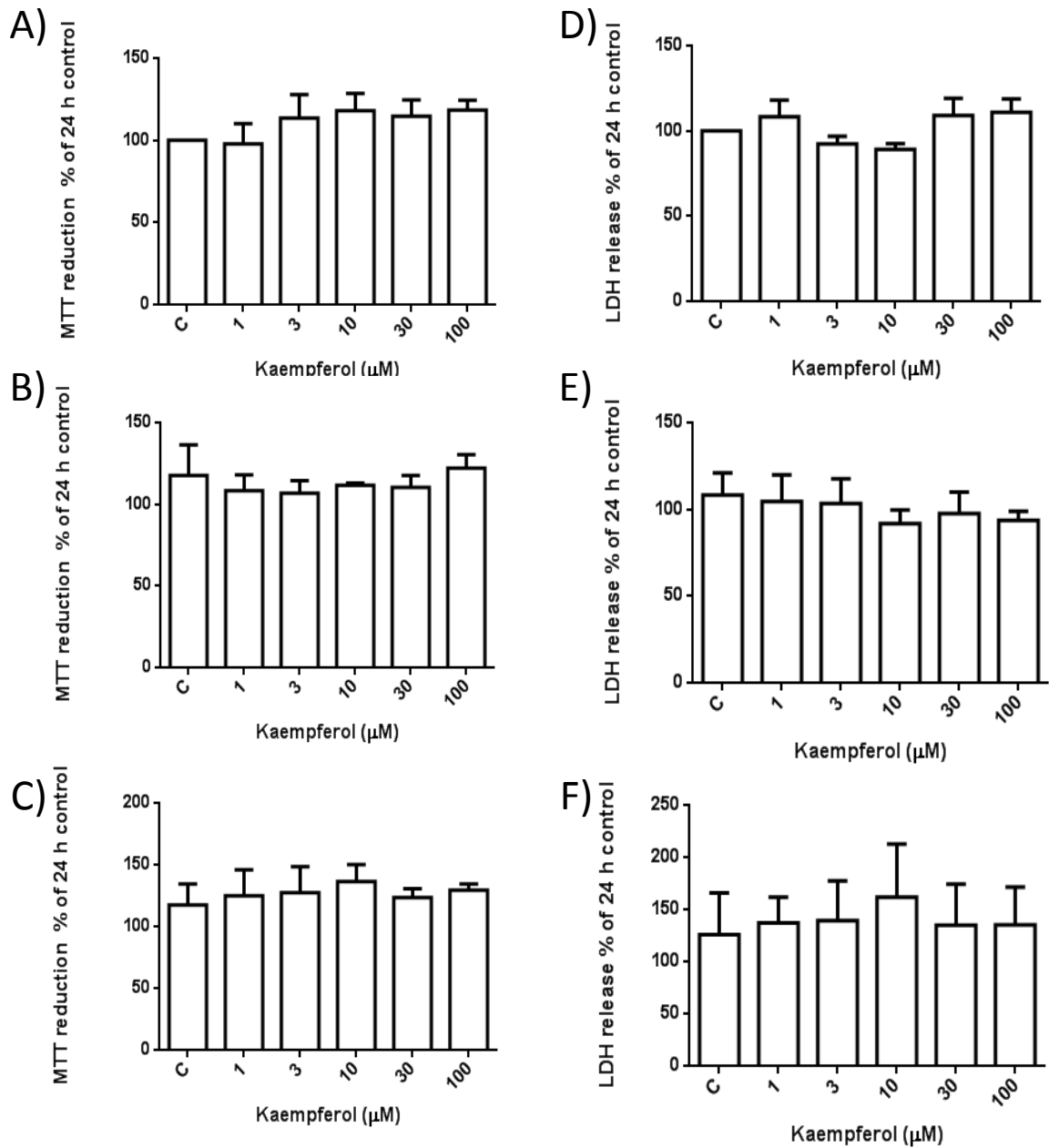


Fig 5.1 Effect of Kaempferol exposure on proliferating H9c2 cell viability. MTT reduction (A, B, C) and LDH release (D, E, F) assays showed that kaempferol at all concentrations tested produced no significant changes in viability at time points tested; 24 h (A,D), 48 h (B,E) and 72 h (C ,F). Data are expressed as the percentage of control cells (24 h C =100%) and represent the mean \pm SEM of three independent experiments.

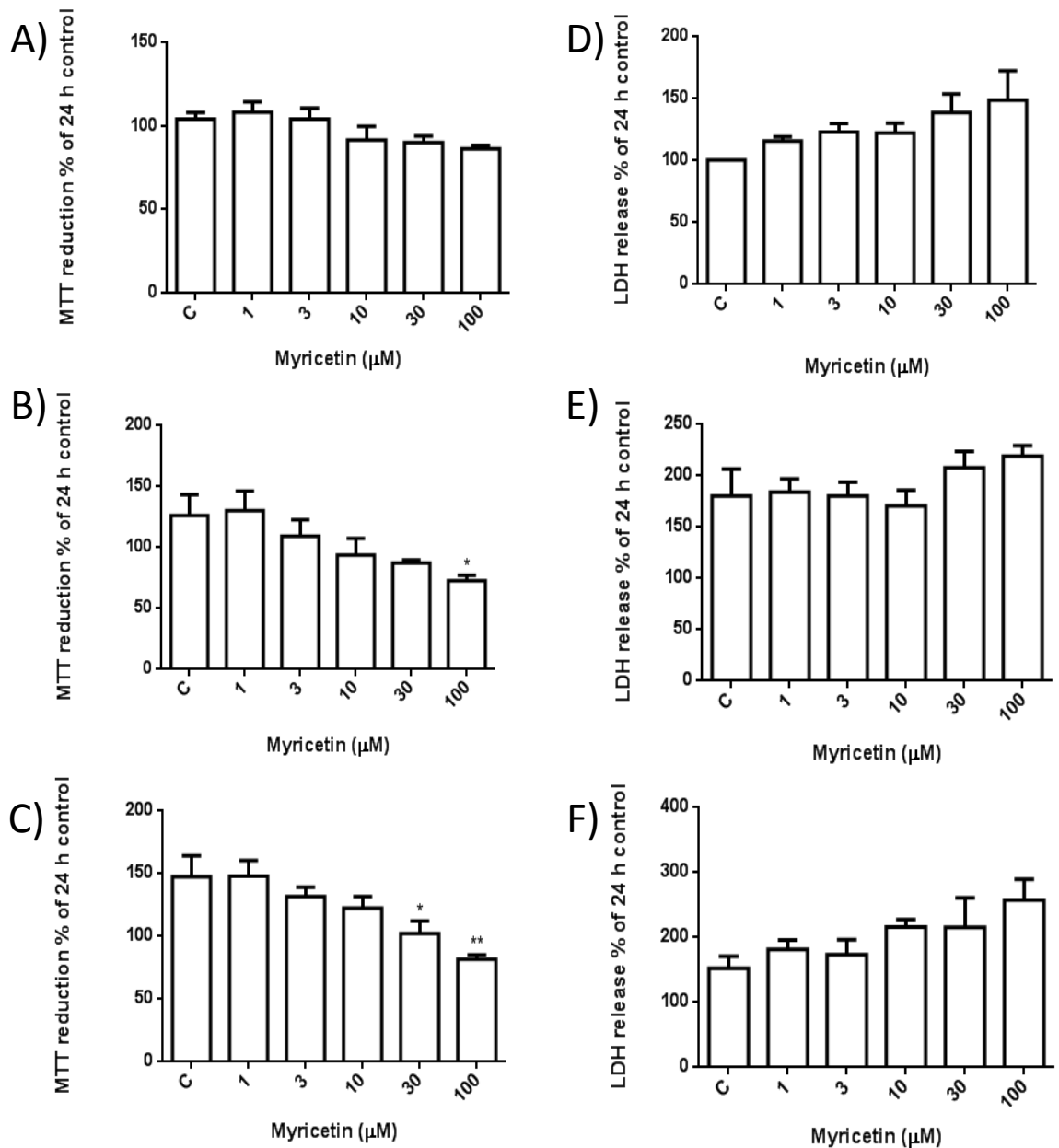


Fig 5.2 Effect of Myricetin on proliferating H9c2 cell viability. MTT reduction (A,B, C) and LDH release (D, E, F) assays. 100 μM myricetin after 48 h exposure (B) caused a significant (*: $p < 0.05$) decrease in MTT reduction. After 72 h as measured by MTT reduction (C) 30 μM (*: $p < 0.05$) and 100 μM (: $p < 0.01$) both caused a significant decrease in MTT reduction. Data are expressed as the percentage of control cells (24 h C =100%) and represent the mean \pm SEM of three independent experiments.**

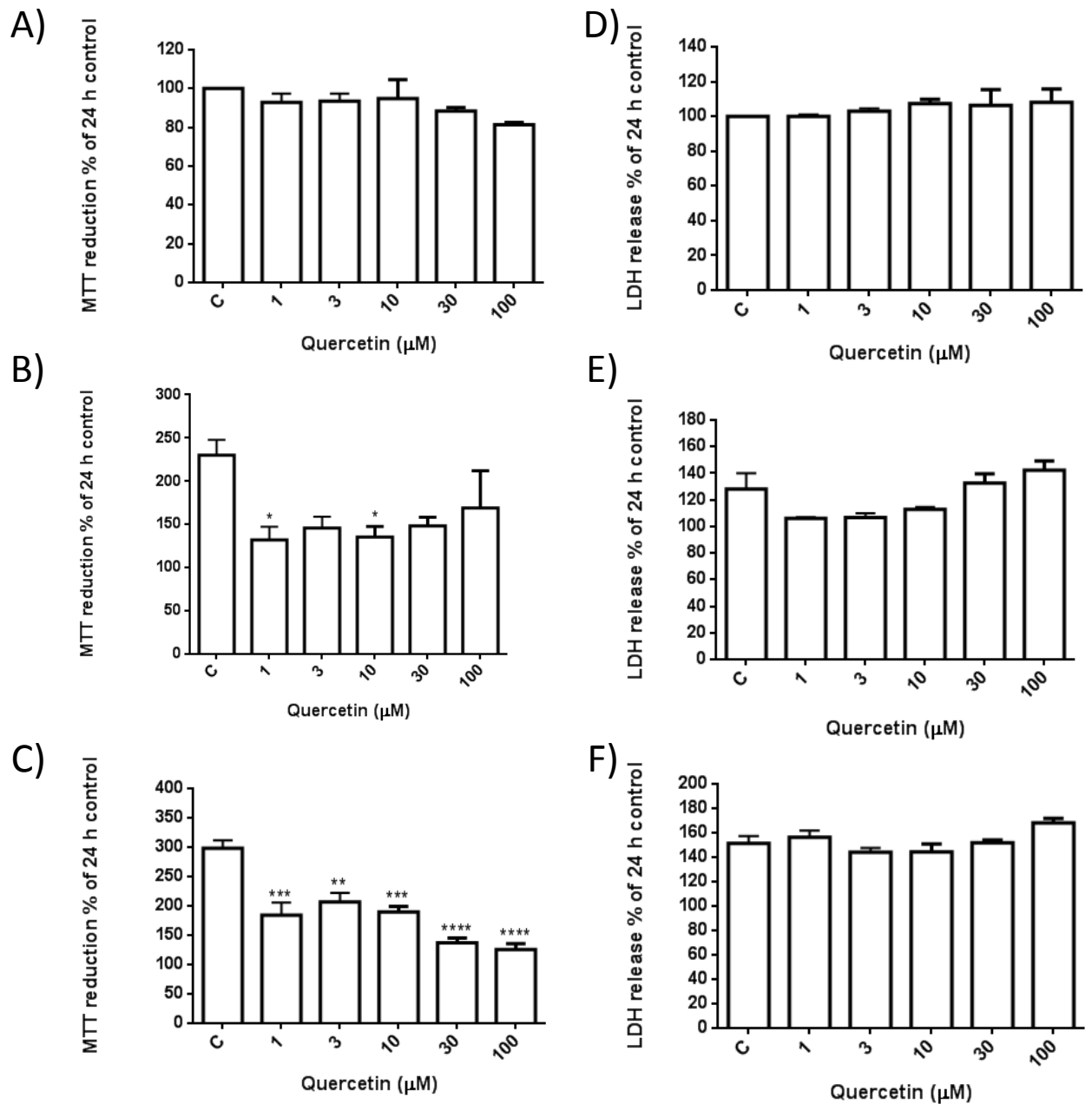


Fig 5.3 Effect of quercetin on proliferating H9c2 cell viability. MTT reduction (A,B, C) and LDH release (D, E, F) assays. 1 μM and 10 μM quercetin after 48 h exposure (B) caused a significant (1 μM & 10 μM, *: $p < 0.05$) decrease in MTT reduction. After 72 h as measured by MTT reduction (C) all concentrations of quercetin caused a significant decrease in MTT reduction (3 μM, **: $p < 0.01$; 1 μM & 10 μM, ***: $p < 0.005$; 30 μM & 100 μM, ****: $p < 0.001$). Data are expressed as the percentage of control cells (24 h C =100%) and represent the mean \pm SEM of three independent experiments.

From these assays shown on Fig. 5.1, 5.2 and 5.3 it is demonstrated that quercetin and myricetin have a significant effect on proliferating H9c2 cell viability, mainly at 30 μ M and 100 μ M concentrations, and after at least 48 h exposure time.

5.2 Cytotoxicity of flavonoids on differentiating cardiomyoblasts

To determine the effects of flavonoids on the viability of H9c2 cells during differentiation, cells were incubated with a flavonoid and well as differentiation medium. The viability of the cells was assayed using MTT reduction and LDH release at three time points, 24 h, 72 h and 7 days. Every 48 h the differentiation medium as replaced along with the relevant concentration of flavonoid.

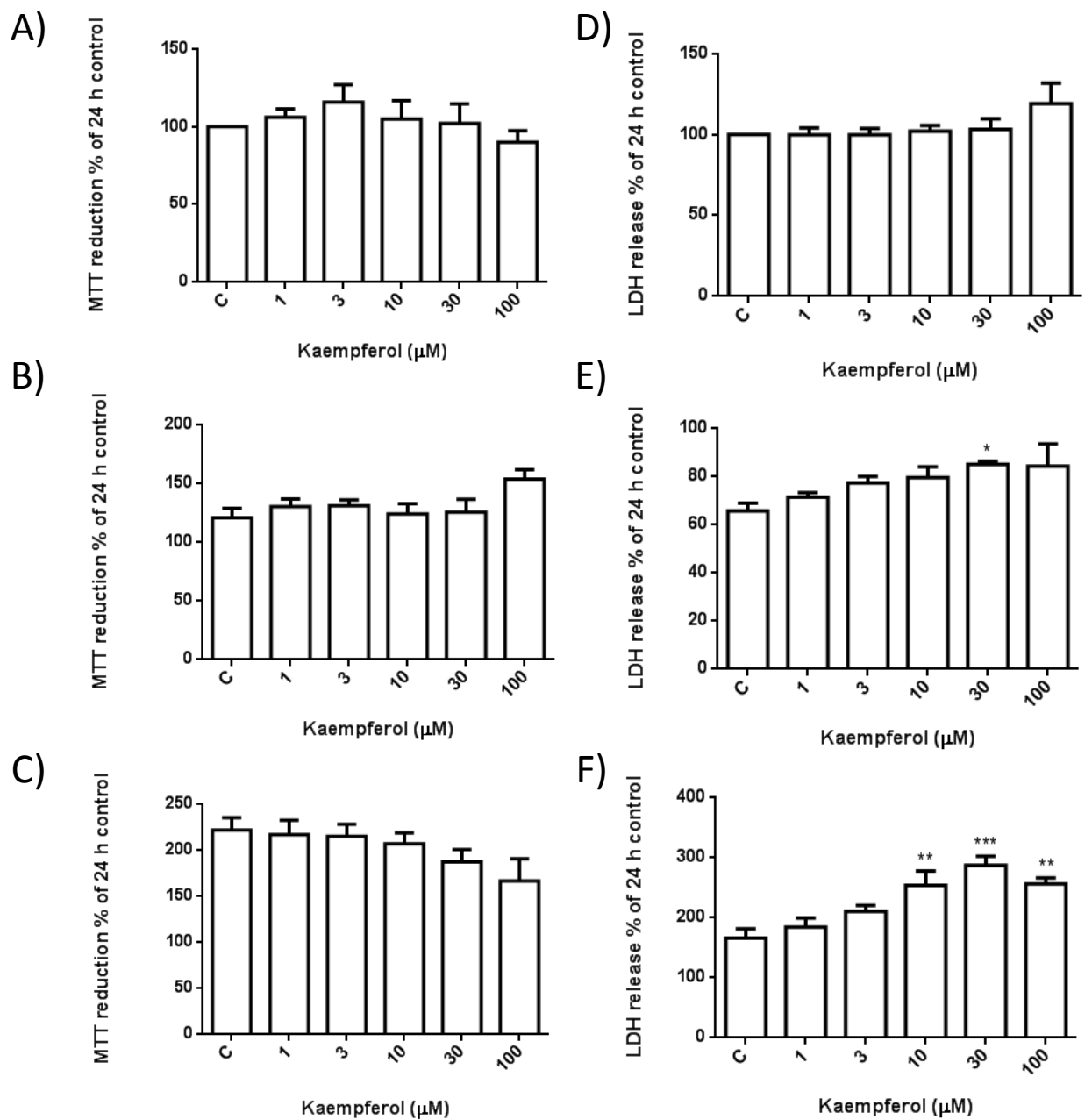


Fig 5.4 Effect of kaempferol on differentiating H9c2 cell viability. MTT reduction (A,B, C) and LDH release (D, E, F) assays. As measured with LDH release 72 h treatment with 30 μM kaempferol (E) caused a significant (*: $p < 0.05$) increase in LDH release compared to the control. After 7 days exposure to kaempferol (F) 10, 30 and 100 μM concentrations elicited a significant increase in LDH release (10 μM & 100 μM, **: $p < 0.01$; 30 μM, *: $p < 0.005$). Data are expressed as the percentage of control cells (24 h C =100%) and represent the mean \pm SEM of three independent experiments.**

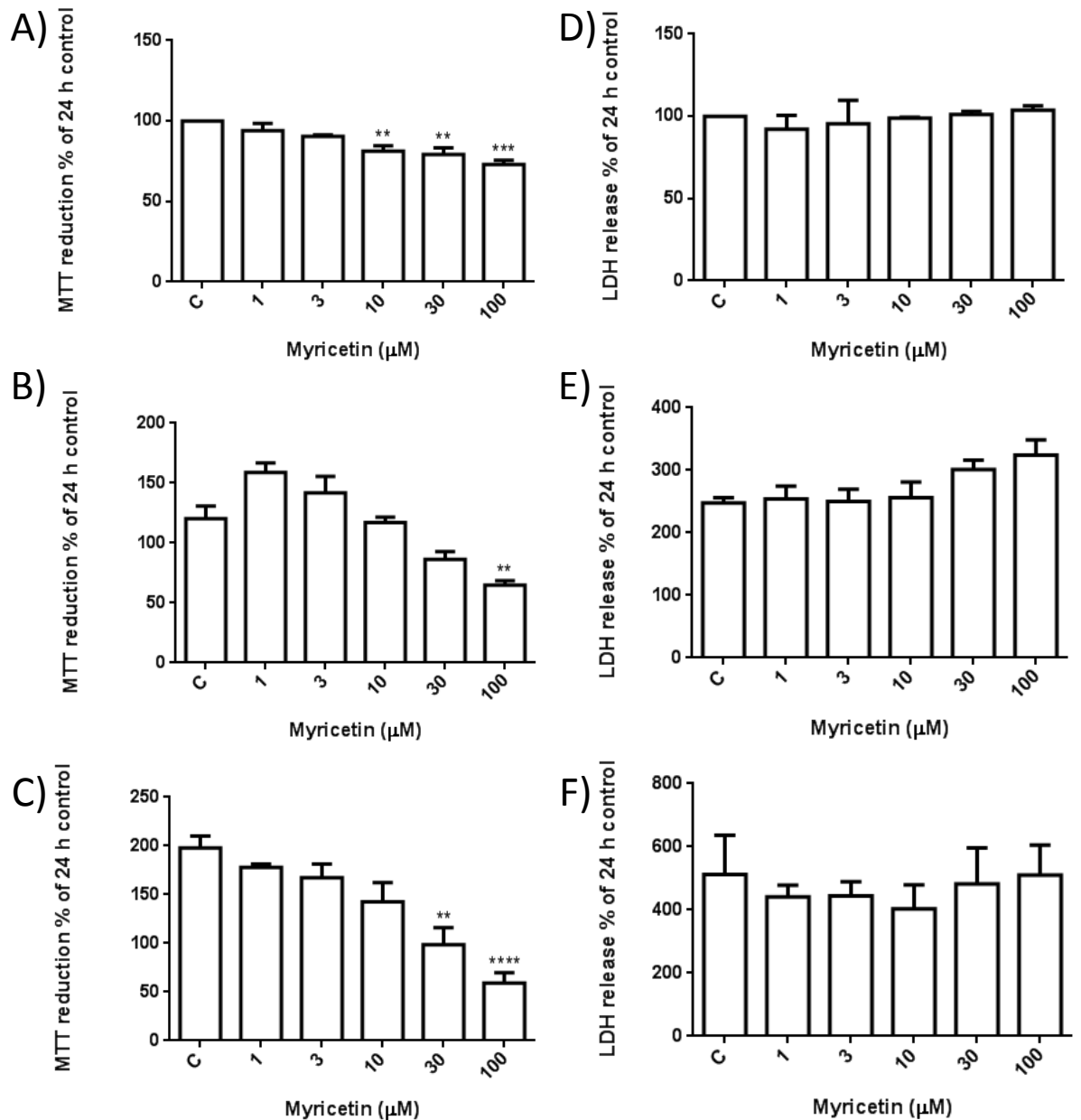


Fig 5.5 Effect of myricetin on differentiating H9c2 cell viability. MTT reduction (A,B, C) and LDH release (D, E, F) assays. As measured with MTT reduction 24 h treatment with 10, 30 and 100 μM myricetin (A) caused a significant (10 μM & 30 μM, **: $p < 0.05$; 100 μM, *: $p < 0.005$) decrease in MTT reduction compared to the control. After 72 h exposure to myricetin (B) 100 μM concentration caused a significant decrease in MTT reduction (**: $p < 0.01$). 7 days exposure to myricetin (C) at 30 μM and 100 μM caused significant decreases in MTT reduction, (30 μM **: $p < 0.01$; 100 μM, ****: $p < 0.001$). Data are expressed as the percentage of control cells (24 h C =100%) and represent the mean \pm SEM of three independent experiments.**

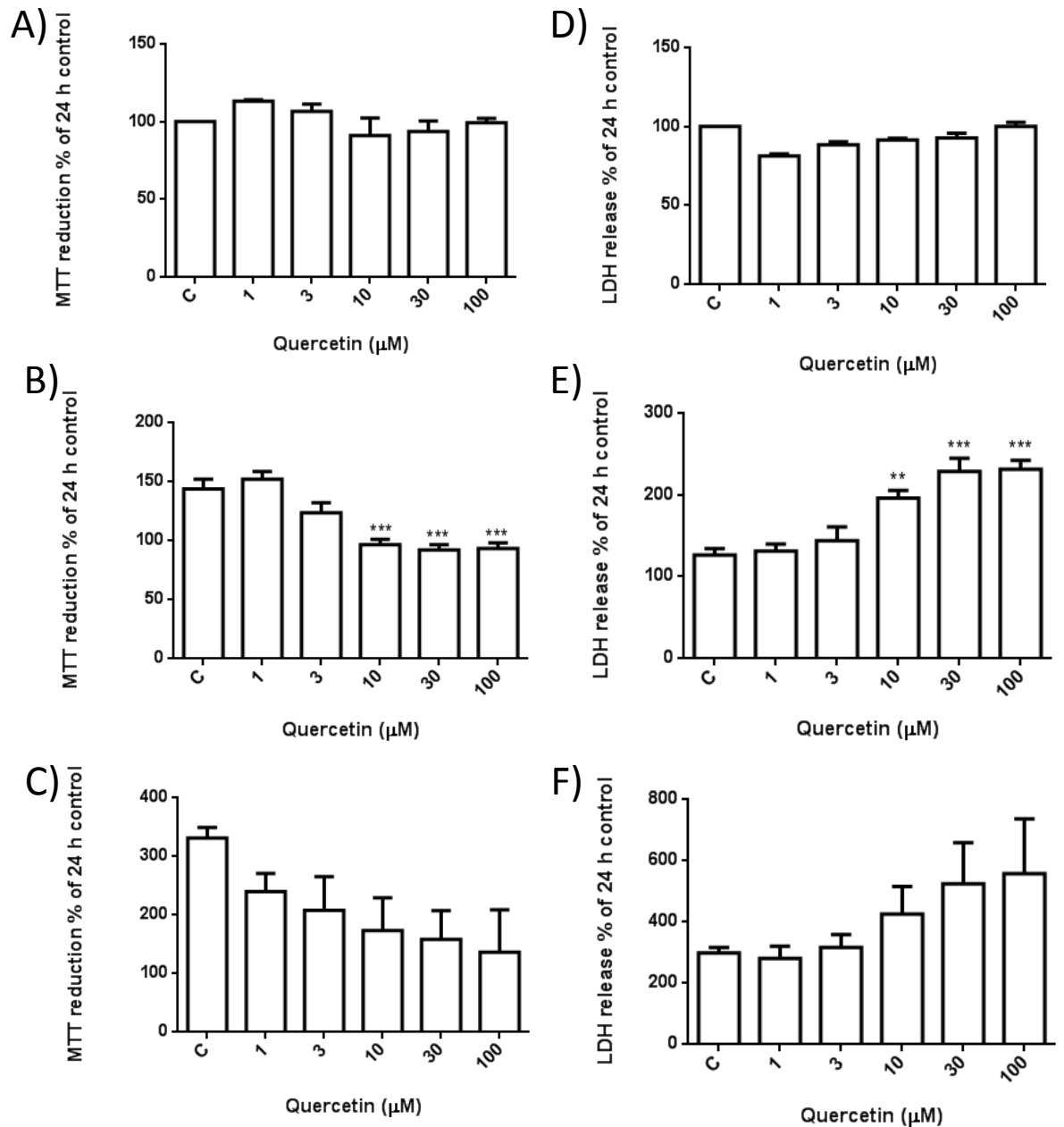


Fig 5.6 Effect of quercetin on differentiating H9c2 cell viability. MTT reduction (A,B, C) and LDH release (D, E, F) assays. After 72 h exposure to quercetin, 10, 30 and 100 μM caused a significant change in both MTT reduction (B) and LDH release (E). The MTT reduction assay (B) showed that 10, 30 and 100 μM caused significant (*: $p < 0.005$) decrease in MTT reduction. The LDH release assay (E) showed 10 μM caused a significant (**: $P < 0.01$) increase in LDH release, whereas 30 μM and 100 μM exposure caused a more significant (***: $p < 0.005$) increase. Data are expressed as the percentage of control cells (24 h C =100%) and represent the mean \pm SEM of three independent experiments.**

Figs 5.4, 5.5 and 5.6 show that quercetin and myricetin have a significant effect on the viability of differentiating H9c2 cells measured by MTT reduction.

5.3 Cytotoxicity of flavonoids on differentiated cardiomyocytes

To measure the effects of exposure to flavonoids on differentiated H9c2 cardiomyocytes, 7 day differentiated H9c2 cells were exposed to a range of concentrations (100, 30, 10, 3 and 1 μM) of flavonoid (quercetin, myricetin or kaempferol). Cell were exposed for 24 h, 48 h or 72 h, after which the viability of the cells was assayed using LDH release and MTT reduction assays.

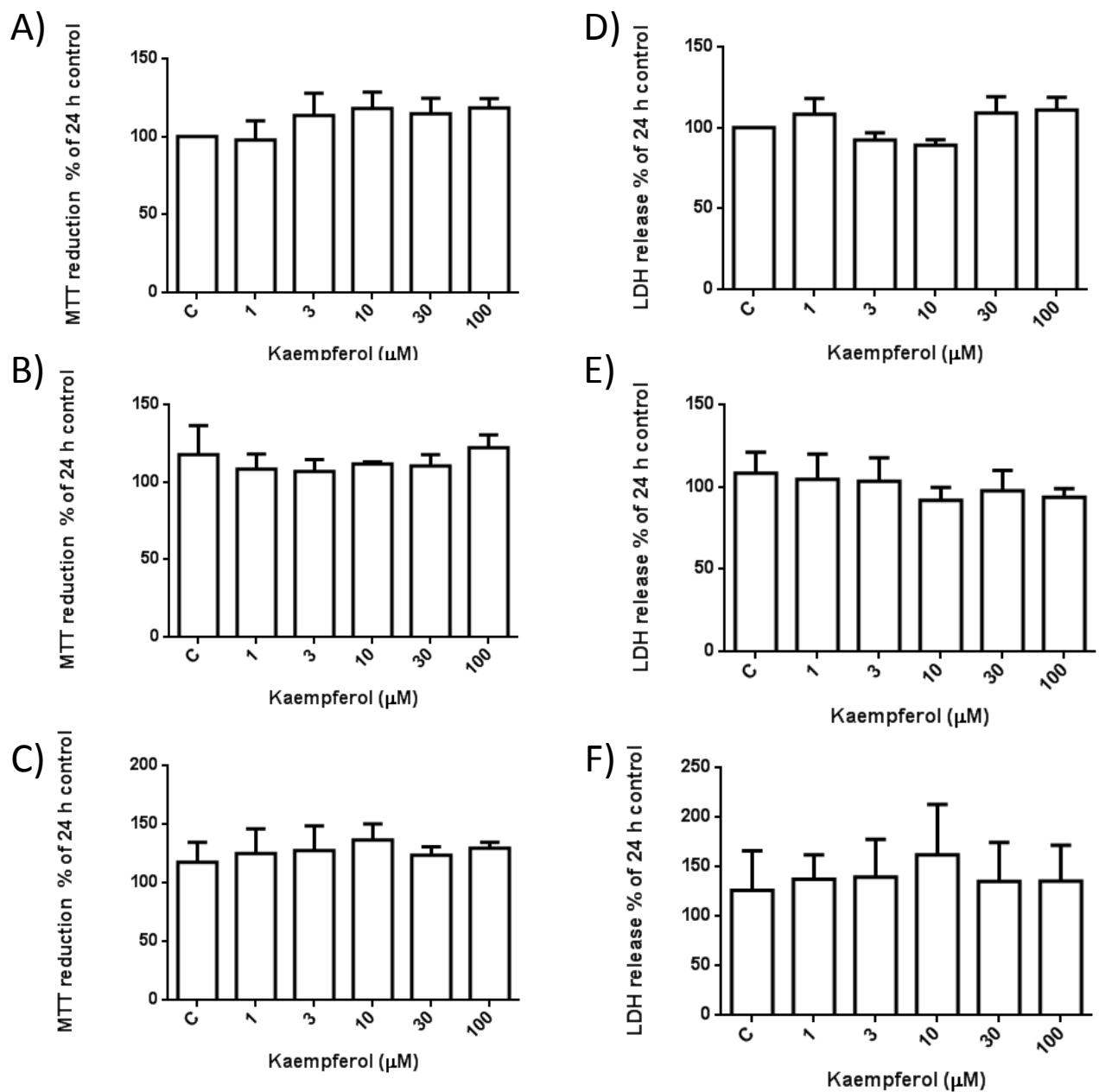


Fig 5.7 Effect of kaempferol on differentiated H9c2 cell viability. MTT reduction (A,B, C) and LDH release (D, E, F) assays. At all concentrations and time points tested (24 h: A & D, 48 h: B & E, 72 h C & F) kaempferol caused no significant changes in LDH release or MTT reduction. Data are expressed as the percentage of control cells (24 h C =100%) and represent the mean \pm SEM of three independent experiments.

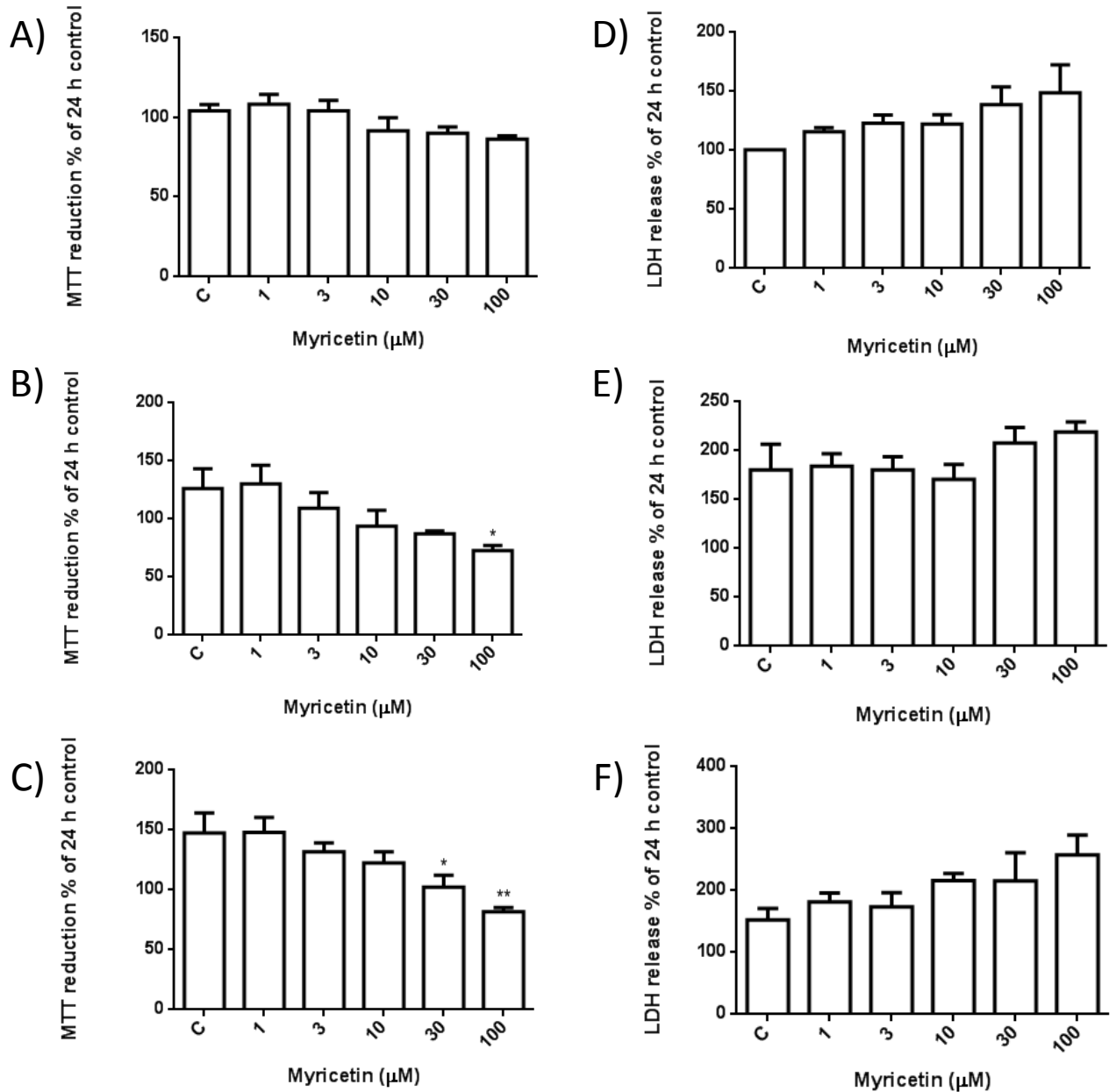


Fig 5.8 Effect of myricetin on differentiated H9c2 cell viability. MTT reduction (A,B, C) and LDH release (D, E, F) assays. After 48 h exposure to 100 μM myricetin (B) there was a significant (*: $p < 0.05$) decrease in MTT reduction. After 72 h (C), exposure to 30 μM and 100 μM myricetin caused significant decreases (30 μM, *: $p < 0.05$; 100 μM, **: $p < 0.01$) in MTT reduction. Data are expressed as the percentage of control cells (24 h C =100%) and represent the mean \pm SEM of three independent experiments.

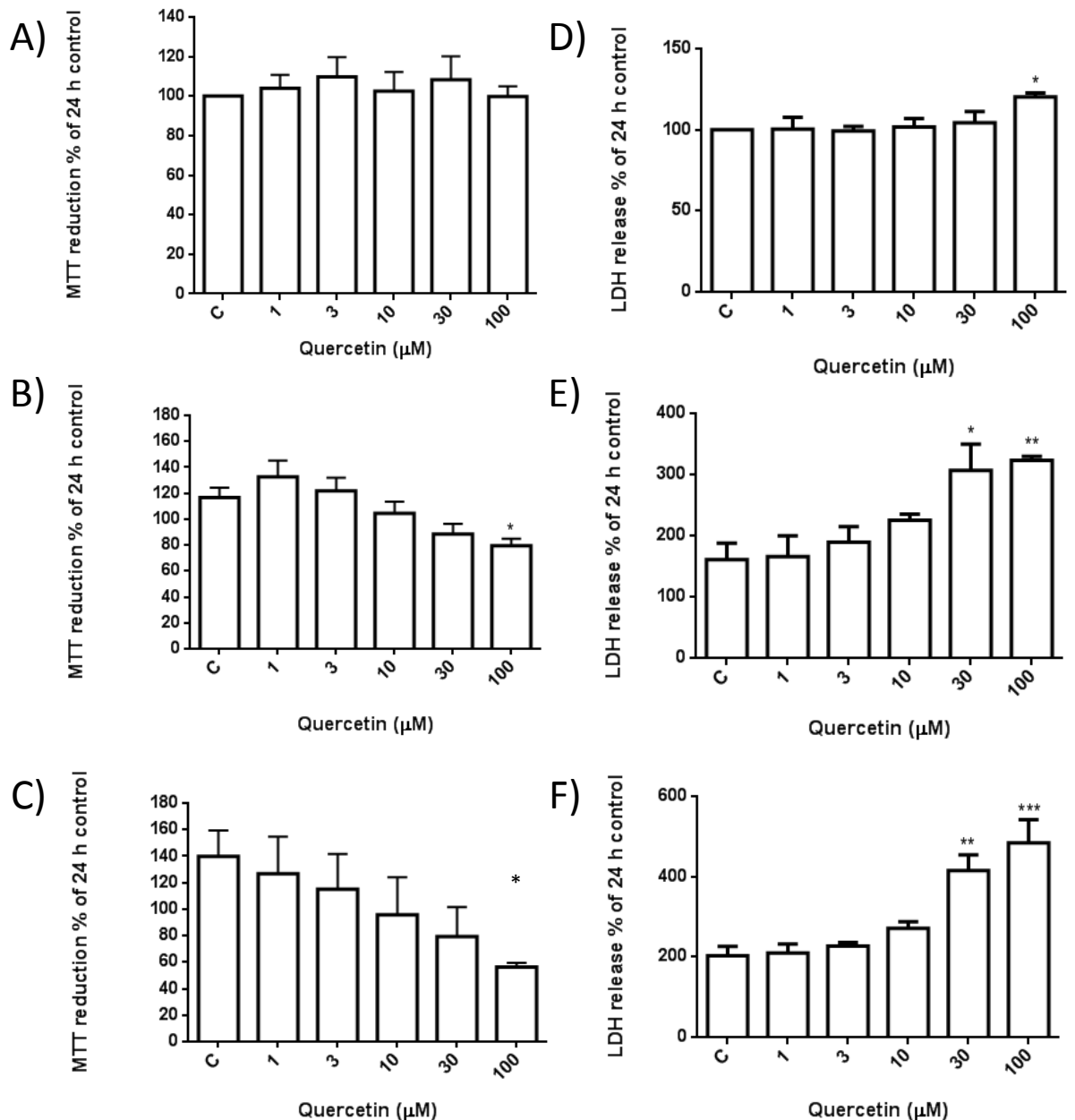


Fig 5.9 Effect of quercetin on differentiated H9c2 cell viability. MTT reduction (A,B, C) and LDH release (D, E, F) assays. 100 μM quercetin treatment for 24 h (D) caused a significant (*: $P < 0.05$) increase in LDH release. After 48 h exposure to 100 μM quercetin both MTT reduction and LDH release assays (B & E) show a significant change (B, *: $p < 0.05$; E, **: $p < 0.01$). The LDH release assay also showed 30 μM quercetin to have a significant effect (*: $p < 0.05$) after 48 h (E). After 72 h exposure to 100 μM quercetin MTT reduction and LDH release assays (C & F) show a significant effect (C, *: $p < 0.05$; F, ***: $p < 0.005$). The LDH release assay also showed 30 μM quercetin had a significant effect (**: $p < 0.01$) after 72 (F). Data are expressed as the percentage of control cells (24 h C =100%) and represent the mean \pm SEM of three independent experiments.

From figs. 5.7, 5.8 and 5.9 it is shown that 30 μM and 100 μM quercetin and myricetin have a significant effect on differentiated H9c2 cell viability after at least 48 h exposure. Both MTT reduction and LDH release showed that 100 μM causes a significant toxic effect after 48 h, this can be seen to be the most reliable method of inducing flavonoid mediated cytotoxicity. The cytotoxicity of 30 μM and 100 μM quercetin exposure is further demonstrated visually in Fig. 5.10.

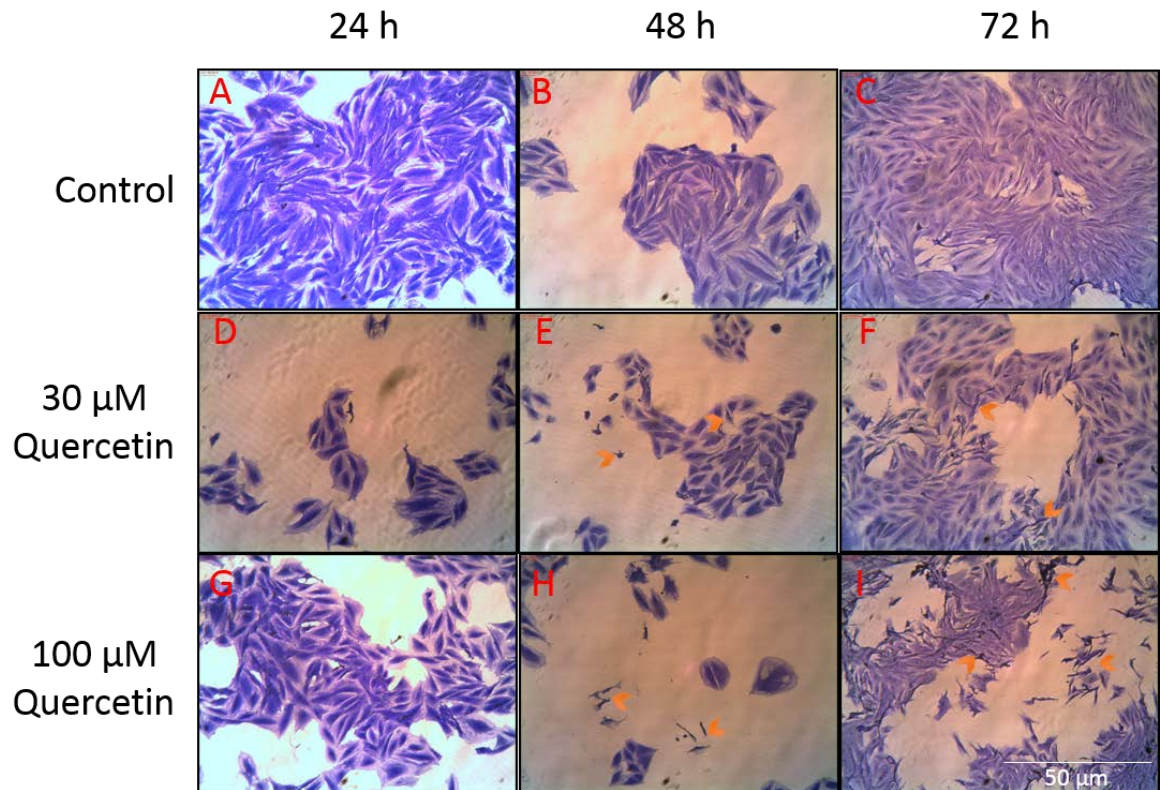


Fig. 5.10 Visible cytotoxic Effect of quercetin exposure on differentiated H9c2 cells. Differentiated H9c2 cells were incubated without quercetin for A) 24 h, B) 48 h C) 72 h, with 30 μM quercetin for D) 24 h, E) 48 h, F) 72 h, or 100 μM quercetin for G) 24 h, H) 48 h, I) 72 h. Visible cell death (red arrowheads) occurs after 48 h exposure to both 30 μM and 100 μM quercetin. Stained with Coomassie blue.

5.4 Cytotoxicity of quercetin metabolites on differentiated cardiomyocytes

To measure the effects of exposure to quercetin metabolites on differentiated H9c2 cardiomyocytes, 7 day differentiated H9c2 cells were exposed to a range of concentrations (100, 30, 10, 3 and 1 μM) of either 3'-*O*-methyl quercetin (Q3M) or quercetin-3-glucorinde (Q3G) . Cell were exposed for 24 h, 48 h or 72 h, after which the viability of the cells was assayed using LDH release and MTT reduction assays.

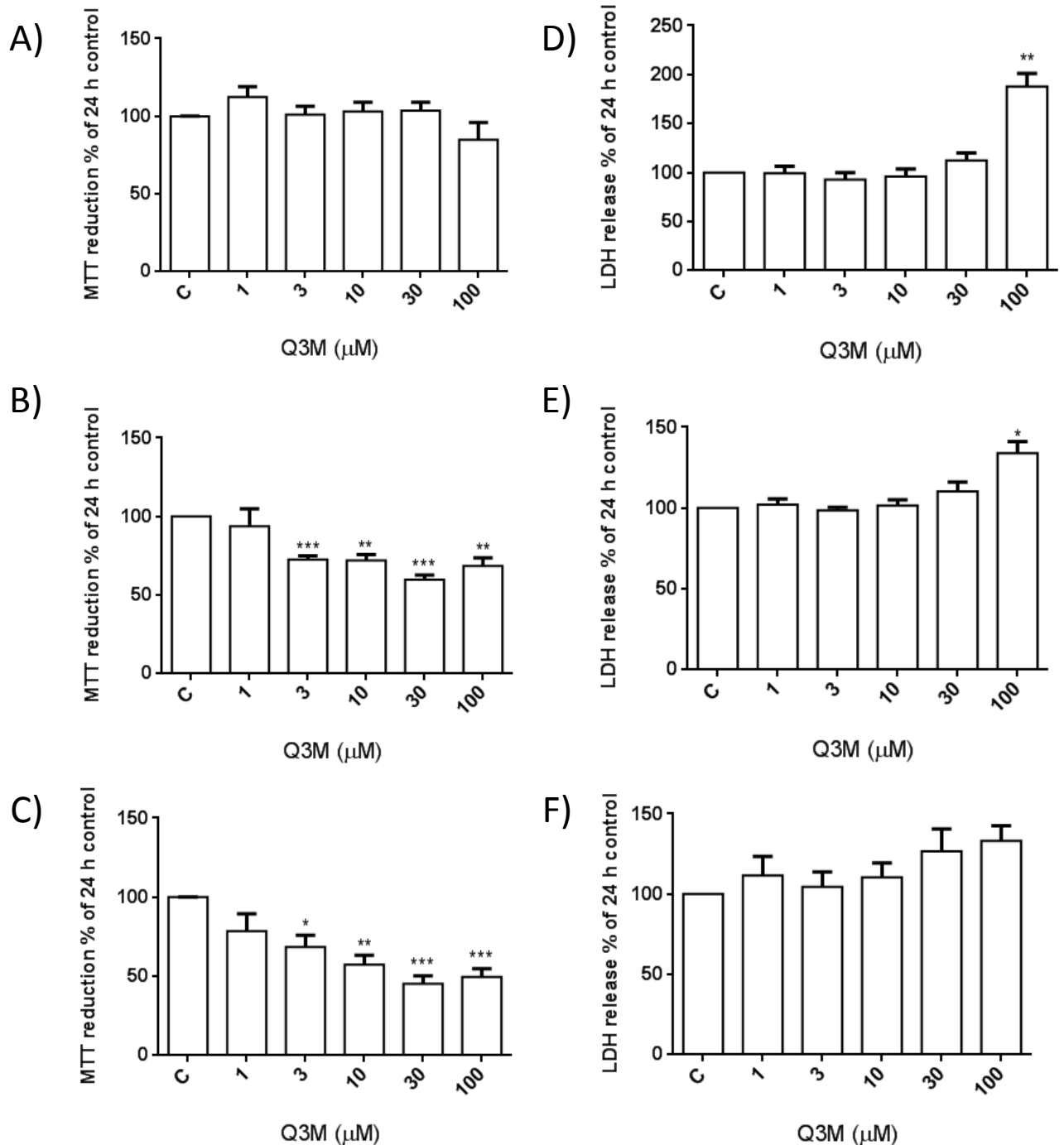


Fig 5.11 Effect of 3'-O-methyl quercetin on differentiated H9c2 cell viability. MTT reduction (A,B, C) and LDH release (D, E, F) assays. After 24 h exposure the LDH release assay (D) shows 100 μM 3'-O-methyl quercetin (Q3M) caused a significant change (*: $p < 0.05$) compared to control. After 48 h exposure (B) showed that 3 μM, 10 μM, 30 μM and 100 μM Q3M caused a significant decrease in MTT reduction (10 μM & 100 μM, **: $p > 0.01$; 3 μM & 30 μM, ***: $p < 0.005$). LDH release (E) also showed 100 μM Q3M caused a significant increase in LHD release (*: $p > 0.05$). After 72 h exposure MTT reduction (C) showed that 3 μM, 10 μM, 30 μM and 100 μM Q3M caused a significant decrease in MTT reduction (3 μM, *: $p > 0.01$; 10 μM, **: $p > 0.01$; 30 μM & 100 μM, ***: $p < 0.005$). Data are expressed as the percentage of control cells (C =100%) and represent the mean \pm SEM of six independent experiments.

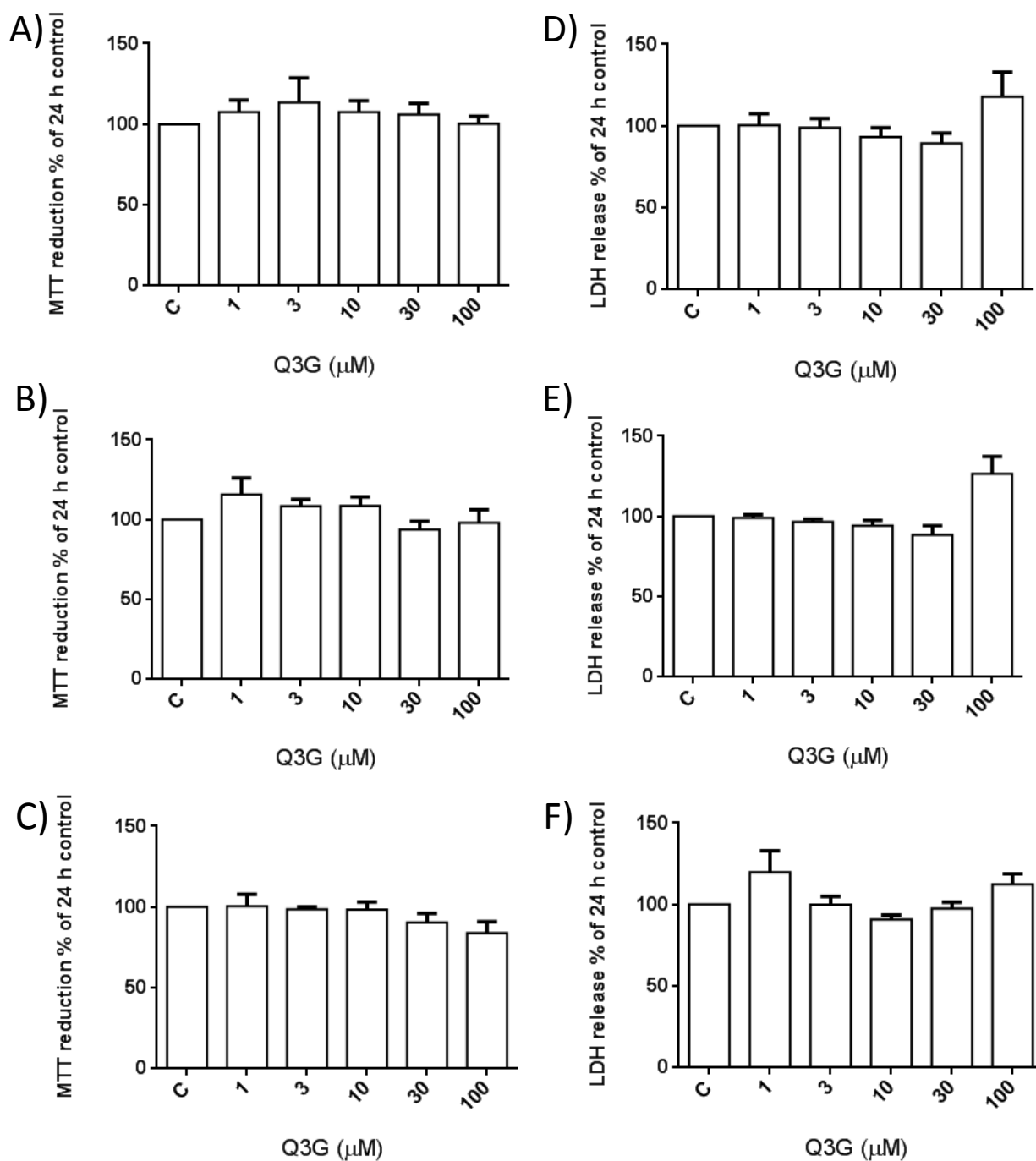


Fig 5.12 Effect of quercetin-3-glucuronide on differentiated H9c2 cell viability. MTT reduction (A,B, C) and LDH release (D, E, F) assays. quercetin-3-glucuronide (Q3G) at all concentrations tested produced no significant changes in viability at points tested; 24 h (A,D), 48 h (B,E) and 72 h (C,F). Data are expressed as the percentage of control cells (C =100 %) and represent the mean \pm SEM of six independent experiments.

5.5 Protein kinase expression associated with flavonoid induced cytotoxicity

As 100 μ M quercetin exposure to differentiated H9c2 cells was shown to produce the most consistent cytotoxicity these parameters were used to test for the effect of flavonoid exposure on protein kinase phosphorylation. Differentiated cells were exposed to 100 μ M quercetin for 24 h, 48 h and 72 h and the phosphorylation of ERK1/2, PKB, p38 MAPK and JNK were monitored using western blotting.

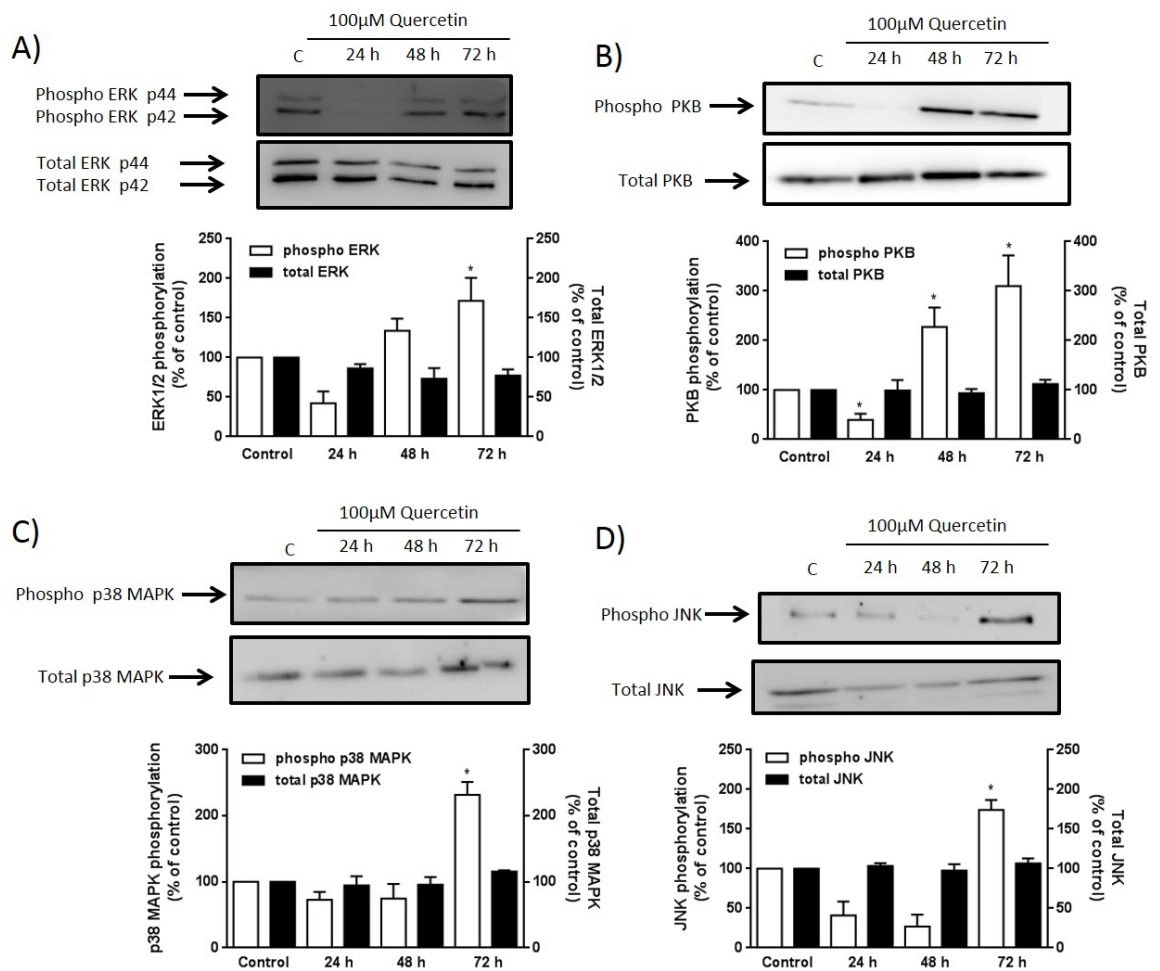


Fig. 5.13 Effect of prolonged quercetin exposure on protein kinase activation. Following exposure to 100 μM quercetin for 24 h, 48 h or 72 h cell lysates were harvested and activation of protein kinases was analysed using western blotting for A) ERK 1/2 B) PKB C)p38 MAPK D) JNK using phosphor-specific antibodies along. Samples were then analysed on separate blots for total versions of the protein kinases using total specific antibodies. It is shown that 72 h exposure to 100 μM quercetin causes a significant (*: $p < 0.05$) increase in phosphorylated levels of A) ERK 1/2 B) PKB C)p38 MAPK and D) JNK. It is also observed that 24 h and 48 h exposure to 100 μM quercetin causes a significant (*: $p < 0.05$) change in B) PKB phosphorylated expression. No significant change was seen in levels of total protein kinase expression for all kinases analysed.

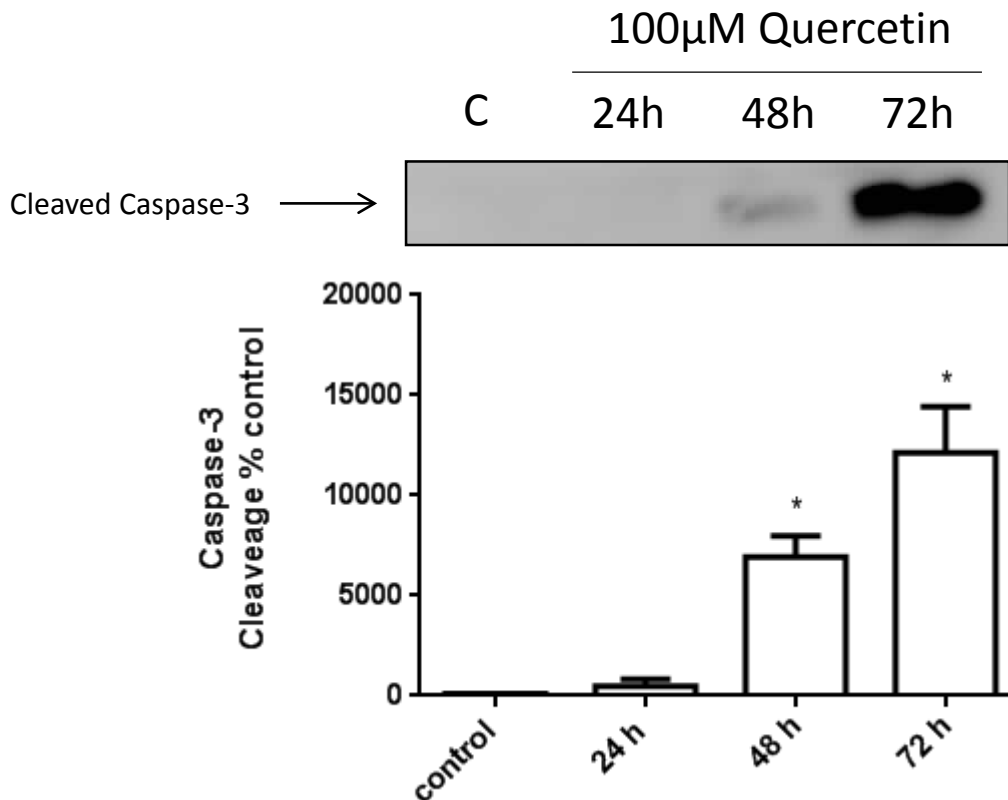


Fig. 5.14 Effect of prolonged exposure to quercetin on caspase-3 activation. Following exposure to 100 μM quercetin for 24 h, 48 h or 72 h cell lysates were harvested and activation of Caspase-3 was monitored with western blotting using anti-cleaved caspase-3 specific antibody. It is shown that 48 h and 72 h exposure to 100 μM quercetin causes a significant (*: $p < 0.05$) increase in caspase-3 activation.

As shown in fig. 5.13, it can be observed that 72 h exposure to 100 μM quercetin causes levels of phosphorylated ERK1/2, PKB, p38 MAPK and JNK to increase. This increase in protein kinase phosphorylation at this time point suggests a relationship between the previously observed incidences of quercetin mediated cell death measured by MTT reduction and LDH release assays. The increased activation of caspase-3 at 48 h and 72 h as shown in fig. 5.14 also coincide with the observation of loss of cell viability at these time points using MTT reduction and LDH release. This suggests a role for apoptosis in flavonoid associated cytotoxicity.

5.6 Intracellular ROS associated with prolonged flavonoid exposure

The potential relationship between flavonoid induced cytotoxicity and intracellular ROS was investigated using the DCFDA assay. Differentiated (7 days) H9c2 cardiomyocytes were exposed to 100 μ M quercetin for 24 h, 48 h or 72 h, and then the presence of intracellular ROS was assayed using the DCFDA fluorescent probe and flow cytometry.

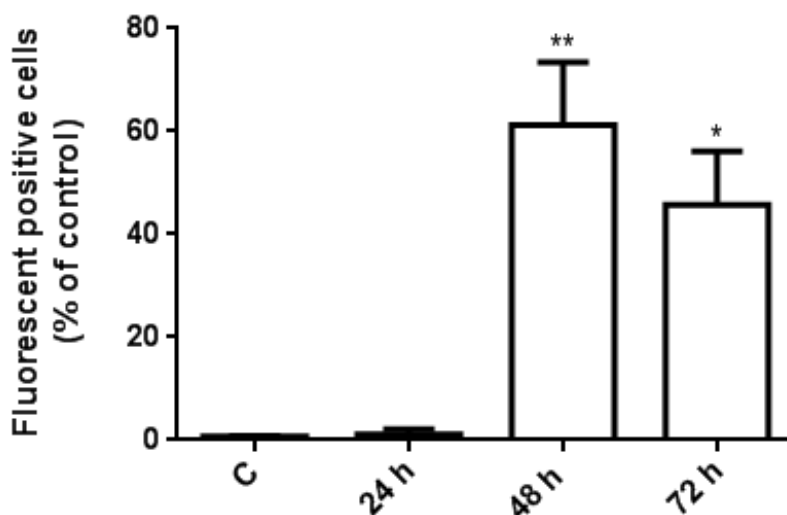


Fig 5.15 Effect of quercetin on reactive oxygen species (ROS) production. Differentiated H9c2 cells were treated with 100 μ M quercetin for 24, 48 and 72 h. ROS production was measured using flow cytometry and the fluorescent probe DCFDA. Both 48 h and 72 h exposure to 100 μ M quercetin caused a significant (*: $p < 0.05$; **: $p < 0.01$) increase in fluorescing cells counted. Data are expressed as the percentage of positive fluorescing cells (10,000 sampled) in each condition, and represent the mean \pm S.E.M of three independent experiments.

As shown on fig. 5.15 both 48 h and 72 h exposure to 100 μ M quercetin caused a significant increase in intracellular ROS. These time points and the concentrations of quercetin match exactly those shown in Fig. 5.10 to cause significant reduction in cell viability, this highlights the possibility that a major mechanism of flavonoid cytotoxicity is causing an increase in intracellular ROS. This pattern of cell death associated events can also be seen with the activation of caspase-3 after 48 h and 72 h exposure to quercetin, further demonstrating the link between flavonoid exposure, ROS production and apoptosis.

5.7 Summary of findings

This chapter identified that flavonoids, as well as having a cytoprotective effect, can have a cytotoxic effect when cells are exposed to concentrations of flavonoid for prolonged periods (> 24 h). Quercetin and myricetin were shown to have a cytotoxic effect on mitotic, differentiating, and differentiated H9c2 cardiomyocytes. Kaempferols cytotoxic effects were observed only in H9c2 cells undergoing differentiation. Quercetin was shown to have the most consistently measurable cytotoxic effect, as the cytotoxicity of 100 μ M exposure was confirmed with both cell viability assays at both 48 h and 72 h exposure times. Of the two metabolites tested 3'-O-methylquercetin was shown to have a cytotoxic effect on differentiated H9c2 cells after 48 h at a 3-100 μ M concentration range. The phosphorylation of ERK1/2, PKB, JNK, p38 MAPK and activation of caspase-3 during prolonged exposure to 100 μ M quercetin was investigated using western blotting. The levels of phosphorylated cell signals was significantly raised after 72 h exposure to 100 μ M quercetin, and caspase-3 activation was significantly increased after 48 h and 72 h exposure to 100 μ M quercetin. The significantly increased phosphorylation occurs when cytotoxicity was observed, and the activation of caspase-3 suggests apoptosis is a consequence of prolonged exposure to quercetin. The potential pro-oxidant effect of prolonged quercetin exposure was investigated using the DCFDA assay to measure intracellular reactive oxygen species. Intracellular ROS was found to be significantly raised after 48 h and 72 h exposure, which links with the previous time point observations with regard to cytotoxic effect, phosphorylation of protein kinases and activation of caspase-3.

5.8 Discussion of flavonoid-mediated cytotoxicity.

i) Cytotoxicity of Flavonoids

In the present study quercetin was shown to have no cytotoxic effect after 24 h exposure on mitotic, differentiating or differentiated H9c2 cells. This finding is in agreement with previous studies that have used only mitotic H9c2 cells, showing that no significant toxicity is associated with quercetin exposure for 24 h with concentrations up to 100 μ M (Angeloni *et al*, 2007). In differentiated cells cytotoxic effects as a result of quercetin exposure were observed after 48 h with 30 μ M and 100 μ M concentrations, with significant reduction in MTT reduction and increases in LDH release. After 72 h exposure significant cytotoxicity

was also observed. Myricetin was also shown to have cytotoxic effects on differentiated H9c2 cells after 48 h exposure. The observation of flavonoid induced cytotoxicity after prolonged (≥ 48 h) exposure has not previously been reported. In mitotic H9c2 cells a similar effect was observed with myricetin and quercetin, as cytotoxicity after 72 h exposure was significant with myricetin concentrations of 30 μM and 100 μM , and all concentrations of quercetin tested. The significant cytotoxic effect was only observable using the MTT reduction assay, although it is known that this is more accurate in detecting cytotoxic events (Fotakis *et al*, 2006). In H9c2 cells undergoing differentiation myricetin, quercetin and kaempferol induced significant cytotoxic effects. Quercetin produced a cytotoxic effect after 72 h exposure with concentrations ≥ 10 μM measured by MTT reduction and LDH release. A concentration of 10 μM would be achievable *in vivo* with supplementation or flavonoid rich foods (Russo *et al*, 2012). Previous studies have identified that quercetin has cytotoxic effects in combination with other drugs in a number of different cell lines (Russo *et al*, 2010; Spencer *et al*, 2003; Repetto *et al*, 2008). The mechanism by which quercetin and other flavonoids induce the observed cytotoxic effect is most likely due to intracellular metabolism into pro-oxidant intermediates, as shown in chapter 1 Fig 1.8 (Metodiewa *et al*, 1998). Intracellular ROS generation associated with quercetin exposure was measured by the DCFDA assay, as shown in Fig. 5.15. Intracellular ROS increased with 100 μM quercetin exposure after 48 h, which coincides with the induction of significant levels of cytotoxicity in differentiated H9c2 cells.

ii) Cytotoxicity of quercetin metabolites

The cytotoxicity of the two major quercetin metabolites 3'-O-methyl quercetin and quercetin 3-glucuronide on differentiated H9c2 cells was also investigated, which showed that quercetin 3-glucuronide has no significant cytotoxic effect. As previously shown in the present study, the lipophobicity of quercetin 3-glucuronide was a probable cause for the lack of protective effect observed. Therefore, this lipophobicity may also be a contributing factor to its lack of cytotoxic effect. Previous studies agree with the observation as a similar metabolite, quercetin 7-glucuronide, was shown to have no significant cytotoxic effect on neuronal cell lines (Spencer *et al*, 2006). Conversely 3'-O-methyl quercetin was shown to induce cytotoxicity after 48 h and 72 h exposure with doses as low as 3 μM . Previous studies

have shown that after 24 h concentrations ranging between 1-30 μM do not induce cytotoxicity in mitotic H9c2 cells, in agreement with this present study (Angeloni *et al*, 2007). Although, cytotoxicity has been induced by 3'-O-methyl quercetin in neuronal cells after 6 h exposure, indicating the toxic potential of the metabolite (Spencer *et al*, 2006). Although a significant decrease in MTT reduction was observed in differentiated cells exposed for 72 h to 3-100 μM 3'-O-methyl quercetin no significant LDH released was observed, suggesting that 3'-O-methyl quercetin may have an effect on mitochondrial function while not inducing a disruption of the cell membrane leading to LDH leakage. Like the parent molecule quercetin, a contributing factor to the cytotoxicity of 3'-O-methyl quercetin is most likely due to intracellular metabolism promoting the production of intracellular ROS, or the deconjugation of the metabolite intracellularly followed by intracellular ROS generation by the metabolism of the aglycone (Viskupičová *et al*, 2008).

iii) Role of cell signalling in flavonoid-mediated cytotoxicity

To investigate more fully the mechanism by which quercetin induces a cytotoxic effect, western blotting was used to monitor the phosphorylation of the pro-survival cell signalling molecules ERK1/2 and PKB, and the pro-apoptosis signalling molecules JNK and p38 MAPK in addition to the activation of the apoptosis marker caspase-3. Quercetin has been shown to induce significant activation of caspase-3 in neuronal cells, which coincides with its cytotoxic effects (Spencer *et al*, 2006). Using western blotting quercetin (100 μM) was able to induce caspase-3 activation after 48 h and 72 h exposure in differentiated H9c2 cells. This suggest that quercetin induces apoptotic cell death after 48 h exposure, which would also suggest that the cytotoxic effect of myricetin and 3'-O-methyl quercetin induce a similar response. As quercetin is known to be a potent inhibitor of MEK1 and P1-3K γ , upstream regulators of ERK1/2 and PKB, it is expected that the mechanism of cytotoxicity of quercetin involves the attenuation of ERK1/2 and PKB activation and the activation of the pro-apoptotic signals JNK and p38 MAPK (Hers *et al*, 2007; Lu and Xu, 2006). Quercetin demonstrates a more potent inhibition of MEK1 than the commercially available and widely used MEK1 inhibitor PD98059 (Lee *et al*, 2008). In the present study, as shown in Fig. 5.13 24 h exposure to 100 μM quercetin significantly attenuated the phosphorylation of PKB and reduced the phosphorylation of ERK1/2. Interestingly after 48 and 72 h exposure the levels of phosphorylated PKB significantly increase, suggesting a bi-phasic pattern of quercetin

interactions with PKB. The actions of quercetin on PKB and ERK1/2 are varied and conflicting, as Angeloni *et al* (2007) reported that quercetin at 30 μ M activates ERK1/2 and PKB in mitotic H9c2 cells. Quercetin mediated activation of ERK1/2 has also been reported in macrophages (Chow *et al*, 2005) pancreatic β cells (Youl *et al*, 2010) and HepG2 cells, where it also induces an increase in JNK, p38 MAPK and PKB phosphorylation (Weng *et al*, 2011). However quercetin has been shown to inhibit the phosphorylation of ERK1/2 and PKB in neuronal cell lines (Spencer *et al*, 2003), and PKB inhibition plays a crucial role in the reported anti-proliferative effects of quercetin on cancer cells (Gulati *et al*, 2006). As shown in Fig. 4.20 24 h exposure to 30 μ M quercetin did not cause a significant effect on the phosphorylated levels of ERK1/2 or PKB, whereas 24 h exposure to 100 μ M quercetin significantly attenuated ERK1/2 and PKB phosphorylation (Fig 4.20 and 5.13). The effect of 24 h exposure to 100 μ M quercetin is analogous to the effect of the two selective inhibitors for MEK1 and PI3K, PD98059 and LY294002 respectively. In the present study exposure to 100 μ M quercetin for 72 h caused a significant increase in the phosphorylated levels of ERK1/2, p38 MAPK, JNK and PKB in the differentiated H9c2 cells. Quercetin induced cytotoxicity can therefore be linked to apoptosis, as both JNK and p38 MAPK are pro-apoptotic cell signals (Mansuri *et al*, 2014). Other mechanisms of quercetin induced cytotoxicity have been shown to be JNK independent (Kim and Lee, 2007). The mechanism by which quercetin induces JNK and p38 MAPK phosphorylation remains unclear, quercetin has been shown to stimulate the upstream kinases TAK1 and MKK3/6 which are associated with p38 MAPK (Chang *et al*, 2012). Clearly, flavonoid induced cytotoxicity involves the modulation of several protein kinases, both associated with survival and apoptosis.

iv) Implications of flavonoid induced cytotoxicity

The findings detailed in this current chapter and chapter 4 present somewhat of a paradox. Quercetin was shown to induce a cytoprotective effect with concentrations \geq 30 μ M after 24 h exposure, whereas after 48 h exposure these same concentrations were shown to cause significant cell death in differentiated H9c2 cells. This present study is the first time these effects have been demonstrated at the same time. Considering the bioavailability of quercetin, with the reported maximal plasma concentration achievable being $<$ 10 μ M, it is unlikely that cardiac cells *in vivo* will be exposed to the concentrations that were observed to cause cytotoxicity in a single dose from dietary sources (Labbé *et al*, 2009). Similarly, as shown in

chapter 4, the doses required to elicit a cytoprotective effect are higher than the currently achievable plasma concentration from dietary sources. Of the metabolites investigated 3'-O-methyl quercetin was shown to cause significant cytotoxicity with doses $\geq 3 \mu\text{M}$. Quercetin and its metabolites in the plasma have been shown to surpass this concentration, furthermore the lipophilicity of quercetin and 3'-O-methyl quercetin suggest it could be accumulated in cells (Labbé *et al*, 2009). Although, when considering the half-life of the quercetin metabolites exposure to the required doses to induce cytotoxicity *in vivo* is unlikely. The results of this chapter therefore represent a phenomenon that is only be created artificially. Despite this, these results highlight that quercetin in particular and flavonoids in general can have major effects on cells under certain conditions, currently achievable in a laboratory.

Chapter 6: Proteomic
identification of
flavonoid mediated
cardioprotective
associated proteins

6.0 Proteomic identification of flavonoid mediated cardioprotective associated proteins.

Exposure to quercetin has been observed to cause inhibition of the MAPK and PI3K pathways in mitotic H9c2 cells in previous studies and differentiated cells as shown in Chapter 4 (Gutiérrez-Venegas *et al*, 2010; Angeloni *et al*, 2012; Angeloni *et al*, 2007; Sun *et al*, 2012; Kim *et al*, 2010; Mojzisoová *et al*, 2009). As these cell signal cascades can lead to the activation of protein expression, it is proposed that flavonoid exposure may lead to the increased expression of proteins associated with these pathways (Courtney *et al*, 2010; Roskoski, 2012). For the first time proteomic methods will be used to investigate the effects of quercetin exposure on protein expression in differentiated H9c2 cells treated with quercetin and differentiated H9c2 cells treated with quercetin and subsequently exposed to oxidative stress.

Quercetin has been previously shown using proteomic methods to induce increased expression of several proteins in mitotic H9c2 cells treated with 1 mM quercetin and 5 mM H₂O₂ (Chen *et al*, 2013). Using the information obtained regarding the concentrations and exposure time of quercetin that induces a cytoprotective effect from this present study, the proteins expressed in differentiated H9c2 cells treated with 30 µM and 100 µM for 24 h will be investigated. Furthermore, protein expression in differentiated H9c2 cells treated for 24 h with 30 µM and 100 µM quercetin prior to oxidative insult from 600 µM H₂O₂ exposure for 2 h will also be investigated. Following identification of proteins by MALDI-TOF MS, western blotting will be used to further measure the expression of the identified proteins.

The nature of the cell signalling cascades and their interaction with flavonoids are complex and remain mostly unknown. It is hoped that using proteomic methods to investigate proteins expressed resulting from quercetin exposure will provide novel insight into the mechanism of flavonoid mediated cytoprotection.

6.1 Two-dimensional gel electrophoresis

To identify novel proteins associated with flavonoid mediated cardioprotection cell lysates from specific treatments were prepared and subjected to two-dimensional gel electrophoresis. Two-dimensional gels were prepared from differentiated H9c2 cells exposed to 600 μM H_2O_2 for 2 h (Fig 6.3), differentiated H9c2 cells pre-treated for 24 h with 100 μM quercetin and then exposed to 600 μM H_2O_2 for 2 h (Fig 6.1) and differentiated H9c2 cells pre-treated for 24 h with 30 μM quercetin and then exposed to 600 μM H_2O_2 for 2 h (Fig. 6.2). Furthermore, Two-dimensional gels were prepared from lysates from cells treated with 100 μM (Fig. 6.4) and 30 μM (Fig. 6.5) without the additional 600 μM H_2O_2 treatment, to determine if the expression of some novel proteins is associated with flavonoid treatment alone. The lysates were prepared using specific 2D gel electrophoresis lysis buffer, as described in section 2.7. Two-dimensional gel electrophoresis was then performed, the gels stained and imaged according to the section 2.7. An example gel from each set of three for each of the treatment conditions are shown below, full sets of the three gels for each treatment can be seen in Appendix 2.

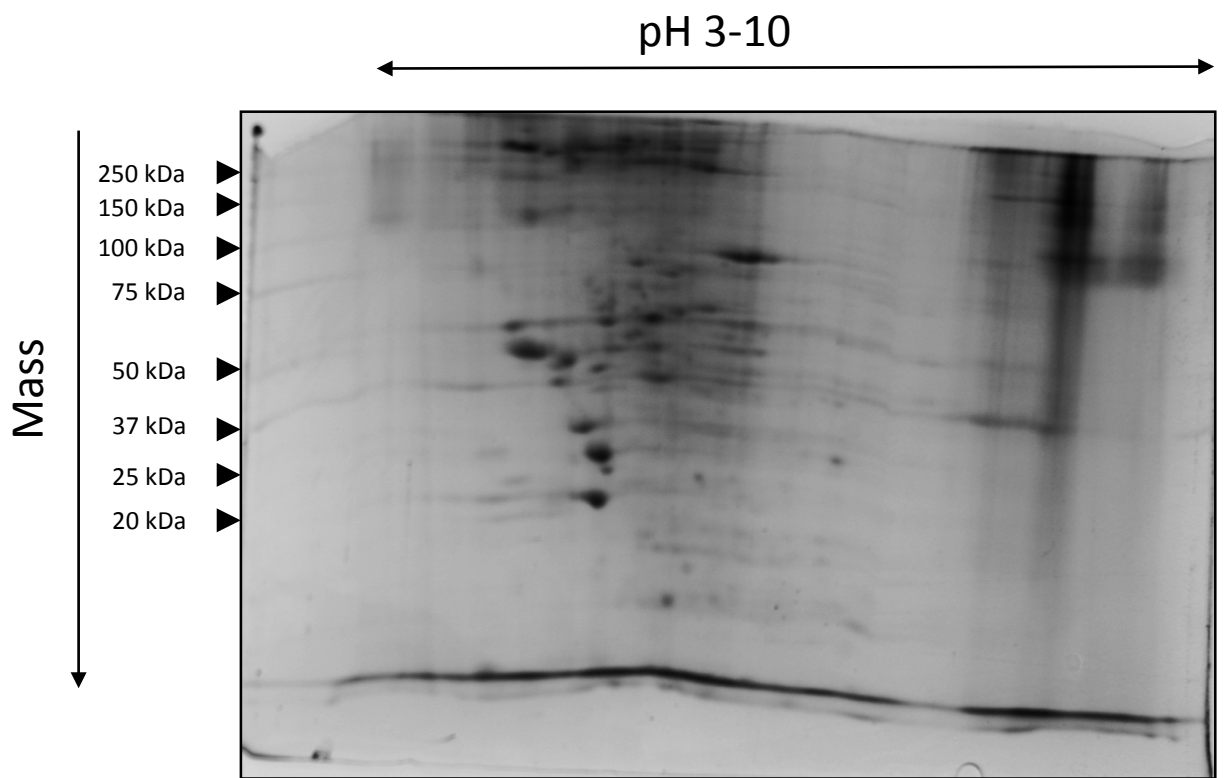


Fig 6.1 Expression pattern of proteins in 100 μ M quercetin pre-treated differentiated H9c2 cells after exposure to H₂O₂. Proteins are separated first according to isoelectric point along a pH gradient, and then according to mass with polyacrylamide gel. Mass (kDa) has been highlighted using protein standards. Image is a representative gel of three separate experiments.

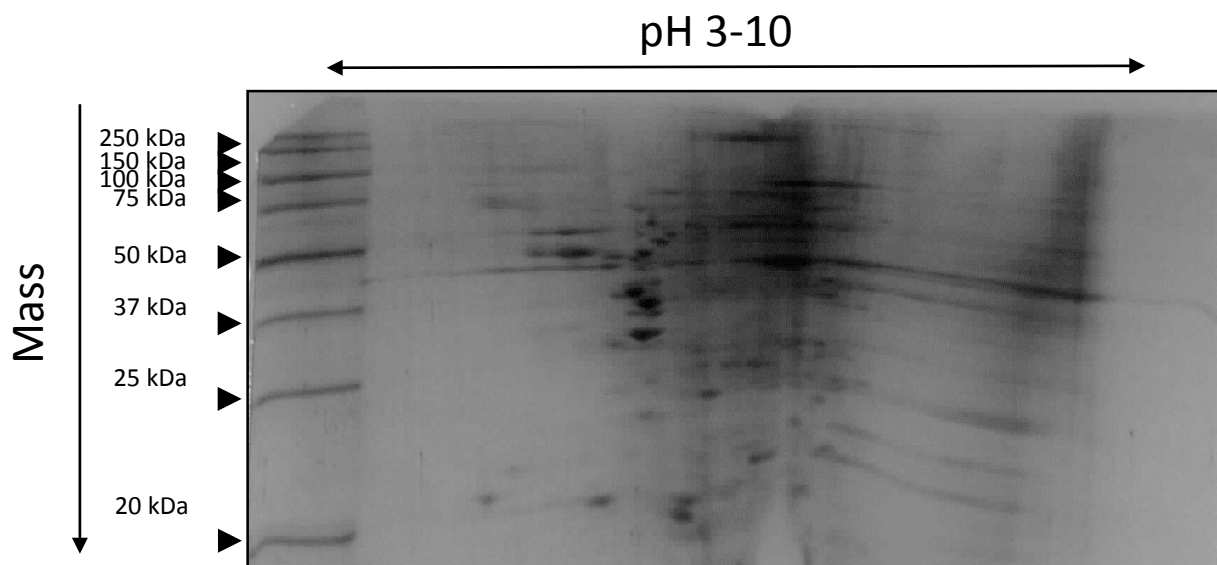


Fig 6.2 Expression pattern of proteins in 30 μM quercetin pre-treated differentiated H9c2 cells after exposure to H_2O_2 . Mass (kDa) has been highlighted using protein standards. Image is a representative gel of three separate experiments.

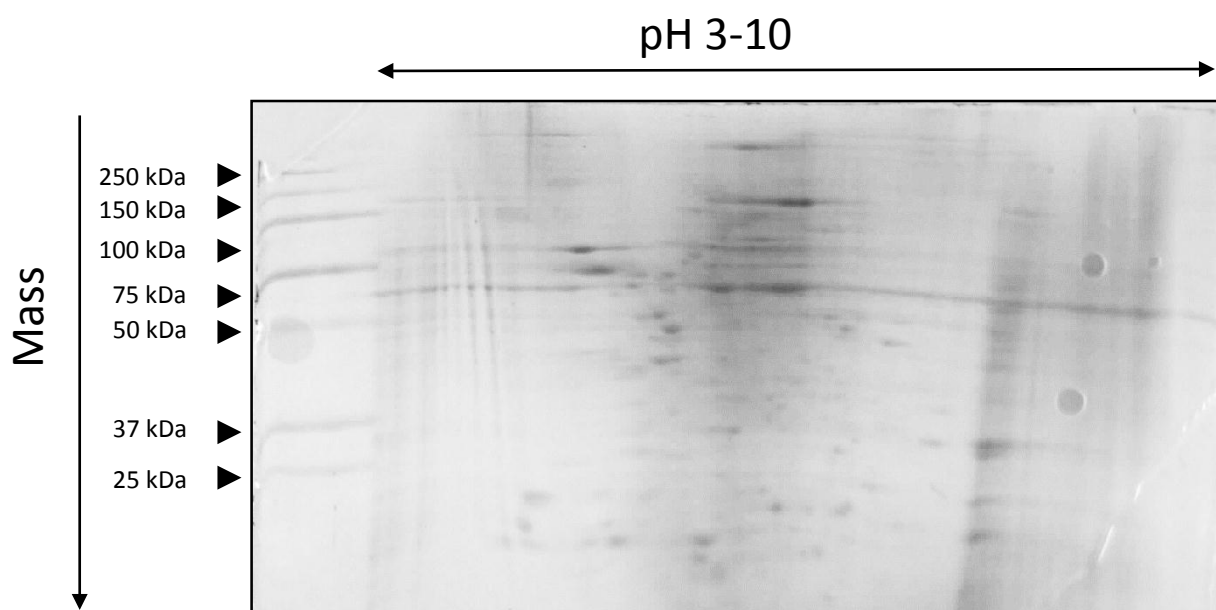


Fig 6.3 Expression pattern of proteins in differentiated H9c2 cells after exposure to H_2O_2 . Mass (kDa) has been highlighted using protein standards. Image is a representative gel of three separate experiments.

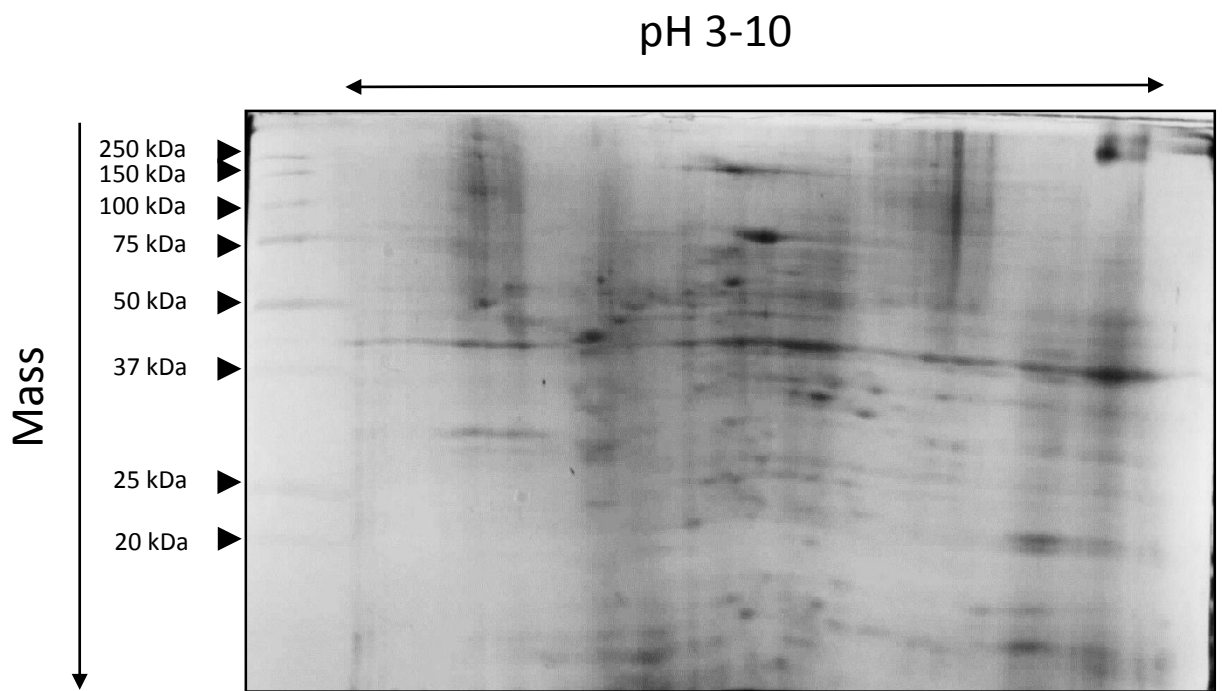


Fig 6.4 Expression pattern of proteins in differentiated H9c2 cells after 24 h treatment with 100 μ M. Mass (kDa) has been highlighted using protein standards. Image is a representative gel of three separate experiments performed separately.

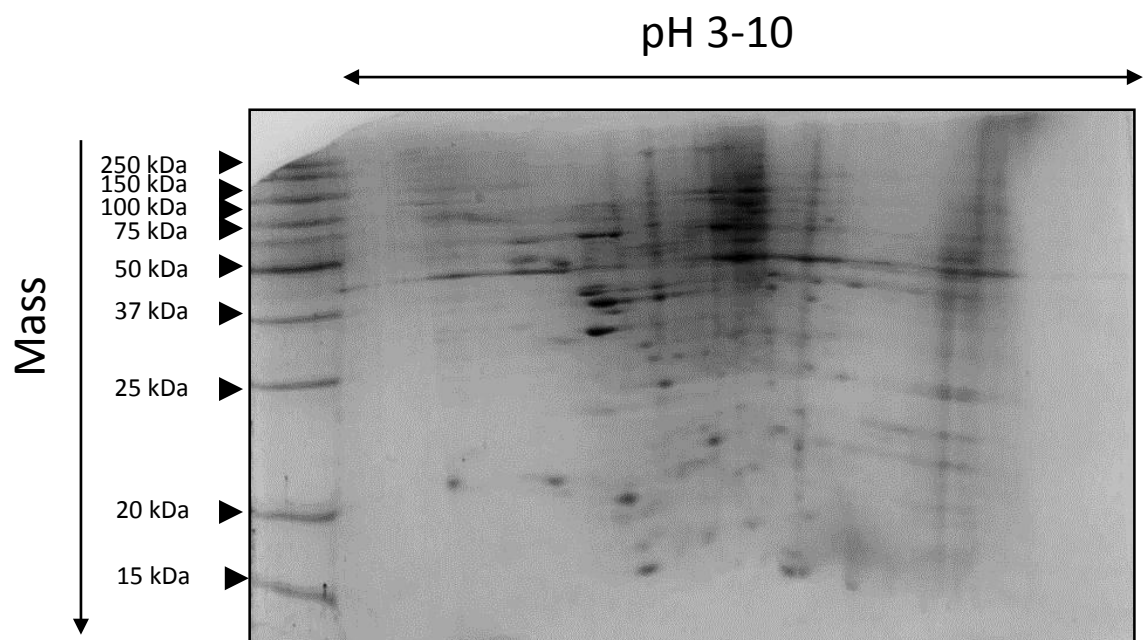


Fig 6.5 Expression pattern of proteins in differentiated H9c2 cells after 24 h treatment with 30 μ M. Mass (kDa) has been highlighted using protein standards. Image is a representative gel of three separate experiments performed separately.

6.2 Progenesis SameSpot analysis

Images of three separate 2D gels of differentiated H9c2 cells exposed to 600 μM H_2O_2 for 2 h and differentiated H9c2 cells pre-treated for 24 h with 100 μM quercetin and then exposed to 600 μM H_2O_2 for 2 h were analysed using Progenesis SameSpot software as described in section 2.7 part ii. Images were aligned to a selected control image, a representative 2D gel of differentiated H9c2 cells exposed to 600 μM H_2O_2 for 2 h was used when determining the effects of 30 μM or 100 μM quercetin pre-treatment. Protein spots were identified by the software, which were confirmed to be viable spots by visual confirmation. Protein spots were then assigned an identity number. The relative density of the protein spots was then calculated and the change in density of the protein spots between the two sets of gels was analysed using the software. The significance of the difference in density was calculated using ANOVA and the protein spots ranked according to their significance, and highlighted on a spot picking map of a reference gel image. Firstly, the difference between differentiated H9c2 cells exposed to 600 μM H_2O_2 for 2 h and differentiated H9c2 cells pre-treated for 24 h with 100 μM quercetin was investigated (Fig 6.6), followed by the difference between differentiated H9c2 cells exposed to 600 μM H_2O_2 for 2 h and differentiated H9c2 cells pre-treated for 24 h with 30 μM quercetin (Fig. 6.8).

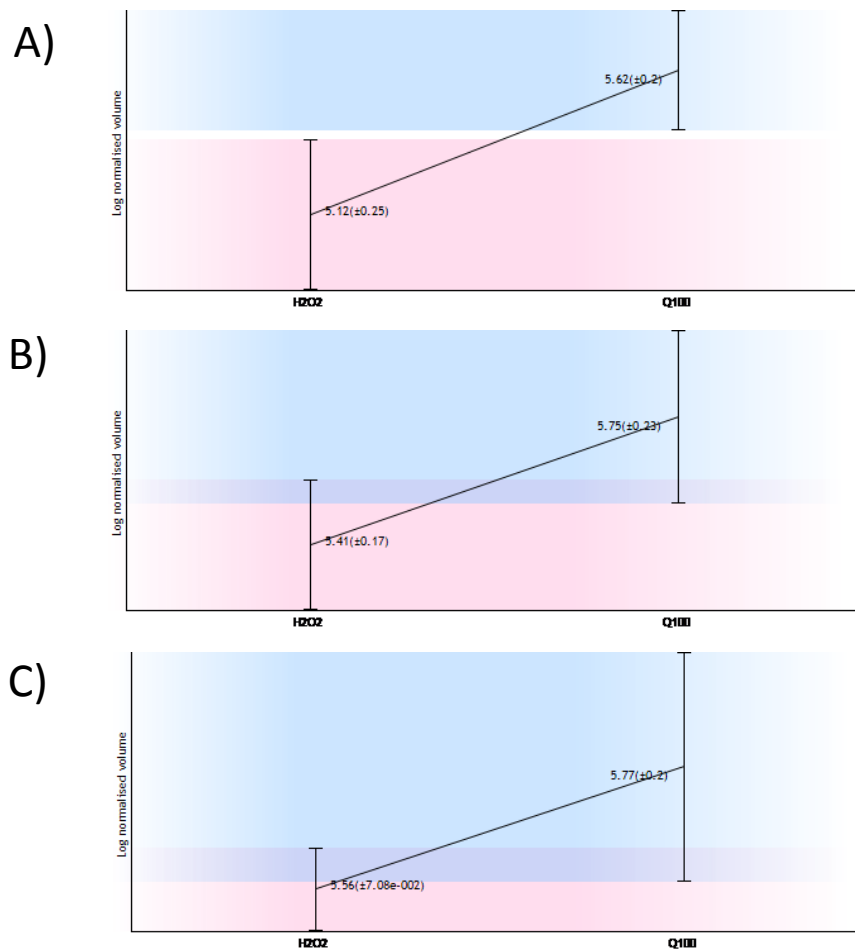


Fig. 6.6 Progenesis same-spot analysis of protein spot densities in 100 μM quercetin pre-treated cells and 600 μM H_2O_2 treated cells. The difference in density between the two sets of gels, differentiated H9c2 cells exposed to 600 μM H_2O_2 for 2 h (H2O2) and differentiated H9c2 cells pre-treated for 24 h with 100 μM quercetin and then exposed to 600 μM H_2O_2 for 2 h (Q100), of three protein spots A) spot ID 8, B) spot ID 28 and C) spot ID 48. Each spot was shown to be of a higher density consistently in the gels of differentiated H9c2 cells pre-treated for 24 h with 100 μM quercetin and then exposed to 600 μM H_2O_2 for 2 h when compared to differentiated H9c2 cells exposed to 600 μM H_2O_2 for 2 h alone. The increase in density of protein spot was found to be significant for each spot using ANOVA analysis . A) *: $p < 0.011$ B) *: $p < 0.023$ and C) *: $p < 0.04$. Data are expressed as the mean log normalised volume of protein spot \pm S.E.M of three independent experiments in each group.

From the analysis shown in Fig. 6.6 spot ID numbers 8, 28 and 48 were found to be significantly more dense in differentiated H9c2 cells pre-treated with 100 μM quercetin for 24 h and then exposed to 600 μM H_2O_2 for 2 h when compared to differentiated H9c2 cells exposed to 600 μM H_2O_2 for 2 h. These spots were then picked from the three gels of the lysates from the differentiated H9c2 cells pre-treated with 100 μM quercetin for 24 h and then exposed to 600 μM H_2O_2 for 2 h, according to the spot picking map (Fig. 6.7).

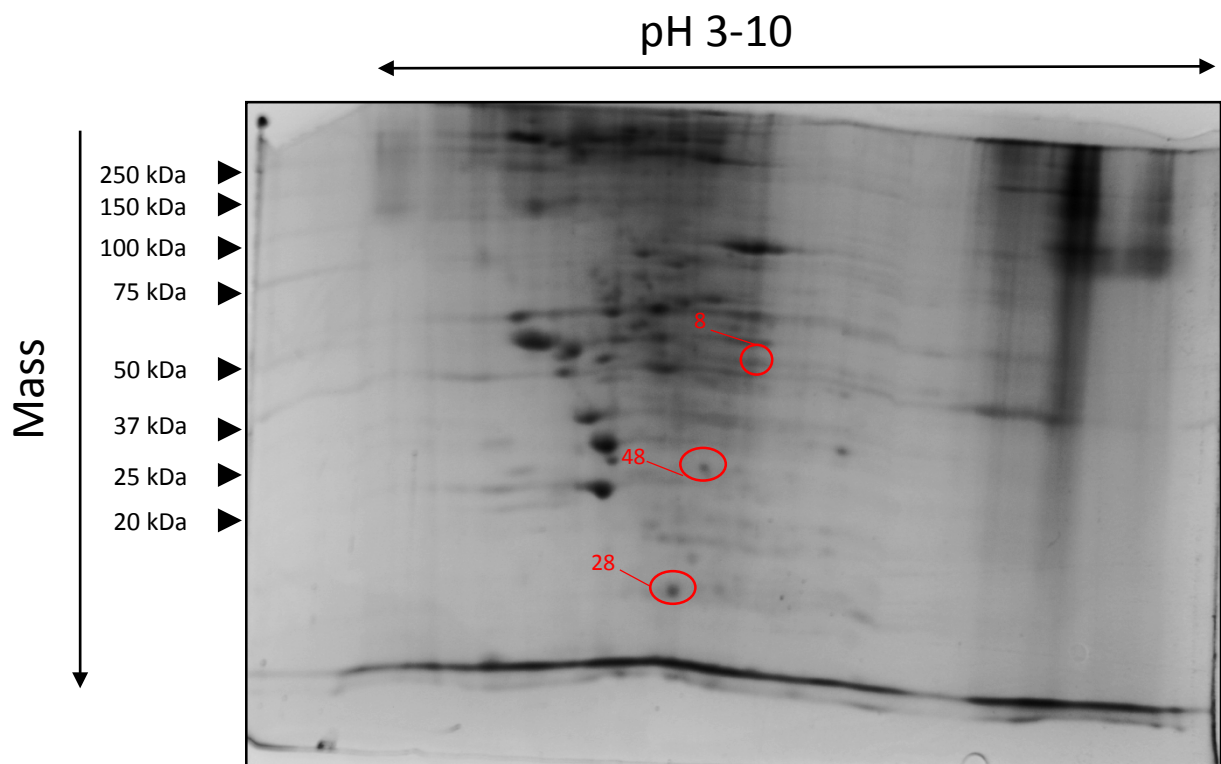


Fig 6.7 Spot picking map of significantly changed protein spots. Spot ID 8 is shown to be approximately 37 kDa, Spot ID 46 between 37 and 25 kDa and spot ID 28 less than 20 kDa.

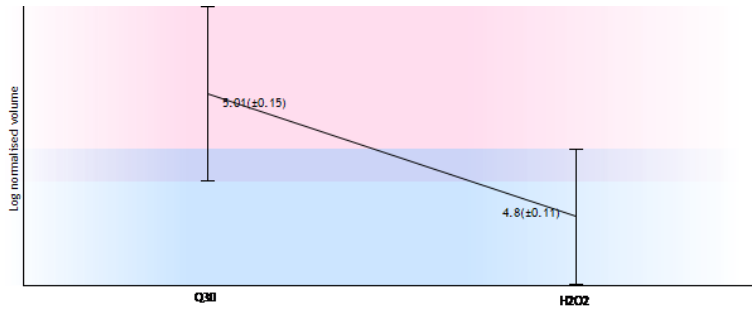


Fig. 6.8 Progenesis same-spot analysis of protein spot densities in 30 μM quercetin pre-treated cells and 600 μM H_2O_2 treated cells. The difference in density between the two sets of gels, differentiated H9c2 cells exposed to 600 μM H_2O_2 for 2 h (H2O2) and differentiated H9c2 cells pre-treated for 24 h with 30 μM quercetin and then exposed to 600 μM H_2O_2 for 2 h (Q30). One spot (ID 14) was found to be significantly (*: $p < 0.028$) upregulated.

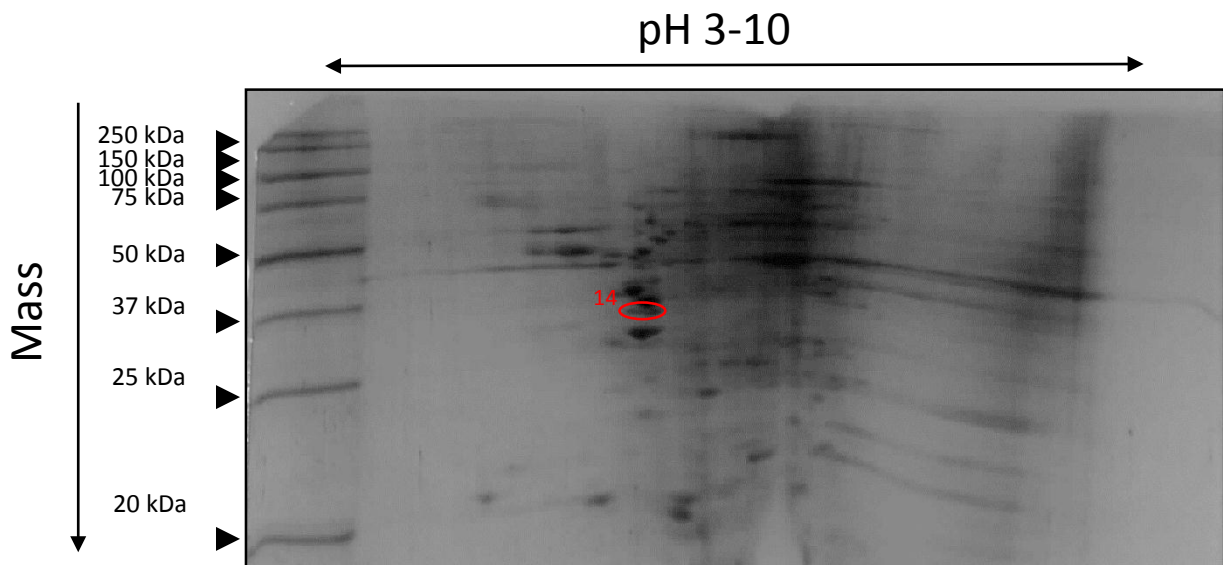


Fig 6.9 Spot picking map of significantly changed protein spots. Spot ID 14 is shown to be approximately 37 kDa.

Spot ID numbers 8, 28 and 48 were found to be significantly more dense in differentiated H9c2 cells pre-treated with 30 μM quercetin for 24 h and then exposed to 600 μM H_2O_2 for 2 h when compared to differentiated H9c2 cells exposed to 600 μM H_2O_2 for 2 h in addition to the previously identified upregulation with 100 μM quercetin pre-treatment. Spot ID 14 was found to be uniquely upregulated with 30 μM quercetin pre-treatment (Fig. 6.8), and was therefore selected for identification. In addition to the 4 proteins highlighted in Figs. 6.7 and 6.9 the cytoskeletal proteins identified in chapter 3.0 (Fig. 3.8 spot picking map) were also shown to be at a higher density after pre-treatment with both 30 μM and 100 μM quercetin compared to cells exposed to 600 μM H_2O_2 for 2 h.

Novel proteins that are induced to be expressed by flavonoid treatment alone was determined by using Progenesis SameSpot analysis to compare 2D gels produced from cells treated for 24 h with 30 μM (Fig. 6.5) or 100 μM (Fig. 6.4) quercetin to each other. Three protein spots (Spots ID 18, 42 and 46) were identified as significant (Fig. 6.10) and visually distinct to enable picking. The density of spots 18 and 46 were significantly increased in cells lysates from cell treated for 24 h with 30 μM quercetin (Fig. 6.11), whereas spot 42 was significantly denser in cells lysates from cells treated with 100 μM quercetin (Fig. 6.12).

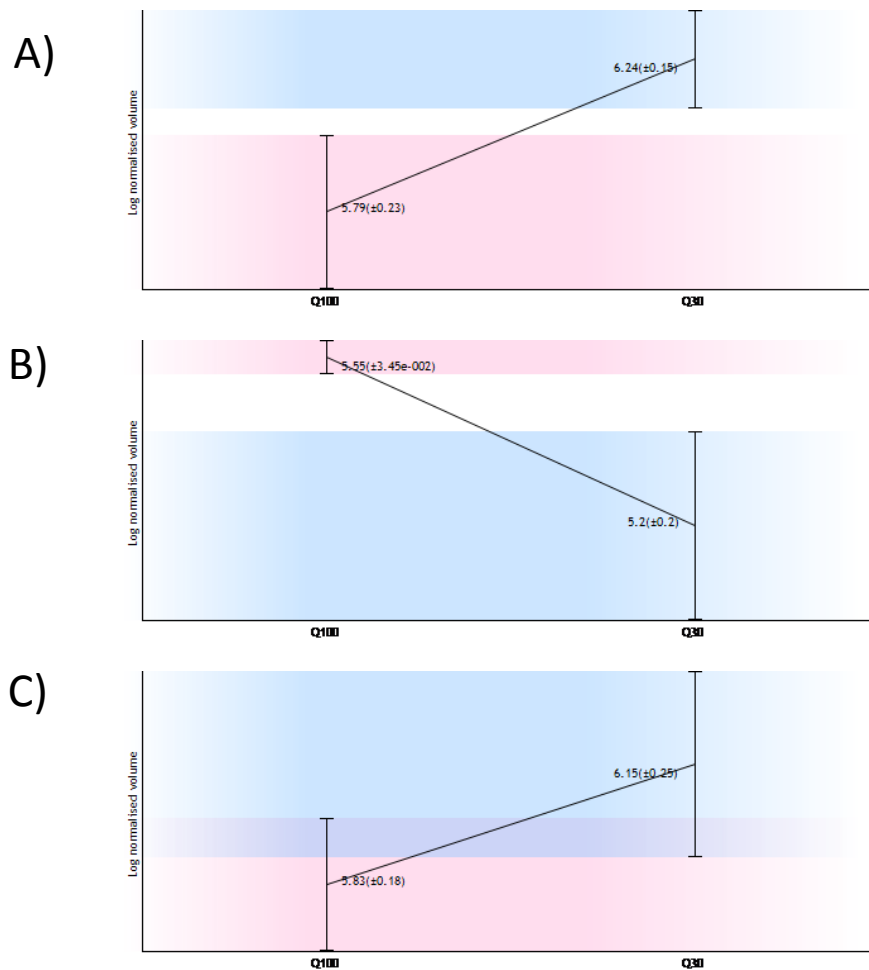


Fig. 6.10 Progenesis sameSpot analysis of protein spot densities in 100 μ M quercetin treated cells and 30 μ M quercetin treated cells. The difference in density between the two sets of gels, differentiated H9c2 cells exposed to 100 μ M quercetin for 24 h (Q100) and differentiated H9c2 cells exposed to 30 μ M quercetin for 24 h (Q30), of three protein spots A) spot ID 18, B) spot ID 42 and C) spot ID 46. The increase in density of protein spot was found to be significant for each spot using ANOVA analysis. A) *: $p < 0.026$ B) **: $p < 0.006$ and C) ***: $p < 0.001$. Data are expressed as the mean log normalised volume of protein spot \pm S.E.M of three independent experiments in each group.

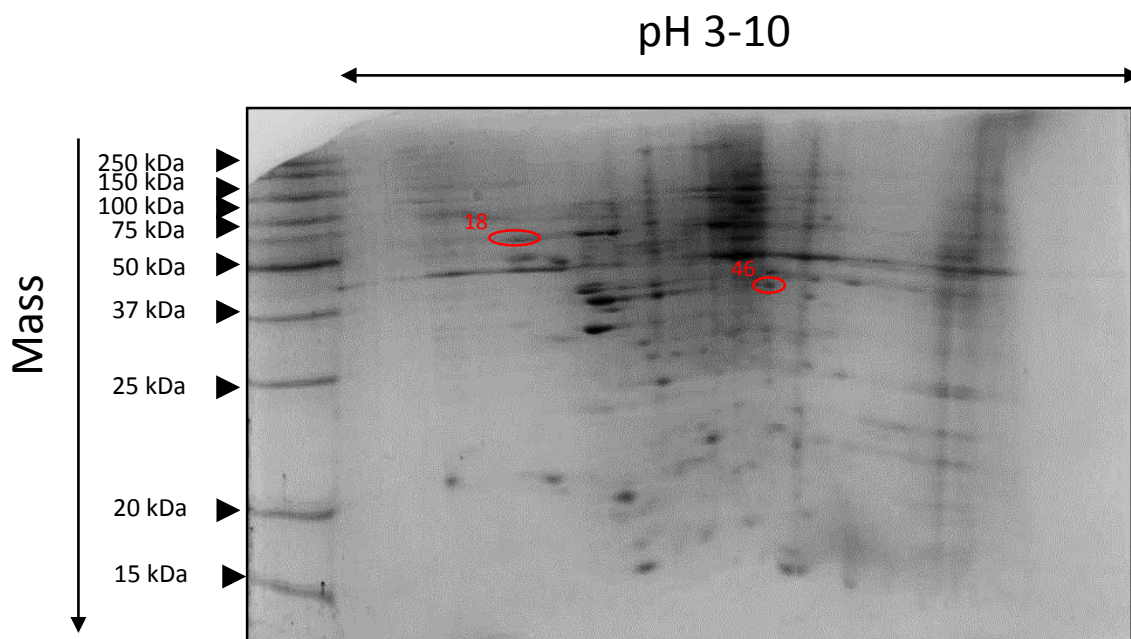


Fig 6.11 Spot picking map of significantly changed protein spots after 30 μM flavonoid treatment. Spot ID 18 is shown to be approximately 75 kDa and spot ID 46 between 37 and 50 kDa. This spot picking map uses a representative gel of cells treated with 100 μM as a reference image.

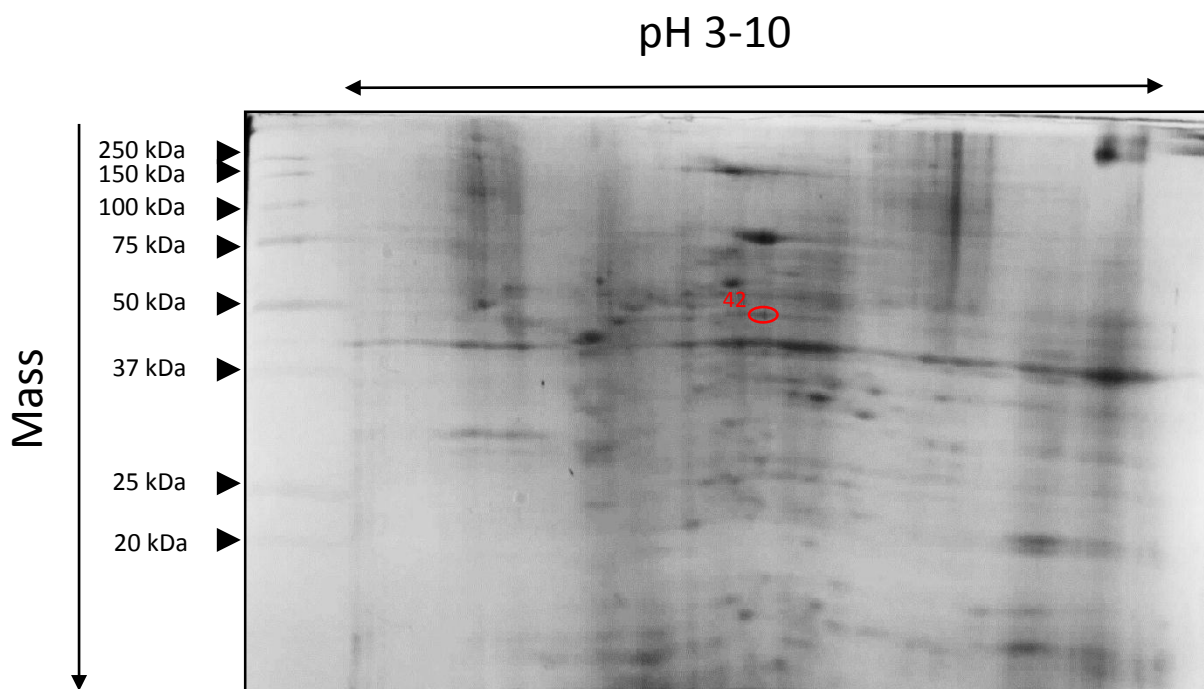


Fig 6.12 Spot picking map of significantly changed protein spots after flavonoid 100 μM treatment. Spot ID 42 is shown to be between 50 and 75 kDa. This spot picking map uses a representative gel of cells treated with 30 μM as a reference image.

6.3 MALDI-TOF MS identification of proteins

The identified spots were tryptically digested, and purified in preparation for MALDI-TOF MS according to section 2.7 part iii and iv. The identity of the proteins found to have an increased expression resulting from flavonoid pre-treatment and subsequent H₂O₂ exposure are summarised in Table 6.13. MALDI-TOF MS/MS data of the proteins found to be expressed in an increased density after 24h exposure to 100 µM or 30 µM quercetin is summarised in table 6.14.

Progenesis spot number	mass	RMS error (ppm)	Identification	PMF Score*	PMF Sequence Coverage (%)	Progenesis score
8	30559	44	Carbonyl Reductase (NADPH) 1	53.5	56	p < 0.011
28	14847	43	Galectin-1	54.5	60	p < 0.023
48	20788	21	Phosphatidylethanolamine-binding protein 1	69.5	74	p < 0.04
14	35844	35	PRKC apoptosis WT1 regulator protein [†]	54		p < 0.028

Table 6.13 Summary of MALDI-TOF MS data of proteins associated with flavonoid induced cytoprotection. The identity of the four spots tested were found to be Carbonyl reductase (NADPH) 1 (CBR1) , Galectin-1, Phosphatidylethanolamine-binding protein 1 (PEBP-1) and PRKC apoptosis WT1 regulator protein (PAWR). *PMF score > 51 considered significant (p > 0.05). [†]PRKC apoptosis WT1 regulator protein was identified in one of the three spot ID 14 analysed with a statistically significant PMF score. PMF sequence coverage and PMF score and RMS error are expressed as the mean of scores from 3 separate protein spots from different gels.

Progenesis spot number	mass	RMS error (ppm)	Identification	Progenesis score	MS/MS Score [#]	MS/MS Peptides
18	107154	92	Glutamate receptor, ionotropic kainate 4	p < 0.026	26	K.GQRSNYALKILQFTR.N
42	36300	40	Annexin-III	p < 0.006	107	K.GELSGHFEDLLLAVVR.L
46	36973	30	Calumenin	p < 0.001	175	K.EEIVDKYDLFVGSQATDFGEALVR.H

Table 6.14 Summary of MALDI-TOF MS/MS data of protein expression associated with flavonoid exposure. Spot ID 18 and Spot ID 46 proteins, Glutamate receptor (ionotropic kainite 4) and Calumenin, were shown to be expressed at a greater density in differentiated H9c2 cells exposed to 30 μ M quercetin for 24 h. Spot ID 42 protein, identified as Annexin-III, was shown to be expressed at a greater density in differentiated H9c2 cells exposed to 100 μ M quercetin for 24 h. [#]MS/MS score > 21 considered significant (p > 0.05). RMS error and MS/MS score are expressed as the mean of scores from 3 separate protein spots from different gels.

From the MALDI-TOF MS data and the Progenesis SameSpot analysis (Table 6.13) it can be seen that CBR-1, galectin-1 and PEBP-1 expression is significantly increased in cell lysates from differentiated H9c2 cells pre-treated for 24 h with 100 μ M quercetin and then exposed to 600 μ M H₂O₂ for 2 h when compared to differentiated H9c2 cells exposed to 600 μ M H₂O₂ for 2 h. This suggests that these proteins are involved in flavonoid mediated cardioprotection. The MALDI-TOF MS/MS data (Table 6.14) for proteins associated with flavonoid treatment shows that different concentrations of quercetin induce the expression of different proteins.

6.4 Western blot confirmation of CBR-1 expression

MALDI-TOF analysis identified CBR-1 expression was increased in of differentiated H9c2 cells pre-treated for 24 h with 100 μM quercetin and then exposed to 600 μM H_2O_2 for 2 h (Table 6.13). Further confirmation of this increase in expression was investigated using western blotting (Fig. 6.15). CBR-1 specific antibodies were used to monitor CBR-1 expression in differentiated H9c2 cells pre-treated for 24 h with 100 μM quercetin and then exposed to 600 μM H_2O_2 for 2 h and differentiated H9c2 cells exposed to 600 μM H_2O_2 for 2 h, α -tubulin was used as a housekeeping protein to ensure even loading.

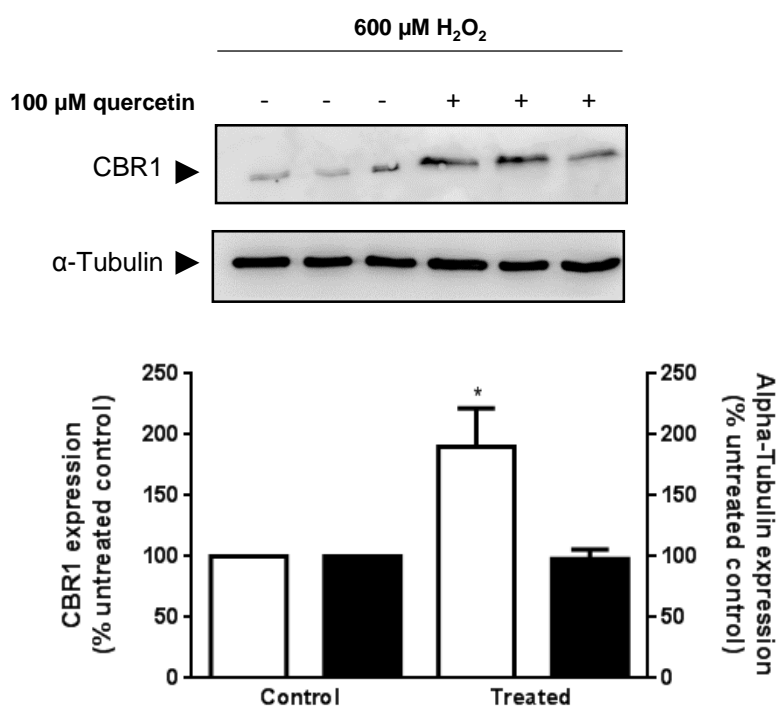


Fig. 6.15 Effect of quercetin pre-treatment on CBR-1 expression during oxidative stress. Cells pre-treated with for 24 h with 100 μM quercetin and then exposed to 600 μM H_2O_2 for 2 h (Treated) showed a significantly (*: $p < 0.05$) increased expression of CBR-1 when compared to the control differentiated H9c2 cells exposed to 600 μM H_2O_2 for 2 h. White bars represent the expression of CBR-1, black bars represent the expression of α -tubulin. Data are expressed as a percentage of control cells (control = 100%) and represent the mean \pm S.E.M of three independent experiments.

From the western blot analysis and mass spectrometry data it can be seen that quercetin pre-treatment followed by oxidative stress causes a significant increase in CBR-1, compared to cells not treated with quercetin. This suggests that CBR-1 has a role in flavonoid mediated cardioprotection.

6.5 Proteomics Discussion

This present study represents the first of its kind in using proteomic methods (MALDI-TOF MS) to investigate the effects of quercetin pre-treatment on differentiated H9c2 cells. Furthermore this present study is, to the author's knowledge, the first to report protein expression resulting from exposure to different quercetin concentrations alone. One previous study investigated the effects of quercetin pre-treatment and subsequent exposure to H₂O₂ on protein expression in mitotic H9c2 cells, however this study used 1 mM quercetin pre-treatment for 1 h and exposure to 5 mM H₂O₂ for 20 min (Chen *et al*, 2013). The concentration of quercetin used in the study by Chen *et al* (2013) is pharmacologically unrealistic (1 mM), as it is far greater than the known concentrations achievable *in vivo* (Labbé *et al*, 2009). Furthermore, when compared to the 600 µM H₂O₂ used in this present study, the 5 mM H₂O₂ used by Chen *et al* (2013) is a less realistic model for oxidative stress caused by ischaemic attack. The proteomic findings of this present study were gained using a more appropriate and accurate model of *in vivo* cardiomyocytes, pharmacologically relevant concentrations of quercetin and an appropriate concentration of H₂O₂ to simulate ischaemia. Proteomic analysis of protein expression during 100 µM and 30 µM pre-treatment and subsequent exposure to 600 µM H₂O₂ identified several novel proteins associated with the quercetin mediated cytoprotective effects. CBR-1, Gelectin-1, PEBP-1 and PRKC apoptosis WT1 regulator protein (PAWR) were identified as being associated with flavonoid mediated cytoprotection, as their expression was up regulated after quercetin pre-treatment and subsequent 600 µM H₂O₂ exposure. Furthermore, Annexin-III, calumenin and Glutamate receptor (ionotropic kainate 4) were shown to be associated with flavonoid treatment alone. Western blotting was used to confirm the increased expression of CBR1 in response to flavonoid pre-treatment and 600 µM H₂O₂ exposure, and CBR1 was shown to have increased expression in cells pre-treated with 100 µM quercetin.

i) CBR1

The enzyme Carbonyl reductase 1 (CBR1) has been previously associated with protection against oxidative stress, although its exact function and role in ischaemia is still not fully understood (Kim *et al*, 2014). CBR1 is an NADPH-dependant cytosolic enzyme belonging to the short-chain dehydrogenase/reductase superfamily found in most tissue including liver, kidney and neuronal tissues. CBR1 metabolises endogenous substrates such as prostaglandin E2 and S-nitroso-glutathione, and is also able to metabolise some xenobiotic substrates (Ito *et al*, 2013). During oxidative stress, specifically exposure to hydrogen peroxide, CBR1 has been shown to have an inhibitory action of the phosphorylation status of MAPKs (p38 MAPK, ERK1/2 and JNK) and PKB cell signalling pathways in HT-22 neuronal cell lines (Kim *et al*, 2014). The specifics of this inhibitory action remains unknown. It is proposed therefore that CBR1 protects ischaemic cell death by inhibition of pro-apoptosis cell signalling pathways. The interactions between flavonoids, including rutin, quercetin and kaempferol, and CBR1 have been previously studied, although not in the context of cardioprotection (Carlquist *et al*, 2008). Most notably CBR1 has been identified as a resveratrol binding protein, with the 3, 5 dihydroxyl group on the 'A' ring of resveratrol identified as contributing to the binding of the CBR1 protein. The importance of the 3, 5 dihydroxyl group is further demonstrated by the binding of CBR1 to the flavonoid 7-monoxyethylrutin, which possesses the same 3, 5 dihydroxyl group as resveratrol (Gonzalez-Covarrubias *et al*, 2008). This 3, 5 dihydroxyl group on the 'A' ring of the flavan nucleus (Fig 1.2) is also present on quercetin and its two major metabolites, thus it may have the potential to interact with the CBR1 enzyme in a similar manner to resveratrol and 7-monoxyethylrutin. The apparent "promiscuity" of the active site of CBR1 may also play an important role in the binding of flavonoid compounds, given that the enzyme already has a large number of substrates (Carlquist *et al*, 2008). The binding of several different flavonoids, including rutin and quercetin, to the active site of CBR1 was reported to cause inhibition of the reducing activity of the enzyme with regard to the interaction with the xenobiotic compound doxorubicin (Carlquist *et al*, 2008). This inhibitory action of flavonoids may have an effect on the potential cytoprotective activity of CBR1. CBR1 was shown to be up regulated in response to 24 h quercetin (100 μ M) pre-treatment during 600 μ M H₂O₂ exposure, with MALDI-TOF MS and western blot. CBR1 has been shown to have

an inhibitory effect on the activation of MAPK and PKB proteins, the same effect was observed in differentiated H9c2 cells with flavonoid pre-treatment and H₂O₂ exposure (Kim *et al*, 2014). This suggests that part of the inhibitory effect of the flavonoids on ERK1/2, JNK and p38 MAPK, PKB may be related to the up-regulation of CBR1. The mechanism of this interaction is unclear, but may involve direct binding of the flavonoid to CBR1, although this has been reported to decrease the reducing activity of the enzyme.

ii) Galectin-1

Galectin proteins are members of the β -galactoside-binding protein family, and are thought to be involved in cellular mechanisms concerned with cell-to-cell interactions, growth regulation and differentiation. Galectin content in cells is known to change in association with differentiation (Gillenwater *et al*, 1998). Galectin-1 was found to be up-regulated in response to quercetin pre-treatment and 600 μ M H₂O₂ exposure. Another member of the galectin family of proteins, galectin-7, was found to be up-regulated in response to quercetin (1 mM) pre-treatment and 5 mM H₂O₂ exposure in mitotic H9c2 cells (Chen *et al*, 2013). The role of Galectin-1 in flavonoid mediated cytoprotection remains unclear, but it can be inferred that as galectins play a role in differentiation, it is possible they may influence the protein kinases ERK1/2 and PKB, which were shown to be inhibited as a result of quercetin pre-treatment (Gillenwater *et al*, 1998). If indeed galectin-1 has an effect on ERK1/2 and PKB then it may be intrinsically linked to the flavonoid mediated cytoprotective mechanism. Further investigation into the role of galectins is needed to fully understand their place in the cytoprotective mechanism mediated by flavonoids.

iii) PEBP-1

PEBP-1 (Phosphatidylethanolamine-binding protein 1), also known as Raf-1 kinase inhibitory protein (RKIP) is a known negative regulator of MAPK signalling pathways, partially MEK/ERK1/2 pathways (Zeng *et al*, 2013). This negative regulation is a result of direct binding of PEBP-1 to Raf-1 at two activation sites. It has therefore been shown to be a regulator of cellular migration, an inhibitor of non-apoptosis cell death and also displays tumour suppressive activity (Hassan *et al*, 2011). To the authors knowledge, this present study represents the first incidence of PEBP-1 observed in relation to flavonoid mediated cytoprotection. The up-regulation of PEBP-1 after flavonoid pre-treatment and 600 μ M

H₂O₂ exposure links with the observed inhibition of MAPK signalling proteins. Along with CBR1, PEBP-1 seems to be a potential cause of the inhibition of ERK1/2, PKB, JNK and MAPK p38 observed after flavonoid pre-treatment. The cause of the up-regulation of PEBP-1 in response to flavonoid pre-treatment and 600 µM H₂O₂ exposure is unclear, although PEBP-1 is known to be negatively regulated by PKC phosphorylation, which may be influenced by quercetin pre-treatment (Zeng *et al*, 2013).

iv) PRKC apoptosis WT1 regulator protein (PAWR)

PAWR, also known as prostate apoptosis response-4 (Par-4), is a protein implicated to be involved in the regulation of apoptosis, identified in prostate cancer cells. It is suggested that PAWR induces apoptosis by inhibition of NF-κB and activation of the pro-death Fas signalling pathway (Chakraborty *et al*, 2001). Relatively little else is known about the mechanism of action or role of PAWR, save that it may be able to mediate the activation of the ERK1/2 cell signalling pathway (Pereira *et al*, 2013). It has been shown that in CF-7 cells increased PAWR expression resulted in reduced ERK phosphorylation (Pereira *et al*, 2013). This suggests that the involvement of PAWR in flavonoid mediated cytoprotection is through its activity as an inhibitor of ERK1/2, along with several other proteins identified in the present study. Although only identified in one incidence, the involvement of PAWR is plausible in its capacity as a negative regulator of ERK1/2.

v) Annexin-III

Annexin-III was shown to be up-regulated in response to exposure to 100 µM quercetin in differentiated H9c2 cells when compared to 30 µM quercetin treated cells. Annexin-III is a member of the annexin family of calcium-dependent membrane-binding proteins. Members of this family are involved in cytoskeletal interactions, membrane fusion and cell signalling pathways in its capacity as a substrate for protein kinases (Barton *et al*, 1991). Annexin-III has been previously shown to be up-regulated in response to intracellular ROS generated by treatment with glucuronic acid (Kim *et al*, 2003). Annexin proteins were also identified as being up-regulated in response to quercetin pre-treatments and exposure to H₂O₂ (Chen *et al*, 2013). The induction of annexin-3 expression by quercetin exposure may result from the generation of intracellular ROS by quercetin metabolism (Metodiewa *et al*, 1999). The increased expression of annexin-3, and heat shock proteins, has been shown to

be related to the stimulation of phosphorylation of MAPK signals such as the pro-apoptotic signals JNK and p38 MAPK and other MAPK proteins such as ERK1/2 (Kim *et al*, 2003). In the present study annexin-3 was observed after 24 h exposure to 100 μ M quercetin, which was shown to have no cytotoxic effect in chapter 5. Although, this increased expression of annexin-3 may be a precursor to the cytotoxic effects and increased JNK, p38 MAPK, ERK1/2 and PKB phosphorylation observed after \geq 48 h quercetin exposure. Further investigation is necessary to determine the precise role in flavonoid induced cytotoxicity.

vi) Calumenin

Calumenin is a universally expressed multiple EF-hand Ca^{2+} binding protein, of the CREC (Cab45, reticulocalbin, ERC-45, calumenin) family, with several functions. Calumenin is known to be expressed at particularly high levels in cardiac cells (Lee *et al*, 2013). Calumenin expression is increased in response to stress to the sarcoplasmic reticulum (SR), which can be caused by ischaemia, oxidative stress and exposure to ROS. The expression of calumenin has been shown to be similar to other molecular chaperones of the SR, which are known to have protective effects against ischaemic cell death (Lee *et al*, 2013). In neonatal rat cardiomyocytes, which are similar to the differentiated H9c2 cells used in the present study, increased calumenin expression was shown to have a protective effect against sarcoplasmic reticular stress, which can result from ischaemic attack. The increased expression of calumenin as a response to 24 h quercetin (30 μ M) exposure may potentially lead to the protective effects observed in previous chapters. Calumenin is suggested to down-regulate pro-apoptotic cell signals (Lee *et al*, 2013). Exposure to quercetin may stimulate moderate sarcoplasmic reticular stress, leading to overexpression of calumenin and other SR chaperone proteins, which then allows cells to react to a subsequent incident of oxidative stress, this may explain partially the cytoprotective effect of flavonoid pre-treatment. Further investigation into the action of flavonoids on ER resident chaperone proteins may further expand the understanding of flavonoid mediated cytoprotection.

vii) Glutamate receptor (ionotropic kainate 4)

Glutamate receptor (ionotropic kainate 4) or GRIK4 is a member of the ionotropic kainite receptor family of proteins, which are known to be activators of ERK1/2 and other members of the MAPK family (Fuller *et al*, 2001). Furthermore, flavonoids are known to be able to bind and activate other proteins including GABA_A and GABA_C receptors (Goutman *et al*, 2013). The increased expression of this protein in response to 24 h quercetin (30 µM) exposure may lead to the increased expression of upstream regulator proteins. This in turn may influence the phosphorylation state of MEK and PI3K family proteins (Fuller *et al*, 2001). This may relate to the modulation of MEK and PI3K family proteins by flavonoids during their cytoprotective and cytotoxic effects.

viii) Summary

From these findings it is clear that the mechanisms of flavonoid mediated cytoprotection and cytotoxicity are complex and interrelated. Several known regulators of the cell signalling proteins investigated in this study were identified using proteomic methods. This present study is the first to identify these proteins as being involved in the cytoprotective and cytotoxic mechanisms of flavonoids.

Chapter 7:

Conclusions

and further

work

7.1 Results summary and further work

This present study for the first time used differentiated H9c2 cells to investigate the cytoprotective and cytotoxic effects of exposure to flavonoids. Mitotic H9c2 cells which have been used in previous studies, have a great many metabolic and morphological differences to differentiated H9c2 cells, which provide a better model for *in vivo* cardiomyocytes (Gutiérrez-Venegas *et al*, 2010; Angeloni *et al*, 2012; Angeloni *et al*, 2007; Sun *et al*, 2012; Kim *et al*, 2010; Mojzisoová *et al*, 2009; Pereira *et al*, 2011; Dangel *et al*, 1996; Branco *et al*, 2013). This body of work further demonstrated these differences by investigating protein expression with proteomic methods for the first time. It was shown that differentiated H9c2 cell express tropomyosin alpha-1, alpha-4 and beta chain in a significantly greater concentration than mitotic H9c2 cells. Actin and vimentin were also shown to be expressed in a significantly greater concentration than mitotic H9c2 cells. The increased sensitivity of differentiated H9c2 cells to oxidative stress was also demonstrated. Considering these differences, as well as the other reported differences between mitotic and differentiated H9c2 cells, future studies using H9c2 cells as a model for *in vivo* cardiomyocytes should consider using the differentiated H9c2 cells as the model cell.

From the investigation into flavonoid mediated cytoprotection concluded that quercetin was shown to have a cytoprotective effect, specifically able to protect differentiated H9c2 cells from H₂O₂ treatment with a pre-treatment time of 1 h as well as 24 h with concentrations of quercetin about 30 µM. A pre-treatment of 24 h with 100 µM myricetin was necessary to protect differentiated H9c2 cells from H₂O₂ treatment induced cell death. Kaempferol was not observed to induce a significant protective effect after 24 h pre-treatment with a 1-100 µM range of concentrations. Protection from hypoxia induced cell death was achieved with 24 h pre-treatment with a concentration of 100 µM quercetin. Of the two quercetin metabolites tested 3'-O-methyl quercetin was found to exhibit a similar protective effect to quercetin against cell death caused by H₂O₂ exposure, whereas quercetin-3-glucorinde showed no protective effect. As previously stated in chapter 4, the evidence for the plasma levels of flavonoid achievable *in vivo* suggest that the observations of cytoprotection in this present study may not translate to observable cardioprotection resulting from dietary flavonoids in humans (Labbé *et al*, 2009). However, the results presented in chapter 4 highlight that quercetin has potent cellular effects under laboratory

condition, particularly with regard to MAPK and PI3K signalling. Further research is required into the intracellular accumulation of flavonoids and their metabolites, this will lead to an enhanced understanding of the conditions necessary for flavonoids to provoke a cytoprotective effect under laboratory conditions as well as *in vivo*. This present study proposes that a major mechanism of flavonoid mediated cytoprotection in differentiated H9c2 cells is inhibition of cell signalling molecules, which is supported by observations made in several other studies (Gutiérrez-Venegas *et al*, 2010; Mansuri *et al*, 2014; Sun *et al*, 2012; Angeloni *et al*, 2007). However, specific kinase inhibitors were unable to mimic the cytoprotective effect of quercetin, necessitating further studies into the relationship between kinase inhibition and cytoprotection. As quercetin is a non-specific inhibitor it may be able to inhibit multiple kinases at the same time, therefore a study into the effect of multiple inhibitors used concomitantly on differentiated H9c2 cells may provide more insight into this mechanism.

Chapter 5 showed that, as well as having a cytoprotective effect, quercetin and 3'-O-methyl quercetin had a cytotoxic effect on differentiated H9c2 cells after 48 h exposure. Prolonged exposure to 100 μ M quercetin was also shown to coincide with significant phosphorylation of ERK1/2, PKB, p38 MAPK and JNK after 72 h, as well as causing significant activation of Caspase-3 after 48 h. Investigation into intracellular ROS generation revealed significant levels after 48 and 72 h exposure to 100 μ M quercetin. These observations agree with previous studies that have shown the activation of these kinases by ROS, and the pro-oxidant intracellular metabolism of quercetin (Kamata and Hirata, 1999; Clerk *et al*, 1998; Pham *et al*, 2000; Takeishi *et al*, 1999; Metodiewa *et al*, 1999). As with the concentration of flavonoid required to invoke a cytoprotective effect, the concentrations of flavonoid it induce cytotoxicity are greater than those than can be achieved *in vivo* from dietary sources (Labbé *et al*, 2009). This observation further demonstrates the need for further research into the intracellular accumulation of flavonoids and the concentration of flavonoid retained by cells. As this study showed that at high concentrations intracellular ROS generation resulting from quercetin exposure likely leads to cytotoxicity.

The proteomic investigation into the effect of quercetin treatment on protein expression after oxidative stress revealed that several proteins associated with cell signal regulation are expressed. Specifically CBR-1, Geletin-1, PEBP-1 and PAWR were shown to have

increased expression in differentiated H9c2 cells after exposure to oxidative stress from H₂O₂. Of these proteins CBR-1 and PEBP-1 are known to have MAPK regulatory functions, and PAWR is thought to have a similar function (Kim *et al*, 2014; Zeng *et al*, 2013; Pereira *et al*, 2013). These results show that quercetin may influence a number of MAPK regulatory mechanisms downstream of ERK1/2.

Three proteins were shown to be expressed after exposure of differentiated H9c2 cells to 100 and 30 µM quercetin. Calumenin has particular importance to this present study as it is reported to be expressed in response to SR stress, leading to a protective effect (Lee *et al*, 2013). This result suggests that exposure to quercetin (30 µM) may lead to SR stress, and induce a protective effect during subsequent episodes of oxidative stress. Although this was only observed after exposure to 30 µM quercetin, which is greater than the maximum plasma concentration of flavonoids achievable from dietary sources, this observation draws attention to another potential mechanism for flavonoid induced cytoprotection. Further studies investigating protein expression in H9c2 cells utilising lower concentrations of flavonoid, in particular concentrations that could be achieved *in vivo*, would further illustrate the effects of flavonoid on protein expression that may lead to a cytoprotective effect.

To be translatable to understanding flavonoid mediated cardioprotection *in vivo*, future studies should focus on investigating the effects of concentrations of flavonoid that are achievable via dietary consumption. More studies into the intracellular accumulation of flavonoids are required to reveal the exact concentrations of flavonoid achievable *in vivo* heart cells. As this present study and previous studies have shown, flavonoids are able to have potent effects in model cell lines at concentrations above 30 µM (Gutiérrez-Venegas *et al*, 2010; Mansuri *et al*, 2014; Sun *et al*, 2012; Angeloni *et al*, 2007). Using an animal model to study the effects of dietary flavonoids will further develop the understanding of this mechanism, as well as the general mechanism of flavonoid mediated protection from CVD.

As flavonoids are ubiquitous in the diet, and numerous flavonoids are present in a single dietary source, future studies could consider using mixtures of flavonoids to better reflect how flavonoids are encountered by *in vivo* cells. Furthermore, other plant polyphenols such as tannins could be introduced to this mixture to simulate the polyphenolic content of wine.

7.2 General conclusions

This present study has provided novel data contributing to the understanding of the cardioprotective mechanisms of dietary flavonoids and their metabolites, specifically in the model H9c2 cell line. For the first time, investigations into the protective mechanisms of dietary flavonoids were performed using differentiated H9c2 cells as a model for *in vivo* cardiomyocytes. Furthermore the cytotoxic effect of long term exposure to flavonoids and flavonoid metabolites was investigated, with flavonoids showing some cytotoxic activity. The findings of this study suggest that flavonoids are potent modulators of cell signalling molecules under certain conditions, and that this can be both beneficial and fatal to cells. This is further demonstrated by the novel proteins identified in this study, many of which play a role in the regulation of MAPK or PI3K cell signalling pathways. Although, the concentrations required to provoke these effects was greater than concentrations available to *in vivo* cardiomyocytes.

7.3 Concluding remarks

In conclusion, this study has shown that flavonoids, particularly quercetin, can provide protection against hypoxia and H₂O₂ induced cell death in differentiated H9c2 cells. This protection is most probably due to the modulation of cell signalling molecules of the MAPK and PI3K families. Several novel proteins associated with MAPK and PI3K regulation were shown to be upregulated in the presence of quercetin. Furthermore, flavonoid induced cytotoxicity was shown to occur after extended periods of exposure, most likely due to intracellular metabolism of flavonoids forming pro-oxidants and ROS. The data presented in this present study will contribute to increasing the body of knowledge concerning the protective effects of flavonoids, and their cytotoxic potential. Hopefully this study will lead to further investigations into the complex nature of flavonoid induced cytoprotection, leading eventually to more effective therapies against ischaemic attacks.

Chapter 8:

References

8.0 References

Angeloni C, Hrelia S (2012). Quercetin reduces inflammatory responses in LPS-stimulated cardiomyoblasts. *Oxid Med Cell Longev*, **2012**: 583901.

Angeloni C, Spencer JPE, Leoncini E, Biagi PL, Hrelia S (2007). Role of quercetin and its *in vivo* metabolites in protecting H9c2 cells against oxidative stress. *Biochimie*, **89**, 73-82.

Angelone T, Pasqua T, Di Majo D, Quintieri AM, Filice E, Amodio N, Tota B, Giammanco M, Cerra MC (2011) Distinct signalling mechanisms are involved in the dissimilar myocardial and coronary effects elicited by quercetin and myricetin, two red wine flavonols, *Nutrition, Metabolism & Cardiovascular Diseases*, **21**, 362-371

Barnes S, Prasain J, D'Alessandro T, Arabshahi A, Botting N, Lila MA, Jackson G, Janle EM and Weaver CM (2011) The metabolism and analysis of isoflavones and other dietary polyphenols in foods and biological systems, *Food Funct*, **2**, 235-244

Barton GJ, Newman RH, Freemont PS, Crumpton MJ (1991) Amino acid sequence analysis of the annexin super-gene family of proteins, *Eur. J. Biochem.*, **198**, 749-760

Bhaskar S , Kumar KS , Krishnan K, Antony H (2013) Quercetin alleviates hypercholesterolemic diet induced inflammation during progression and regression of atherosclerosis in rabbits, *Nutrition*, **29**, 219–229

Branco AF, Sampaio FS, Wieckowski MR, Sardão VA, Oliveira PJ (2013) Mitochondrial disruption occurs downstream from β -adrenergic over activation by isoproterenol in differentiated, but not undifferentiated H9c2 cardiomyoblasts: Differential activation of stress and survival pathways, *The International Journal of Biochemistry & Cell Biology*, **45**, 2379–2391

Calderón-Montaño JM, Burgos-Morón E, Pérez-Guerrero C and López-Lázaro M (2011) A review on the Dietary Flavonoid Kaempferol, *Mini-Reviews in Medicinal Chemistry*, **11**, 298-344

Carlquist M, Frejd T, Gorwa-Grauslund MF, (2008) Flavonoids as inhibitors of human carbonyl reductase 1, *Chemico-Biological Interactions*, **174**, 98–108

Chakraborty M, Qiu SG, Vasudevan KM, Rangnekar VM (2001) Par-4 Drives Trafficking and Activation of Fas and FasL to Induce Prostate Cancer Cell Apoptosis and Tumor Regression, *CANCER RESEARCH* **61**, 7255–7263

Chambless LE, Folsom AR, Sharrett AR, Sorlie P, Couper D, Szklo M, Nieto FJ (2003) Coronary heart disease risk prediction in the Atherosclerosis Risk in Communities (ARIC) study, *Journal of Clinical Epidemiology*, **56**, 880–890

Chang YC, Lee TS, Chiang AN (2012). Quercetin enhances ABCA1 expression and cholesterol efflux through a p38-dependent pathway in macrophages. *J Lipid Res*, **53**, 1840-50.

Chang WT, Shao ZH, Yin JJ, Mehendale S, Wang CZ, Qin Y, Li J, Chen WJ, Chien CT, Becker LB, Hoek TLV, Yuan CS (2007) Comparative effects of flavonoids on oxidant scavenging and ischemia-reperfusion injury in cardiomyocytes, *European Journal of Pharmacology*, **566**, 58–66

Chatzizisis YS, Coskun AU, Jonas M, Edelman ER, Feldman CL, Stone PH (2007) Role of Endothelial Shear Stress in the Natural History of Coronary Atherosclerosis and Vascular Remodeling, *Journal of the American College of Cardiology*, **49**, 2379–2393

Chen YW, Chou HC, Lin ST, Chen YH, Chang YJ, Chen L, Chan HL. (2013) Cardioprotective Effects of Quercetin in Cardiomyocyte under Ischemia/Reperfusion Injury, *Evidence-Based Complementary and Alternative Medicine*, **2013**.

Choi EN (2011). Kaempferol protects MC3T3-E1 cells through antioxidant effect and regulation

of mitochondrial function, *Food and Chemical Toxicology*, **49**, 1800–1805

Choi YJ, Jeong YJ, Lee YJ, Kwon HM, Kang YH (2005). (-)Epigallocatechin Gallate and Quercetin Enhance Survival Signaling in Response to Oxidant-Induced Human Endothelial Apoptosis, *J. Nutr.* **135**: 707–713

Chow J-M, Shen S-C, Huan Sk, Lin H-Y, Chen Y-C (2005). Quercetin, but not rutin and quercitrin, prevention of H₂O₂-induced apoptosis via anti-oxidant activity and heme oxygenase 1 gene expression in macrophages. *Biochem Pharmacol*, **69**, 1839-51.

Clerk A, Fuller SJ, Michael A, Sugden PH (1998). Stimulation of “stress-regulated” mitogen-activated protein kinases (stress-activated protein kinases/c-Jun N-terminal kinases and p38-mitogen-activated protein kinases) in perfused hearts by oxidative and other stresses. *J Biol Chem*, **273**, 7228-34.

Comelli M, Domenis R, Bisetto E, Contin M, Marchini M, Ortolani F *et al* (2011). Cardiac differentiation promotes mitochondria development and ameliorates oxidative capacity in H9c2 cardiomyoblasts. *Mitochondrion*, **11**, 315-326.

Courtney KD, Corcoran RB, Engelman JA (2010) The PI3K pathway as drug target in human cancer, *Journal of Clinical Oncology*, **28**, 1075-1083

Dangel V, Giray J, Ratge D, Wisser H (1996) Regulation of β -adrenoceptor density and mRNA levels in the rat heart cell-line H9c2, *Biochem. J.*, **317**, 925-931

Dong Q, Chen L, Lu Q, Sharma S, Li L, Morimoto S, Wang G. (2014) Quercetin attenuates doxorubicin cardiotoxicity by modulating Bmi-1 expression. *Br J Pharmacol.*, **171**, 4440-54

Edinger AL and Thompson CB (2004), Death by design: apoptosis, necrosis and autophagy, *Current Opinion in Cell Biology*, **16** ,663–669

Edwards RL, Lyon T, Litwin SE, Rabovsky A, Symons JD, Jalili T (2007). Quercetin Reduces Blood Pressure in Hypertensive Subjects, *The Journal of Nutrition*, **137**, 2405–2411

Egert S, Bosy-Westphal A, Seiberl J, Kürbitz C, Settler U, Plachta-Danielzik S, Wagner AE, Frankl J, Schrezenmeir J, Rimbach G, Wolfram S, Müller MJ (2009). Quercetin reduces systolic blood pressure and plasma oxidised low-density lipoprotein concentrations in overweight subjects with a high-cardiovascular disease risk phenotype: a double-blinded, placebo-controlled cross-over study, *British Journal of Nutrition* , **102**, 1065–1074

Fotakis G, Timbrell JA (2006). In vitro cytotoxic assays: comparison of LDH, neutral red, MTT and protein assay in hepatoma cells following exposure to cadmium chloride. *Toxicology Letts*, **160**, 171-77.

Fuller G, Veitch K, Ho LK, Cruise L, Morris BJ (2001) Activation of p44/p42 MAP kinase in striatal neurons via kainite receptors and PI3 kinase, *Molecular Brain Research*, **89**, 126–132

Gau GT and Wright RS (2006) Pathophysiology, Diagnosis, and Management of Dyslipidemia, *Curr Probl Cardiol*, **31**, 445-486

Geybels MS, Verhage BAJ, Arts ICW, van Schooten FJ, Goldbohm RA, and van den Brandt PA (2013) Dietary Flavonoid Intake, Black Tea Consumption, and Risk of Overall and Advanced Stage Prostate Cancer, *Am J Epidemiol*, **177**, 1388–1398

Gillenwater A, Xu XC, Estrov Y, Sacks PG, Lotan D, Lotan R (1998). Modulation of galectin-1 content in human head and neck squamous carcinoma cells by sodium butyrate, *International journal of cancer*, **75**, 217-224

Glaeser H, Bujok K, Schmidt I, Fromm MF, Mandery K (2014) Organic anion transporting polypeptides and organic cation transporter 1 contribute to the cellular uptake of the flavonoid quercetin, *Naunyn-Schmiedeberg's Arch Pharmacol*, **387**, 883–891

Goutman JD, Waxemberg MD, Doñate-Oliver F , Pomata PE, Calvo DJ. (2013) Flavonoid modulation of ionic currents mediated by GABA_A and GABA_C receptors, *European Journal of Pharmacology*, **461**, 79 – 87

Gulati N, Laudet B, Zohrabian VM, Murali R, Jhanwar-Uniyal M (2006). The antiproliferative effect of quercetin in cancer cells is mediated via inhibition of the PI3K-Akt/PKB pathway. *Anticancer Res*, **26**, 1177-82.

Guo Y and Bruno RS (2015) Endogenous and exogenous mediators of quercetin bioavailability, *Journal of Nutritional Biochemistry*, **26**, 201–210

Gutiérrez-Venegas G, Bando-Campos CG (2010). The flavonoids luteolin and quercetin inhibit lipoteichoic acid actions on H9c2 cardiomyocytes. *Int Immunopharmacol*, **10**, 1003-09.

Hansson GK (2005) Inflammation, Atherosclerosis, and Coronary Artery Disease, *N Engl J Med*, **352**, 1685-1695.

Hassan MH, Klett D, Cahoreau C, Combarous Y (2011) Straightforward isolation of phosphatidyl-ethanolamine-binding protein-1 (PEBP-1) and ubiquitin from bovine testis by hydrophobic-interaction chromatography (HIC), *Journal of Chromatography*, **879**, 2935–2940

Hausenloy DJ and Yellon DM (2007) Preconditioning and postconditioning: United at reperfusion, *Pharmacology & Therapeutics*, **116**, 173–191

Heim KE, Tagliaferro AR, Bobilya DJ (2002). Flavonoid antioxidants: chemistry, metabolism and structure-activity Relationships, *Journal of Nutritional Biochemistry*, **13**, 572–58

Hers I, Vincent EE, Tavaré JM (2011). Akt signalling in health and disease. *Cell Signal*, **23**, 1515-27.

Hescheler J, Meyer R, Plant S, Krautwurst D, Rosenthal W, Schultz G (1991). Morphological, biochemical and electrophysiological characterization of a clonal cell (H9c2) line from rat heart. *Circ Res*, **69**, 1476-86.

Hsieh SR, Hsu CS, Lu CH, Chen WC, Chiu CH, Liou YM (2013) Epigallocatechin-3-gallate-mediated cardioprotection by Akt/GSK-3 β /caveolin signalling in H9c2 rat cardiomyoblasts, *Journal of Biomedical Science*, **20**, 86

Ito Y, Mitani T, Harada N, Isayama A, Tanimori S, Takenaka S, Nakano Y, Inui H, Yamaji R (2013) Identification of Carbonyl Reductase 1 as a Resveratrol-Binding Protein by Affinity Chromatography Using 4'-Amino-3,5-dihydroxy-trans-stilbene, *Journal of nutritional science and vitaminology*, **59**, 358-364

Kageyama K, Ihara Y, Goto S, Urata Y, Toda G, Yano K, Kondo T (2002) Overexpression of Calreticulin Modulates Protein Kinase B/Akt Signaling to Promote Apoptosis during Cardiac Differentiation of Cardiomyoblast H9c2 Cells, *J. Biol. Chem.*, **277**, 19255-19264

Kamata H, Hirata H (1999). Redox regulation of cellular signalling. *Cell Signal*, **11**, 1-1

Kawai Y, Nishikawa T, Shiba Y, Saito S, Murota K, Shibata N, *et al* (2008). Macrophage as a target of quercetin glucuronides in human atherosclerotic arteries: implication in the anti-atherosclerotic mechanism of dietary flavonoids. *J Biol Chem*, **283**, 9424-34.

Kim DS, Kwon DY, Kim MS, Lee YC, Park SJ, Yoo WH *et al* (2010) The involvement of endoplasmic reticulum stress in flavonoid-induced protection of cardiac cell death caused by ischaemia/reperfusion. *J Pharm Pharmacol*, **62**, 197-204.

Kim DS, Ha KC, Kwon DY, Kim MS, Kim HR, Chae SW, Chae HJ, (2008) Kaempferol Protects Ischemia/Reperfusion-Induced Cardiac Damage Through the Regulation of Endoplasmic Reticulum Stress, *Immunopharmacology and Immunotoxicology*, **30**, 257–270

Kim JM, Yoon MY, Kim J, Kim SS, Kang I, Ha J, Kim SS (1999). Phosphatidylinositol 3-Kinase Regulates Differentiation of H9c2 Cardiomyoblasts Mainly through the Protein Kinase B/Akt-Independent Pathway, *Archives of Biochemistry and Biophysics*, **367**, 67–73

Kim YH, Lee YJ (2007). TRAIL apoptosis is enhanced by quercetin through Akt dephosphorylation. *J Cell Biochem*, **100**, 998-1009.

Kim YN, Jung HY, Eum WS, Kim DW, Shin MJ, Ahn EH, Kim SG, Lee CH, Yong J, Ryu EJ, Park J, Choi JH, Hwang IK, Choi SY. (2014) Neuroprotective effects of PEP-1-carbonyl reductase 1 against oxidative-stress-induced ischemic neuronal cell damage, *Free Radical Biology and Medicine*, **69**, 181–196

Kyoung AK, Zhi HW, Rui Z, Mei JP, Ki CK, Sam SK, Young WK, Jongsung L, Deakhoon P, Jin WH (2010) Myricetin protects cells against oxidative stress-induced apoptosis via regulation of PI3K/Akt and MAPK signalling pathways. *Int J Mol Sci*, **11** 4348-4360

Labbé D, Provençal M, Lamy S, Boivin D, Gingras D, and Béliveau R (2009) The Flavonols Quercetin, Kaempferol, and Myricetin Inhibit Hepatocyte Growth Factor-Induced Medulloblastoma Cell Migration, *The Journal of Nutrition*, **108**, 646-652

Lee JH, Kwon EJ, Kim DH (2013) Calumenin has a role in the alleviation of ER stress in neonatal rat Cardiomyocytes, *Biochemical and Biophysical Research Communications*, **439**, 327–332

Lee KW, Kang NJ, Heo YS, Rogozin EA, Pugliese A, Hwang MK *et al* (2008). Raf and MEK protein kinases are direct molecular targets for the chemopreventive effect of quercetin, a major flavonol in red wine. *Cancer Res*, **68**, 946-55

Lodi F, Jimenez R, Moreno L, Kroon PA, Needs PW, Hughes DA, Santos-Buelga C, Gonzalez-Paramas A, Cogolludo A, Lopez-Sepulveda R, Duarte J, Perez-Vizcaino F (2009) Glucuronidated and sulfated metabolites of the flavonoid quercetin prevent endothelial dysfunction but lack direct vasorelaxant effects in rat aorta, *Atherosclerosis*, **204**, 34–39

Lu Z, Xu S (2006). ERK1/2 MAP kinases in cell survival and apoptosis. *IUBMB Life*, **58**, 621-31.

Malhotra R, Lin Z, Vincenz C, Brosius FC III (2001). Hypoxia induces apoptosis via two independent pathways in Jurkat cells: differential regulation by glucose. *Am J Physiol Cell Physiol*, **5**, 281

Mansuri ML, Parihar P, Solanki I, Parihar S (2014). Flavonoids in modulation of cell survival signalling pathways, *Genes & Nutrition*, **9**, 400

Ménard C, Pupier S, Mornet D, Kitzmann M, Nargeot J, Lory P (1999) . Modulation of L-type channel expression during retinoic acid-induced differentiation of H9c2 cardiac cells. *J Biol Chem*, **274**, 29063-070.

Mendoza MC, Er EE and Blenis J (2011) The Ras-ERK and PI3K-mTOR pathways: cross-talk and compensation, *Trends in Biochemical Sciences*, **36**, 320-328

Metodiewa D, Jaiswal AK, Cenas N, Dickançaité, Segura-Aguilar J (1999). Quercetin may act as a cytotoxic prooxidant after its metabolic activation to semiquinone and quinoidal product, *Free Radical Biology & Medicine*, **26**, 107–116

de Moissac D, Gurevich RM, Zheng H, Singal PK, Kirshenbaum LA (2000). Caspase activation and mitochondrial cytochrome C release during hypoxia-mediated apoptosis of adult ventricular myocytes. *J Mol Cell Cardiol*, **32**,53-63.

Mojzisová G, Sarisský M, Mirossay L, Martinka P, Mojzis J (2009). Effects of flavonoids on daunorubicin-induced toxicity in H9c2 cardiomyoblasts. *Phytother Res*, **23**, 136-39.

Morecroft I, Doyle B, Nilsen M, Kolch W, Mair K and MacLean MR (2011). Mice lacking the Raf-1 kinase inhibitor protein exhibit exaggerated hypoxia-induced pulmonary hypertension, *British Journal of Pharmacology* , **163**, 948–963

Murry CE, Jennings RB, Reimer KA (1986). Preconditioning with ischemia: a delay of lethal cell injury in ischemic myocardium, *Circulation*, **74**, 1124-1136

Nishimuro H , Ohnishi H , Sato M, Ohnishi-Kameyama M, Matsunaga I, Naito S, Ippoushi K, Oike H, Nagata T, Akasaka H, Saitoh S, Shimamoto K and Kobori M (2015) Estimated Daily Intake and Seasonal Food Sources of Quercetin in Japan, *Nutrients*, **7**, 2345-2358

Peluso I and Palmery M (2015) Flavonoids at the pharma-nutrition interface: Is a therapeutic index in demand? *Biomedicine & Pharmacotherapy*, **71**, 102–107

Pereira MC, De Bessa-Garcia SA, Burikhanov R, Pavanell,AC, Antunes L, Rangnekar VM, Nagai MA (2013) Prostate apoptosis response-4 is involved in the apoptosis response to docetaxel in MCF-7 breast cancer cells, *International journal of oncology*, **43**, 531-538

Pereira SL,Ramalho-Santos J, Branco AF, Sardão VA, Oliveira PJ, Carvalho RA (2011) Metabolic Remodeling During H9c2 Myoblast Differentiation: Relevance for In Vitro Toxicity Studies, *Cardiovasc Toxicol*, **11**, 180–190

Perez A, Gonzalez-Manzano S, Jimenez R, Perez-Abuda R, Haroe JM, Osunaa A, Santos-Buelga C, Duarte J, Perez-Vizcaino F (2014) The flavonoid quercetin induces acute vasodilator effects in healthy volunteers: Correlation with beta-glucuronidase activity, *Pharmacological Research*, **89**, 11–18

Pham FH, Sugden PH, Clerk A (2000). Regulation of protein kinase B and 4E-BP1 by oxidative stress in cardiac myocytes. *Circ Res*, **86**, 1252-58.

Pimentel FA, Nitzke JA, Klipel CB, de Jong EV (2010) Chocolate and red wine – A comparison between flavonoids content, *Food Chemistry*, **120**, 109–112

Qian F, Wei D, Liu J, Yang S (2004) Molecular Model and ATPase Activity of Carboxyl-Terminal Nucleotide Binding Domain from Human P-Glycoprotein, *Biochemistry (Moscow)*, **71**, S18-S24

Reed J (2002) Cranberry Flavonoids, Atherosclerosis and Cardiovascular Health, *Critical Reviews in Food Science and Nutrition*, **42**, 301-316

Repetto G, del Peso A, Zurita JL (2008). Neutral red uptake assay for the estimation of cell viability/cytotoxicity. *Nature Protocols*, **3**, 1125-31.

Romero M, Jiménez R, Sánchez M , López-Sepúlveda E, Zarzuelo MJ , O'Valle F, Zarzuelo A, Pérez-Vizcaíno F, Duarte J (2009) Quercetin inhibits vascular superoxide production induced by endothelin-1: Role of NADPH oxidase, uncoupled eNOS and PKC, *Atherosclerosis*, **202**, 58–67

Roskoski Jr R (2010). ERK1/2 MAP kinases: Structure, function, and regulation, *Int. J. Mol. Sci*, **11**, 4348-4360

Ross R (1999) Atherosclerosis- an inflammatory disease, *Mechanisms of Disease*, **340**, 115-126

Rozengurt E, Sinnott-Smith J, Kisfalvi K (2010) Crosstalk between Insulin/Insulin-like Growth Factor-1 Receptors and G Protein-Coupled Receptor Signaling Systems: A Novel Target for the Antidiabetic Drug Metformin in Pancreatic Cancer, *Clin Cancer Res*, **16**, 2505-2511

Russo M, Spagnuolo C, Tedesco I, Bilotto S, Russo GL (2012). The flavonoid quercetin in disease prevention and therapy: facts and fancies. *Biochem Pharmacol*, **83**, 6-15.

Russo M, Spagnuolo C, Volpe S, Mupo A, Tedesco I, Russo GL (2010). Quercetin induced apoptosis in association with death receptors and fludarabine in cells isolated from chronic lymphocytic patients. *Br J Cancer*, **103**, 642-8.

Schaper J, Kostin S (2005). Cell death and adenosine triphosphate: the paradox. *Circulation*, **112**, 6-8.

Selmin O, Thorne PA, Caldwell PT, Johnson PD, Runyan RB (2005) Effects of trichloroethylene and its metabolite trichloroacetic acid on the expression of vimentin in the rat H9c2 cell line, *Cell Biology and Toxicology*, **21**, 83–95.

Serra A, Macia A, Romero MP, Reguant J, Ortega N, Motilva MJ (2012) Metabolic pathways of the colonic metabolism of flavonoids (flavonols, flavones and flavanones) and phenolic acids, *Food Chemistry*, **130**, 383–393

Shimoi K, Saka N, Nozawa R, Sato M, Amano I, Nakayama T and Kinae N (2001) Deglucoronidation of a flavonoid, luteolin monoglucuronide, during inflammation, *Drug metabolism and disposition*, **29**, 1521-1524

Simon HU, Haj-Yehia A, Levi-Schaffer F (2000) Role of reactive oxygen species (ROS) in apoptosis induction, *Apoptosis*, **5**, 415–418

Spencer JPE, Rice-Evans C, Williams RJ (2003). Modulation of pro-survival Akt/protein kinase B and ERK1/2 signaling cascades by quercetin and its *in vivo* metabolites underlie their action on neuronal viability. *J Biol Chem*, **278**, 34783-93.

Spencer JPE, Kuhnle GGC, Williams RJ, Rice-Evans C (2003) Intracellular metabolism and bioactivity of quercetin and its *in vivo* metabolites, *Biochem. J.*, **372**, 173–181

Sun B, Sun GB, Xiao J, Chen RC, Wang X, Wu Y (2012). Isorhamnetin inhibits H₂O₂-induced activation of the intrinsic apoptotic pathway in H9c2 cardiomyocytes through scavenging reactive oxygen species and ERK inactivation. *J Cell Biochem*, **113**, 473-85.

Takeishi Y, Abe J, Lee J-D, Kawakatsu H, Walsh RA, Berk BC (1999). Differential regulation of p90 ribosomal S6 kinase and Big-mitogen-activated protein kinase 1 by ischemia/reperfusion and oxidative stress in perfused guinea-pig hearts. *Circ Res*, **85**, 1164-72.

Tatsumi T, Shiraishi J, Keira N, Akashi K, Mano A, Yamanaka S, Matoba S, Fushiki S, Fliss H, Nakagawa M (2003). Intracellular ATP is required for mitochondrial apoptotic pathways in isolated hypoxic rat cardiac myocytes. *Cardiovasc Res*, **59**, 428-40.

Viskupičová J, Ondrejovič M, Šturdík E (2008). Bioavailability and metabolism of flavonoids, *Journal of Food and Nutrition Research*, **47**, 151–162

Wang ZH, Kang KA, Zhang R, Piao MJ, Jo SH, Kim JS, Sang SS, Lee JS, Park DH, Hyun JW (2010). Myricetin suppresses oxidative stress-induced cell damage via both direct and indirect antioxidant action. *Environ. Toxicol. Pharmacol*, **29**, 12–18.

Weng CJ, Chen MJ, Yeh CT, Yen GC (2011). Hepatoprotection of quercetin against oxidative stress by induction of metallothionein expression through activating MAPK and PI3K pathways and enhancing Nrf2 DNA-binding activity. *New Biotechnol*, **28**, 767-77.

Williams RJ, Spencer JPE, Rice-Evans C (2004). FLAVONOIDS: ANTIOXIDANTS OR SIGNALLING MOLECULES? *Free Radical Biology & Medicine*, **36**, 838 – 849

Williamson G, Barron D, Shimoi K, Terao J (2005). *In vitro* biological properties of flavonoid conjugates found *in vivo*. *Free Radic Res*, **39**, 457-69.

Youl E, Bardy G, Magous R, Cros G, Sejalon F, Virsolvy A *et al* (2010). Quercetin potentiates insulin secretion and protects INS-1 pancreatic β -cells against oxidative stress damage via the ERK1/2 pathway. *Br J Pharmacol*, **161**, 799-814

Zara S, di Giacomo V, Rapino M, Di Valerio V, Cataldi A (2010). Morphological and molecular events during H9c2 differentiation: role for pPKC δ /SC35 interaction, *IJAE*, **115**, (Supplement)

Zeng L, Ehrenreiter K, Menon J, Menard R, Kern F, Nakazawa Y, Bevilacqua E, Imamoto A, Baccarini M, Rosner MR (2013) RKIP regulates MAP kinase signaling in cells with defective B-Raf activity, *Cellular Signalling*, **25**, 1156–1165

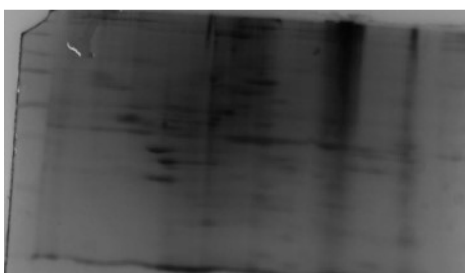
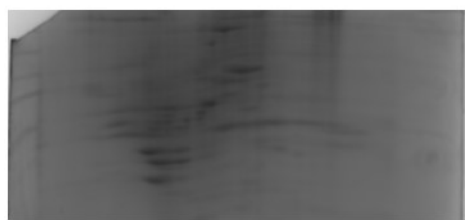
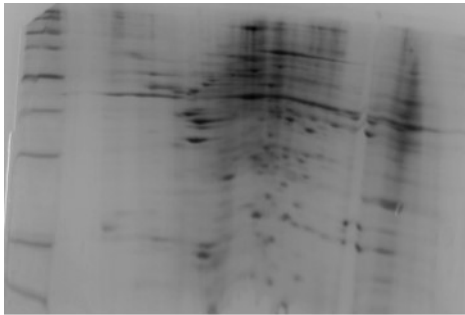
Appendix I

Bruker peptide calibration standard II content

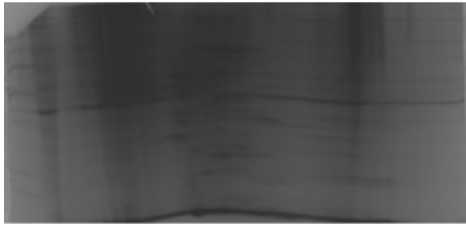
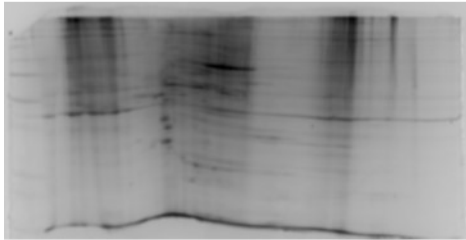
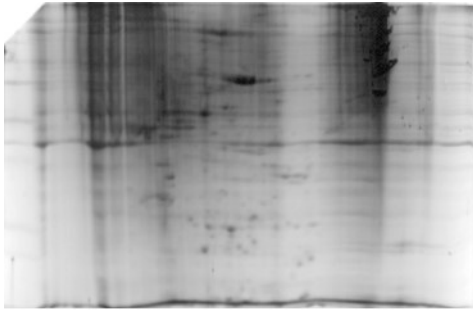
Peptide	Average Monoisotopic Mass
Angiotensin II	1046.5418
Angiotensin I	1296.6848
Substance P	1347.7354
Bombesin	1619.8223
ACTH (1-17)	2093.0862
ACTH (18-39)	2465.1983
Somatostatin 2	3147.4710

Appendix 2

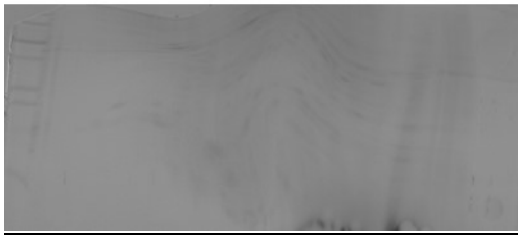
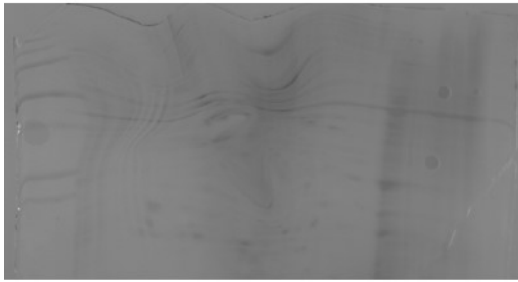
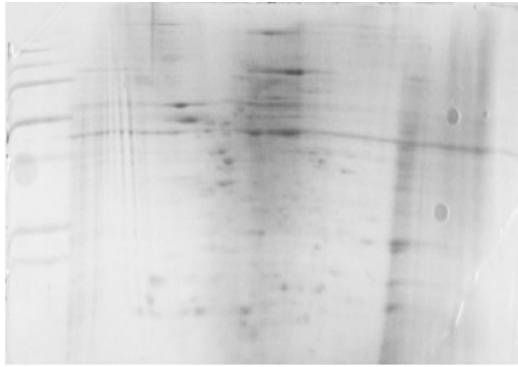
Proteomic gels produced by two-dimensional gel electrophoresis



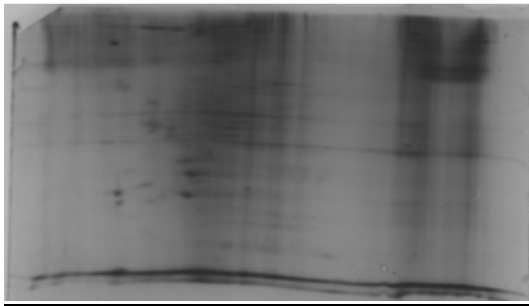
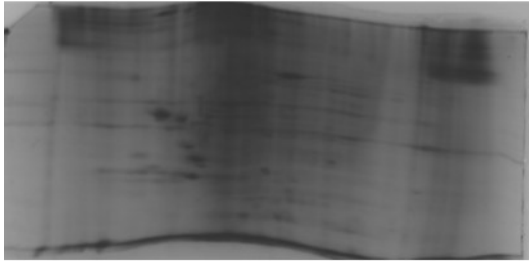
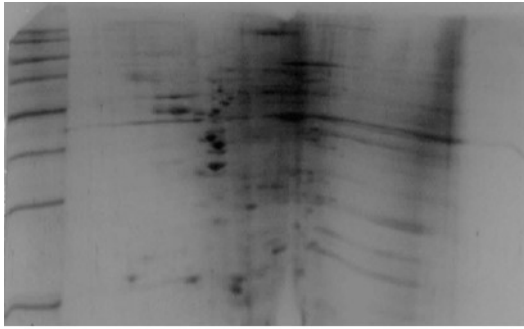
A.1 Proteomic gels of differentiated H9c2 cell lysates.



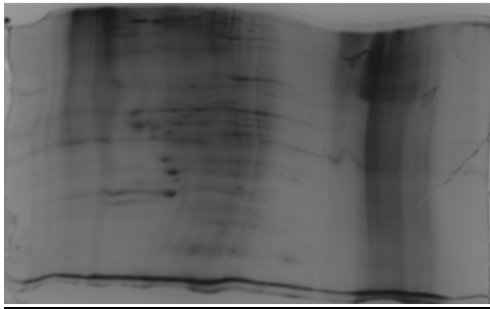
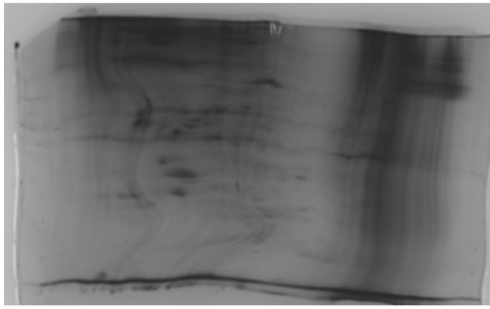
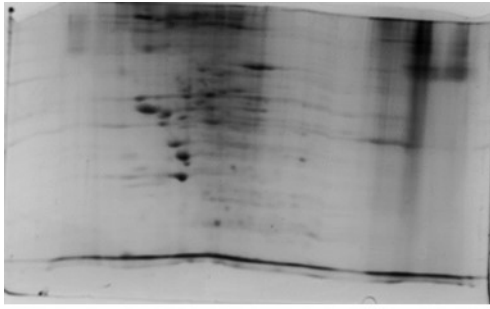
A.2 Proteomic gels of mitotic H9c2 cell lysates.



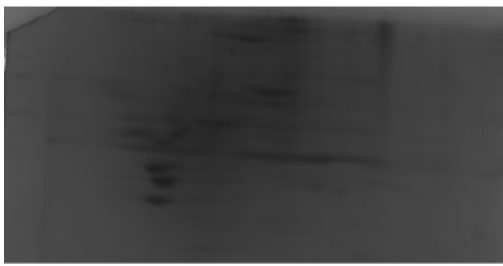
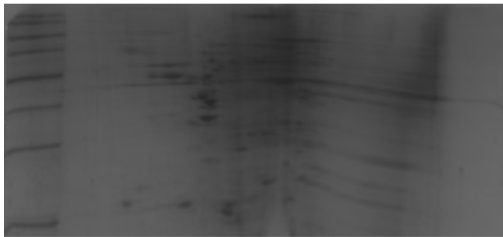
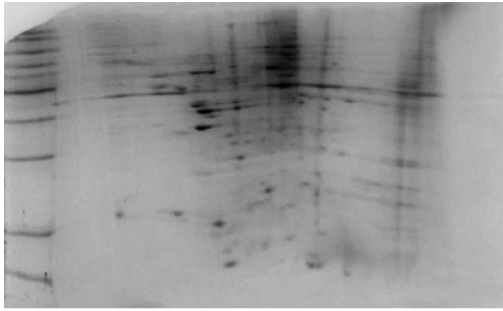
A.3 Proteomic gels of differentiated H9c2 cells exposed for 2 h to 600 μM H_2O_2 cell lysates.



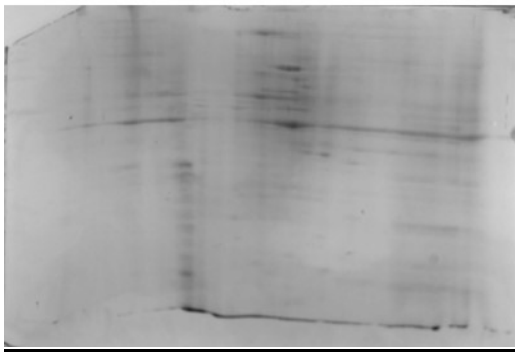
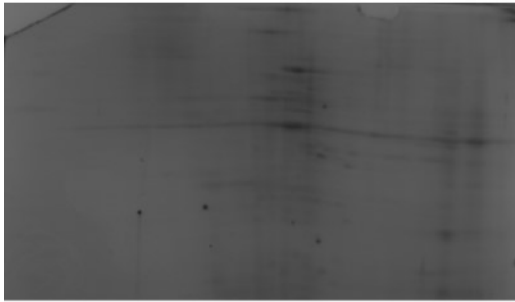
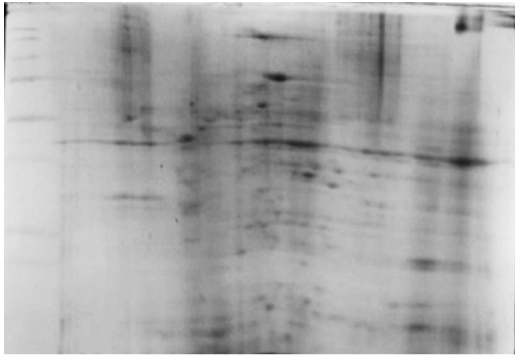
A.4 Proteomic gels of differentiated H9c2 cells 24 h pre-treated with 30 μ M quercetin followed by 2 h exposure to 600 μ M H_2O_2 cell lysates.



A.5 Proteomic gels of differentiated H9c2 cells 24 h pre-treated with 100 μM quercetin followed by 2 h exposure to 600 μM H_2O_2 cell lysates.



A.6 Proteomic gels of differentiated H9c2 cells exposed for 24 h to 30 μ M quercetin cell lysates.



A.7 Proteomic gels of differentiated H9c2 cells exposed for 24 h to 100 μ M quercetin cell lysates.